Reliable Flexibility Provision from Distribution Systems to Enable Higher Grid Utilization by Curative Operation

Methods to Analyze Distributed Flexibility Potentials and Algorithms to Calculate Flexibility Sets that Can Be Safely Provided by Distribution Grids

TECHNISCHE
UNIVERSITÄT
DARMSTADT

Electrical Engineering and Information Technology Department

Technik und Ökonomie Multimodaler Energiesysteme

Reliable Flexibility Provision from Distribution Systems to Enable Higher Grid Utilization by Curative Operation
Methods to Analyze Distributed Flexibility Potentials and Algorithms to Calculate Flexibility Sets that Can Be Safely Provided by Distribution Grids

Accepted doctoral thesis by Till Jakob Kolster

Date of submission: 30.01.2022
Date of thesis defense: 18.07.2022

Darmstadt – D17, Technische Universität Darmstadt

Erklärungen laut Promotionsordnung

§ 8 Abs. 1 lit. c PromO

Ich versichere hiermit, dass die elektronische Version meiner Dissertation mit der schriftlichen Version übereinstimmt.

§ 8 Abs. 1 lit. d PromO

Ich versichere hiermit, dass zu einem vorherigen Zeitpunkt noch keine Promotion versucht wurde. In diesem Fall sind nähere Angaben über Zeitpunkt, Hochschule, Dissertationsthema und Ergebnis dieses Versuchs mitzuteilen.

§ 9 Abs. 1 PromO

Ich versichere hiermit, dass die vorliegende Dissertation selbstständig und nur unter Verwendung der angegebenen Quellen verfasst wurde.

§ 9 Abs. 2 PromO

Die Arbeit hat bisher noch nicht zu Prüfungszwecken gedient.

Darmstadt, 30.01.2022

_____

T. Kolster

Zusammenfassung

Die Anforderungen an den Betrieb der Stromnetze im Zuge der fortschreitenden Dekarbonisierung der Energiesysteme steigen stetig an. Immer mehr dezentral installierte erneuerbare Energiequellen tragen zur Energieversorgung bei und verursachen höhere Transportbedarfe in den Stromnetzen. Da der hierfür notwendige Netzausbau sowohl aus Akzeptanzgründen stockt und große Kosten verursacht, als auch zeitlich nicht mit der notwendigen Geschwindigkeit durchgeführt wird, um die Ziele des Pariser Klimaschutzabkommen einhalten zu können, sind die Übertragungsnetzbetreiber und Regulierungsbehörden angewiesen, innovative Konzepte zu entwickeln, um eine höhere Netzauslastung zu ermöglichen. Eine Möglichkeit hierfür ist der Wechsel vom präventiven n-1 sicheren Netzbetrieb zu einem kurativ n-1 sicheren. Um einen solchen Wandel zu ermöglichen, werden betriebliche Freiheitsgrade benötigt, die aus verschiedenen Quellen stammen können.

In dieser Arbeit wird untersucht, ob und wie Anlagen in Verteilnetzen Flexibilität bereitstellen können, die für eine kurative Netzbetriebsführung genutzt werden kann. Dabei werden die Fahrpläne der verteilt installierten Anlagen so verändert, dass die daraus resultierenden Lastflussänderungen zu Entlastungen von Engpässen im Übertragungsnetz führen. Diese verteilten Anlagen können Stromerzeuger wie Windkraft- oder Photovoltaikanlagen sein, aber auch flexible Lasten, wie zum Beispiel Power-to-Heat Anlagen oder Wärmepumpen.

Zwei Kernfragen dieses Konzepts werden dabei analysiert: Erstens, gibt es in den deutschen Verteilnetzen genügend Flexibilität, um jene für einen kurativen Übertragungsnetzbetrieb zu nutzen? Und zweitens, wie kann ein Verteilnetzbetreiber die Flexibilität seines Netzes berechnen, die sicher bereitgestellt werden kann? Beide Fragen werden methodisch unabhängig voneinander bearbeitet, da es bei der ersten um eine Potentialabschätzung in zukünftigen Energiesystemen geht, bei der zweiten aber um die tatsächliche Anwendung in bereits real existierenden Stromnetzen.

Um die erste Kernfrage zu erforschen, wird ein Energiesystemmodell für Deutschland im Jahr 2030 erstellt und die verfügbare Flexibilität für den kurativen Übertragungsnetzbetrieb berechnet. Dabei werden Zeitpunkte ausgewählt, in denen ein Ausfall von Übertragungskapazität zu kritischen Zuständen im Netz führt und die verfügbare Flexibilität in den an den kritischen Korridor angrenzenden Regionen berechnet. Die Ergebnisse zeigen, dass insbesondere Power-to-Heat wertvolle Flexibilität in den Situationen bieten kann, in denen

Übertragungskapazitätsverluste zu kritischen Zuständen führen. Zusammen mit Flexibilität aus Windkraft reicht die von beiden Technologien bereitgestellte Leistung, um in 40 % dieser Situationen die Netzbelastung wieder auf sichere Werte zu reduzieren. In den übrigen 60 % der Situationen muss entweder die für eine kurative Netzbetriebsführung notwendige Flexibilität aus anderen Quellen ergänzt werden oder das Netz weniger stark ausgelastet werden.

Die zweite Kernfrage wird durch die Entwicklung eines schnellen und robusten Optimierungsansatzes zur Netzbetriebsführung ergründet. Durch die Optimierung werden die Flexibilitäten der einzelnen Erzeuger und Lasten so eingesetzt, dass ein sicherer Zustand im Flexibilität bereitstellenden Verteilnetz gewährleistet ist. Die hierbei hergeleitete analytische Lösung der Netzrandbedingungen die einen sicheren Netzzustand garantieren, kann als untergeordnetes Problem der Optimierung eingebunden werden, sodass ein großer Teil des Gesamtproblems bereits vor Optimierung berechnet werden kann. Die Robustheit des Ansatzes zeigt sich dabei nicht nur durch die garantierte Einhaltung von Randbedingungen, sondern auch durch ein stabiles Konvergenzverhalten. Diese Methode wird sowohl auf einem einfachen Testnetz als auch einem realen Verteilnetz erfolgreich getestet.

Diese Arbeit zeigt, dass Flexibilität aus den Verteilnetzen sowohl in den für den kurativen Netzbetrieb relevanten Größenordnungen vorhanden ist, als auch für einen solchen genutzt werden kann. Der hier entwickelte Ansatz zur Berechnung und Bereitstellung von Flexibilität kann auf realen Netzen zur Anwendung gebracht werden und bietet durch die inhärenten Robustheitsbedingungen die notwendige Sicherheit und Geschwindigkeit, um in einer kurativen Netzbetriebsführung genutzt zu werden.

Abstract

Operating power grids in the course of the ongoing decarbonization of energy systems is increasingly challenging. More and more decentral renewable energy sources are contributing to the supply of electricity and cause higher transport demands in the power grids. The necessary grid expansion is running behind schedule required to meet the targets of the Paris Climate Accords for reasons of social acceptance and high costs. Therefore, transmission system operators as well as regulatory authorities are investigating new approaches to enable higher network utilization. One way to alleviate the situation, is to shift from preventive n-1 safe grid operation to curative n-1 safe grid operation. To enable such a change, operational degrees of freedom are needed, which can stem from different sources.

In this work, the focus is on flexibility provided by distribution grids and how it can be used as an operational degree of freedom for curative grid operation. Flexibility allocated by adapting the schedules of distributed energy sources is provided in such a way, that the resulting power-flow changes relieve congestion in the transmission system. These distributed energy sources can be generators, such as wind-power or photovoltaic power plants, as well as flexible loads, such as power-to-heat plants or heat pumps.

Two key questions in the context of this concept are treated in this thesis: Firstly, is there enough flexibility in the German distribution grids to use those grids for curative transmission grid operation? And secondly, how can a distribution system operator calculate the flexibility of his grid that can safely be provided?

To answer the first question, an energy system model of Germany in the year 2030 is set up and available flexibility for curative transmission system operation is calculated. Time-steps are selected, in which a loss of transmission capacity leads to critical states in the grid, and the available flexibility in the regions adjacent to the critical corridor is calculated. Results show, that especially power-to-heat can provide valuable flexibility in situations where transmission capacity losses lead to critical states and, together with flexibility from wind-power, in 40 % of these situations the power provided by these two technologies is sufficient to reduce power-line loadings back to safe values. In the remaining 60 % of situations other sources must complement the flexibility necessary for curative operation or the utilization of the grid has to be reduced accordingly.

The second question is answered by the development of a fast and robust optimization

approach to limit the allowed ranges in power injection changes from individual energy resources in order to guarantee a safe state in the flexibility-providing distribution grid. The derived analytical solution of the boundary conditions that ensure a secure state in the grid can be integrated as a subordinate problem of the optimization, so that a large part of the overall problem can be calculated before optimization. The robustness of the approach is not only shown by the guaranteed compliance with boundary conditions, but also by a stable convergence behavior. This method is successfully tested on both a conceptual test grid and a real distribution grid.

This work shows both that flexibility from the distribution grids is available in orders of magnitude relevant for curative grid operation, and that it can be used for such operation. The approach developed in this thesis to calculate and provide flexibility can be applied to real grids and offers the necessary security and speed needed for curative grid operation due to the inherent robustness.

Contents

List of Figures

List of Tables

1. Introduction

The Intergovernmental Panel on Climate Change (IPCC) reports, that current levels of CO_2 and other climate gas emissions into the atmosphere will lead to catastrophic changes in the earth's climate [1]. Even worse, if so called tipping-points are crossed, changes in the earth's ecosystem become irreversible and a further loss of biodiversity and habitable land area is inexorable [2]. Therefore, it is imperative to remain inside the planetary boundaries [3], the limits for consumption and emissions set by our planet and its ecosystem.

One key step to remain inside these planetary boundaries is the transition from fossil fuel energy systems to such, that are shaped by renewable electricity generation. However, renewable energy sources (RES) are often sited further away from load centers than fossil fuel-fired electricity generators [4]. As a consequence, electric transmission demand is rising and novel approaches to better utilize existing and future transmission infrastructure are needed.

One such approach is curative n-1 safe grid operation, a concept that needs flexibility from different sources to properly function. In a curative grid operation, those transmission grid capacities, that currently serve as a buffer for unexpected malfunctions, are used for transmitting additional electric power. Their role to act as safety against outages is taken over by other assets which provide the necessary flexibility for such a change in grid operation [5]. The potential of flexible energy resources from distribution systems to constitute at least a part of the needed flexibility is evaluated in this thesis.

1.1. Motivation

Since over 150 years, the scattering effect of infrared light by CO_2 is known, and so are its impacts onto the atmosphere of our home planet [6]. Even earlier, in the 1820s, Joseph Fourier formulated his theory about the Greenhouse-effect [7].

Figure 1.1 shows the CO_2 concentration in the earth's atmosphere, displaying the so called hockey-stick curve [9]. From the early experiments of Eunice Newton Foote [6], John Tyndall [7], and Svante Arrhenius [10], it is known that CO_2 concentration in the atmosphere has a significant impact on the Greenhouse-effect.
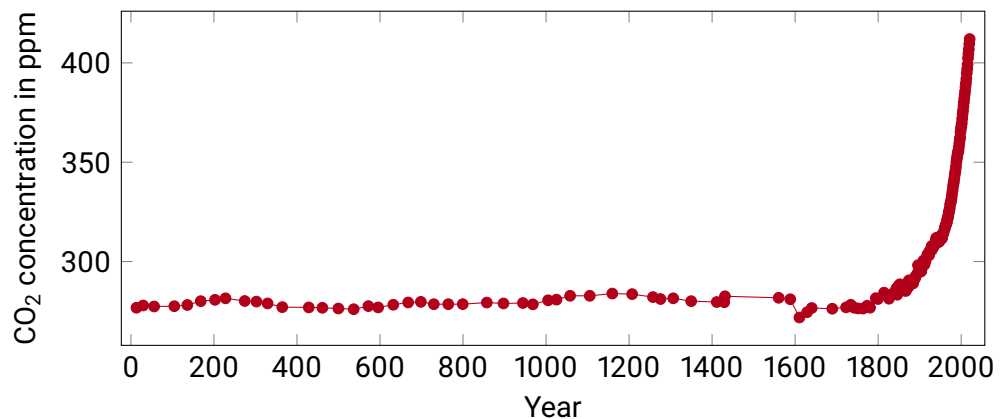
Figure 1.1.: CO_2 concentration in earth's athmosphere, reconstructed from ice core records and merged with atmospheric measurements, data from [8].

1.1.1. Role of the Energy Sector in Greenhouse Gas Emissions

The majority of CO_2 emission and emission equivalents stems from burning fossil fuel [11]. In Figure 1.2, the emission share of different sources are pictured, showing that coal, gas, and oil cause the greatest part of emissions.

The energy sector, using a large part of these resources to generate electricity and heat, is the sector responsible for the most emissions. In Germany, the emission share of the energy sector is 30 % [12]. Therefore, it is of special interest to reduce emissions from this sector, as it has the biggest impact. In addition, reductions in emissions are easier to achieve in the energy sector than in other sectors, as the technologies are not only readily available, but also most cost effective (see Figure 1.3).

1.1.2. Renewable Energy Sources to Supply Our Energy Needs

Known for a time almost as long as the Greenhouse-effect is the photovoltaic principle, discovered in 1839 by Edmond Becquerel [13]. First modern silicon solar cells have been invented in 1954 [14]. While their use was at first limited to specialized applications, as for example Vanguard 1, the oldest human made satellite still in space [15], since 2010 even in Germany alone, several Gigawatts were installed in new PV capacity each year [16]. These days, direct conversion of solar irradiation into electrical energy via PV is seen as one of the main power sources of the future, with costs lower than those for electricity from conventional, fossil fuel fired power plants [17]–[19].

2
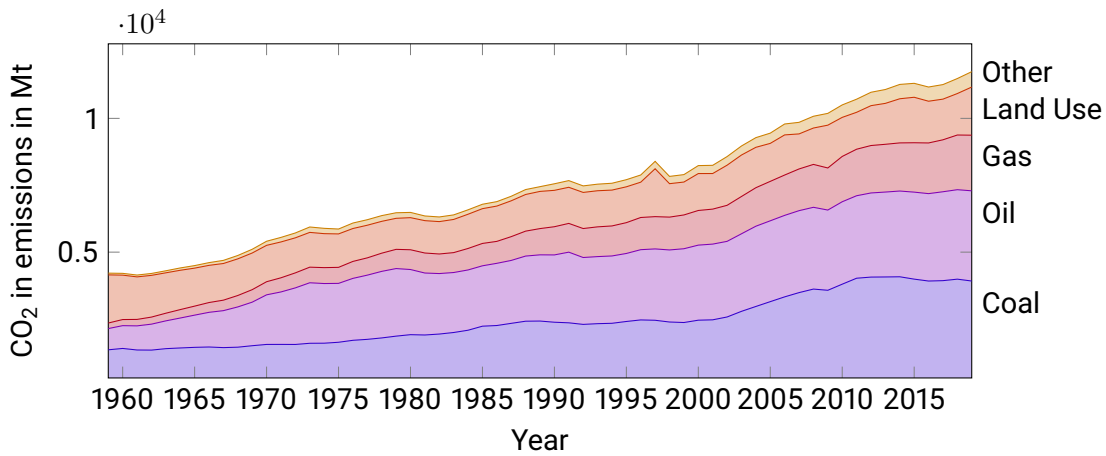
Figure 1.2.: CO_2 emissions in Mt by source. Land use change includes deforestation and drainage of wetlands. Data from [11].

The history of harnessing energy from wind goes back a long time, at least to 200 B.C., when Persians used wind mills to grind grains [20]. At least since 1887, modern wind mills, those that convert wind-power into electricity, are in use [21]. Similar to some people today, residents saw such technology as the devils work [21]. Not much later, in 1891, wind-power was even used to power electrolysis in Denmark for energy storage [22]. Denmark kept being at the forefront of the usage of wind-power, with the first wind-turbine of a power rating of over 1 Megawatt being constructed by the pupils and teachers of the Tvind school in 1978 [22]. Such power ratings were only used in production wind-turbines in the late 1990s.

However, even at the multi-Megawatt scales at which individual wind-turbines are being built, they are still small in comparison to the power plants which used to generate almost all of the electricity in our energy system. Typical nuclear, large coal and lignite-fired power plants have electrical power ratings of up to about a Gigawatt. Hydro power, also being one of the renewable energy sources, is not broadly available in many regions of the world and often carries great ecological costs [23], making energy systems dominated by renewables still an exception today. Due to the smaller size of wind-turbines and PV-farms and the corresponding power injections in the range of a few kilowatts to several Megawatts, those energy sources are often connected in lower voltage levels than fossil fuel powered plants. Typically, these lower voltage levels correspond to low voltage, 400 V (LV) and medium voltage, 3 to 35 kV (MV) distribution grids, while for larger farms high voltage, 60 to 110 kV (HV) sub-transmission or distribution grids are chosen as connecting grids [24]. This dispersion, in contrast to the concentration of power in transmission grids, is why these renewable energy sources are

often called distributed energy resources (DER) [25].

Since levelized cost of electricity of these distributed energy resources (DER) are decreasing, their installed capacity rises and is set to rise even further in the future [26], especially in countries that have set a political agenda to reduce CO_2 emissions like Germany [27]. Figure 1.3 shows the development of different renewable energy sources (RES) in terms of costs and installed capacities, outlining the development that has been done in the last decades. Such developments are often seen as trends, in this case it is often talked of three or four "D"s, decarbonization, decentralization, digitalization, and sometimes democratization to describe the changes in our energy systems.
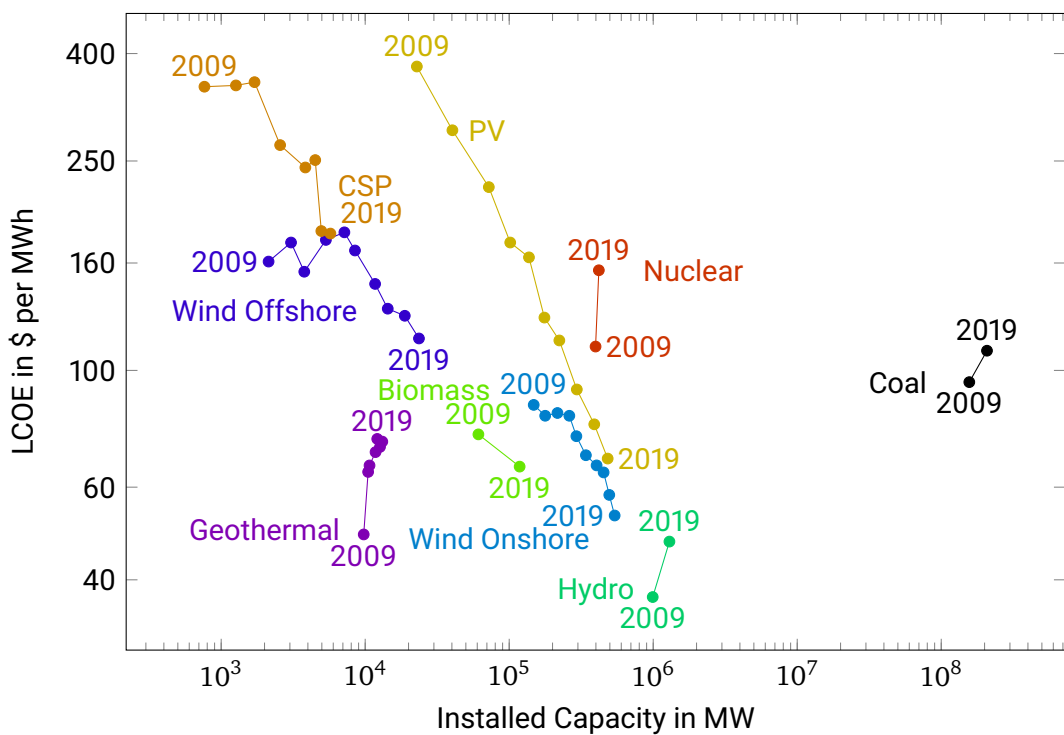
Figure 1.3.: Development of globally installed generation capacity and globally weighted LCOE. While renewable energy sources (RES) like photovoltaics (PV) or wind-power show strong downward trends for costs, coal and nuclear power remains have rising costs. Data for RES from [18], for nuclear and coal from [28], [29], inspired by similar graphic in [30].

1.1.3. Changing Generation Technologies Lead to Increasing Transmission Needs

Changes in energy systems are not only caused by shifts in production, but also by changes in consumption and regulation. In the EU, many of those regulatory changes in recent years are part of the EU Clean Energy Package, a set of EU directives aimed to increase energy performance in buildings [31], energy efficiency [32], renewable energy penetration in energy systems [33], and create an energy union [34]. The latter is of great importance for electricity markets and transmission, as it mandates a fully integrated internal energy market in the EU. It forces transmission system operators (TSOs) to better utilize transnational interconnectors and to enhance or expand their grids to comply with minimum requirements for these interconnectors. The EU commission has the right to split or reconfigure electricity market zones in the EU if countries do not comply. For the lower voltage levels, the Clean Energy Package also shifts rights to citizens to form renewable citizen energy communities to strengthen local value creation, leading to the already mentioned 4th "D" of democratization. Local markets are made possible by digitalization of DER, allowing distributed assets to exchange information and even to automatically bid on markets.

For distribution grids and their operators, the distribution system operators (DSOs), the EU Clean Energy Package and its implementations into national laws brought large changes, too. Not only are these DSOs part of biannual European network development plans, they also form a new association, the European distribution system operators (EU DSO Entity), similar to the existing European network of transmission system operators for electricity (ENTSO-E). They partake in redispatch, which is broadened to include renewable energy sources (RES) and combined heat and power (CHP). In Germany the Clean Energy Package is implemented in several laws, including the Netzausbaubeschleunigungsgesetz [35], the Erneuerbare-Energien-Gesetz [36], the Kraftwärme-Kopplungs-Gesetz [37], and the Energiewirtschaftsgesetz [38]. The process of including DERs of a nominal power of >100kW and those generators that are remotely controllable by their connecting grid operators into the redispatch is called Redispatch 2.0 [39]. This process changes the number of power-generating facilities that are subject to the redispatch process from about 80 to 80000 [40].

Most distributed energy resources (DERs) are not installed close to load centers unlike most conventional power plants, but at places that are favorable for electricity generation. These are locations with high irradiance for PV, or such that are especially windy for wind-turbines. In the EU, highest irradiances are in the southern countries, for example Spain, Italy, or Greece, while best conditions for wind-power can be found offshore and at the coasts, for example Ireland and Denmark. In addition to these natural conditions, population density and political factors can heavily influence the location where renewable DERs are installed, leading to a very inhomogeneous and more decentral distribution of electricity generation.

In Germany, most wind-power is installed in northern parts of the country[1], while for PV, the opposite is true, even though not in the same extent[2]. This inhomogeneity leads to rising transmission demands. As the electricity market in Germany is not divided into several zones and does not use nodal pricing, these transmission demands are directly translated into a need for more transmission capacity. Otherwise redispatch costs, costs that are caused by a mismatch in market result and transmission capacity, keep rising [43]. To account for these rising transmission demands, the TSOs together with their regulatory authorities develop so called network development plans, for example the ten year network development plan (TYNDP) and midterm adequacy forecast (MAF) on European level, and the Netzentwicklungsplan (NEP) on a national level in Germany. After consolidation, these plans are turned into individual construction projects. However, in this last stage the grid expansion is lagging behind plans [44], [45], mainly due to complex planning phases which often include several legal disputes. These delays were one reason for the German Netzausbaubeschleunigungsgesetz (grid expansion acceleration law) [35], trying to accelerate the processes that otherwise might hinder a successful energy transition.

The delays in transmission grid expansion has the potential to limit the integration of renewable energies. As a consequence, fossil fuel powered energy sources have to produce electricity, while simultaneously renewable energy that is available cannot be injected into the grid. In order to counter this phenomenon, several approaches exist. Since transmission grid operation and electricity market processes are intertwined, a short description of the electricity market in Germany follows.

1.1.4. Electricity Market and Transmission System Operation in Germany

There are several different types of electricity markets being operated worldwide. In general, they all bring the market participants' bids and offers to match. One of the main differences in market design is how the costs of transport and losses are attributed to the price of electricity.

In the European Union and some neighboring countries[3], TSOs are associated in the ENTSO-E, coordinating the operation of transmission grids for electricity. In the area where transmission grids are operated by the member-TSOs, the bidding zones, in which bids and offers are matched, span over hundreds of nodes. Inside one of such bidding zones, transmission capacities are assumed to be sufficient. If transmission constraints are present, a redispatch is performed. Redispatch is a process in which TSOs instruct power plant operators

---

[1]In 2021, only about 7 % of the total wind-power capacity of Germany is installed in Baden-Württemberg and Bavaria which have a combined area share of almost 30 % [41].

[2]In 2021, about 41 % of the total PV capacity of Germany is installed in Baden-Württemberg and Bavaria [42].

[3]Albania, Bosnia and Herzegovina, Switzerland, United Kingdom, Iceland, Montenegro, Republic of North Macedonia, Norway, and Serbia

to change their power injections to relieve congestion in the grid. In the EU, if bidding zones display structural congestion, they can be split [34].

In the ENTSO-E-area, large parts of the electricity trade is accomplished at or before the day-ahead market closing, which happens at 14:30 each day. Grid operators, however, start planning their operations long before, since some reserve power plants can take up to a week in preparation to partake in the operation. In the week-ahead planning process (WAPP), demand and renewable energy production forecasts are taken into account, to determine how much and when reserve power is needed. This is done on national and international levels, to gain an estimate how much transmission capacity will be available on the interconnectors. After day-ahead market closing, a good estimate of all demands and generation schedules in hourly resolution is available. With these estimates, TSOs perform the preventive redispatch. In this step, the market result is turned into a power-flow calculation, showing TSOs if a safe and reliable operation is possible. If not, a redispatch is performed. In addition, TSOs need to buy energy to balance expected transmission losses. Redispatch and balancing power costs are distributed across grid users of each bidding zone. Figure 1.4 shows the relevant planning processes on European and national level.

In other electricity markets[4], transmission constraints are included in the matching process by introducing marginal prices calculated by a security constrained optimal power flow (SCOPF), resulting in so called nodal prices [48]. These are prices that can differ for each node or bus in the grid. In theory, nodal prices can counter lagging grid expansion by incentivizing local electricity production and thereby reducing transmission demand. However, if nodal markets only have few market participants at each node, the liquidity, e.g. the simultaneous interest in buying and selling, may be too low for a functioning market. Therefore, in [49], a split into two bidding zones has been evaluated as an optimal for Germany. This is not desired politically [50], since it would probably lead to higher costs of electricity in the southern federal states. However, the EU commission will start a procedure to split Germany into two bidding areas, if the structural congestion in north-south direction is not remedied [34], [51].

---

[4]For example large parts of the USA [46], [47], and New Zealand[48]

	Preventive Redispatch Processes	Capacity Calculation Processes
2 Day-Ahead	08:30-09:30 Week-ahead planning process (WAPP), optimizing demand for reserve power plants up to 7 days ahead, twice a day 11:30-12:30 WAPP 2, same calculation as in WAPP for a second time	16:00-19:00 Day-2 congestion forecast (D2CF), grid analysis without knowledge of market 19:00-08:30 Day-ahead congestion calculation (DACC), calculating grid capacities for the international market
Day-ahead	14:30 Day-ahead market closure 16:30-17:30 Preventive Redispatch 1 (pRD1), same as WAPP but with knowledge of market 18:00-22:00 Day-ahead congestion forecast (DACF) to calculate a European common grid model (CGM) for each hour	20:00-22:00 Intra-day congestion calculation (IDCC), calculating additional international grid capacities (NTCs)
Business-Day	From 00:00 Intraday congestion forecast (IDCF), calculating CGM not necessarily free of bottlenecks, coordination of measures by TSCNET (regional security coordinator) From -1 h Close to real-time operation (C2RT) Realtime Corrective regime	

Figure 1.4.: Timeline of the market and grid operation planning processes in the ENTSO-E. In curative operation, planning processes are the same, but curative redispatch is performed in realtime.

1.1.5. Curative Grid Operation to Increase Grid Utilization

As grid expansion in Germany is lagging behind the increasing need of transmission capacity [45], regulators and government started looking for alternative and additional approaches to increase the capacity of the transmission grid. One such approach is the shift from a preventive n-1 safe operated system, to one which is curative n-1 safe.
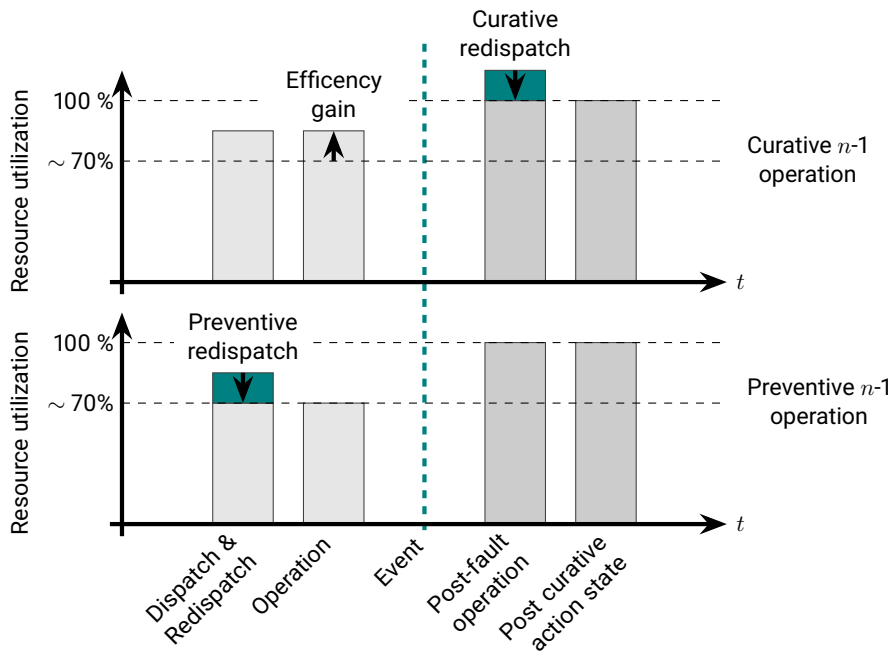
Figure 1.5.: Preventive and curative operation: In preventive operation the utilization of an arbitrary power line might be reduced to ensure an inherently safe post-fault operation. In curative operation preventive redispatch is omitted or reduced, resulting in an efficency gain. Sufficient flexibilities have to be present to perform a curative redispatch in case of an equipment malfunction, here displayed as the vertical dashed line. In the post curative action state restoring remedial actions are needed to return to a n-1 safe regime.

Currently, the basic principle how reliability is guaranteed in most transmission grids is by applying the preventive n-1 principle. This means, that the TSO takes care to establish a state in which one of n pieces of operating equipment can fail without causing overloading

or violation of operating limits on any other piece of equipment. The grid is then n-1 secure[5]. For example, given a simple grid of two buses and two parallel power lines between them, to be operated n-1 secure, both lines have to be operated at maximum 50 % of their nominal capacity. If one line fails, the other can take the extra transmission loading without being overloaded. In a meshed grid such as typical transmission grids, this threshold of 50 % moves upward to a value closer to 70 %. TSOs keep contingency lists to gain an overview over all possible contingencies and an additional list of restoring remedial actions, to be ready for equipment malfunction during operation.

In order to achieve a power-flow in the grid that allows for a preventive n-1 operation, the schedules of power plants might need to be adapted in the redispatch process, as outlined in Figure 1.4. The more congestion there is in the grid, the more the TSOs need to intervene, and the higher are redispatch costs. Figure 1.5 shows this process in the lower half on the left, where average resource utilization is reduced.

The idea behind curative n-1 operation is to increase the resource utilization of the grid, reducing preventive redispatch, and, in case of an equipment failure or critical outage, have sufficient flexibility to reduce the power-flow on the critical branch before operational boundaries are violated. At all times when there is no equipment malfunction, resource utilization is higher, allowing more transmission to take place at costs of higher losses[6] and operational complexity. It is absolutely imperative, that sufficient curative remedial actions are ready during curative operation to guarantee a reliable electricity supply and that restoring remedial actions are also available to return to a n-1 safe state after the curative remedial actions. The general concept of curative operation and its efficiency gains are displayed in Figure 1.5.

To evaluate the potential of curative n-1 transmission grid operation in Germany, the InnoSys 2030 consortium [52], a multi disciplinary research initiative, was established by the four German TSOs, a few DSOs, universities, research facilities and industry. In this consortium, a first concept was developed, how curative operation can be put into production [53].

In this context, it is important to distinguish between the terms "preventive", "reactive", "corrective", and "curative". While the difference between "preventive" and "curative" is explained above, the terms "reactive" and "corrective" have not yet been mentioned. While the term "corrective" is often used synonymously to the term "curative", some people or corporations in the area of TSOs use it in the sense of restoring remedial actions, a measure to return to a n-1 safe state, while others use it as a preventive action, for example a change in topology. In the case of the term "reactive", there is also ambiguous use: In [54], the term

---

[5]For a more detailed definition, see N-1 principle in the Glossary.
[6]As currents rise with the transmitted power, ohmic losses also rise

"reactive" is used like the term "curative" is used in the scope of this thesis, while some DSOs use it as the reaction to an unexpected event, for example for feed-in management.

In this thesis, the term "curative" is used in the sense of curative remedial actions as defined by [5] A4-D1.2.:

> **Definition 1: Curative Remedial Action**
>
> Remedial action refers to any measure applied in due time by a TSO in order to fulfill the n-1 security principle of the transmission power system regarding power-flows and voltage constraints. *Curative* remedial actions are those needed to cope with and to rapidly relieve constraints with an implementation delay of time for full effectiveness compatible with the temporarily admissible transmission loading (TATL). They are implemented after the occurrence of the contingencies TATL.

There are different technologies that can be used to provide operational degrees of freedom to the TSOs in order to enable curative operation. These can be the TSO's operating material, like high voltage direct current (HVDC) systems, phase shifting transformers (PSTs), or especially developed assets for curative operation, like grid boosters, or flexible energy resources in distribution and transmission grids [53], [55]. These different technologies and their key parameters are listed in Table 1.1.

Table 1.1.: Different options for curative remedial actions and their key indicators, compiled and discussed in the InnoSys consortium [52].

Measure	Activation Time	Mode of Action
Grid Booster	<1 s	Strategically positioned energy storage to either quickly and controllably inject or withdraw power from grid. If realized as a battery, storage capacity allows 15-30 minutes of power injection or withdrawal. Planned power ratings range from 50 to 500 MW.

Measure	Activation Time	Mode of Action
High voltage direct current systems (HVDC)	<1 s	HVDC systems can transport active power between their inverter stations. If the HVDC is realized as a voltage source converter (VSC), reactive power can be supplied at inverter stations. Due to their controllability and large control area, HVDC systems can quickly and continuously alter power-flows over large areas of the grid. Planned HVDC systems in Germany have a power rating of 2 GW. Since the direction of the power-flow can be chosen, this results in a flexibility of ±2 GW per system.
Impedance compensation	<1 s	By changing the capacitance of a power line, the power-flow over said line can be altered. This can be done with fixed capacitors or variable capacities, as for example with a thyristor-controlled series compensator (TCSC) or static synchronous series compensator (SSSC).
Phase shifting transformer (PST)	<1-20 s	PSTs can shift voltage angles and thereby alter power flows in the grid. They introduce a source of controllability and can be used to align the utilization of several power lines, increasing the total transmission capacity of the grid. If the PST uses mechanical switches, each voltage step takes about 3-5 s to switch, while also leading to a reduction in equipment lifetime.
Topological switching	3-60 s	Topological switching alters the routes the electricity can take through the grid. Electrical meshes or loops can be opened or closed by circuit breakers, relieving or adding power-flows to different power lines.

Measure	Activation Time	Mode of Action
Power to heat (P2H) and power to gas (P2G)	1-100 s	P2H and P2G plants are facilities that use electricity to generate either heat or synthetic gases. While P2G plants currently need many full load hours (flh) to be operated profitably, P2H plants often improve their profitability from their property of being quickly dispatchable loads. In case of congestion, these assets can be switched on or off for a relatively small compensation due to their low CAPEX and OPEX. Central P2H plants have power ratings from 5 to 150 MW.
Conventional redispatch	>300 s	Redispatch from conventional electricity generation sources provides the most power, but is slow. The fastest sources here are gas engines, which are only available in the ∼10 MW range. Single cycle gas turbines offer power gradients of up to 15% of their installed capacity per minute, taking 300s to reach full power [56]. Depending on the individual power plant, nuclear, coal or lignite fired power station can take longer. In addition, in many countries, a coal phase-out is already underway.
Reduce offshore wind-power	<20 s	Offshore wind-power in Germany is mostly connected via HVDC connectors. These are in the direct control of TSOs, making the reduction of injection fast and reliable. To balance the missing power injection, other generation has to be acquired on the opposite end of the congestion. Offshore wind farms reach installed capacities of up to 1 GW.

While curatively usable measures like grid boosters, PSTs, or FACTS elements[7] need to be built by grid operators, with their costs being spread across grid users, energy resources are paid for by market participants directly in order to use them for generating electricity or other commodities from electricity, for example heat in the case of P2H. In some cases, these resources are already existing and can gain additional revenue if they provide flexibility.

---

[7]These include SSSCs, TCSCs, and STATCOMs.
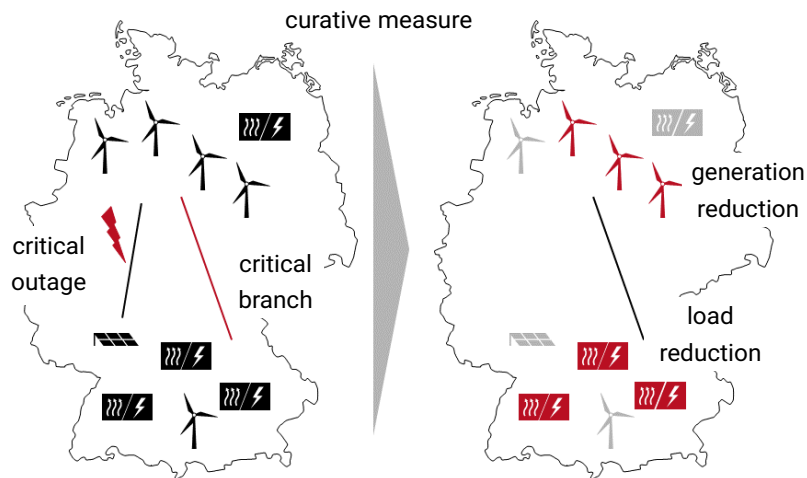
Figure 1.6.: Usage of distributed flexibility to relieve a congestion in the transmission grid. After a critical outage on the left transmission line, a parallel line becomes the critical branch. A reduction of generation in the north and of load decreases the line loading on the critical branch.

1.1.6. Distribution System Flexibility for Curative Operation

In Table 1.1, different technologies that can be used to provide flexibility for a curative n-1 safe operation are listed. Each one of them can be used as either as primary source of flexibility, being scheduled for a contingency, or as collateral, in case the primary source is not available. The same is true for flexibility from distribution grids. In the following, the general concept to use such flexibility is illustrated.

In a situation with a high share of electricity generated from RES, electricity has low energy-dependent costs, and many flexible loads will make use of it. Such a situation can coincide with great transmission need, for example on windy winter days when the transmission grid is operated at maximum capacity. As a consequence of a contingency, for example the outage of a transmission line, the n situation becomes the n-1 situation. To relieve the congestion on the critical branch, flexible loads on the south of the congestion reduce their electricity consumption, while RES in the north lower their feed-in.

These flexible loads are mainly connected in distribution grids, therefore the problem remains, that the TSO, in whose grid the congestion happened, has to know how much flexibility is present before the critical outage happens. Therefore, DSOs need to continuously run a flexibility aggregation algorithm in the background and communicate the values for

upward flexibility, that is a reduction in load or increase in generation, and downward flexibility, an increase in load and reduction in generation, to the relevant TSO.

As displayed in Figure 1.6, during the *n*-1 situation, the TSO requests the flexibility, upward flexibility in the south, and downward in the north, from the DSOs. Slow flexibility sources are activated as restoring remedial action, enabling to return to a new *n*-1 safe state. Some DER are unaffected, for example loads in the north and generation in the south, and therefore greyed out in Figure 1.6.

Instead of directly requesting distribution system flexibility, TSOs can also reduce offshore wind-power injections and use grid boosters, only using distribution system flexibility as replacement measure. Even if the flexibility is never requested, it can serve as a collateral security, both in preventive and curative operation.
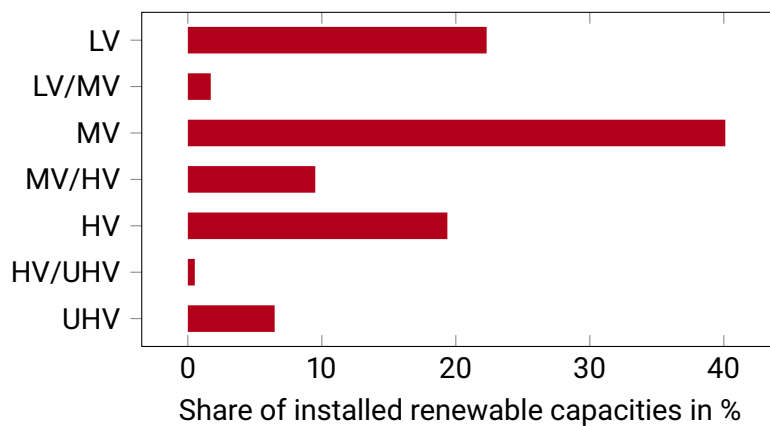
Figure 1.7.: Distribution of renewable generation capacities as a function of voltage levels in Germany. Voltage levels are ultra high voltage, $\geq 220\,\text{kV}$ (UHV), high voltage, 60 to $110\,\text{kV}$ (HV), medium voltage, 3 to $35\,\text{kV}$ (MV), and low voltage, $400\,\text{V}$ (LV). HV/MV means, that the DER is connected in MV, but directly to the next HV station via a HV/MV transformer. Numbers from [24].

Figure 1.3 depicts the global development of installed renewable capacities. In Germany, the same development is happening, shifting a rising proportion of the installed capacities towards RES. As can be seen in 1.7, these RES are being installed mainly (93 %) in the voltage levels of the distribution systems, forcing developments like Redispatch 2.0 [39] to integrate these large numbers of energy resources into grid operation procedures.

Using this distributed generation [25], [57], [58] as a source of flexibility therefore seems to be an obvious choice, if inherent challenges, like the control of several hundreds or thousands of energy resources while remaining in a safe grid state, can be overcome. In addition to

generation, this is also true for controllable loads, which are also assumed to increase in numbers, as heat-pumps, electric vehicles, and central power-to-heat plants enter the markets.

In this thesis, the word flexibility will be used mainly in combination with energy resources, while for HVDCs, FACTS, or PSTs, the term operational degrees of freedom are used, as these assets are in direct control of the grid operators. This reduction in scope of the word flexibility is not exotic in any matter, but in accordance with [59], [60]. The existing scientific literature in this area provides very general definitions, for example [61] defines flexibility "as the potential for capacity to be deployed within a certain time frame." In [62] and [63], definitions are even less specific, as it is seen as "the ability of a power system to cope with variability and uncertainty in both generation and demand". As this thesis focuses on flexibility from distribution systems, its definition follows [64]:

Definition 2: Flexibility

Flexibility of an energy resource is its ability to deviate from its uninfluenced state and to change power feed-in or load upon request. To offer flexibility to a grid operator, the energy resource will communicate an uninfluenced reference feed-in profile together with maximally available upwards and downwards deviations from the reference profile. This deviation is both in active and reactive power.

The flexibility-requesting and flexibility-providing grid operators not only need to know the amount of flexibility, given in units of megawatt and megavar, but also the activation time. This activation time is given by the power-gradients that are mandated and tested in the process of connecting a new generator to the grid or qualifying a flexible load. In German distribution systems, the admissible gradients are normed and given in the VDE AR-N 4120 for HV-grids and VDE AR-N 4140 for MV-grids [65], [66].
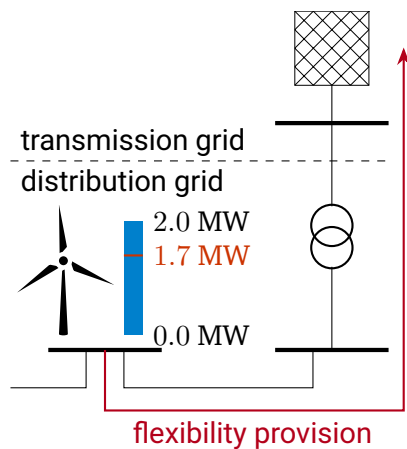
Figure 1.8.: A partly curtailed wind-turbine in a distribution grid providing flexibility that can be used in the transmission grid. Here, the setpoint is at 1.7 MW, with the potential to provide these 1.7 MW as downward flexibility and 0.3 MW as upward flexibility. The dashed line denotes the grid interconnection point (GICP) which seperated the transmission from the distribution grid.

1.2. Objective and Scope

The objective of this thesis is to quantify the value and enable the usage of distribution system flexibility for curative transmission system operation. In the scope of this work, all electrical transmission systems with voltages of 110 kV and lower (HV, MV, LV)) will be called distribution grids in accordance with [58], since they distribute the power regionally in contrast to the inter-regional transmission in transmission systems, which operate with voltages of 220 kV and higher (UHV) [58]. However, even if all the HV, MV, and LV-grids are distribution grids, the focus in this work lies on the HV grids, which are in the direct control of the first-order distribution system operator (DSO). This scope of the work allows to cover flexibility for curative use. Every additional voltage level adds complexity, new operational boundary conditions, and, depending on the local regulations and history, also additional DSOs. This makes it even harder to quickly provide flexibility from LV grids when needed.

The Redispatch 2.0 [39] regulations in Germany force all DSOs to partake in preventive redispatch processes starting 01.10.2021, establishing the communication technologies also necessary for curative operation. This is a shift in the responsibilities of DSOs, whose original task only was the distribution of electricity mainly generated in large plants connected to UHV. As electricity generation by RES shifts power injections into distribution grids, the scope of tasks expands for DSOs. In terms of controlled energy resources, the mode of operation now more resembles that of a TSO in the last decades.
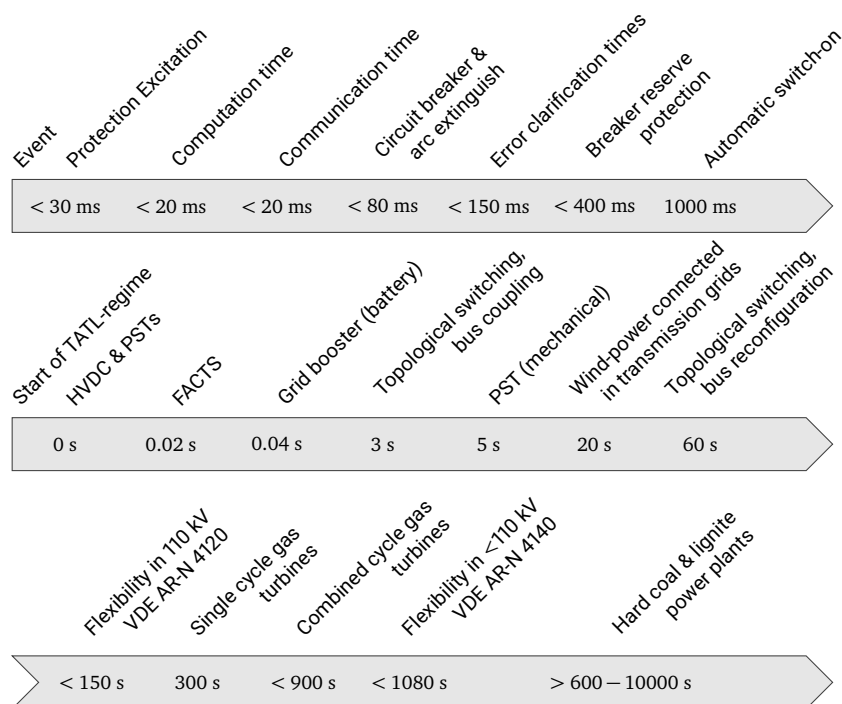
Figure 1.9.: Timescales in curative grid operation after a malfunction. Topmost arrow describes timescales after a critical outage or malfunction event until the source and scope of the error is known. The following arrows start their timings at this point in time, right after the knowledge of the system is complete. All timescales stem from experts in the InnoSys consortium [52].

1.2.1. Timescales in Curative Operation

Figure 1.9 depicts that DSOs of 110 kV grids in Germany can have their energy resources completely (0-100 % or 100-0 %) adjusted in less than 150 seconds, while DSOs of MV-grids might need 18 minutes or 1080 seconds. This difference in time is due to regulatory requirements (VDE AR-N 4120 vs. VDE AR-N 4140) and the use of ripple control receivers instead of RTUs. This holds specifically true for Germany, but in general also for other countries due to increased communication demand if several DSOs are involved.

These timescales are somehow meaningless if the appropriate reaction times during a contingency are unknown. If a reaction is only needed half an hour after an event, flexibility

from households or even old fossil fired power stations can be a relevant source. To get an idea of the time that is left to react, the so called temporarily admissible transmission loading (TATL) and permanently admissible transmission loading (PATL) are important. These describe the admissible power-flows over a branch in the grid and are mostly given in Amperes, since the limiting factor is the thermal expansion of the conductor resulting in sag, caused by ohmic resistance, which is a function of the current. The thermal expansion is also dependent on the surrounding temperature, solar irradiation, and wind speeds, which influence the thermal equilibrium of the conductor. If the sag of a power line becomes too large, safety margins governed by the voltage level and admissible field-strengths at ground level are violated, making it possible to cause a ground fault resulting in a further loss of transmission capacity and might even endanger bystanders life or health. Special high temperature low sag (HTLS) conductors can reduce this phenomenon, but require costly refitting of power lines, which then fall under newer regulation [67], in turn leading to time intensive approval procedures.

Dynamic line rating (DLR) is using observable properties like temperature and wind speed to calculate both PATL and TATL in dependence of the power-flow over the line element. In winter, for example, temperatures are colder and it might be windier, which leads to higher admissible currents or power-flows, leading to a higher PATL and TATL. The TATL is always very strongly conditional of the initial operation conditions of the line [5]. The TATL of the critical branch is the most important one, since it defines the timescales for all curative measures (by definition, the critical branch is the one dictating timescales, since it is closest to failing due to its operational state).

It is important to stress, that the use of TATL does not mean an overloading of any equipment is happening. Only admissible power-flows are transmitted, harming neither any human, nor the environment, nor any equipment. The operation remains inside the operating limits at all times, otherwise overload or short-circuit protection will be triggered. The tripping current is never reached or exceeded if a curative remedial action is performed to plan.

If the critical branch is relieved only in parts because the first set of curative remedial action is not sufficient to achieve a relief strong enough to reach the PATL on all lines, those actions can still be helpful by reducing power-flows over the critical branch and increasing the TATL, as can be seen in Figure 1.10. Here, the first action is done just in time to gain leeway for a second measure that reduces the current back to the PATL. The sooner after an equipment failure an action happens, the more thermal inertia remains for further measures. Of course, this is also true for the effectiveness of a measure: the more an action reduces the current on the critical branch, the better.

In the InnoSys consortium [52], it was decided to simplify this smooth process into three steps defining the time intervals after which the different measures are active. These intervals are:
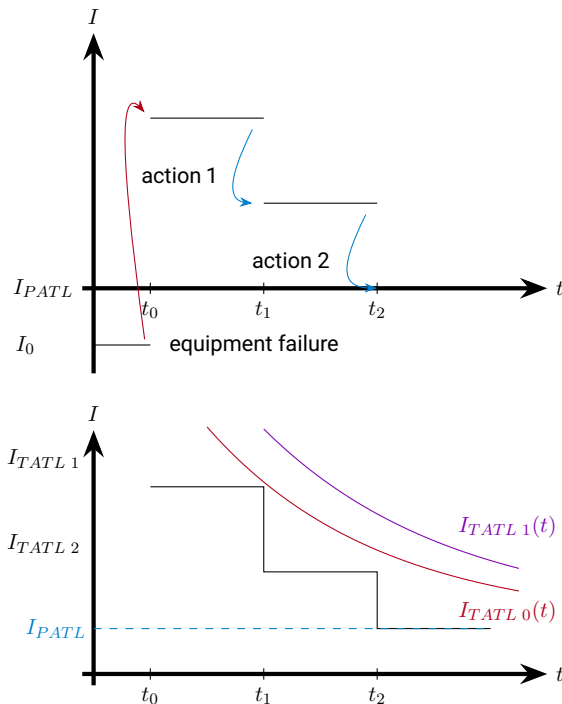
Figure 1.10.: Effect of curative actions on the TATL at the critical branch. In the upper half, two actions at time t_1 and t_2 lower the current on the critical branch back to the PATL after a critical equipment failure at t_0. In the lower part, the time-dependence of the $I_{TATL}(t)$ is depicted in red and purple, displaying that i.) the longer a current is needed to be above I_{PATL}, the lower it has to be, and ii.) fast measures flatten the $I_{TATL}(t)$ curve. For short time intervals, the T_{TATL} can be very high due to thermal inertia. Graphic redrawn after original work in the InnoSys consortium [52].

1. very fast, < 1 s

2. fast, < 2 min

3. slow < 15 min

The measures in category 1 are faster than the grid control center. As a consequence, activation must be independent of the control center, while other measures can be either activated via the grid control, even with human oversight, or directly via special protection schemes (SpPS), which are predefined measures or combinations of such that are automatically activated when certain protections trigger, e.g. a combination of circuit breakers or overload protections. The control center gets updated values via SCADA every five seconds, another five seconds go by until all other grid operators get informed (via telecontrol application service element (TASE) 2.0) by the one operating the failed equipment.

Figure 1.11 shows the structure of data exchange between the different levels in grid control. The control instance that is highest in the hierarchy, the control center, is also the slowest, as it accumulates data from many substations, which in turn collect data from measurement equipment at the substation or via a remote terminal unit (RTU) that is connected

to measurement equipment. In case of a short circuit, this path is too slow to control circuit breakers from the control center. Therefore, decentral protective relays, logic controllers, and fault recorders are used to directly trigger protections, if the measurement data they receive provokes the pre-programmed logic. All events in the first row in Figure 1.9 are happening on this level of control. For special protection schemes (SpPS) that use wide-area monitoring, data from other substations might be used and is received via RTUs.

State estimation, the process in the grid control center that homogenizes all measurement data into a consistent picture of the grid, can take about one minute to converge, shorter for simpler grids, and longer for larger grids or inconsistent measurement data. This means, that most measures need to be pre-planned, pre-computed, and ready to be implemented right when the error is clarified[8], to return to safe operating states on all equipment as quickly as possible. To make sure that all measures are available when needed, computations have to be performed continuously in the background in short cycles.

In order to use flexibility from distribution grids, the process might look like the following:

1. An equipment malfunction occurs. After the automatic switch-on fails, the SpPS trigger the grid booster.

2. After about 5s, the grid operator at the TSO control center receives the information on the error and the triggered grid booster. The operator now has about 2 minutes, until the TATL is exceeded.

3. The control center suggests to call for distribution system flexibility, because it identified the correct entry from the contingency list and offers options from the pre-computed reaction matrix.

4. The TSO enables the suggested measure and a request for flexibility is sent to the corresponding DSOs.

5. A few seconds later, in the DSO control centers, the request is displayed to the DSO's operator in his control center.

6. The DSO releases the call, the command is sent to the RTUs connected to the DER via the distribution system substation automation or via the DER's control center, if it exists. At the same time, the operator acknowledges the execution to the TSO.

7. The DER adapt their power injection.

---

[8]Error clarification is the process to determine the type of the error, e.g. a singlepole short circuit or a ground fault. It is performed after error detection.

8. The DSO operator receives data from his substations, confirming the change in power injections. The TSO is informed that the measure has been executed.
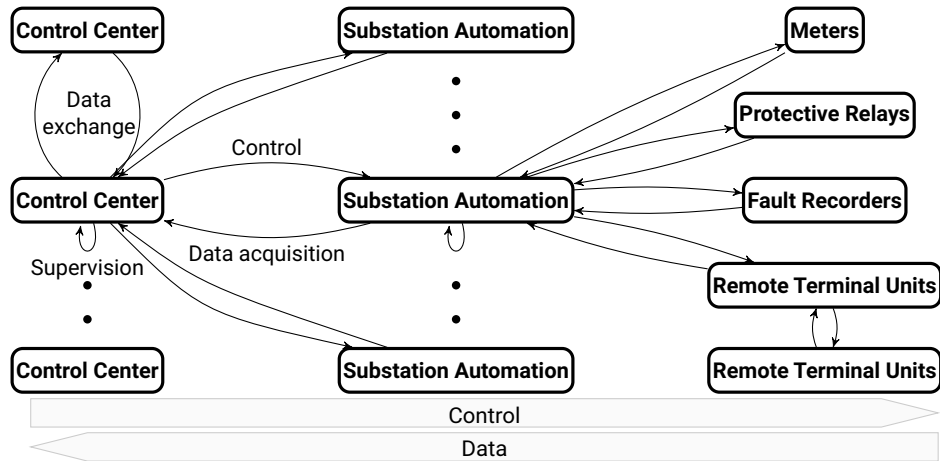
Figure 1.11.: Schematic structure of the cascading structure how the control center, substation automation, and substation automation controlled hardware interact. Supervisory control and data acquistion (SCADA) is used on each level to obtain data, supervise the state, and control subordinate devices. The next level in this graph would be operating equipment like circuit breakers, switches, disconnectors, tap changers,PMUs ,RTUs, and further equipment to measure and control the power-flow in the grid.

1.2.2. Key Challenges in Distribution System Flexibility Provisioning

Provisioning of flexibility from distribution grids therefore meets several key challenges:

1. Is it available when it is needed? To guarantee the same reliability as preventive n-1 operation, operational degrees of freedom must be certainly available. If this operational degree of freedom is flexibility from distribution grids, it must be evaluated if generation or load is indeed ready to be adapted and such in a controllable way within consistent reaction times.

2. Can it be guaranteed, that the aggregated flexibility of all the flexible assets does not interfere negatively with grid operation on any voltage level, especially in the grid of the connecting grid operator?

3. Can this process of aggregating safe flexibility be performed in sufficiently short timescales dictated by TATLs and variance from RES?

4. How can the amount of aggregated flexibility that is provided and called for be correctly communicated in complex grid topologies with several grid interconnection points?

These challenges can be condensed into two research questions:

> **Research Questions**
>
> 1. Are flexible assets in distribution grids a viable source of flexibility for curative transmission system operation?
>
> 2. How can flexibility from underlying grids be safely and quickly aggregated and offered for curative use?

These are the two research questions treated in this thesis. As they provide more than enough substance for a doctoral thesis, the following sub-areas will not be processed in detail and are left for further research:

- Technical implementations of flexibility provisioning, including details pertaining SCADA systems, control via RTUs or similar technology.

- TSO command center applications and integration. While the objective of this thesis is provisioning of distribution system flexibility to TSOs, the TSO's planning processes and operation procedures are not part of it, neither are the command center applications like security constrained optimal power flow (SCOPF) or dynamic security assesment (DSA).

- Dynamic assessments of security are not examined, as this goes beyond the scope of the thesis and the researchers' abilities.

- Other sources of flexibility, namely those listed in table 1.1, and their potential in curative operation.

- Flexibility markets for either individual or aggregated flexibilities.

- Preventive usage of distribution system flexibility, even though evaluation is possible with the same approach, as the focus lies on different aspects in preventive operation.

- Grid planning. Even though the approach and algorithms developed in this thesis can be used to identify bottlenecks in grids, this is not part of the thesis.

- Regulatory aspects or market designs to counter congestion in transmission or distribution grids.

- Detailed analysis, which assets are best suited for distribution grid flexibility in terms of of inertia or generator designs outside the applicable norms VDE AR-N 4120 and 4140.

- Different communication protocols or data standards to exchange information between TSOs and DSOs.

- Demand side management as a means to increase flexibility ranges apart from flexible DERs that are designed to provide flexibility to grid operators as part of their business model.

- Approximations of the number of flexible assets. While answering the first research question, this thesis takes data provided by German grid operators as ground truth without additional approximations how many more or less flexible assets might exist in the year 2030.

- Transformation paths of the modeled energy system. While the optimization framework used in this thesis is able to model transformation paths, this is out of the scope and not part of this thesis.

The two research questions, while thematically linked, are methodically far apart. Especially the details needed in the modeling of grids in both questions are different. Therefore, in addition to the partitioning into Analysis, Modeling, Method, and Results, this thesis is also split into two parts, each one addressing one research question as shown in Figure 1.12.

| Concept and goal: make flexibility from distribution grids available for corrective transmission system operation |

Quantifying flexibility potential from distribution grid flexibility for corrective transmission grid operation:

- Energy system modeling

- Identification of critical timesteps via simulated redispatch

- Identification of critical corridor loadings via simulated loss of transmission capacity

$\Rightarrow$ Determine if flexibility from distribution grid has a potential for curative grid operation in an energy system dominated by renewable energy sources.

Implementation and demonstration of algorithms to reliably offer and request flexibility:

- Interface between DSO and TSO control center to calculate aggregated and safe setpoints

- Safely and quickly disaggregate request on single assets

- Use of robust optimization to reliably be able to calculate safe flexibility limitations

$\Rightarrow$ Usage of a flexibility service agent on a grid to show distribution system flexibility can be used in curative grid operation.

| Potential and implementation of distribution grid flexibility for corrective grid operation is determined, tested, and demonstrated |

Figure 1.12.: Structure of the thesis. Research questions are answered in methodically largely independent parts.

Table 1.2.: Structure of the thesis.

	Research question 1.	Research question 2.
Introduction	Motivation, introduction of key terms and concepts, definition of the scope, research questions, literature review, and research gap.	
Analysis	What is necessary to calculate the potential of distribution system flexibility? What are the features an energy system model needs to exhibit to determine if distribution system flexibility is a viable degree of freedom for curative grid operation in energy systems dominated by renewables?	What are the properties an algorithm needs to produce for calculating safe aggregated flexibility? How can algorithms guarantee a safe grid operation while minimizing flexibility limitations?
Modeling	Framework for energy system modeling, outlining of modeling assumptions, and input data.	Distribution grid modeling and power-flow calculation. Linearization of power-flows.
Method	Calculation of the distribution system flexibility potential via two approaches: simulated redispatch and correlation of bottlenecks with available assets.	Introduction of the flexibility cluster and application of robust optimization onto the calculation of safe flexibility aggregation.
Results	Total distribution grid flexibility potential for curative transmission grid operation in Germany in dependence of the boundary conditions	Applicability of linearization, demonstration of the robust optimization approach on a test grid and a real grid
Conclusion	Discussion of the results, neglected aspects for further research, outlook.	

1.3. Literature Review

This part of the thesis analyzes scientific literature in the area of calculation of distribution system flexibility potential and how it is best provided in curative transmission system operation. Some research has been done that only touches one part of the research question, so either estimating the potential or discussing the provisioning, while others are looking at both aspects. Therefore, part of the literature review is not cleanly cut in two parts discussing each side in isolation, but covers both sides in one section.

Sources of Flexibility in Distribution Grids

In distribution grids, flexibility, as defined above, can stem from many different sources: RES like small-scale rooftop PV to multimegawatt wind-farms, heat-pumps, decentral batteries, and central sector coupling elements, like P2G- or P2H-plants. Already today, there are different companies aggregating many small-scale batteries in households to provide the connecting grid with flexibility [68]–[70].

Impacts of Rising Shares of Renewables

Since installed RES-capacities are steadily rising world-wide due to their low costs for generating electricity [71], a lot of work has been done to assess how flexibility in distribution grids can enable integrating even more RES without the need of grid expansion. A prominent study in this area is [72], in which the integration of RES into the German energy system is discussed. Different approaches are examined, from demand side management (DSM) to increase flexibility, to usage of new high temperature conductors, or voltage support at times with a very high share of renewable generation. The study does not answer, how renewables may also help the transmission grid, neither is curative operation in the scope. Interestingly, the aims of the study, to integrate a renewable share of 39 % into the German electricity grid, has been achieved before its target in 2020 (40.3 % in 2018). Recommendations from the study include storage and grid expansion, as well as enhanced European cooperation.

Consequences for Grid Operation

If grid expansion is performed, costs can be significantly reduced by taking flexibility options into account during the planning process, as is shown in [73]. Interestingly, the algorithms developed for grid operation in Chapter 7 can also be used exactly for this purpose by artificially introducing flexible assets in the grid and evaluating how often and to which power they need to be limited. Demand response alone, at least in Germany, is shown in [74]

to be insufficient to balance out or integrate large amounts of surplus renewables generation. This might be different in other countries, as presented in [75]. Here, analysis shows that flexibility needs are driven by the individual energy system, its portfolio of power generation, and its size.

Alternatively, using a virtual power plant (VPP) is another popular approach in trying to integrate more RES into the grid, as is shown in [76]. Here, different electricity generation technologies are combined to reduce uncertainty and variability in power injection. These technologies aggregate wind-power, PV, biomass, and batteries to emulate the behavior of conventional power plants. This VPP can be dispatched as if it were a conventional fossil power plant.

Integrating High Shares of Renewables

Which sources are best suited to provide flexibility on different time-scales in energy systems with high renewable energy shares is the focus in [77], matching different generation and storage assets to the tasks and services in the energy system for which they are best suited. One key outcome is that up to a share of 35 % renewable energy from wind-power and PV, no technical barriers are existent, provided that the grid is expanded adequately. Only when reaching higher shares of RES, flexibility from these assets and loads becomes an important contribution to keep the system stable. Much higher RES shares of up to 80 % have been analyzed in [78], resulting in a "flexibility gap" between supply and demand side that needs to be filled. In addition to network expansion, dynamic assessment of power transfer capability, or dynamic line ratings, are mentioned. These are also one cornerstone in the InnoSys concept for curative grid operation and are also recommended in [72].

To close this flexibility gap, different methods to incentivize flexibility provision are analyzed in [79], [80], from local market designs to specific monetary compensations for different sources of flexibility in households.

Flexibility Markets

Many studies in the area of distribution system flexibility are focused on market aspects and therefore only of peripheral interest in the scope of this thesis. In [81], many different market models are compared in their usefulness to provide flexibility to the grid. In this study, the authors claim a great potential for market platforms for flexibility provisioning, while also noting, that their success might be limited by the risk that some participants might generate illicit profit from market manipulation. Some work, like [82], also cover the area between markets and system operation and show, that a better cooperation between TSOs and DSOs indeed leads to cost reductions and smaller amounts of re-dispatch.

Provisioning Distributed Flexibility to Transmission Grids

Flexibility in distribution systems for the use by transmission system operators has been the focus of several research projects, for example EU-Sysflex [83], SysDL2.0 [84], IMOWEN [85], Interplan [86], DA/RE [87], and enera [88]. Those projects mainly take the perspectives of transmission and distribution system operators, dealing with coordination between different grid levels, assuming flexible assets. Integration of many flexible assets into system operation concepts without having to deal with exploding complexity due to a quickly rising number of assets in lower grid levels is also the focus of another research project, REGEES [89], and a doctoral thesis [90]. Both these works heavily influenced this thesis, since REGEES is one of the precursor projects to InnoSys 2030 [52], in which the author of [90] plays a part. However, none of these projects deal with curative system operation, which has stricter requirements for speed and reliability.

1.3.1. Calculation of Distribution System Flexibility Potential

In this subsection of the present thesis, existing scientific work pertaining analysis or calculation of distributed flexibility potential is examined. At first, approaches that do not rely on integrated energy system modeling are analyzed. Afterwards, energy system models that can be used to calculate the flexibility potential from distribution grids are examined. Finally, the research gap is identified which is to be addressed in present thesis.

Aggregation Approaches

To calculate flexibility potentials, or approximate them for future scenarios, there are different approaches. Many authors focus on the role of demand side management, from industry, commercial sectors, or households, for either existing energy systems [72], [91], [92], or future scenarios [93], [94]. However, in these studies the focus lies on calculating the total available flexible power from different processes, not in quantifying how often this power is indeed available. In [93], for example, to approximate flexibility needs in different scenarios, residual load curves are used. Then, DSM in different sectors is approximated and compared to the flexibility needed. In many assumptions these scenarios for 2050 are already outdated, for example P2H-systems and DSM from industrial processes. Independent from their assumptions, the main problem with many studies approximating future flexibility is that the operational state of the energy resources is not taken into account. Also, the regional distribution of flexibility offers and needs is not considered when trying to match them. The grid that is needed to transmit the energy to clear this imbalance is not being modeled, which can lead to vastly different results, as will be shown in this thesis.

Ancillary Services from Distribution Grids

Other authors, e.g. in [95], are trying to tackle this point by showing that distribution grids can serve the reactive power needs of the transmission grid in an energy system supplied solely by RES. Here, the flexibility from distribution grids is used to replace one of the tasks conventional power plants are fulfilling these days, providing reactive power to stabilize the transmission grids voltage profile. To assess this claim, the connection of synthetic and actual distribution grids to a German transmission system is simulated. Then, reactive power needs are derived for the transmission grid and it is assessed, if the providing distribution grids can indeed cover the needs. The basis for this study is a 100 % renewable scenario taken from [96]. Similar work for the flexibility potential to provide curative transmission system operation has not been performed so far, but might be possible within the same model.

A more general approach to calculating future distribution grid flexibility is performed in [90], where many studies estimating such flexibility are analyzed and compared to estimations based on data provided by the regulator like [97]. A flexibility potential between 10.8 GW to 18.7 GW is determined for Germany, with 3.8 GW to 5.9 GW from industry and commerce, comparable to the 6 GW in the 2030c scenario of the Netzentwicklungsplan 2030 [98]. However, potentials analyzed in [90] are in parts estimations of current flexibilities, in contrast to the 2030 scenario taken as basis in the InnoSys research project. As in other studies, operational states are omitted in [90] and results are therefore not usable if flexibility needs to be correlated to different states in the transmission grid.

For existing distribution grids, an approximation of the flexibility that can be provided for different transmission system scenarios has been performed in [99]. However, even in the scenario with a high RES-penetration, the possibility of curtailed RES providing flexible incremental generation is not considered. Only a few researchers even consider this option or have the tools to include it into their simulation.

Consideration of Operational States

In general, summing up installed capacities, neglecting operation-schedules and -states, leads to overestimation of available flexibility. To counter this, in [100], simultaneity factors are used to reach adjusted data, in [101], residual load curves are used as means for the same goal. These approaches can deliver time-series of percentages of the flexibility that is available. Of course, these heavily depend on the meteorological year that is used and, in general, are not locally resolved. In Germany, the electricity market and power-flows strongly correlate with wind availability in the north of the country, since most wind-farms are located there. This is also not expected to change significantly, but rather intensify, since offshore wind-power is increasingly being integrated into the electricity sector. If just using simultaneity factors

or residual load curves that are not regionally resolved, flexibility exigency (e.g. southern Germany) cannot be correlated with supply (e.g. northern Germany), and usefulness for the grid remains unknown.

Integrated Modeling to Determine Flexibility Needs

For such detailed knowledge, especially where (geographically) flexibility is available, an integrated model is required. Such modeling is performed in many works, for example in [96], [102]–[106]. While this list can be extended by many more entries, these are chosen due to their ability to theoretically assess the question, if distribution system flexibility is existent, and if the availability meets the exigency. To answer this question, the model needs sufficient spatial resolution, e.g. on the scale of large distribution grids, and a transmission system model. This grid model is needed to assess when the grid is in need of a distribution system to increase or decrease load or generation, hence the exigency. On the other hand, operational states of all assets in the distribution grids are needed to calculate the supply of such set-point changes of either loads or generators.

Approaches to Model Energy Systems

To obtain the information about both the state of the grid and the energy resources, both loads and generators, an energy system model is needed. There are many different types of energy system modeling software, using different approaches for different goals and desired accuracy. One such goal is resource planning, a planning process, in which present or future load and generation scenarios meet a grid, in order to identify which changes to the grid lead to the best overall performance. In Germany, theses processes are regularly performed in the Netzentwicklungsplan, in European surrounding this is done by the ENTSO-E in the TYNDP and MAF. The outcome of such models might be a list of preferred options how to enhance the infrastructure to support grid operators in the political processes, that are needed before investments into the grid are being done. An example of such a modeling framework is [107], where a market simulation is performed in a very fine granularity, and then the result of this simulation is cast upon the grid. Contingency analysis might follow in order to determine the stability if a loss of generation, load, or transmission capacity occurs. In addition, if the model of the grid and connected assets is sufficiently accurate, dynamic simulations can show instabilities due to oscillations or resonances when transitioning between two states in the grid, for example before and after the tripping of a circuit breaker. Such a model is suited to the task that is performed here. However, the amount of details and the corresponding work, that goes into a model such as the Netzentwicklungsplan, is significantly higher than what is possible during a PhD. A review of other modeling approaches for the application as planning

tools can be found in [108]. Especially for the European scope, not only limited to electrical transmission system planning, but also for example gas transmission, a review of models and tools to make the European energy transition possible and understandable, not only for scientist and modelers, but also politicians and public stakeholders, can be found in [109].

Modeling Energy Systems with High Shares of Renewables

The need for curative grid operation rises with higher shares of renewables and the corresponding transmission patterns. Modeling high shares of renewables therefore is important to asses the impacts of curative operation. Many modeling approaches are delving into the question if a 100 % renewable energy system is possible, and if so, how. These studies can cover a range of scales, from regions like Bavaria [110], to smaller countries like Denmark [111], to countries like Germany [106], or even whole continents like Europe [112], [113]. If a not completely renewable energy system is to be modeled, CO_2-attribution is key to realize how CO_2-emissions (and other climate gasses) can be reduced. This is highly non-trivial as shown in [114] and [115], especially when storage options come into place. Some energy system models also focus on specific challenges inside the whole energy system, like transport [116], hydrogen storage [117], or global shipping [118], just to name a few. A paper thematically very close to this thesis is [119], in which curtailments of RES in Europe are analyzed for scenarios spanning the years 2030 to 2050. Due to differences in scenarios, results can not directly be compared, but the phenomenon that is being observed remains the same.

Setting the Correct Spatial and Temporal Scope

To reduce computational costs in simulating as well as needed man-power in creating the energy system model, the correct spatial and temporal scope of the model have to be set. Depending on this scope, especially county- or continent wide models need spacial aggregation to be computed in reasonable times. The choice of scale is dependent not only on the desired accuracy and run-time, but also on the research questions that are to be answered. If impacts of measures on specific power lines are of interest, of course the resolution has to be sufficiently fine. For larger models, power transmission between countries might be of interest, so a coarser resolution might do. In [120], the role of spatial scale is evaluated, and it is shown, that the choice of scale heavily influences modeled system costs. Especially questions of grid expansion and storage, e.g. posed in [121], need a higher resolution to be answered reasonably.

Not only in spatial scales, but also in temporal ones, different resolutions can be chosen. However, time-series aggregation and choice of representative days can very well approximate a simulation with many more time-steps [122], [123]. This way, a lot of run time can be

saved and model sizes be reduced.

Key Aspects in the Calculation of Useful Flexibility

As energy system modeling is only a part of this thesis, it will not be covered in in more detail. However, two great review papers can give such an overview in a length not possible here. These two papers are [124] and [125].

In Table 1.3, the key aspects to calculate distribution system flexibility potential for curative transmission grid operation are listed. A detailed and consistent calculation of said potential can only be performed if all aspects are present in the approach chosen for the task.

An evaluation if these aspects are available in existing research is shown in Table 1.4. As can be seen, the potential of "de-curtailing" renewable generation is not being determined in any work analyzed here.

With many of those models cited here it is possible to answer the first research question: calculating if distribution system flexibility has a meaningful potential for curative transmission system operation. Some models might even be better suited than the one chosen in this work, due to their extraordinary level of detail in the regionalization of the scenario and the grid modeling. However, to the knowledge of the author, no such a study has been performed covering this area of research except [64]. The level of detail might not be as high as possible with other modeling approaches, but is adequate to answer the first research question of this thesis.

Table 1.3.: Necessary modeling aspects to calculate distribution system flexibility potential in curative grid operation

Aspect	Relevance for the calculation of flexibility potential
Curative grid operation	Currently, transmission grids are operated preventively n-1 safe to increase reliability and resilience. Curative n-1 safe operation helps to increase the utilization of the grid and can, given enough flexibility, achieve the same reliability as before. Flexibility potentials useful for curative grid operation have to fulfill stricter requirements than those for preventive operation.
High shares of renewables	Curative grid operation becomes relevant in energy systems with high transport demands. These energy systems are often characterized by high shares of electricity generated by RES. Therefore, the assessment how much flexibility is available for curative grid operation is best performed in an energy system model with a high share of renewables.
De-curtailment of renewables	As capacity factors or full load hours (flh) of RES are lower than those of conventional power plants, especially base load plants, installed capacities need to be much higher in energy systems dominated by RES. However, the power injection of those energy resources is correlated. This leads to energy systems, where sometimes RES will be curtailed due to a lack of consumers or transmission capacity. The flexibility from these curtailed RES can be used by "de-curtailing" them, providing an additional source of upward distribution system flexibility.
Integrated modeling	Only in an integrated model the correlation of availability and need for flexibility can be appropriately determined. This is especially true if such flexibility is used for curative grid operation.

Table 1.4.: Research gap in the calculation of the distribution system flexibility potential for curative transmission grid operation. "+"-signs mean that the aspect is taken into account, "-"-signs mean that it is not.

Publication	Curative grid operation	High share of renewables	Flexibility calculation including de-curtailments	Integrated modeling
[72]	-	-	-	-
[91]	-	-	-	-
[92]	-	-	-	-
[93]	-	+	-	-
[94]	-	+	-	-
[90]	-	+	-	-
[100]	-	+	-	-
[101]	-	+	-	-
[102]	-	+	-	+
[104]	-	+	-	+
[96]	-	+	-	+
[105]	-	+	-	+
[106]	-	+	-	+
[107]	-	+	-	+
Present thesis	+	+	+	+

1.3.2. Provisioning of Distribution System Flexibility

Provisioning flexibility from one grid level to another consists of several steps, which are, depending on the chosen approach, done in sequence or at once, therefore, making it harder to compare them. In essence, the desired result is one or several numbers describing the power or change in power that can be provided at corresponding grid interconnection points between the providing and the requesting grid. The steps that are performed are either, in a two stage process, limiting individual flexibility of energy resources and aggregation of such flexibility, or, in a one stage process, optimization of the flexibility range at one or multiple grid interconnection points. Upon request, disaggregation onto individual energy resources has to be performed to execute the request.

Reliability Requirements

The primary objective when providing flexibility is to keep the providing grid in a secure state, whether or not a request is executed. After calculating the available flexibility, it is imperative, that the flexibility that was communicated, is assuredly available in case of a contingency. If the underlying grid has several grid interconnection points, it is also important for the requesting operator to know how the provided flexibility is distributed among them.

TSO-DSO Interface and Preference Cascade

To quickly and safely provide flexibility, the interface between different operators, mostly TSOs and DSOs, must be clearly defined. In [126], the options for coordination at the TSO-DSO interface are detailed. In this concept, retrieval of flexibility can be done for individual energy resources or for aggregates, while stating that the connecting grid operator of the energy resource is responsible both for assurance, that his grid is operated safely, the decision to grant a request, and the execution of said request. In addition, the preference-cascade from local needs to global needs is defined: Since in general, the lower the voltage level, the less options are available for the operator to retain a safe operating state or achieve one after a malfunction, the higher the priority when requesting flexibility, with the highest priority of course lying at the connecting grid operator.

This preference-cascade as well as the necessity of a safe operating state in the providing grid is also highlighted in [127]. Here, the coordination between grid operators is examined in the context of an intra-day flexibility market during a phase with reduced operating margins for operators or energy resources ("Gelbe Ampelphase").

Coordinating TSOs and DSOs

One thesis already mentioned is [90], in which different coordination interfaces for a vertical cooperation between grid operators are evaluated. The $PQu(t)$-approach at the center of that thesis is defining the interface at each grid interconnection point (GICP) in a PQ-plane, that is dependent on the voltage $u(t)$ at the GICP. Integrating over the observed time-steps returns a $PQ\forall u$-area, which is similar to the output desired in present work. Here, the goal is to provide a setpoint range at the GICP that is reliable, independent of the voltage which might change during a critical outage. Again, aggregation of these flexibility-planes is bottom up, from the lowest to the highest voltage level.

Another project harmonizing the interface between grid operators is the generation and load data provision methodology (GLDPM), being implemented with the help of the ENTSO-E's common grid modeling standard (CGMES). Goal of the GLDPM is to be able to model transmission systems better by including (simplified) models of distribution grids. With the results from these models, inter-zonal power-flows can be better extrapolated into the future, leading to less uncertainty in free cross-border transmission capacities, which in turn can lead to a lower market price for electricity. An overview over grid simplification methods that can be used to integrate distribution grids into the transmission grid power-flow calculations can be found in [128].

Provisioning of Ancillary Services

In [84], the authors are looking into another aspect of distribution system flexibility: ancillary services. In this research project, including universities, grid operators, and companies, the focus is on maintaining frequency and voltage stability, grid operation, and re-establishment of power generation after blackouts using energy resources from distribution grids. As in the second part of the present thesis, detailed knowledge of the providing grid, including its state and the state of all connected energy resources, is necessary. In this case, two real grids from MITNETZ STROM and ENSO Netz are used to test the developed SysDL platform. A similar scoping is chosen in [129], where the focus lies on Volt/Var control by optimizing reactive power provision from wind-parks in the 110 kV level to reduce losses on both the TSO's as well as DSO's level. In addition to [95], there is a lot of work regarding different aspects of reactive power management in distribution grids, for example [130], where the potential of reactive power from distribution grids is assessed, to [131], where distributed energy resources (DER) are used to stabilize both the distribution and transmission systems voltages. In [132], voltage response from active distribution network (ADN) is explored using both central and decentral control algorithms, while in [133] model predictive control is used to regulate the systems voltages. All these works share the same root-problem with some

of the work done in this thesis, it being that controlling a lot of individual DERs becomes exponentially difficult when their numbers rise, therefore novel approaches to keep control in the connecting grids are needed.

Approaches to Calculate Safe Flexibility Ranges

In order to limit the possible flexibility range or plane at the GICP, different approaches can be chosen.In [134], for example, an optimal power flow (OPF)-based optimization problem is formulated, whose result are cost-dependent flexibility areas in which a safe and reliable operating state of the providing grid is guaranteed. This is of course very relevant for market-based provisioning of flexibility, which might be happening in the future in the planning process. However, prices are less relevant in a curative operation, where the re-establishment of a safe state is in the focus. In Germany, discrimination-free usage of power to resolve bottlenecks in the grid is required by law from the system operator. This means, that cheaper sources must be used first, but in case of an emergency, the operator can use all sources expedient to a resolution of the critical outage [38]. In addition, renewable energy resources must only be curtailed, if it saves a multiple of the curtailed amount from non-renewable sources[9], making a price attribution very hard [36].

The opposite approach to offering flexibility at the GICP is done in [89]. Here, as in the present thesis, optimization is done bottom up, limiting each individual assets flexibility to stay inside the safe operating boundaries instead of optimizing the area at the GICP.

Improving the methodology from [134], in [135] a linearized OPF is used in a loop. Linear branch constraints are achieved by using regular polygons, for which the constraints are evaluated piece-wise. The boundaries of the flexibility ranges of each individual flexible asset are also linearized as convex polygons. Optimization itself is done in a loop, in which the convex solution space is explored iteratively. The result of this optimization is, as in present work, a P-Q-area, in which each desired set-point can be chosen by the TSO without risking an unsafe state in the providing grid. A similar approach to communicating the aggregated flexibilities is done in [136], but no real optimization is performed in that publication, only a justification of sampling, which is feasible in the view of the author due to short run-times of power-flows. However, in both works only grid topologies with single GICP are tested and evaluated, with run-times, in the case of [135], that are longer than what is to be expected using robust optimization.

A comparison, if OPF or Monte-Carlo based approaches are more suited to the problem of aggregating flexibilities is done in [137]. The authors explain, that for smaller grids, Monte-Carlo style sampling approaches, as for example performed in [138], [134], or [139],

---

[9]This is called priority dispatch.

work well and are sufficiently quick, while for larger grids OPF-based approaches are better suited. To circumvent the inherent disadvantage of random sampling, that the whole area is to be sampled, in [89] the problem is expected to be convex, allowing sampling in "corners" and performing power-flow calculations only in the edge-cases, while neglecting the bulk of uninteresting states. A similar procedure is also advised in [137], where the choice of sampling approaches is evaluated to have a significant effect. In either way, this approach is unsuitable for real time applications, at least on real, larger grids, especially in a curative operation regime.

Dealing with Uncertainty and Robustness

In [140], a geometrical approach is being taken to evaluate the solution plane, where for every voltage angle ϑ, an optimization using an OPF is performed. The step-size $\Delta\vartheta$ is variable and defines the accuracy, to which the aggregated flexibility matches the available flexibility. This approach has the advantage that different active-reactive power capability curves for different RES can be considered, but again can be very slow on real grids.

A similar approach, but including uncertainty and reliability is developed in [141]. Here, uncertainty from PV and loads are added by optimizing several times for different scenarios, which are created by picking the injections from slices of their respective probability distributions, returning results for seven different uncertainties, varying from $\pm 3\sigma$ to 0σ. In addition, single line outages are introduced and its impact evaluated. The results are similar to what one would get using robust optimization in addition to a contingency analysis simulating equipment outages, but computationally much more intensive. However, this sampling-over-standard-deviations approach has the advantage, that the maximal uncertainty that is to be accepted can be actively chosen.

Another way to incorporate robustness is taken in [142]. Here, a number of different scenarios is generated and a linearized optimal power-flow performed, to increase performance. As in [140], individual flexibility ranges are approximated using polygons, which in addition to the sampling in scenarios also forces a sampling in voltage angles ϑ. Robustness is then achieved by using only those flexibilities of the assets, that are certain in all scenarios. This seems like a very promising approach, but for each time-step for which the flexibility range at the GICP is to be calculated, the algorithm takes about 500 seconds in a 33 bus model, which is unsuitable for curative and real-time applications. This is also the reason, why the concept developed in [140] is meant for planning processes and not operation.

Key Aspects for Curative Flexibility Provision from Distribution Grids

In Table 1.5, the three main aspects for calculating aggregated safe flexibility from distribution grids are listed. The publications whose subject is the calculation of distribution system flexibility are assessed with respect to these three aspects. In Table 1.6, the results of this assessment are included. As is visible, none of the approaches that are taken into consideration is suitable for curative flexibility provisioning, leaving a research gap for the present thesis.

Robust optimization [143], a method to ensure boundary conditions are obeyed for uncertain input data, seems like a promising way to solve problems in the context of power-flow calculation. Indeed, two applications of robust optimization in power systems are [144] and [145]. In [145], uncertain renewable generation is taken into account in a robust OPF in a mixed AC and DC power system, where voltage, power-flow, and frequency limits have to be obeyed, whereas in [144], a dispatch problem is solved using robust optimization and linearized power-flows.However, no work has been found using robust optimization for flexibility aggregation or for curative use.

In the present thesis, an approach is being developed that uses linearization of power-flows in connection with robust optimization in a bottom-up process, with the objective to achieve fast computation times even on large, real grids, robust convergence and results, and the potential for flexibility provision via several GICPs. These qualities enable such an approach to be suitable for safe and reliable distribution grid flexibility provision for curative transmission system operation.

Table 1.5.: Aspects and behavior of importance for the calculation of safe distribution system flexibility for curative transmission system operation.

Aspect	Relevance for the safe provisioning of distributed flexibility
Grid size and scaling	While sampling approaches work very well on small grids, they display bad scaling behavior when increasing the number of flexible assets. OPF based approaches have less scaling issues, but are still too slow for curative operation. Intelligent sampling as used in [89] and advocated for in [137] can alleviate runtime problems, but lack robustness. In general, linear optimization programs are solved much faster than nonlinear ones, an effect that increases with problem size.
Robustness	Both with respect to convergence as well as input errors, optimization methods need to be robust to be used in curative operation. While there are several approaches including uncertainties and generating robust results, especially [141] and [142], those approaches are also very slow and only suitable for planning purposes. Nonlinearities in AC-power-flow can also lead to convergence problems in the optimization, where finding a good starting point becomes a challenge for large problems.
Several GICPs	While there is a lot of work addressing flexibility from distribution grids, most only consider one GICP between transmission and distribution grid. This is a conceptual problem, since the flexibility that is being optimized is that at the GICP, not the flexibility of the grid. It is hard to prove, that a flexibility potential calculated this way is free of discrimination, as a different combination of setpoints and assets might lead to the same potential. In order to be in accordance with regulation, requests for flexibility have to be free of discrimination, something that can be guaranteed by a bottom-up approach, minimizing individual flexibility limitations.

Table 1.6.: Research gap in the aggregation and provisioning of distribution system flexibility for curative transmission grid operation. "+"-signs mean that the aspect is taken into account and the behavior is compatible with the research question, ○-signs show that the behavior adequate, but not optimal, while "-"-signs mean that the aspect is not considered or the behavior is not adequate for curative operation.

Publication	Scaling behavior	Robustness	Several GICPs
[138]	-	+	-
[139]	-	+	-
[89]	○	○	+
[134]	-	+	-
[135]	○	+	-
[136]	-	+	-
[137]	○	○	-
[140]	○	+	-
[141]	○	+	-
[142]	○	+	-
Present thesis	+	+	+

Summary

In this introduction, the setting, in which the present thesis is embedded, is outlined. The need for an energy transition and the corresponding shift from electricity generation by fossil fuel-fired power plants to renewable energies is outlined and so are its implications:

- Renewable energy sources (RES) are installed at locations with favorable conditions which can cause higher transmission demand.

- RES are mostly installed in lower voltage levels than fossil fuel-fired power plants.

- The higher transmission demand causes a need for grid expansion, which can be accompanied by innovative measures to increase grid utilization in order to lower the overall costs of the energy transition.

- One such innovative measure is curative grid operation, which can increase grid utilization by shifting the safety margins from power-lines to other assets that provide the necessary flexibility for such a shift.

- A possible source for this flexibility are the distribution grids, in which most loads and RES are installed. If these loads and generators can quickly and reliably be coordinated to provide their flexibility, they can be integrated in a curative transmission system operation.

Based on these points, two research questions are formulated:

1. Are flexible assets in distribution grids a viable source of flexibility for curative transmission system operation?

2. How can flexibility from underlying grids be safely and quickly aggregated and offered for curative use?

As the literature analysis shows, both questions have not yet been answered, providing a task that is set for this thesis.

2. Analysis

This chapter deals with the requirements to solve the research questions and how to best tackle them. Since this thesis addresses two aspects of distribution system flexibility for curative transmission grid operation, which need conceptually completely different approaches to be answered, this part of the work is split in two. First, requirements concerning the calculation of the distribution system flexibility are addressed, this part closely follows the publication [64]. After an overview of the challenges and the necessity to perform such a calculation, the second part follows, covering the development of an algorithm to reliably provide flexibility from one grid level to another.

2.1. Calculation of the Flexibility Potential from Distribution Grids

In order to assess the viability of flexibility from distribution grids, two questions have to be answered:

1. How large is the flexibility potential?

2. Is it available when and where it is needed?

To answer them, not only the information how many assets of which type and power are installed in the grid is needed, but also how they are operated in the energy system that is to be operated curatively. Figure 2.1 shows the concept of using flexibility from two distribution grids or regions. At different times, these regions offer varying flexibility due to the operational states of the connected energy resources. A power-to-heat plant, for example, can only offer a decrease in load, if it is running, and a wind-turbine a decrease in power injection only if it is turning. On the other hand, operational states of power lines or corridors in the transmission system are dominated by macro weather situations and the inhomogeneity of installed generation capacities. In Germany, a large part[1] of the wind-power capacities are installed in the north of the country, a situation that likely will stay this way or even escalate,

---

[1]As stated earlier, only about 7 % of the total wind-power capacity of Germany is installed in Baden-Württemberg and Bavaria which have a combined area share of almost 30 % of Germany [41].

due to increasing numbers of offshore wind farms. On windy days, the transmission system will therefore show large transports from north to south, especially during night times or in winter, when PV-based generators mainly installed in the south of Germany are not able to inject much power due to the relative position of the PV panels and the sun. If, in such a situation, a loss of transmission system capacity occurs, upward flexibility ΔP^{up} is needed in the southern regions or grids, and downward flexibility ΔP^{down} is needed in northern regions to counteract the transmission loss. Upward flexibility means a decrease in load or increase in electric power injections, while for downward flexibility the opposite is true. The closer to the location of the failure this flexibility is injected into the transmission grid, the higher is its sensitivity to relieve the remaining transmission lines. In addition, less of the power that is to be compensated is shifted onto other transmission lines. The goal of the calculation of available flexibility is to get an estimate, how often distribution system flexibility is available in the regions whose power and load injection changes have a high sensitivity to a potentially failing line, and, if flexibility is available, how much energy can be compensated to relieve the transmission grid.

2.1.1. Sources of Flexibility

The flexibility potential $\Delta \hat{P}$ is a function of the chosen technologies and sources of flexibility. The more sources are considered, the higher the potential will be. Some sources can only be used for downward flexibility ΔP^{down}, while others provide only upward flexibility ΔP^{up}. Some, for example batteries, if neither completely empty nor fully loaded, can provide both ΔP^{down} and ΔP^{up}. In the following, a few sources of flexibility are listed. It is shown why they are or are not considered as suitable sources for flexibility in a curative operation.

Renewable Energy Sources

Flexibility from RES can be obtained in two ways: curtailing the output power or de-curtailing curtailed RES. Curtailment of RES is already a present phenomenon in Germany [35]. It is an option grid operators can choose to relieve the grid from bottlenecks. In an energy system that is dominated by RES, the total available generation power in the energy system can regularly be in oversupply, such that many RES are operated below their maximally available generation power. De-curtailing these curtailed RES can then be used as a source of flexibility that will increase in importance and abundance with rising shares of RES in an energy system.
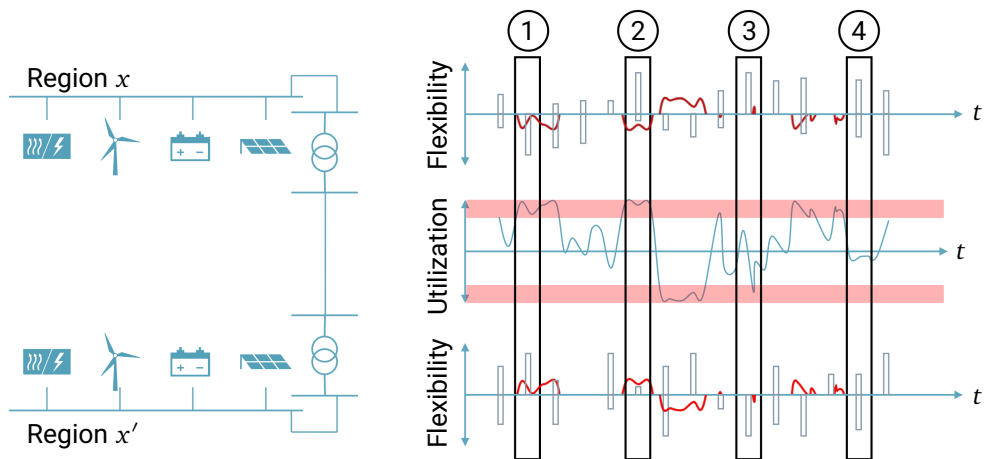
Figure 2.1.: Concept of flexibility from sub-transmission grids for use in a curative transmission system operation. Upward and downward flexibility potentials of regions x and x' are plotted above and below the utilization $P_{xx'}$ of the connecting transmission corridor. Intervals of critically high utilization are shown as light red bands. Sections of the utilization profile within the critical intervals are also plotted as red traces in the top and bottom panels to allow for better comparison to the available flexibility potential. Four cases are shown to outline different scenarios: In case 1, there is enough flexibility to allow curative operation within a critical time-step. In case 2, flexibility is available but not enough to allow curative operation (see red lines). In case 3, the power-flow is in the opposite direction from x' to x and enough flexibility potential is available. In case 4, flexibility is available but not needed.

In case of curtailed RES, the future regulations regarding which RES will be curtailed first are not known yet. The optimization process used here will always select the which asset to curtail based on costs, the source of energy with lowest costs will be curtailed last. To influence the order in which curtailments are performed and analyze the impact of a change in this order, additional costs can be introduced.

In Germany, gradients for power injection changes are set and enforced by connecting grid operators, which, depending on the voltage level, demand that connected RES satisfy the VDE-AR-N 4120 [65] in HV or VDE-AR-N 4140 in MV. These regulations describe power injection gradients that need to be obeyed. These gradients are limited from 0.33 % to 0.66 % of the installed power per second, resulting in a full shut-down or ramp-up in 2.5 to 5 minutes. These regulations exists to increase dynamic stability and reduce the need for a dynamic security assesment (DSA), since the gradients that can be performed by most RES are much greater than those defined in the regulation and can lead to dynamically unstable states.

Flexible Loads

Besides curtailments, power to heat (P2H) is another option to provide both upward and downward flexibility. P2H assets are low-cost, often large scale loads and therefore installed in MV and HV and already used for demand side management today [146]. There are also small scale P2H-assets in households, but residential appliances are not controllable by grid operators, installed in low voltage levels and no candidate for the first generation of assets to be integrated into curative system operation. Already today, the business model for power-to-heat is to provide ancillary services to grid operators [147]–[149].

Decentral Batteries

Decentral batteries are primarily used to store energy generated from PV installations on private homes are another source of flexibility. Aggregated mostly by manufacturers, they are already used to provide flexibility today by Lichtblick, Sonnen, or Tesla [68]–[70], [150]. These batteries can provide upward flexibility via two ways: Either they can increase their power output or decrease their power input. The case where these batteries are loaded from the grid is not planned yet in any business model in Germany[2] due to the grid levies on both charging and discharging electricity. It is therefore not considered as a source of flexibility in this work.

---

[2]In South Australia, this is already happening [151].

Possible Additional Sources of Flexibility

In this work, only sources of flexibility that either are already used to provide flexibility or fulfill the necessary requirements to do so in the near future are taken into account in the calculation of the flexibility potential. A second category of assets is listed below that can either provide flexibility to markets or be used preventively. In the future, the situation might change and those assets can also be included in a curative grid operation. This only makes sense as a second step, after the integration of assets listed above.

The sources not taken into account for the calculation are:

- E-cars

- Heat-pumps and other decentral electrical heating

- Flexible small loads

- Power-to-gas

- Combined heat and power and Biomass

- Demand side management

Most of them are either not controllable by grid operators or mainly connected in LV-grids. Power-to-gas will be connected in HV or even UHV and might also be controllable by DSOs. However, since the CAPEX of the P2G assets are so high, they need to run more or less continuously to be economically feasible and are not meant to be controlled quickly as for example P2H assets.

In the scenario used here, biomass is modeled without flexibility. In the official German grid development plans, biomass is modeled as continuous output, as that is the current observed behavior. This behavior is due to the incentives for farmers that operate most biomass plants, which does not explicitly favor provisioning of flexibility.

Demand side management is an exception, as it is both already in use for flexibility provision and controllable by grid operators. It is not included in the calculation here, as it is harder to model due the fact that the load is only shifted and not curtailed.

2.1.2. Setting the Correct Modeling Scope

Every model is a compromise between the desired or possible degree of realism on one side and feasibility on the other side. To strike the right compromise and calculate realistic estimations of available flexibility without modeling each single energy resource itself, a few challenges have to be addressed. Especially finding the sufficient temporal and spatial resolution to

maintain a desired degree of accuracy while keeping computation times reasonable and data acquisition manageable is of interest.

Additionally, the scope of the modeled system has to be set, to be able to exhibit phenomena caused by the macro system, also while maintaining a manageable size. This scoping is not only necessary in spatial dimension, but also temporal, limiting the number of time-steps that are simulated during a model run.

These decisions are also influenced by the available computation- and man-power. A large group of people could increase spatial resolution with manual data handling, while for individual modelers such an undertaking is prohibitively time-consuming. An example of such very detailed models is [106], where every sector is modeled with very high level of detail, down to the physical properties of each asset. Still, while some components of the model are treated with high accuracy, a consistent level of modeling accuracy is hard to achieve. Macroscopic, large-scale changes caused by legislation, activists, and innovations can still substantially change a model result. The farther one tries to look into the future, the more a model becomes a set of guesses, and increasing accurate technical simulations can only provide spurious accuracy.

In essence, ideally the scope in terms of time, space, and physical detail is chosen in such a way, that the phenomena which are of interest can be observed, while not spending too much time and effort on unnecessary or even spurious accuracy. In the following, the main phenomena relevant for the research questions are listed:

- Super-national power-flows shaping large scale transmission patterns.

- Inter-regional power-flows shaping local transmission schedules.

- Regions the size of HV-distribution grids offering flexibility.

- A set of time-steps to get a picture of the system in different states.

- Temporal resolution larger than dynamic time scales but small enough to get a picture of all relevant processes.

After a model with such properties is set up, determination of critical time-steps has to follow, during which the flexibility needs to be present for a curative operation.

2.1.3. Building a Sector Coupling Energy System Model

There are many different approaches how to set up an energy system model. The type of model being chosen depends on the research to conduct with it. Here, the question to answer is how much flexible power is available from each region in the model, given a transmission

grid equipment failure in a future energy system. To do this, at first, a scenario for the energy system is set up, in this case it is a German energy system dominated by RES and set in the year 2030.

It can be assumed about the future, that market mechanisms remain intact: sources of electricity with low costs of generation will be in front of more expensive ones in the merit order. This means, that the use economic optimization of the energy system to model its energy resources' schedules, as the optimizer will set a preference for electricity sources to minimize costs while satisfying energy demands. This optimizer hereby mimics the behavior of many market participants that try to fulfill their needs while only paying as much as necessary. As the information available to the optimizer is complete, its performance will be better than the market, and, as a result, the total costs are lower. Nevertheless, usage of optimization to simulate markets is a standard procedure.

Another assumption that can be assumed with low uncertainty about future energy systems is, that sector coupling will grow in importance. Sector coupling means, that the electricity, transport, and heat sector are intertwined, in most cases by using electrical power to provide energy for the heat or transport sector. This is due to the dwindling relevance of fossil energy sources in a decarbonized energy system, where the sources producing electricity at the lowest costs are PV or wind-power, depending on the region [17]–[19]. Already today, this sector coupling is at work: electric cars and bicycles are being used in rising numbers, as well as trains, which run on electric power already since the 1840s [152]. In Germany, electric trains are in use since 1879 [153]. In the heating sector, electric resistance heaters and storage heaters have also been in use for many years [154]. Essentially, sector coupling is nothing entirely new or revolutionary, but its importance is likely to grow due to falling electricity prices or surplus renewable energy during times with good weather conditions.

Sector coupling can play a critical role in flexibility provision due to its ability to shift flexibility from one sector to another, for example shifting the time when an electric vehicle is being charged or a heat pump operates. Especially in the heat sector, flexibility is present due to the thermal inertia involved in space heating and the extremely low costs of thermal storage, which undercut electricity storage options by at least one order of magnitude [155]. Thermal storage can be combined with power-to-heat plants, especially for district heating, to use surplus energy and provide flexibility to the electricity grid [147].

One approach to allow sector coupling in a model is to formulate demands in useful energy. This means, that instead of formulating the optimization problem by telling it how much gasoline is needed for transports in cars, the need is formulated in person-kilometers. In the case of space heating, the needed energy is not normed cubic meters of natural gas, but kilo Watt hours or Joules of thermal energy. The optimization is then free to choose over the options that provide these useful energies the ones that are most cost effective or emit least CO_2.

CO_2 emissions can be included in the model by using emission factors. Each time one source of energy is converted into another, for example natural gas into heat, such a factor can be added to the model. If emissions from one sector are not of interest, they can be omitted, too. The optimizer can be given both a total of emissions that can't be surpassed, leading to an accounting price for them determined by the marginal cost to avoid further emissions, or a fixed price per unit of emission. Of course, these emissions can be generalized, accounting not only for CO_2, but also for other emissions like methane or nitric oxides. In the case of the model used here, the German grid development plan sets an emission target in millions of tons of CO_2 and an expected CO_2 price. Depending on the scenario and the costs of renewable energy and storage options, either the emission target or the price becomes an active boundary for the optimization process.

2.1.4. Data Needs for an Integrated Energy System Model

In dependence of the scope of the model, the corresponding data is needed. Input data for a model being able to estimate distribution system flexibility has to include at least the following:

- Regionally resolved installed capacities: Once the spatial scope and resolution is set to an adequate level, data is needed to model the energy system at this level. For each region, both the generation capacities and loads are needed to be able to calculate the local need or surplus in energy at each time-step. Generation capacities include both conventional and renewable energy sources. For a sector coupling model, as used here, these capacities not only include electricity but also heat or transport. The electrified part of the transport sector is included in the electric load curve while other transport capacities are not modeled to reduce model complexity. For the heat sector, generation capacities include both electrical sources for heat generation, like heat pumps and power-to-heat assets, as well as gas- or oil-based heating options. In the model used here, the heat demand is split in industrial, commercial, and residential demands, again split in district heat and local heat generation. For each of these sectors, capacities are either given by the scenario, in the case of electrified heat generation, or left to be built by the optimizer. This optimization is done in accordance to the regional loads, in the case of both heat and electricity. One main difference is, that heat cannot be transported over region boundaries, while electrical power can, if transmission capacity is sufficient. In short, data to fill the following regional distributions needs to be present:

    - Renewable and conventional generation capacities for both electricity and heat

    - Electrical and thermal loads

- Transmission capacities

Of course, data is not always available in the correct regional resolution. If the data is only available in finer resolution than the modeled one, aggregation methods can be used. In case of a coarser resolution, a disaggregation has to be performed. For this model, data needed in resolution of regions is in parts only available on a country level, for example for electricity and heat demands. In these cases, values for Germany are taken and distributed among the regions according to the distribution of gross domestic product (GDP) and population, each with the same weight. In the case of installed electricity and heat generation, synthetic methane or hydrogen production, data is made available by the German transmission grid operators on an asset level. Together with the information where each asset is installed, regional distributions can be calculated by simply adding up assets in each region.

- Time-series: Energy system models can be point models, both in time and space. This means, that the spatial or temporal resolution is reduced to zero. In the spatial case, the loss of accuracy if reducing the resolution is analyzed in [120]. This loss in accuracy is caused mainly by not considering transport limits, while in the temporal case, the variabilities of both loads and generators have to be considered. It is obvious, that the reduction by one hour of 8670 in a year does not change a lot in the outcome, if any representative hour is chosen. In [156], the author claims, that a robust reduction to 10 hours per year is possible, if the only source of variability are loads. In [123], this claim is backed up, showing that 10 well chosen time-steps can be sufficient. However, if storage, especially seasonal storage is part of the model, a choice of typical days in the course of a year is necessary [122]. Both to be on the safe side modeling electricity and heat storage as well as to be able to plot the behavior of the energy system smoothly for whole weeks, the time span was chosen to be 12 weeks in hourly resolution. This way, the model returns not only useful data, but it is also possible to generate more easily explainable graphs.

Both the temporal and the spatial reduction have the potential to reduce the computational effort of performing an optimization. In this case, the spatial resolution is set by the necessity to model transmission corridors between distribution grids, therefore further reduction in model size is more easily achieved by reducing the number of time-steps being modeled. In the case of this model, 12 representative weeks are chosen as a compromise between accuracy and computation time. According to the work cited before, this is sufficient to get an accuracy comparable with the general level of detail in the model.

Temporal variability in demands and generation have to be covered by a model for

it to gain explanatory power[3]. This variability takes place on different scales, for example intra day, with peaks in demand at noon and in the evening, with workdays differing from weekends, and intra annual, with higher demands in the winter than in the summer in areas where heating is important, or the other way around, if cooling demands are more important. The same is valid for electricity generation by renewables, where, in the case of PV, the power is highest at noon, and summers provide better conditions than winters[4]. Time-series that incorporate the demand and availability values for renewable generation, and to lesser extent also fossil generation, need to be included in the energy system model at sufficient temporal resolution. Dynamic phenomena are those that are in the time scales of a single to a few periods of the grid frequency. However, observing those phenomena needs a much higher degree of detail in grid modeling than for static processes. In addition, dynamic processes are mainly of interest for transient behavior, for example after the activation of a circuit breaker. Such processes are not in the focus of this thesis, therefore hourly profiles are deemed to be sufficient. Those time-series are needed in the following sectors:

- Load or demand curves on a regional level for both heat and electricity.
- Renewable generation curves on the same level for wind-power, PV, and hydro power.

Time-series might differ from region to region, as the composition of loads is different or, in larger models, the time zone is playing a role. In this model, time-series for both generation and demand of electricity are provided by grid operators. In the heating sector, time-series on a country level are used. This assumption of simultaneous change in heat demand across the regions in Germany is not assumed to be limiting the model accuracy, especially since heat is not transported between regions.

- Technology data: In the optimization process, there are several technologies for the optimizer to choose from to satisfy demands. For example, during noon in summer, the optimizer can use conventional as well as renewable electricity generation, while in other time-steps the choice is rather between different conventional generation sources. To correctly choose between these options, the model needs technology data. This data is used to determine which option or combination of options is most cost efficient, given CO_2 prices or boundaries. The set of data needed includes:

  - Efficiency factors: How much of the input energy, e.g. chemical energy in the form of natural gas, is being converted into heat, electricity, or losses. In case of

---

[3]The explanatory power of a model is its "ability to decrease the degree to which we find the explanandum surprising" [157]

[4]The closer one gets to the equator the less this is true, as excessive heat lessens the efficiency of solar cells.

storage, how much of the input energy can be retrieved?

– Capital and operational costs: What are the costs of building one unit or megawatt of this technology? What are the annual costs for keeping it operational, what are the costs caused by wear of the equipment?

– Raw material costs: Costs to extract coal, lignite, natural gas, or even uranium, and those to import. In case of biomass, costs to plant, harvest, and transport.

– Availability: All equipment is subject to wear. During the lifetime of a power plant, several planned outages to perform maintenance are to be included in the model.

– Operational boundaries: Electricity generation technologies work on different principles resulting in different operational boundaries. While some technologies, for example gas engines, can ramp up and down their output power in less than a minute, others carry more inertia, for example lignite or coal power plants [56]. In the case of lignite power plants, mining of the lignite takes place close by in surface mining, requiring pumps to keep the mining pit free of water and large equipment due to the low energy density of the raw material. Therefore, the power plant cannot only be viewed as a power plant, but as a system including the lignite extraction. Economics require minimal usage factors, describing that a lignite power plant cannot just run in the winter and be dormant during the summer.

– CO_2 factors: To be able to calculate the total emissions and in order to reduce them to the boundary set by the model parameters, CO_2 emission factors are needed for each technology. These factors determine how much CO_2 is emitted when converting one from of energy form into another.

• CO_2 emission prices or limits: In addition to CO_2 emission factors, to calculate a cost optimal usage of all assets, CO_2 prices are necessary. If a limit for CO_2 is set, shadow prices will be generated by the optimizer.

• A scenario to form a cohesive picture, set boundaries, and fill in gaps: A cohesive scenario is very important, since with rising model complexity, there will be missing data points for e.g. individual technologies. It is necessary to be able to fill them with the help of previous scientific or public data, but this data will probably not match the chosen scenario. Therefore, it is imperative, to deliver a reason why some parameters differ in comparison with other studies.

2.1.5. Choice of Scenario for the Energy System Model

In the case of this thesis, the scenario in which the model is set is one that was agreed upon in the InnoSys 2030 consortium, which in turn is based on the Netzentwicklungsplan 2030c [98]. This scenario was slightly modified in number of e-cars and installed offshore capacities, but offers the bulk of the data needed for the model. In addition, similar data for German grid-neighbors stems from a study on the decarbonization of the German energy system [158], which itself is based on [159] and [160].

2.1.6. Choice of Modeling Method

In addition to specific details how to model which sector, a general question has to be answered: Which method to model the energy system is chosen and is it suitable to the task? Here, the method chosen for modeling is optimization. To determine, if it is indeed a suitable method to model energy systems, a look at the history of optimization can help.

One of the fathers of linear optimization, Leonid Witaljewitsch Kantorowitsch, wrote about mathematical methods of organizing and planning production, in other means, optimal economical planning in 1939 [161]. In the Union of Soviet Socialist Republics at that time, the use of five-year plans meant, that the economy had to develop in accordance to a central planner. If this planner did indeed plan optimally, the economy would take an optimal path. In this case, the use of mathematical optimization to model the economy is obviously a valid choice as both the model and the planner use it. However, even though the electricity market is highly regulated, it is by no means similar to a five-year plan. In addition, the electricity market is only one part of an energy system. One could argue, that the ENTSO-E's midterm adequacy forecast (MAF) and ten year network development plan (TYNDP) and the Bundesnetzagentur's Netzentwicklungsplan (NEP) are some sort of central planning, but they only describe desired or expected basic conditions in the electricity sector, to which the grid planning has to adapt.

In a functioning market, however, each market participant tries to optimize his or her own participation, resulting in a distributed instead of a central optimization [162]. In cases with many market participants, this distributed optimization can, given sufficient information, achieve results almost as optimal as a central optimization, but at smaller computation costs [163]. The central optimization therefore determines an upper bound of optimality. This also means, that, of course with a deviation in accuracy, one can model individual market participants with an optimization approach. This deviation in accuracy is probably smaller than the uncertainty about future installed capacities and distributions of assets.

Summary

In this chapter, the requirements to calculate the potential of distributed flexibility sources for curative n-1 safe transmission grid operation are analyzed:

- To know, when certain flexible energy resources can offer flexibility, it is necessary to know if they operate and at which power. An energy system model can answer these questions and approximations about flexibilities can be made.

- In an energy system dominated by RES, the installed capacity is much higher than the peak demand due to lower full load hours (flh). This phenomenon can lead to times where more electrical energy can be produced at no marginal costs than can be used or transmitted, resulting in valuable flexibility.

- To answer the question when equipment malfunction in the transmission grid leads to a need for flexibility, national and super-national power-flows have to be analyzed.

- To get a full oversight of an energy system's behavior, it is necessary to analyze different load and generation scenarios.

- Correlation of times and locations when and where flexibility is needed and when it is present can help determine if flexibility from distribution grids is a viable and useful concept for operational degrees of freedom in a curative grid operation.

To answer the first research question and calculate the potential of flexibility from distribution grids for curative use, an energy system model has to be set up with the above mentioned qualities.

2.2. Development of Algorithms to Calculate Safe Flexibility Sets

In this part, the requirements to solve the second research question, which deals with the problem, how flexibility from distribution grids can be safely and quickly aggregated and offered for curative use, are outlined. The methodology needed to answer this question is different from the methodology for the first question, as the level of modeling detail for the flexibility-providing grid needs to be much higher.

2.2.1. Operational Boundaries in Electrical Grids

To calculate the flexibility potential in an energy system, fleets of DER are modeled. To model the impact of individual setpoint shifts due to requests for flexibility at an individual grid interconnection point (GICP), such an approach is not sufficient. The reason is that a high level of detail of the flexibility-providing distribution grid is needed to determine if any occurring states in the process of providing flexibility are violating operational boundaries. Such boundaries can be divided in two groups:

- Voltage bounds for all buses: Normal voltage bounds in HV are set to ±10 % of their reference voltage [164]. For a 110 kV grid, this means the voltage must be between 99 kV and 121 kV. This is due to several factors: Equipment to transport electrical energy needs to be isolated from the ground to prevent electrical charge carriers from recombining while being transported. The isolation needs to be adapted to the potential or voltage the charges carry. In HV- and MV-systems, isolation is in large parts achieved by distancing charge carrying equipment from each other and the ground, letting the air play the role of an isolator. To prevent short circuits and electric arcs, the distances have to be planned accordingly to the voltage level, with higher voltages requiring higher distances. If, by an inappropriate choice of setpoints for the energy resources in the distribution system, the voltage becomes too high, short circuits can occur resulting in damage or destruction of operating equipment and subsequently in blackouts. If voltages drop too much, the security of supply is threatened, leading to reduced power outputs of connected appliances or even damaged equipment.

- Current or power-flow bounds for all branches or power lines: In 110 kV grids, normal overhead lines have maximum transmission capacities of up to 343 MVA [165]. These power lines are essentially metal ropes or cables carrying electric charges. Overhead lines, which are the backbone in HV- and MV-grids usually use aluminum as material for the conductor and steel to absorb forces due to the mechanical stretching of the material. Depending on the resistance of the material, the current flowing through it will heat it up. The more current flowing through a conductor, the higher the power loss that is converted into heat. Most materials have a positive thermal expansion, leading to a increasing sag of the power lines with increasing temperatures. To keep the conductor as far away from the ground as necessary, current or power-flow limits are calculated for each branch in a grid.

One of the grid operators tasks is to always ensure a safe operating state, defined as follows:

> **Definition 3: Safe Operating State**
>
> A grid is in a *safe operating state* if neither current nor voltage limits are exceeded and all operating equipment is used within its operating limits.

All the n_{FA} flexible energy resources in a grid can change their power injections by some amount $\delta p_{\text{FA}n}$, $\delta q_{\text{FA},n}$ within the upper and lower bounds for active $\delta p_{\text{FA},n,\max}^{(0)}$, $\delta p_{\text{FA},n,\min}^{(0)}$ and reactive power $\delta q_{\text{FA},n,\max}^{(0)}$, $\delta q_{\text{FA},n,\min}^{(0)}$. These boundaries define the initial flexibility set $F^{(0)}$:

> **Definition 4: Initial Flexibility Set**
>
> The *initial flexibility set $F^{(0)}$* of a distribution grid or distribution grid section is the set of all possible individual setpoints within the individual flexibility boundaries in said grid or section.

In case the DSO has to provide flexibility to the TSO however, he wants his grid to remain in a safe operating state. In a future energy system with thousands or even millions of flexible assets, it is imperative to check first, if by providing their flexibility, the safe operating state is left by the activation of setpoint changes by the many assets in the distribution grids. The purpose of the algorithm developed in this thesis is to check, if any violations of boundary conditions can happen by the activation of setpoint changes, and if that is the case, limit individual flexibilities to guarantee a safe flexibility set F:

> **Definition 5: Technically Safe Flexibility Set**
>
> The *technically safe flexibility set F* of a distribution grid or distribution grid section is a subset of $F^{(0)}$. All combinations of individual flexibilities in the set lead to a safe operating state.

To determine this technically safe flexibility set F, individual initial flexibilities are limited so that all combinations of flexibilities lead to a safe operating state:

$$\delta p_{n,\min} \leq \delta p_n \leq \delta p_{n,\max} \qquad\qquad n = 1,\ldots,n_{\text{FA}} \qquad (2.1)$$
$$\delta q_{n,\min} \leq \delta q_n \leq \delta q_{n,\max} \qquad\qquad n = 1,\ldots,n_{\text{FA}} \qquad (2.2)$$

Knowing these safe flexibility limits for all assets, two tasks remain for a flexibility-providing operator: Aggregation and, in case of a request, disaggregation of said request onto individual assets.

2.2.2. Aggregation of Distributed Flexibilities

At first sight, the aggregation of safe flexibilities is straight forward: since all combinations of setpoints inside the upper and lower limits for active and reactive power are safe to be provided, summing up all $\delta p_{n,\max}$ results in an upper bound for active power, summing the $\delta p_{n,\min}$ leads to a lower bound. Of course, the same is valid for reactive power. However, losses have to be considered to not over- or underestimate the provided flexibility. These losses or avoided losses are dependent on the state in the grid that is defined by the generation and loads injecting and drawing electrical power, and their spatial distributions. For example, such a state can be a "cold and windy winter day at noon", in which generation is dominated by wind-power in some area of the grid and the load is only little reduced by distributed PV generated electricity. In distribution grids, these states can also be differentiated between those in which the grid is net exporting electricity, and those where it is net importing.

Now, if the aggregated downward flexibility in active power ΔP^{down}, which is an increase in load or decrease in generation, is calculated in a state in which the providing grid is exporting electricity, a request for flexibility provision would result in a reduction of the exports or even to net import. Since transmission losses depend on the line loading, a reduction in export of electricity will lead to less losses and the flexibility aggregating grid operator can actually provide more flexibility than what a simple summing up of the individual flexibilities would return. The opposite is valid if the request for flexibility leads to higher line loading, increasing transmission losses and therefore a decrease in the flexibility that can be provided.

The flexibility-requesting TSO does not know, what the difference in summed up individual and properly aggregated flexibility will be. All he needs to know is how much flexibility is present at which time. However, if the distribution grid has several GICPs to the transmission grid, it is also important how much of the flexibility is provided through which GICP. Figure 2.2 shows this in an example with one wind-turbine in a simple distribution grid with two GICPs. In this case, the wind-turbine is a flexible energy resource connected to the distribution grid at the bus with number 4 . Flexibility provided by this resource will be distributed among the GICP inverse proportional to the impedance of the branches connecting the flexible energy resource to the respective GICPs. In this example, about 30 % of the flexibility is available at the GICP slack-bus 1 and about 70 % at the slack-bus 2.

2.2.3. Multiple Grid Interconnection Points Influence Flexibility Provisioning

Calculating power-flows in an electrical grids is performed by solving systems of equations. To set up these equations, buses have to be categorized by the available information about them to calculate the unknown power-flows. As a function of the known information on buses, they are grouped into three categories:
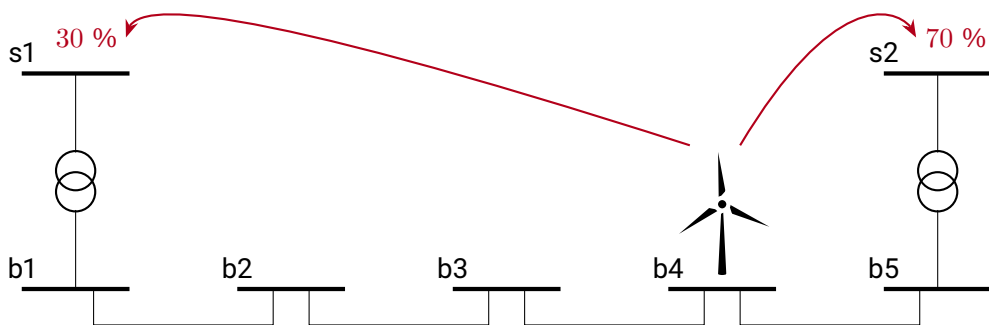
Figure 2.2.: Example for the distribution of flexibility in a distribution grid: About 30 % of the flexibility provided will be available at the slack-bus s1 and about 70 % at slack-bus s2.

- *PQ*-nodes, whose active and reactive power injection or demand is known,

- *PV*-nodes with variable reactive power injections that keep voltages at a fixed setpoint, and

- *Vϑ*-nodes or slack-nodes, which inject or take up the remaining power to balance the system. For at least one of the slack-nodes, the voltage angle is set to a fixed value to take the role of a reference angle.

For the distribution grid, all GICPs are slack-buses, since they balance the missing or surplus generation and have fixed voltage angles, which can also lead to additional power-flows in the distribution grid. Figure 2.3 depicts this phenomenon: A voltage angle difference on the slack-buses leads to a power-flow not only in the transmission grid, but also in the underlying distribution grid. The share of the power-flow that is transmitted via both paths is proportional to the admittances, as they form a parallel connection. As the transmission grid is a more direct route with a greater admittance or smaller impedance, a large part of the power-flow will be transmitted via this route. Also, if superimposed power-flows grow too big, DSOs can open circuit breakers and open loops to change the topology of their grid to reduce superimposed preload.

For the calculation of the technically safe flexibility *F*, the power-flow across the overlying grid is not of importance. However, the superimposed power-flow in the flexibility-providing grid can reduce or increase the flexibility that can safely be provided at the GICPs. If the superimposed power-flow is in opposite direction to the power-flow change caused by

transmission system power-flow $\sim \vartheta_2 - \vartheta_1$

s1, ϑ_1

s2, ϑ_2

superimposed power-flow in distribution system

b1   b2   b3   b4   b5
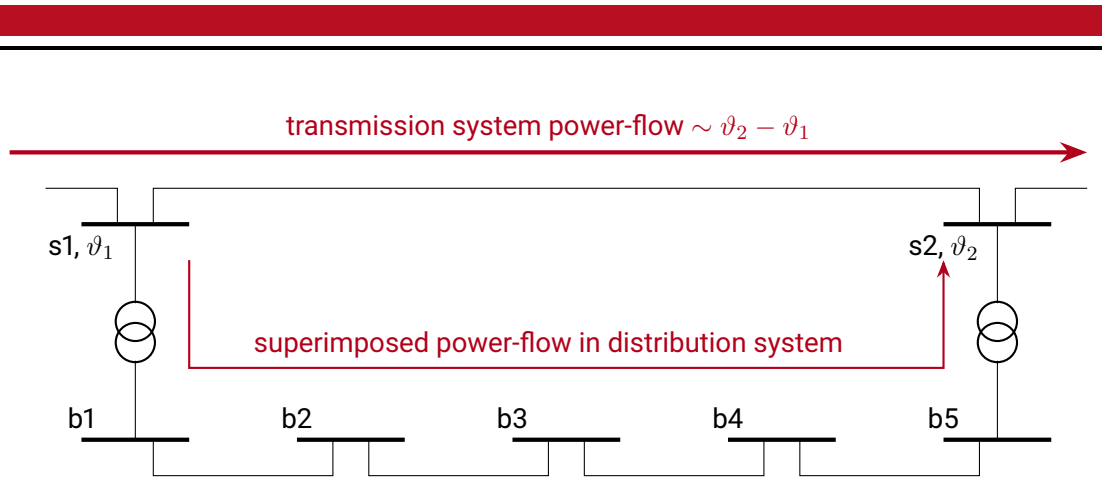
Figure 2.3.: A power-flow in the transmission system proportional to the voltage angle difference $\triangle\vartheta = \vartheta_2 - \vartheta_1$ causes a superimposed power-flow in the distribution system, leading to a preload on its power lines.

flexibility provision, they cancel out and more flexibility can be provided. In the opposite case, if both power-flows are in the same direction, they sum up leading to a reduction in the provision. Another more special case is a malfunction in one of the overlying transmission grid lines, in which case the superimposed power-flow in the distribution grid can suddenly and drastically increase due to shifts in the voltage angles.

Algorithms aggregating distributed flexibility for both preventive and curative operation need to be able to include superimposed power-flows, as they can significantly change the amount of flexibility that can be provided safely.

2.2.4. Runtime Requirements in Curative Operation

Another aspect of great importance for curative operation is the necessary speed the algorithm has to deliver. To use distribution system flexibility in a curative transmission operation regime, its potential has to be evaluated several different times during the planning and operation processes. Figure 1.4 shows the planning processes of TSOs. To keep the same reliability as in preventive operation, curative operation is only performed if enough operational degrees of freedom are available. This means, that not only during the business day, but also in the DACF and WAPP an estimate of flexibility needs to be available for power-flow calculation and contingency analysis. These estimates are not time sensitive as they are not performed in real-time. Tools like [142] can be used for such purposes if they are adapted to function with several GICPs. During the business day in the close-to-real-time operation, however, short

cycles are required to deliver precise and up-to-date calculations of aggregated flexibilities. If a request for flexibility is posted to the DSO, not only the pre-calculated amount of flexibility, but also the disaggregation of the requested amount onto the flexible energy resources must be present any time.
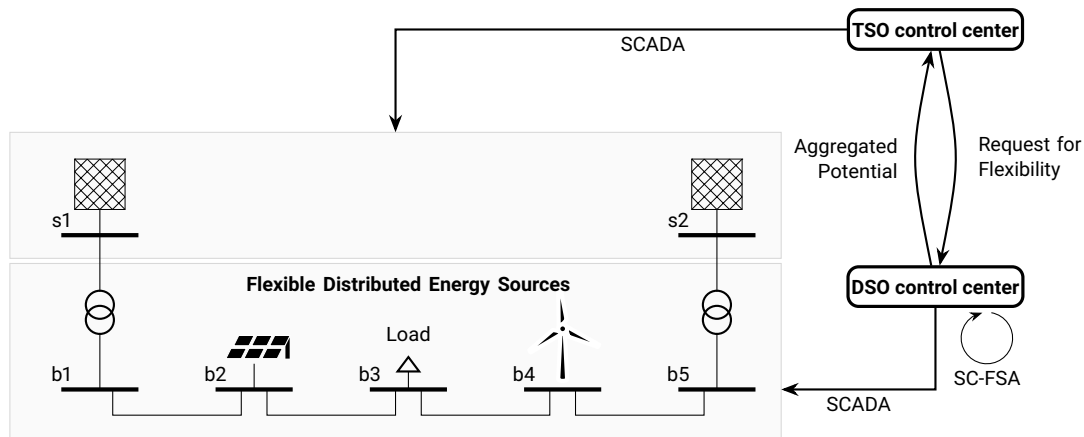
Figure 2.4.: TSO and DSO control centers have communication protocols between each other and control their respective responsibility area. The DSO aggregates flexibility from DER in his grid and, if a request for flexibility is issued, instructs the DER to adapt their power injections. To always know what amount of flexibility can be offered, the security constrained flexibility service agent (SC-FSA) is running continuously in the background.

Figure 2.4 depicts the concept developed in the InnoSys project for aggregating and provisioning of distribution system flexibility. The DSO, who is the connecting grid operator for three exemplary flexible energy resources, does not give away any degree of control, because all requests for flexibility run through his control center. In the DSO control center, the newly developed security constrained flexibility service agent (SC-FSA), which includes algorithms to aggregate F and calculate its distribution onto the GICPs, is running continuously to ensure the offered amount of flexibility is indeed present and safely deliverable. Also, in case of a request for flexibility, the disaggregation of the desired amount onto the individual assets is pre-calculated to ensure a quick execution of the provisioning process. In the context of the InnoSys consortium, this concept is tested in a demonstrator, where both the distribution and the transmission grid are simulated and a model TSO control center is used to test the provisioning of distribution system flexibility.

Summary

In this chapter, the basic requirements to use distributed flexibility sources for curative n-1 safe transmission grid operation have been introduced:

- The safe flexibility set F includes the setpoint ranges in active and reactive power that can be offered and provisioned to the TSO without violating any operational limits or boundary conditions. It is a subset of the initial flexibility set $F^{(0)}$, which is the sum of all flexibilities in the responsibility area of a DSO.

- Since handling many hundreds or thousands of flexible energy resources is not feasible for a TSO and because the DSO needs to remain in control over all energy resources connected in his grid, aggregation functions are necessary. Such a function aggregates the individual flexibilities in F and calculates the distribution to the GICPs between the DSO and TSO.

- In order to improve resilience against losses of GICPs and to reduce power-flows inside the distribution grid, transmission and distribution grids have several GICPs. Small grids might only be connected via two GICPs, while larger grids have close to ten or more. Power-flows over the transmission grid can lead to superimposed flows in the distribution grid, which can reduce F.

- In curative operation, speed is of the essence. Measures have to be executed within timescales set by the TATL and must be guaranteed to be ready if needed.

An algorithm or program of several algorithms for provisioning distribution grid flexibility in a curative regime must be able to meet all the above conditions: It has to quickly calculate the F, with possible superimposed power-flows from the transmission grid, and aggregate the flexibility onto the GICPs.

Part I.

Flexibility Potential from Distribution Grids for Curative Transmission Grid Operation

---

The modeling framework, method, and results in this part of the thesis closely resemble the paper [64].

3. Modeling of the Flexibility Potential

In this chapter, the modeling framework used to calculate the potential of distribution grid flexibility is introduced. In the scope of this thesis, the regional extent of the energy system model is limited to a scenario of Germany in the year 2030. This scenario models about 200 GW of installed electricity generation capacity from wind-power and PV, but the framework and methods can also be applied to other scenarios and energy systems.

3.1. Modeling Framework

The Energy System Development Plan (ESDP) is an energy system modeling framework used in this thesis to model a German energy system. The framework was initially developed in a cooperation of RWTH Aachen and Siemens Technology and is currently being maintained by TU Darmstadt and Siemens Technology. A description of the framework itself can be found in [103]. Using the framework, it is possible to model sector-coupling energy systems in an integrated way, including transmission of electric power, pipelines for hydrogen and natural gas, and boundary models of reduced complexity for enhanced realism. Different optimization suites can be coupled, allowing for linear and non-linear programs as well as mixed-integer program. The results of a modeling run are schedules for all simulated assets, necessary capacity additions, costs, and modeled emissions.

A model in the ESDP framework consists of several components:

- Modeling equations: A set of equations describing the objective function and boundary conditions. These equations are provided by the framework and are not regularly modified for a model.

- Commodities: Depending on the desired complexity and scope of the model, different commodities are modeled. Examples for commodities are not only electric power or heat, but also coal or biomass.

- Conversion processes: Conversion processes can convert one or combination of commodities another. A coal-fired power plant for example converts coal to heat, electricity, and losses.

- Transport processes: To transport a commodity from one region or country to another, a transport process is needed. Electricity can only be transported between regions, if the modeled transport capacity is existent and sufficient.

- Data: Both technology data as efficiencies and costs as well as capacity curves from RES are needed to provide the framework with the necessary information to simulate a realistic model.

- Scenarios: Each model can be simulated in several scenarios, which can differ in general conditions as for example cost of capital or CO_2-prices.

In the following, these components are introduced.

3.1.1. Modeling Equations

The central objective function used in the framework is a total cost optimization of both capital expenditure (CAPEX) and operating expenses (OPEX) while CO_2 or other emission limits can be set and CO_2 costs be added. The objective function is:

$$\min(\text{CAPEX} + \text{OPEX}) \tag{3.1}$$

There are different boundary conditions that restrict the solution space if wanted:

- The most important boundary condition is the necessity that demands for all commodities have to be supplied at all times and places. Some parts of the demands can be shifted in time. However a large part of the a demand has to be supplied for each modeled region and time-step. To match both supply and demand in times with surplus power, a slack variable is introduced. This boundary condition can be formulated the following way:

$$\sum_{\text{Cp}} Ca^{\text{gen}}_{\text{Cp},t,x,c} + trp^{\text{in}}_{t,x,c} + Slack_{t,x,c} = \sum_{\text{Cp}} Ca^{\text{dem}}_{\text{Cp},t,x,c} + trp^{\text{out}}_{t,x,c} \qquad \forall\, t,x,c, \tag{3.2}$$

where t is the time variable, x the spatial variable, c the commodity. Cp stands for the conversion process generating (left side) or consuming (right side) the commodity with capacity Ca, while trp denotes the transport which transmits the commodity c in and out of the region x at time t.

- CO_2 or other emission boundaries: The framework offers the option to include both a price for emissions and a limit. If an emission price is set, costs are included according to the emission factors given to the model. These costs are added to the OPEX and

help determine a new, cost optimal result. If an emission limit is set, the modeling framework will calculate a price for emissions which is set by the costs that are needed to keep emissions inside the limit. If both price and limit are provided to the optimizer, a shadow price emerges if the emission price is not enough to lead to a modeled state obeying the limit. Otherwise, the given price is set as the minimum. The boundary condition can be formulated the following way:

$$\sum_{t}\sum_{x}\sum_{Cp} emission(Cp, x, t) \leq \max(emission) \tag{3.3}$$

In essence, summed emissions in the modeled time period need to be equal or less than the given allowed maximum.

- Temporal availability: For conventional energy sources, an availability factor is used to determine if total installed capacities are sufficient. In the case of renewable energy sources with a high variability in availability, time-series are used to describe if and to what extend the renewable energy sources (RES) can supply power. Each conversion process can only be used to the extend given by the temporal availability:

$$Ca_{Cp,t,x,c} + Slack_{t,x,c} = Avail_{Cp,t,x,c} \cdot Ca_{Cp,x,c} \qquad \forall\, Cp, t, x, c \tag{3.4}$$

In words, this equation denotes that the capacity of a conversion process at time t and region x producing or consuming commodity c is equal to the availability for that process times its time independent capacity. The slack variable is used to account for surplus generation.

- Spatial availability: Similar conditions as for temporal availability are also valid for spatial availability. An example are lignite power plants: Due to the low energy density of lignite, it is mined and burned in close proximity. There are only few lignite powered power plants that do not have direct access to a lignite mining pit[1]. The spatial availability is not only important for capacity additions, but also for initial capacities that can be given as regional distributions:

$$Ca_{Cp,x,c} \leq Avail_{Cp,x,c} \cdot Ca_{Cp,c} \qquad \forall\, Cp, x, c \tag{3.5}$$

Again describing the equation in words, the capacity to produce or consume a commodity c via the conversion process Cp in region x is limited to the availability for this conversion process and commodity.

---

[1] One exception to the rule was the Kraftwerk Klingenberg in Berlin, which was lignite fired until 2017 [166].

- Inter-regional distributions, as for example electrical grids or pipelines, are also subject to the spatial availability boundary conditions. In this case, the availability is not bound to one region, but to a combination of two regions. In the scope of this thesis, grid expansions are not considered, but an existing grid is given.

- There is a range of additional boundary conditions, that are needed to achieve the degree of realism necessary to answer the research question. Those are:
    - Transport restrictions for the commodities.
    - Minimum capacity factors: Lignite power plants, for example, are not commercially viable, if they only run half a year.
    - Proportions of energy output: Even in cogeneration of heat and electricity, the respective shares are not freely adaptable.
    - Must-run times: Certain technologies have a fixed, often uniform energy output.
    - Storage restrictions: commodities can only be stored up to a boundary set by the modeled storage capacity.
    - C-rates: The C-rate of an energy storage unit is the ratio of its output or charging power to its storage capacity. For home-storage batteries this ratio is often close to one, for grid boosters, it is closer to four, resulting in the fact that they can run at full power for one fourth of an hour.
    - Technologies: For each technology, a range of data is provided to the optimizer: OPEX and CAPEX, lifetimes, capacities, spatial and temporal availability, emission factors, efficiencies, and more, depending on the respective technology.

3.1.2. Commodities and Conversion Processes

Commodities are not only objects that can be touched like a piece of coal or a bucket of oil, but also services as the transport of a person or a piece of cargo for a certain distance. To determine the optimal use of the input energy, demands are set in useful energy demands, as for example kWh of low-temperature heat or person-kilometer. The optimizer then has several options to satisfy the useful energy demands using different conversion processes or combinations of conversion processes. Heat, for example, can be either generated by burning natural gas at home or by burning it in gas-turbine in a power plant and using the generated electricity to operate a heat pump. The optimizer will choose the cost-optimal solution. This results in all transport being done via public transport, walking, or bicycles, which is optimal in terms of costs and CO_2 emissions, but not realistic. Therefore, output shares can be used to define how much of each commodity is supplied by which conversion process. As the

model here is not used to calculate additional capacities needed in a future energy system, but mainly to solve a dispatch problem, these output shares are given by the scenario and existing capacities.

In dependence of the desired modeling details and process, conversion processes have many sub-processes. Burning hard coal in a coal-fired power plant for example, is modeled by converting chemical energy bound in hard coal to thermal energy in hot steam, to electrical energy, district heat, and losses. For conventional power generation sources, these processes contain several steps, as outlined above, while for renewable energy sources, they are more simple, for example from solar irradiation to direct current in the solar cell to alternating current, which can be injected into distribution grids.

3.1.3. Transport Processes and Regions

In the ESDP framework, regional modeling is supported. This means, that the optimizer solves the optimization problem for each defined region itself while also optimizing the total system. If regions have no connections to other regions via inter-regional distributions, which are used to model transmission capacities, the regions act individually and are optimized separately. This means, that for each region capacities, costs, and operation schedules are determined without influence from other regions, only defined by their own time-series and variable sets.

All commodities are transported without any barriers or losses inside the regions where they are generated. For electricity this means, that a region is modeled as a single bus in a grid model. Sometimes, this concept is called "copper-plate", as the electricity is available everywhere without losses in a region. For transport between regions, the process is either explicitly modeled, allowed, or disallowed, depending on the commodity that is to be transported. The transport of electricity, for example, is explicitly modeled: a grid is included in the model, upon which an exchange of electricity is possible according to the modeled capacities. In the case of hard coal, a free-flowing transport is assumed. This means, that hard coal can be imported in every region of the model. An example for the third case, disallowed transport, is heat. Heat can only be used in the region where it is generated.

If transport of a commodity is possible, the optimizer has the option to shift its production from one region to another. This will happen, if the result has lower total costs. If transmission capacities are explicitly modeled, losses can be added to increase the degree of realism.

In the model developed here, not only Germany is modeled, but also its grid-neighboring countries, those that share an interconnector with Germany. Those countries are: Poland, Czech Republic, Austria, Switzerland, France, Luxembourg, Belgium, Netherlands, Great Britain, Denmark, Norway, and Sweden. Germany itself is split into 38 regions, whose boundaries or borders are defined by the European NUTS 2 classification. This spatial

resolution is chosen to be able to correctly model the international electricity exchange due to varying renewable energy injections and to model German regions in the approximate size of larger HV distribution grids.

In order to answer the research question and to calculate the flexibility potential from distribution grids for curative transmission system operation, is is necessary to know when the transmission system is in a state where a malfunction leads to a critical state. To get this information, a model of the transmission grid is needed with its operation schedule.

To obtain this information, a German transmission grid model that is planned to be in place in the year 2030 was supplied by the four German TSOs. This model is transformed from the Common Information Model [167] (CIM) standard into a Matpower format [168]. This Matpower format is a simplified model, where the modeling detail is reduced to a bus-branch model from the CIM model, which includes circuit breakers (node-breaker model). The Matpower model is then transformed into a inter-regional distribution readable in ESDP, more details to this process can be found in Subsection 3.2.5.

3.1.4. Data and Scenarios

Data is provided to the framework in different forms: point data, as for example an efficiency, a capacity, or a price, and multi-dimensional data. Multi-dimensional data can be a time-series for a demand or the distribution of a capacity among regions.

Scenario data is used to quickly set the model into another surrounding without the need to completely rewrite it. If, for example, the effects of a change in weighted average cost of capital (WACC) onto the installation of additional PV-capacity is analyzed, the scenario data is changed while the rest of the model remains the same.

In the following section, the process of preparing the necessary data for the modeling process is detailed.

3.1.5. Framework

Figure 3.1 shows the general setup and modeling process in ESDP: Input data to define variables and boundary conditions are defined in a spreadsheet and turned into an optimization problem using GAMS [169]. An optimizer, in this case CPLEX [170], is used to read the problem and solve it. The results can then be read and analyzed.

3.2. Data and Scenario Preparation

Figure 3.1 conceptually shows the input data for the optimizer. In this section, the data used for the model and the process how to make it accessible for the ESDP framework are outlined.
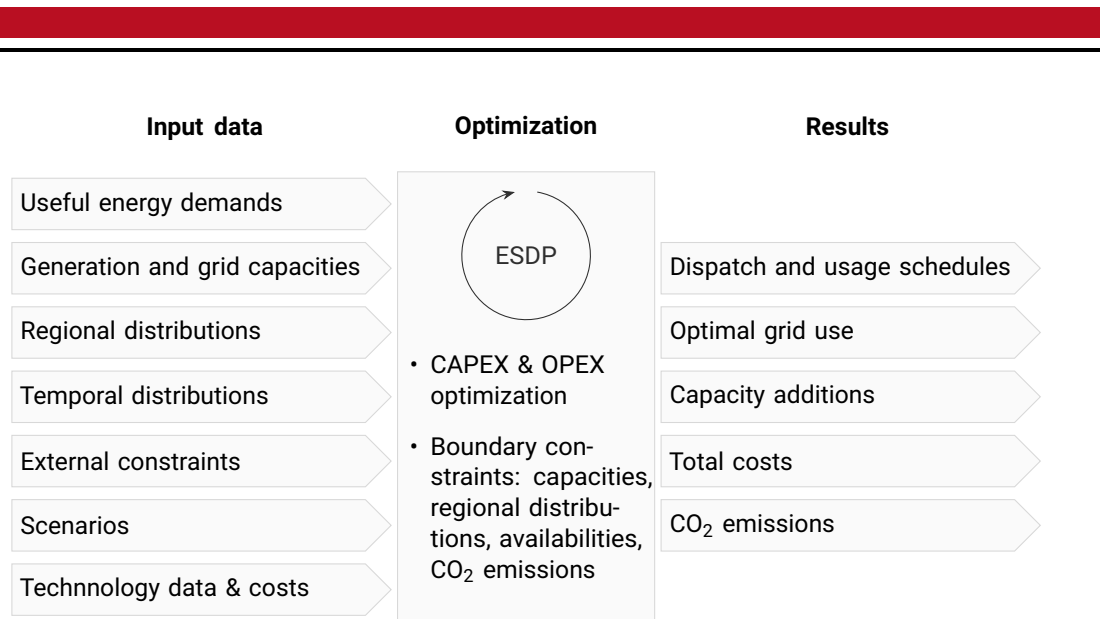
Figure 3.1.: The structure of the energy system modeling process with ESDP.

3.2.1. Technology Data

Technology data is all data that defines how conversion processes work. In table 3.1, the sources for the different technologies are found. CO_2 data was provided by the TSOs and stems from the Netzentwicklungsplan 2019 [98].

Table 3.1.: Technology data in the energy system model and its sources.

Conversion process	Sources
Biomass plants	[19], [171]
P2G & P2H	[146], [147], [172], [173]
Conventional power plants	[19], [56], [174]–[177]
RES	[176]
Miscellaneous	[178]–[181]

This technology data defines the following characteristics of the conversion processes:

- CO_2 emissions in kg/kWh

- Storage efficiencies:Round-trip efficiency when storing and later withdrawing energy in this conversion process.

- Maximum efficiencies and energy splits: The ration between input and output energy. For example in a combined cycle gas power plant, up to 59 % of the chemical energy stored in the gas is converted into electrical energy, up to 36 % into district or central heat, and at least 15 % are losses.

- Maximum market shares: Electric cars are much more energy efficient than those using an internal combustion engine. Therefore, the optimization process will prefer e-cars. However, in the scenario the assumption is that only 10 million e-cars are in use in 2030. The ratio between the output commodity provided by both technologies can be set according to the share of e-cars in the transport system.

- Technical and financial depreciation periods, investment costs, and operational costs are needed to determine which technology can provide a commodity at the lowest cost.

- Minimum capacity restrictions: Lignite and coal power plants are not able to run just for a few hours, since each time the power plant is turned on and off reduces the lifetime significantly, as it is also a function of its thermal cycles. In addition, lignite power plants are bundled with open pit mines, that constantly need energy for pumping out groundwater. Not running the power plant therefore puts the operator under great financial stress, leading to the power plant nearly always running.

3.2.2. Time-Series

Many parts of an energy system are time dependent: demands are higher during the day than during the night, weekdays higher than weekends, and the earths orbit and inclination put more irradiation onto Germany in summer than in winter, while the weather provides more wind during winter than summer. All these phenomena need to be taken into account to model different states in the energy system. Some time-series data is only available on national levels, other data is resolved in smaller units and will be referenced in Subsection 3.2.4.

In Table 3.2, the sources for the time-series data used in the model are referenced. Heat demands are further split between decentral, district, and industrial heat. Run of river data, is only available as an averaged time-series and is split between the regions according to the installed capacities.

Table 3.2.: Time-series data in the energy system model and its sources

Conversion process	Sources
Electricity demand	[98]
Heat demand	[182]
Run-of-river availability	[98]

3.2.3. Regional Data

Each region in the model, these are 38 German regions and its 12 grid neighbors, has different installed capacities, technologies, and demands due to their population, industry, and regulatory framework. In France, for example, electricity is generated mainly by nuclear power plants, while in Germany those are not in place any longer in 2030. Lignite power plants are installed in Poland, North Rhine-Westphalia, Saxony and Brandenburg, while in other German regions there are no lignite or even hard coal power plants. Offshore wind-power can only be installed offshore, which is impossible in Bavaria or Switzerland and so on. To model these phenomena, regional distributions are used.

Sometimes, regional distributions are also used to allocate time-series onto regions, as for example with heat demands in Germany, which are allocated according to 50 % population and 50 % GDP. This disaggregation method is an assumption, but also in use in [183]. In addition, less than 10 % of the heat demand is supplied by electricity in the modeled scenario. This means, that the distribution onto the regions does not play a role as long as sufficient demand in heat is available in each region.

Table 3.3.: Regional data in the energy system model and its sources.

Conversion process	Sources
Electricity & heat demand	[184]
Non-German heat demand	[182]
Installed generation capacities	[98]
Non-German generation capacities	[159], [160]

International data is taken from an internal unpublished study at Siemens, which is based on the ENTSO-E's TYNDP and MAF. This data is used for all installed capacities outside Germany.

Figure 3.2.: Geographical scope of the energy system model. In addition to the 38 German NUTS 2 regions, there are 12 grid neighbors.

3.2.4. Time-Regional Data

Time-regional data is a combination of time-series data and regional data, essentially regionally resolved time-series. This data is used if time-series are very different for different regions, for example solar irradiation is very different in Bavaria than it is in Sweden.

The EMHIRES [185], [186] database offers regionally and temporally resolved capacity factors for both wind-power and PV. This data is used for the neighboring countries, while for Germany time-series are provided for individual wind farms. This data is aggregated to the NUTS 2 level in which the regions are modeled. As listed in Table 3.4, the demand time-series are taken from Heat Roadmap for Europe [182] and multiplied by the respective yearly energy demands from Eurostat [184]. Generation time-series for run-of-river and storage-hydro power plants, especially important in Sweden, Norway, and Switzerland, are also taken from [182].

Table 3.4.: Time-regional data in the energy system model and its sources.

Conversion process	Sources
International electricity demand	[182], [184]
PV capacity factors	[98]
Non-German PV capacity factors	[185]
Wind-power capacity factors	[98]
Non-German wind-power capacity factors	[186]
Offshore wind-power capacity factors	[98]
Non-German hydro capacity factors	[182]

3.2.5. Inter-Regional Data

The ESDP framework includes grid data as inter-regional data. The optimizer has the option to instantaneously shift commodities from one region to another via inter-region links that have an associated capacity. In a real world scenario, this would be similar to a grid with completely controllable power-flows, e.g. a HVDC grid or one with PSTs at every node. Inside the regions, power-flows are unrestricted and losses are added via additional conversion processes representing the transmission and transformer losses.

The inter-regional distribution representing the grid is derived by taking a real grid model and calculating the transmission capacity between pairs of regions. This is done via a process in which the power injection in one region and the load in the other region is increased until operational boundaries are violated. If the grid is operated preventively n-1 safe, a transmission reliability margin (TRM) of about 30 % of the resulting capacity is subtracted to mimic the operation in real-life. This factor of 30 % is calculated taking the square root of the number of connections between regions and multiplying it with a safety factor of 100 MW. This TRM is individually calculated for each connection between two regions.

An inter-regional distribution with optimally controlled power-flows is not a real grid with AC-power-flow, but it is an approach often taken and sufficiently exact to be used in this context [187].

After converting the grid model from the CIM standard to a Matpower case format, the model is translated into inter-regional data in the process outlined above. Interconnectors to neighboring countries are directly supplied with the grid data, therefore no transformation is necessary. Exports and imports are limited to 15 GW at all times, distributable onto the individual interconnectors by the optimizer. The thinking process behind the limitations is to model current political behavior, where countries try to protect local energy producers, for
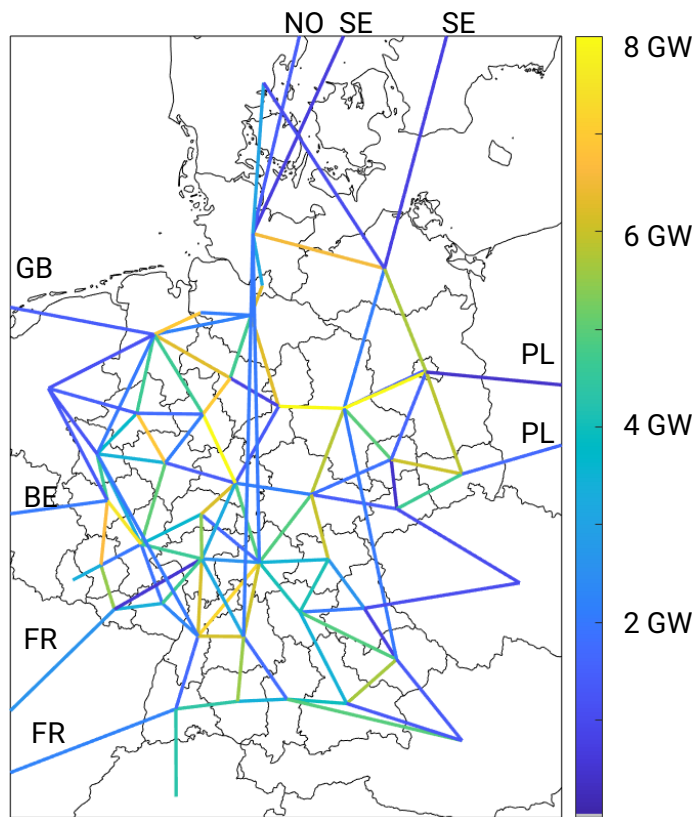
Figure 3.3.: Transmission grid as modeled in ESDP. Transmission capacities of corridors are encoded in color. Country codes are given where interconnectors leave the plotting area. Connection from Berlin to Brandenburg is barely visible as the distance between the center of both regions is very small.

example coal firing power plants in Poland. Already today, phase shifting transformer (PST)s are installed to reduce power-flows caused by RES from Germany into Poland [188].

Figure 3.3 shows the inter-region data aggregated and used in this thesis. Some corridors, e.g. Saxony-Anhalt to Brandenburg or Brandenburg to Berlin have more than 8 GW capacity, but the scale is cut off to allow better comparison to other corridors in Germany.

3.3. Scenario Generation

The largest parts of the scenario are set by the Netzentwicklungsplan (NEP) 2030c. In the InnoSys consortium, a few changes are performed to adapt the scenario to be more in line with developments the grid operators are seeing or expecting to happen. Changes include a shift of 1 GW offshore wind-power from the North Sea to the Baltic Sea and 10 million e-cars in Germany. The scenario in the surrounding countries is taken from the associated European

plans, MAF and TYNDP.

3.3.1. German Regions

For Germany, the scenario data is plotted in Figure 3.4. The installed capacity reaches almost 300 GW, with over 104 GW PV, 86.5 GW onshore and 17 GW offshore wind-power. Nuclear power plants are phased out, and there is 9 GW lignite power plant capacity and 8 GW hard coal power plant capacity remaining. Natural gas capacity slightly increases from 29.6 GW to 33.2 GW.
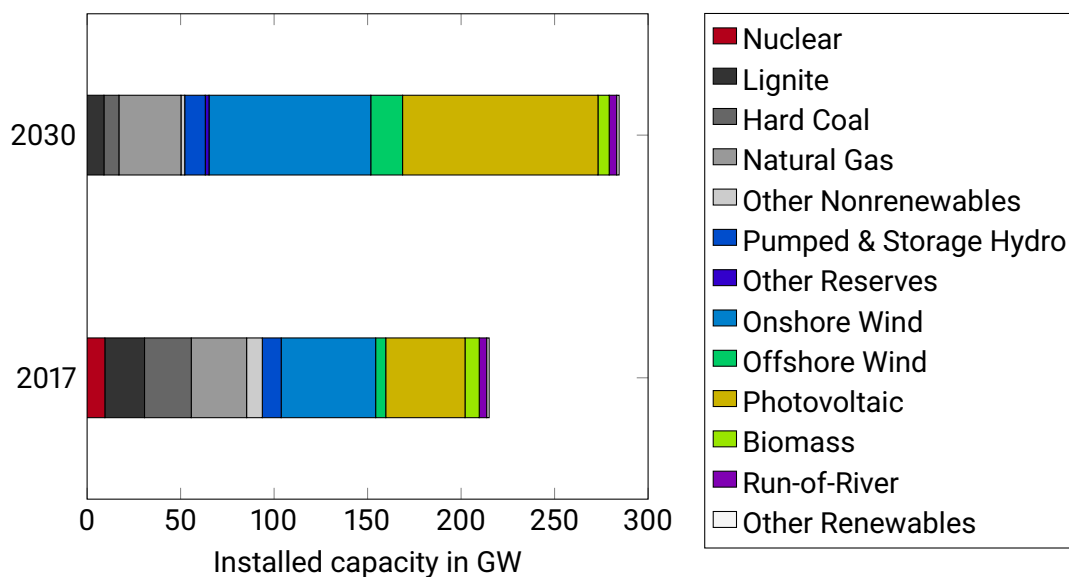
Figure 3.4.: Scenario data for Germany in the energy system model: Installed generation capacities in Gigawatt.

In addition to these generation capacities, there are 16.1 GW[2] power to heat (P2H) and 3 GW power to gas (P2G) capacities[3], 10.1 GW PV home storage batteries, 6 GW demand side management (DSM), 10 million e-cars and 4.1 GW heat pumps.

---

[2]Power to heat only refers to resistive heaters, as heat-pumps are modeled separately.
[3]2.4 GW Power-to-hydrogen and 0.6 GW Power-to-methane.

3.3.2. Neighboring Countries

In Table 3.5 the installed capacities for the neighboring countries in the model are listed. These stem from [160] and [159]. Values smaller than 50 MW have been omitted from the table but have been included in the model. This concerns values for Luxembourg and run-of-river capacities in Denmark. Tidal power plants are not expected to be rolled out in 2030 in meaningful numbers, as well as wave-power or other more exotic power generation techniques.

Table 3.5.: Installed generation capacities in neighboring countries in 2030 in GW. Values smaller than 50 MW are omitted from the table.

GW	AT	BE	CH	CZ	FR	UK	LU	NL	NO	PL	SE	DK
Nuclear	0	0	1.1	4	52.2	5.7	0	0.5	0	0	6.9	0
Lignite	0	0	0	4.8	0	0	0	0	0	7.4	0	0
Hard Coal	0	0	0	0.3	0	0	0	0	0	13.8	0	0
Gas	4.2	6.4	0	1.4	11.5	30.8	0	12.2	0.4	5.7	0	0.4
Onshore Wind	5	3.3	0.4	1	36.3	16.1	0.2	6.7	3.3	9.2	9.2	5.6
Offshore Wind	0	2.3	0	0	7	22.2	0	11.5	0	2.3	0	2.3
PV	4.5	5.1	5.6	3.5	31.4	24.5	0.2	11.4	0.4	2.4	1.3	2.9
Run-of-River	4.7	0.1	4.1	0.4	13.6	0.1	0	0.04	34.5	1	15.8	0
Pumped and Storage Hydro	10.8	1.3	13.6	1.0	13.5	1.8	1.3	0	1.3	1.4	1.8	0

Summary

In this chapter, the modeling approach and assumptions to create a model capable of serving as a basis to calculate the potential of distributed flexibility sources for curative n-1 safe transmission grid operation are outlined. The key aspects are:

- The objective of the modeling approach is cost optimization, minimizing capital expenditure (CAPEX) and operating expenses (OPEX).

- Boundary conditions include temporal and spatial restrictions, matching of demand and supply, export/import restrictions, as well as CO_2 emission limitations.

- Formulating demands in useful energy provides the optimizer with the ability to chose the best combinations to generate commodities.

- Regionalization is necessary to model grids and grid restrictions, while in the regions commodities are assumed to flow freely. The correct scope in the regionalization is not only dependent on the research questions that need to be answered, but also a function of available computation time, manpower, and data. Since the knowledge about a future energy system is limited, more data and a higher amount of details can easily lead to fictitious accuracy.

- The modeled scenario is dominated by large amounts of renewable energy sources (RES), especially wind-power and PV, which together amount to about 200 GW capacity.

All the data and boundary conditions that are listed above are used to create an energy system model with the purpose of determining the distribution system flexibility potential. However accurate the method and the model might be, the results are only directly applicable in the scenario that is chosen. Nevertheless, some phenomena will appear in many scenarios and can be considered robust, as for example the mismatch of generation capacities and installed loads, which leads to curtailments of renewable energy sources (RES).

4. Method for Calculating the Flexibility Potential

This chapter describes the method to calculate the potential of distribution system flexibility. Basis of the method is the energy system model characterized in the previous chapter. Two of the methods to determine the flexibility potential from distribution grids developed during the course of the thesis are explained in detail in the following sections.

4.1. Sources of Flexibility

For both methods, to allow for comparability, the sources of flexibility are the same. These sources are assigned to one of two categories: upward flexibility ΔP^{up} or downward flexibility ΔP^{down}. Upward flexibility can be generated by increasing power injection or decreasing loads, while for downward flexibility the opposite is true. Downward flexibility is used on the power injecting side of the grid to reduce power injections, while upward flexibility is needed at the receiving side for balancing.

4.1.1. Selection Criteria

Methodologically, all modeled assets, that are able provide flexibility, can be included in the determination of the flexibility potential. As the focus here lies on curative grid operation, the choice of the sources considered in the calculation is governed by two aspects:

1. The asset providing the flexibility is connected in HV-grid or

2. The asset is already used for real-time flexibility provision somewhere in the world.

Both aspects are formulated because of the time restrictions in curative grid operation: In many countries, as for example in Germany, different voltage levels are operated by different operators. Each operator included in a call for flexibility contributes to an increase in the activation time because of delays caused by communication and calculation times needed for a safe grid operation. Even for a single operator, these calculations have to be performed

on each voltage level separately if the grid model does not include all voltage levels. In Subsection 2.1.1, possible sources of flexibility are listed and their qualities with respect to curative grid operation determined.

4.1.2. Allocation to Voltage Levels

Due to the time delays that increase with each grid or voltage level, in this thesis the focus lies on the first voltage level below the transmission grid, namely the 110 kV HV grids, sometimes called sub-transmission grids. The data provided by the grid operators and used in the energy system model described in the previous section does not include this information. In [24], a breakdown of the installed capacities per technology and voltage level can be found. This data is considered trustworthy as it is collected by the regulatory authority.
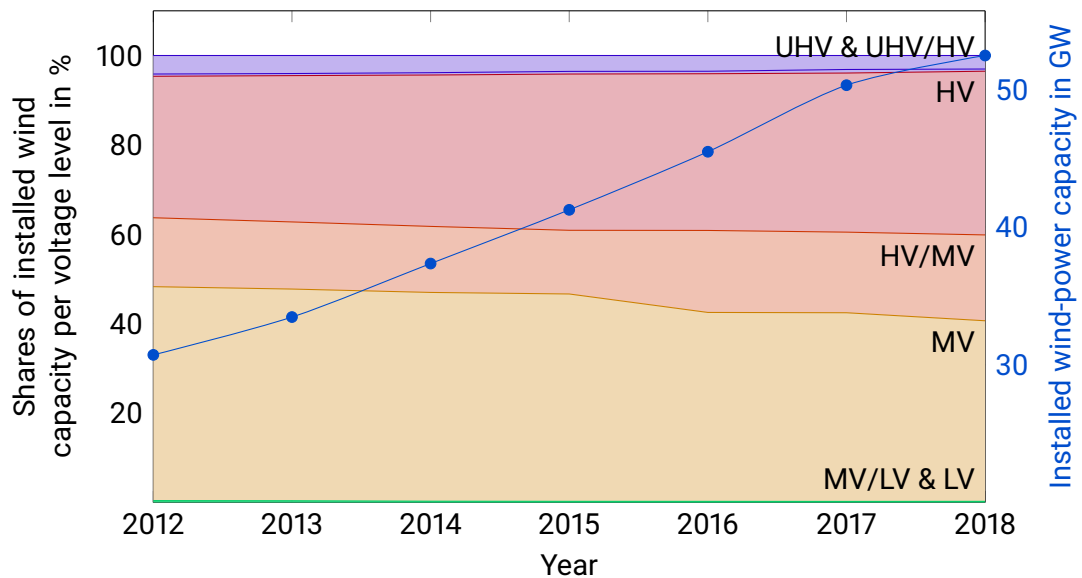
Figure 4.1.: Installed wind-power capacity shares per voltage level in Germany and total installed capacity of wind-power (blue line). Data from [24].

With the help of this data, voltage level shares V_T as a function of the technology T can be determined. Based on this data, a trend can be deduced: In 2012, about 32 % of all wind-power was installed in HV and another 15 % in the HV/MV transmission level. Due to rising capacities of the individual wind-power plants and their rising penetration in the grids, connecting voltage levels rise, leading to about 37 % of the wind-power being connected in

HV in 2018 and another 19 % in HV/MV. Figure 4.1 shows the voltage shares and the total installed wind-power capacity in Germany.

If this trend of larger wind-power plants and therefore higher connecting voltage levels continues, about 40 % of the installed capacity can be assumed to be connected in the 110 kV HV grids in 2030 and another 25 % in the HV/MV level.

For PV in Germany, these numbers differ, as only 7 % of the installed capacity is currently connected directly via HV and via MV directly at HV stations. About 35 % are installed in MV distribution grids and another 54 % in LV. A trend for bigger individual installation sizes for PV in Germany is not visible in the data from [24]. It is hard to determine which share of installed PV capacities will be connected in which voltage level in 2030. This is especially true for Germany, where regulation for larger and smaller PV farms differs significantly, shaping the market in either direction depending on the current government.

Table 4.1.: Preferred voltage levels to connect loads in Germany. Data from the ARGE FNB OST [189], [190] via [52].

Power of the connected load in kW	Preferred voltage level
≤ 30	existing house connections
30 to 300	LV grid
300 to 6000	MV grid
6000 to 15 000	MV/HV transformer level
≥ 15 000	HV grid

In the German Renewable Energy Sources Act [36] it is stated, that the grid operators must choose the correct voltage level for RES that are to be connected to the grid. Normally, the closest grid is chosen. However, if another voltage level is determined to be more economically feasible, this voltage level can be chosen. Above a power injection of 30 kW, it is not clearly defined which voltage level is the correct one and the grid operator has to determine it.

For loads, the process is also not very strict. Table 4.1 shows an overview. Power-to-heat assets with power in the single to triple digit power ratings in megawatt are mostly connected in MV and high voltage, 60 to 110 kV (HV), also due to stability issues caused by the steep gradients possible with this technology.

The voltage allocation factors for each technology V_T can be approximated with this information, giving the possibility to estimate how much of the distribution system flexibility is installed in the first or second distribution grid level and therefore available in time for

curative grid operation.

4.2. Calculation via Simulated Redispatch

The first method that is used to get an approximate of the total flexibility potential is based on the market process in Germany: A dispatch and following redispatch process are simulated. At first transmission constraints are relaxed for the dispatch, then they are reintroduced for the redispatch. The method is performed in three steps:

1. Regionally resolved energy system model: To determine the capacities for the following modeling runs, in a first simulation the necessary capacities are optimized in the process while the grid is set as constraint. The results are saved and fed back into the model setup. This step ensures that there are enough capacities for all commodities.

2. Dispatch or market process: The grid constraints are relaxed so that at each time-step the electricity generators with the lowest costs are chosen to generate the necessary power. The output of this simulation run are dispatched power generator schedules $\bar{P}_T^{\text{disp}}$ and loads $\bar{L}_T^{\text{disp}}$. Both these variables are matrices, with operation schedules for each time-step and region for all relevant technologies T.

3. Redispatch process: The same input model as in step 2. is used, but this time the grid constraints are set to normal. This simulates the redispatch process as performed in Germany in the day-ahead congestion forecast (DACF). Results are $\bar{P}_T^{\text{red}}$ and $\bar{L}_T^{\text{red}}$.

After performing the simulation runs, results from step 2. and 3. are compared. They differ when transmission constraints are active in step 3. The difference $\vec{P}^{\text{diff}}$ can be expressed as a shift between stage 2. and 3.:

$$\vec{P}^{\text{diff}} = \sum_x \sum_T \left| \bar{P}_T^{\text{disp}} - \bar{P}_T^{\text{red}} \right|, \tag{4.1}$$

where the sums over T and x are over technologies and regions and the resulting vector is of dimension t.

By sorting the entries in vector $\vec{P}^{\text{diff}}$, an order from least necessary redispatch to most is obtained. This list shows when the grid is under the most duress and therefore might need flexibility. In essence, the method is not made to calculate the amount of flexibility, but to identify time-steps when flexibility is needed.

The amount of flexibility that is present at these critical time-steps can be determined from the results of the simulation in step 3. The flexibilities stem from the technologies chosen for each analysis and voltage level allocation can be performed with the factors listed in Table 4.1 and displayed in Figure 4.1.

4.3. Calculation via Correlation of Bottlenecks and Available Assets

A second method is developed to be able to correlate flexibilities with the transmission corridors for which the provided flexibility is needed. While in the first approach the result is the total flexibility present at critical time-steps, here only the flexibility from regions adjacent to congested transmission corridors is taken into consideration. This second approach is more suitable to quantify the flexibility that is indeed helpful to cure a temporary increased load on a branch in the transmission grid.
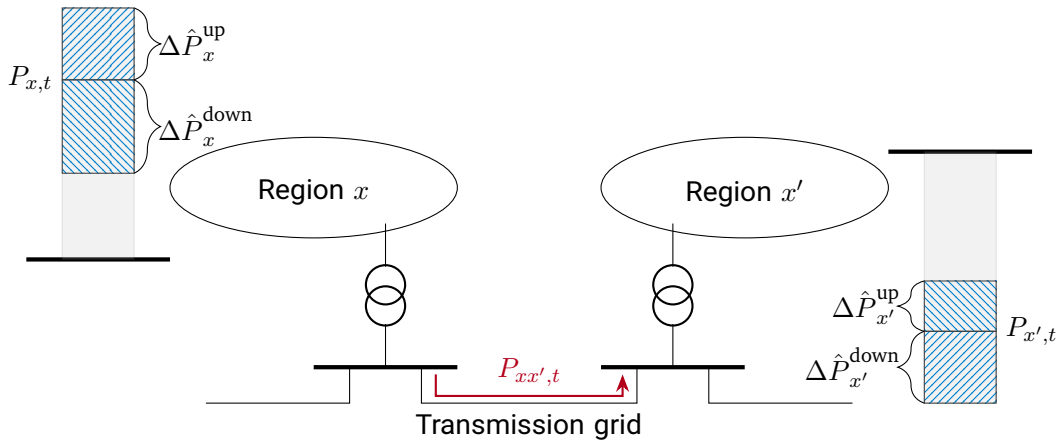
Figure 4.2.: Concept to calculate the flexibility potential available per corridor. A region x, injecting power $P_{x,t}$ into the transmission grid, provides an upward flexibility potential $\Delta\hat{P}_x^{\text{up}}$ and downward flexibility potential $\Delta\hat{P}_x^{\text{down}}$. The transmission grid corridor transports the power $P_{xx',t}$ between regions x and x'. Region x' imports power $P_{x',t}$ with flexibility potentials $\Delta\hat{P}_{x'}^{\text{up}}$ and $\Delta\hat{P}_{x'}^{\text{down}}$.

Figure 4.2 shows the concept for two regions x and x'. The power-flow $P_{xx',t}$ at time t is from x to x'. If a loss of transmission capacity occurs between both regions, upward flexibility $P_{x'}^{\text{up}}$ is needed in region x' and P_x^{down} is needed in region x to return to a safe state.

Not only the regions directly connected by the transmission corridor that is affected by the malfunction can contribute flexibility, but also neighboring regions can provide additional flexibility. In Figure 4.2, a region to the left of x could also provide downward flexibility ΔP^{down}, and a region to the right of x' could provide upward flexibility ΔP^{up} to even out the burden caused by the outage and help relieve the critical branch.

To determine when each transmission grid corridor is in a critical state, losses of transmission capacity are simulated using the results of a simulation of the energy system model. These results include the schedules or utilization factors for each modeled corridor, as the utilization is calculated by dividing the transmitted power $P_{xx',t}$ between two regions x and x' at time t by the maximal allowed capacity $P_{xx'}^{\max}$. Now, for all corridors and all times, a loss of 2 GW transmission capacity is simulated. This is the capacity a HVDC systems provides or a 380 kV power line with modern conductors:

$$380 \text{ kV} \cdot \sqrt{3} \cdot 3 \text{ kA} \approx 2 \text{ GW} \tag{4.2}$$

After such a transmission capacity loss, it is evaluated if the remaining capacity is sufficient to transmit the power on the corridor. If not, the time-step is added to the set of critical time-steps $t_{xx'}^{\text{crit}}$ for this corridor:

$$t_{xx'}^{\text{crit}} = \{t | P_{xx',t} > P_{xx'}^{\max} - 2 \text{ GW} \wedge P_{xx',t} > \frac{1}{2} P_{xx'}^{\max}\} \tag{4.3}$$

As given in Equation 4.3, another condition must also be satisfied for a classification as critical time-step: The transmission corridor usage at time t has to be at least half of its capacity $P_{xx'}^{\max}$, to be considered as a critical time-step. This condition is introduced to model corridors transmission capacity $P_{xx'}^{\max} < 4$ GW, as they consist of at least two parallel systems[1]. For example, if a corridor has a rating of $P_{xx'}^{\max} = 3$ GW and only 1.2 GW is used, a loss of 2 GW would only affect one of at least two parallel power lines, of which the other one still provides enough transmission capacity.

Figure 4.3 depicts a critical and a noncritical situation: While on the left, the power-flow $P_{xx',t}$ at time t is relatively high, so that a loss of 2 GW transmission capacity leads to a critical state, on the right $P_{xx',t}$ is lower, so that even after an outage the transmission corridor still has some remaining buffer and transmission capacity. The area that is colored in red on the left also depicts the amount of power that needs to be compensated to return to a safe state in which the restoring remedial action can be performed.

The power $P_{xx',t}^{\text{drop}}$ that needs to be compensated can be calculated using:

$$P_{xx',t}^{\text{drop}} = \min\left(\max(P_{xx',t} - (P_{xx'}^{\max} - 2\text{GW}), 0), P_{xx',t}\right) \tag{4.4}$$

The power that can be used for this task stems from the adjacent regions x and x' and, if not sufficient, from regions adjacent to them. To calculate the flexibility potential present at that time, a simple sum of admissible technologies T is sufficient:

$$\Delta \hat{P}_{x',t}^{\text{up}} = \sum_{T} \Delta \hat{P}_{x',t,T}^{\text{up}} \cdot V_T \tag{4.5}$$

---

[1]HVDC-systems are exempt from this rule, as they can't loose fractions of their transmission capacity.
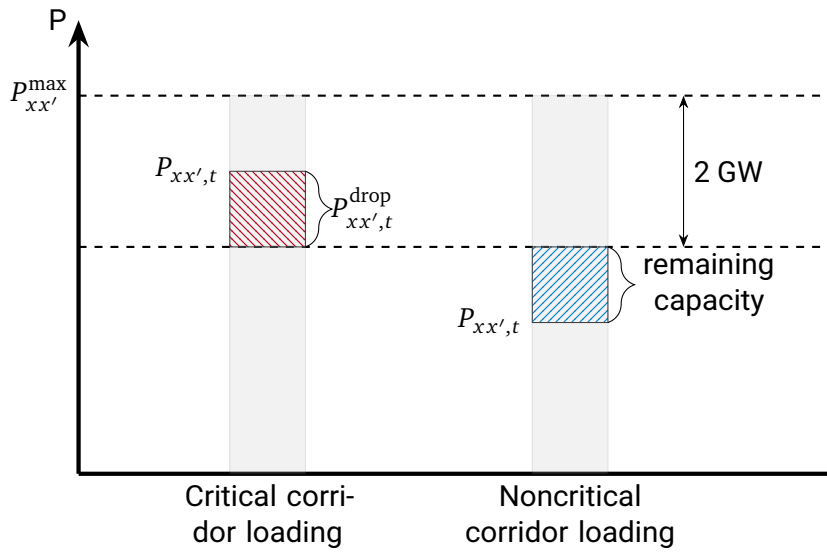
Figure 4.3.: Concept of the power that has to be compensated after a loss of 2 GW transmission capacity.

If additional regions are taken into account, the sum has to be expanded over the set of regions considered.

A symmetric flexibility potential can be defined for the corridor, determining the amount of power that can be compensated by upward flexibility potential in the receiving and downward flexibility potential in the sending region:

$$\Delta \hat{P}^{*}_{xx',t} = \min(\Delta \hat{P}^{\mathrm{up}}_{x',t}, \Delta \hat{P}^{\mathrm{down}}_{x,t}) \tag{4.6}$$

In most cases when the transmission corridor can turn critical after a loss of transmission capacity, many RES are injecting power. This means, that curtailment is more easily achieved than increasing generation on the receiving end, making upward flexibility ΔP^{up} more valuable. Since the impact individual assets have on transmission lines that are not directly connected to them is relatively low[2], the exact location where the flexibility is provided is not relevant, as long as it is on the right side of the congestion. Since the applicable distance is hard to determine for distribution grid flexibilities that are already spread out via the

---

[2]Analysis via PTDF in the InnoSys consortium [52] have shown, that the sensitivity of a grid booster connected to a bus in the transmission grid quickly drops to less than 10 % for transmission lines connected to a neighboring node.

GICPs between the distribution and transmission grid, in this study only direct non-mutual neighbors are included for providing the respective flexibility.
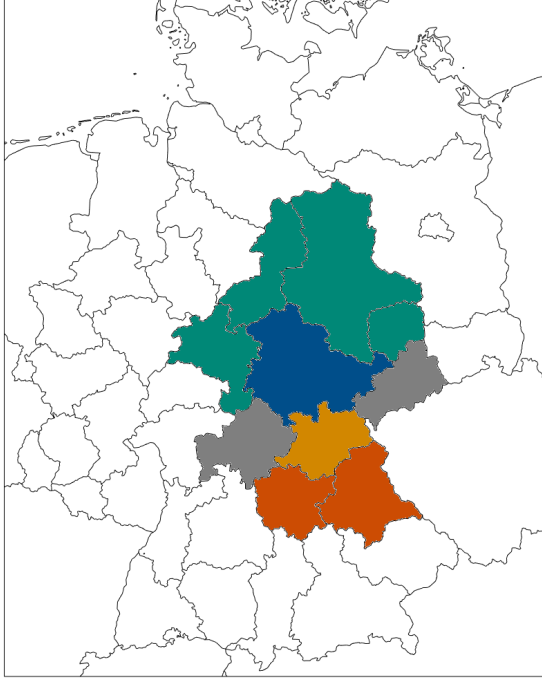
Figure 4.4.: Example: Regions admissible to provide flexibility. Between the blue region (Thuringia) and the light orange one (Upper Franconia) a transmission corridor needs flexibility. Regions in light and dark orange provide upward flexibility, while regions in blue and green provide downward flexibility. Grey regions are mutual neighbors and provide neither.

Figure 4.4 shows an example for admissible regions to provide flexibility during a critical time-step.

To analyze the provided flexibility, several measures are developed. At first, it is important to know how much of the missing power $P^{\text{drop}}_{xx',t}$ can be compensated by the flexibility provided in the admissible regions. This compensated power is calculated with the following formula:

$$\Delta P^{\text{comp}}_{xx',t} = \min(P^{\text{drop}}_{xx',t}, \Delta \hat{P}^{*}_{xx',t}) \tag{4.7}$$

This variable $\Delta P^{\text{comp}}_{xx',t}$ is called the correctively compensated power per transmission corridor xx' and time-step t. This power is only needed in case of an outage and might therefore never be requested and provided. The compensated power $\Delta P^{\text{comp}}_{xx',t,T}$ per technology T can also be calculated or a voltage level dependency can be added.

To get an understanding how much the compensated power by distribution system flexibility

helps to achieve a curative operation, corridor specific averages can be calculated:

$$\langle \Delta P_{xx'}^{\text{comp}} \rangle = \frac{\sum_{t \in t_{xx'}^{\text{crit}}} \Delta P_{xx',t}^{\text{comp}}}{\left| t_{xx'}^{\text{crit}} \right|} \tag{4.8}$$

Summing over time provides measures in dimensions of energy:

$$E_{xx'}^{\text{comp}} = \sum_{t \in t_{xx'}^{\text{crit}}} \Delta P_{xx',t}^{\text{comp}} \tag{4.9}$$

By further summing up over all transmission corridors xx', a total correctively compensated energy approximation can be obtained:

$$E^{\text{comp}} = \sum_{xx'} E_{xx'}^{\text{comp}} \tag{4.10}$$

The same measures are also available for the hypothetical energies that are necessary in case of simulated outages:

$$E_{xx'}^{\text{drop}} = \sum_{t \in t_{xx'}^{\text{crit}}} P_{xx',t}^{\text{drop}} \qquad E^{\text{drop}} = \sum_{xx'} E_{xx'}^{\text{drop}} \tag{4.11}$$

The time constant used in this thesis is hours, resulting in gigawatthours of dropped energy for gigawatts of dropped power. If another time constant is used, the resulting unit also changes. The dropped energy $E_{xx'}^{\text{drop}}$ and the compensated energy $E_{xx'}^{\text{comp}}$ per corridor can also be compared, to get a compensated share:

$$S_{xx'}^{E} = \frac{E_{xx'}^{\text{comp}}}{E_{xx'}^{\text{drop}}} \tag{4.12}$$

To determine how often distribution system flexibility is present in sufficient amounts to base a corrective operation on it, there is a binary measure defining if flexibility is sufficient:

$$\Theta_{xx',t} = \begin{cases} 1 & \text{if } \Delta P_{xx',t}^{\text{comp}} > \Delta P_{xx',t}^{\text{drop}} \\ 0 & \text{else} \end{cases} \tag{4.13}$$

This measure can be evaluated per corridor to provide insight where flexibility is present in large amounts when it is needed to operate the transmission grid curatively:

$$S_{xx'}^{t} = \sum_{t \in t_{xx'}^{\text{crit}}} \frac{\Theta_{xx',t}}{\left| t_{xx'}^{\text{crit}} \right|} \tag{4.14}$$

To be able to better discuss the results later on, $S^t_{xx'}$ is named flexibility-sufficiency-index. Summing over all links, a meta-measure how often distribution grids can provide sufficient flexibility to operate the transmission grid curatively can be obtained:

$$S^t = \sum_{xx'} \frac{S^t_{xx'}}{\# \text{ links}},$$

(4.15)

where # links is the number of corridors or inter-region-links to normalize the measure. A similar meta-measure can also be obtained for compensated energies:

$$S^E = \sum_{xx'} \frac{S^E_{xx'}}{\# \text{ links}}$$

(4.16)

Summary

In this chapter, two methods are introduced to determine the contribution that distribution system flexibility can provide for curative grid operation:

- An energy system model provides schedules for all modeled assets, including the information when certain predefined assets can change their power injection or load to supply flexibility.

- RES are mainly connected in HV distribution grids or lower. The higher the voltage level, the quicker these assets can be activated. Wind-power is more often installed in HV than PV, making it a more valuable source for distribution system flexibility for curative use.

- Certain technologies offer great potential, but are mainly installed and connected in LV grids. Inclusion of these technologies in curative operation is unlikely in the near future, which is why heat-pumps and electrical cars are not considered. Assets that are already used to provide ancillary services like decentral batteries are included in the scope.

- A simulated dispatch-redispatch process provides time-spans in which the grid is in a state of high utilization. A global measure of flexibility can be calculated for these time-steps to determine the flexibility potential. However, it is not possible to correlate locations where flexibility is present and where flexibility is needed via this approach.

- Therefore, a transmission-corridor-resolved measure is used to fill this knowledge gap by simulating transmission capacity losses. Losses are expected to amount to a maximum of 2 GW transmission capacity, which defines how much power needs to be compensated to achieve a safe operation.

5. Results for the Flexibility Potential

In this chapter, the calculation results of the distribution system flexibility potential are outlined. At first, the results derived by the simulated redispatch process introduced in Section 4.2 are presented. The transmission grid corridor resolved results follow in Section 5.2.

In both result sections, the German energy system is modeled for 12 weeks in a hourly resolution to get a sample of different states in the grid. The chosen weeks are the first week of each month, always beginning with Mondays. This way, the sample is representative for one year.

Possible sources of flexibility from distribution grids are introduced above in Subsection 2.1.1. The following results only use the technologies listed in Table 5.1. It shows that there are three main sources of flexibility considered here: curtailment and de-curtailment of RES, flexible loads as P2H, and decentral batteries.

5.1. Flexibility Calculation by Simulated Redispatch

To obtain results for a flexibility potential that is not resolved onto individual transmission system corridors, the simulated redispatch process introduced in Section 4.2 is used. It calculates the difference in all schedules in the energy system before and after introducing grid constraints. The amount of redispatch is the difference between the injected power in these two set-ups. All simulated time-steps are sorted by the calculated amount and for illustration the top 10 % of these time-steps are evaluated.

In these time-steps, the flexibility options from table 5.1 are evaluated and the results for upward flexibility potential $\Delta \hat{P}^{\text{up}}$ are shown in Figure 5.1. The results show that the calculated flexibility has a median of about 11 GW in available upward flexibility potential for wind-power. Multiplying the values for wind-power with a voltage share V_T of 40 % corresponding to the HV-level, a median of 5 GW remains.

P2H shows only little variability, which is due to the fact that it is always running if the availability of RES is high, which coincides with the time-steps with high redispatch amounts. In fact, it is always running above 99 % of the full capacity in these time-steps.

Table 5.1.: Sources of flexibility to calculate the distribution system flexibility potential.

Upward flexibility ΔP^{up}	Downward flexibility ΔP^{down}
• Increase of power injection from curtailed wind-power	• Curtailment of wind-power electricity generation
• Increase of power injection from curtailed PV	• Curtailment of PV electricity generation
• Power-to-heat curtailment	• Increase of load from power-to-heat
• Decrease of charging power of decentral batteries	
• Increase of decentral battery power output	

The figure also depicts the significantly smaller amount of flexibility from PV in comparison with wind-power. PV installations are distributed more homogeneously, leading to less transmission demand on sunny days in comparison with windy days and therefore less curtailment due to bottlenecks.

Flexibility from higher voltage levels is much more accessible for curative transmission grid operation than flexibility from lower voltage levels. The installed wind-power capacities are mainly installed in such higher voltage levels. To test the influence of changes in the merit order onto the flexibility potential, a sensitivity analysis is performed. This analysis is performed to asses the impact of possible future regulation determining which RES are curtailed first in situations with surplus electricity generation capacities. To model a priority dispatch for wind and PV generated power, artificial OPEX are added to both technologies, to influence which one shall be curtailed first by the cost optimal energy modeling process.

The artificially added marginal costs must be in the correct order of magnitude, to not change the merit order for other generators but still lead to a difference for the electricity generated by wind-power and PV. In table 5.2 the costs that are used are listed.

The energy system model is extended to include these costs, and the dispatch-redispatch tool chain described in Section 4.2 is re-run. The same analysis as performed for Figure 5.1 is repeated in two scenarios with prioritized power injection once from PV and once from
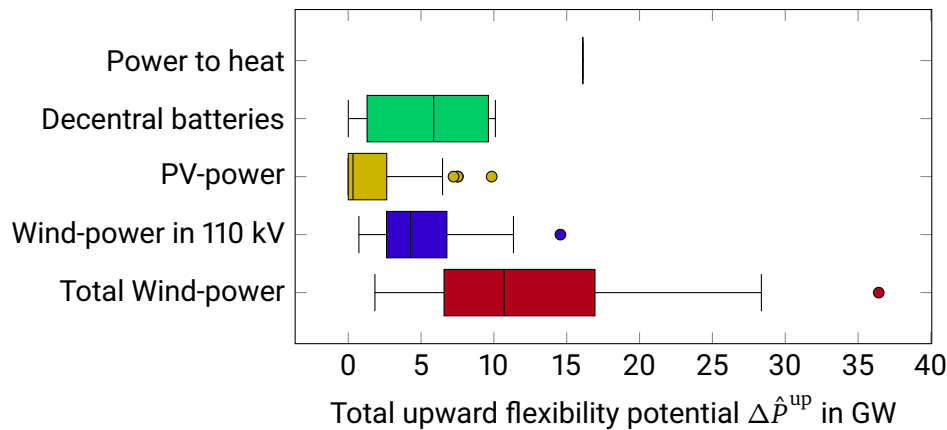
Figure 5.1.: Results for the flexibility potential calculation from approximated redispatch for a twelve-week simulation: Upward flexibility potential $\Delta \hat{P}^{\mathrm{up}}$ from different sources at times with 10 % largest simulated redispatch volumes.

wind-power. In Figure 5.2, the upward flexibility in these scenarios is compared.

Flexibility potentials for power-to-heat and decentral batteries are unaffected by these costs and not shown in Figure 5.2. For PV and wind-power, the figure shows that if PV is prioritized, its flexibility potential vanishes, while the prioritization of wind-power does not have such strong effects. Wind-power has a large share in the generation in critical time-steps. Decreasing its costs does not significantly change the flexibility potential from curtailment. The correlation of redispatched power and wind-power injection is stronger than the one of redispatch and power injection by PV.

For curative grid operation, this is good news, since the result for flexibility from wind-

Table 5.2.: Artificially added marginal costs for wind-power and PV to simulate priority dispatch effects.

Technology	Equal marginal costs	Marginal costs in sensitivity with prioritized wind-power	Marginal costs in sensitivity with prioritized PV
PV	0 €/kWh	0.005 €/kWh	0 €/kWh
Wind-power	0 €/kWh	0 €/kWh	0.005 €/kWh
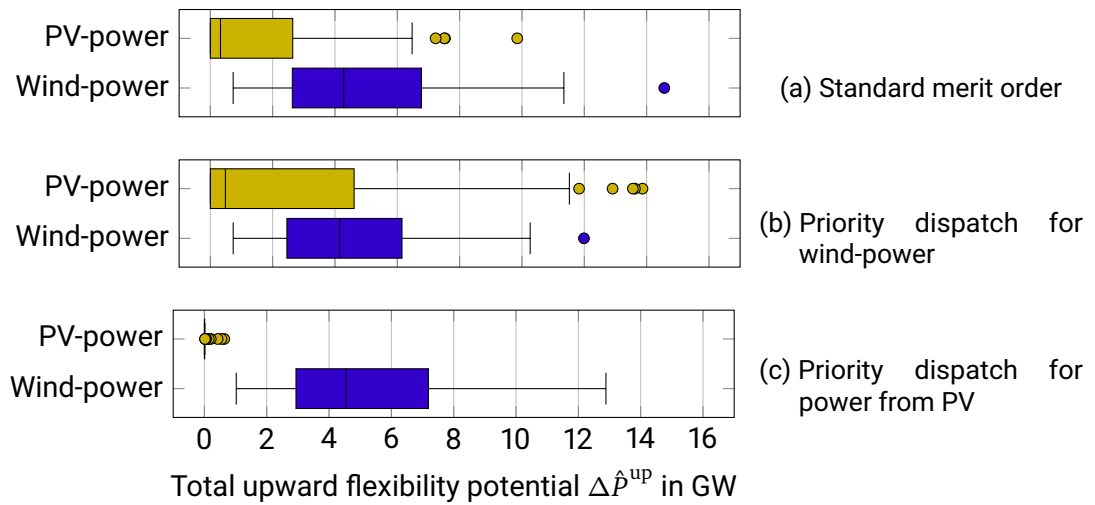
Figure 5.2.: Upward flexibility potential $\triangle \hat{P}^{\mathrm{up}}$ from wind-power in 110kV grids and from PV installations. The box plots in (a) are the same results as in Figure 5.1. Figures (b) and (c) show flexibility potentials for different OPEX assumptions.

power is robust against changes in the merit order caused by future regulation that could prioritize lower voltage power injections. In addition, flexibility from power-to-heat is very robust, as it is not influenced by changes in the merit order. It displays little variability at times when the grid is operated at its capacity. It is not known, how much P2H will be installed in 2030, but in an energy system a high share of RES, flexible demand will evolve in order to utilize surplus generation. This might be in form of P2H, but can also be charging infrastructure for e-cars or novel battery technology.

The above results give aggregate values for flexibility potentials summed over the whole modeled region. Independent of the possible sources of flexibility, these amounts are not correlated with regions or transmission corridors where flexibility might be needed.

5.2. Transmission Corridor Resolved Flexibility Potential

As the global flexibility potential calculation does not provide information if flexibility is present where it is needed after a grid malfunction, the transmission corridor resolved flexibility analysis is performed as described in Section 4.3. In this analysis, the focus is on the spatial distribution of the flexibility and the correlation of possible critical transmission system outages with flexibility availability.
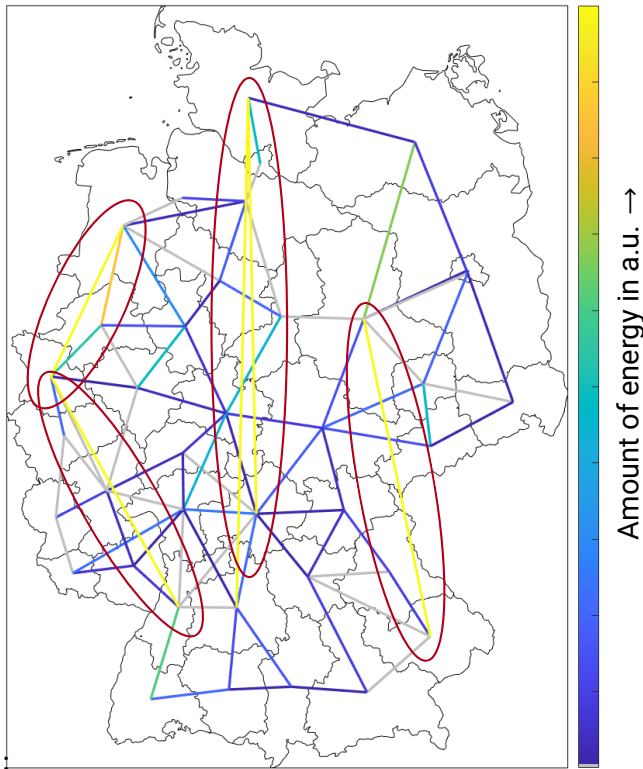
Figure 5.3.: Distribution of dropped energy $E_{xx'}^{\mathrm{drop}}$ on transmission corridors. Units are not given since only the distribution onto the corridors is of interest here. Grey corridors never become critical as defined by Equation 4.3. Red ellipses are drawn around HVDC-corridors that display large values for $E_{xx'}^{\mathrm{drop}}$.

Figure 5.3 depicts the distribution of the dropped energy $E_{xx'}^{\mathrm{drop}}$ from region x to region x' as introduced in Equation 4.11. This quantity is calculated by simulating all possible outages and adding up the power that needs to be compensated due to these outages. The sum of this power is then plotted for each corridor. This means, that the quantity itself is hypothetical, as it describes a sum over all possible outages. The distribution, which describes the relation of these summed up energies, is of interest as it describes the risk of transmission system outages on different corridors.

As one can see, the HVDC-corridors show the highest values for $E_{xx'}^{\mathrm{drop}}$, because their capacity is only 2 GW each and they are used preferably for north-south energy transmission as losses are smaller than via the AC-grid. It is important to note that for corridors with transmission capacity greater than 2 GW, it is less probable that an outage on it becomes critical, as the outage is simulated with the same value of 2 GW for all corridors. As a consequence, the less often a transmission corridor can become critical, the lower the dropped energy $E_{xx'}^{\mathrm{drop}}$.

The same is true for compensated energy. Compensation for dropped energy is only calculated if a time-step is critical in a simulated transmission loss. Only the combination of

both dropped and compensated energy can provide more valuable insights, as it shows the value of the flexibility potential.
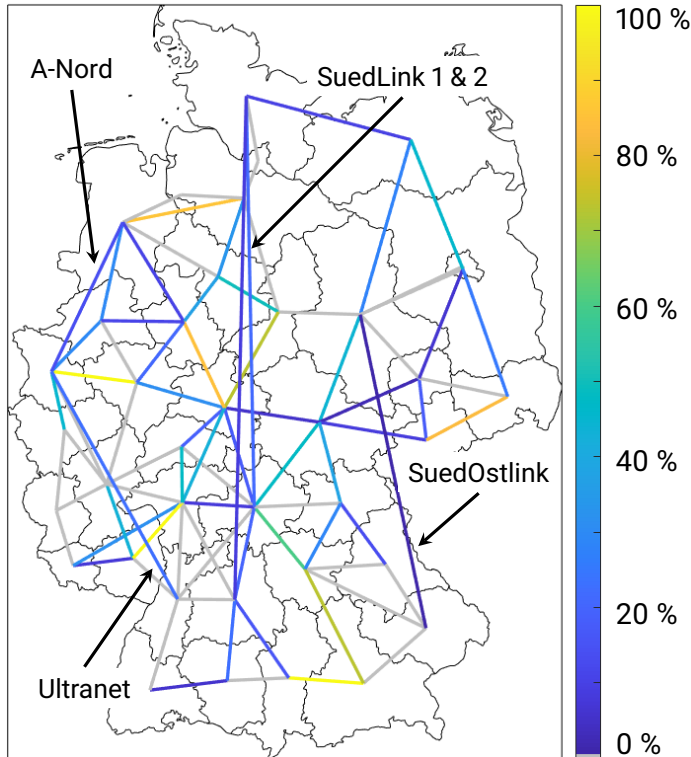
Figure 5.4.: Visualization of the flexibility-sufficiency-index, describing how often distribution flexibility potential is sufficient to completely compensate simulated transmission corridor losses. Only wind-power and P2H are included as flexibility sources here as they are two of the sources that can be included in curative measures with the least effort.

The flexibility-sufficiency-index introduced in Equation 4.14 is used to evaluate this value. It describes the share of time-steps in which the distribution system flexibility potential is sufficient to compensate a loss of transmission capacity. In Figure 5.4, this measure is plotted, but only including flexibility from wind-power and P2H, two technologies mainly installed in upper voltage levels and therefore especially suited to the task of quickly providing flexibility for curative use. Instead of P2H, any other flexible and controllable load that is installed in similar orders of magnitude can be chosen.

The calculated flexibility potential is only sufficient on a few corridors, on which the total dropped energy, as shown in Figure 5.3, is relatively low. Of the five north-south running HVDC corridors, the share is only above 10 % for the Ultranet project, which connects Osterath in close to Düsseldorf and Philippsburg in northern Baden. For the other four HVDCs, A-Nord, SuedLink 1 and 2, and SuedOstLink, on which dropped energies are relatively high, $S_{xx'}^t$ is below 10 %. Note, that even for seemingly low values of $S_{xx'}^t$, distribution system flexibility

potential can still be relevant. In curative grid operation, each measure has to be collateralized by other measures to ensure no cascading outages happen. Even small amounts of flexibility that are not enough to entirely compensate the transmission capacity loss of a corridor can be used as part of a curative measure or as a collateral for it. Also, if, for example, 200 MW are missing to completely compensate a transmission capacity loss, the corridor loading can be reduced by the appropriate amount and still be operated curatively with the corresponding avoided redispatch. In addition, even if distributed flexibility only compensates a part of the transmission capacity losses, it can increase TATLs and therefore allow slower flexibility options to partake in curative operation.
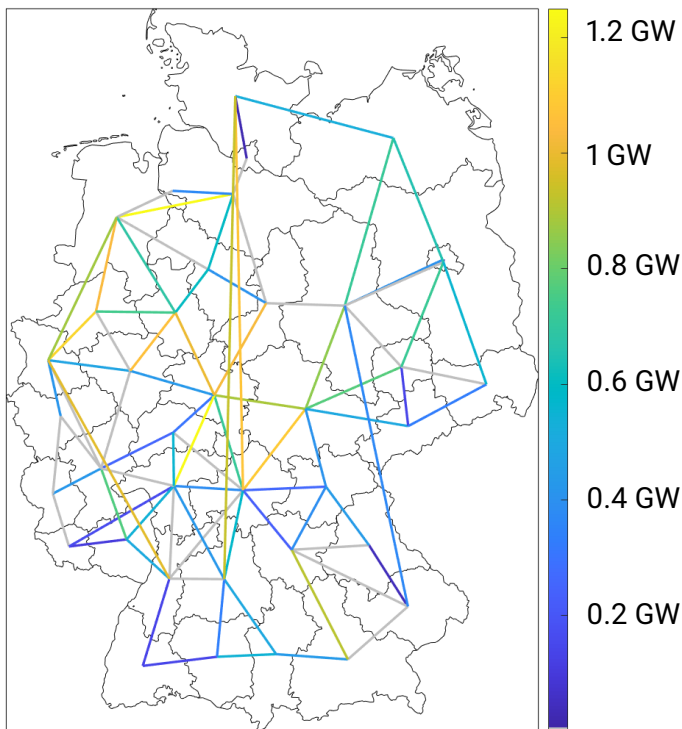
Figure 5.5.: Averaged compensated power per corridor $\langle P_{xx'}^{\text{comp}} \rangle$ introduced in equation 4.8. Only wind-power and P2H are included as flexibility sources here. Graphic previously published in [64].

Taking a look at the power that flexibility from distribution grids do compensate in average, the picture changes significantly. Figure 5.5 depicts the results of this analysis. The graph shows the average compensated power per corridor $\langle P_{xx'}^{\text{comp}} \rangle$ with flexibility from P2H and wind-power. Even though other flexibility sources as PV and decentral batteries are not included, the calculated amounts reach gigawatts on several corridors. Especially for four of the five HVDCs, the results are significant, only the most eastern located SuedOstLink has a $\langle P_{xx'}^{\text{comp}} \rangle$ of below 750 MW. This is in parts due to the fact that the receiving region

Lower Bavaria only has two neighboring regions that can assist in providing flexibility. A cross-border cooperation with the Czech Republic or Austria in curative redispatch would contribute to increase this potential.
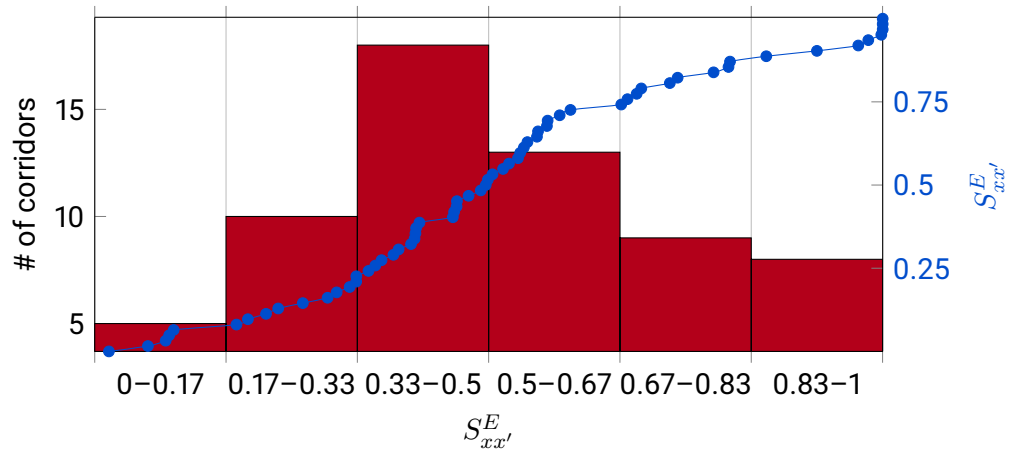
Figure 5.6.: Histogram of the share of compensated power per corridor $S^E_{xx'}$. Technologies for upward flexibility potential $\triangle \hat{P}^{\mathrm{up}}$ are curtailed wind-power and P2H. Blue line is the data used for the histogram, sorted and plotted into the respective bars.

Figure 5.6 depicts the histogram over the share of compensated power per corridor $S^E_{xx'}$. For 30 of the 63 corridors that become critical[1], $S^E_{xx'} \geq 0.5$ holds. This means, that for over half of the all transmission corridors, flexibility from distribution grids can compensate at least half of the power in cases when and where it is needed. If not only P2H and wind-power are used for upward flexibility potential $\triangle \hat{P}^{\mathrm{up}}$, but also the other options from Table 5.1, 49 out of the 63 corridors that can become critical have compensated energy shares of greater than 50 % ($S^E_{xx'} \geq 0.5$).

In Table 5.3, the different results for compensated transmission losses as a function of the used technologies for upward flexibility $\triangle P^{\mathrm{up}}$ and the total compensated energies or time-steps are listed. As becomes visible, power-to-heat is the technology providing the biggest part of $\triangle \hat{P}^{\mathrm{up}}$. This is due to the fact that P2H, serving as a low-cost flexible load, is always running in situations with high renewable power injections and possibly critical grid situations. However, this also means that if P2H was not using this power, it would be

---

[1]22 are never critical

Table 5.3.: Overview of compensated energies S^E (Equation 4.16) and share of time-steps S^t (4.15) where distribution system flexibility potential is sufficient to solely compensate dropped power as a function of upward flexibility $\Delta P_{xx'}^{\mathrm{up}}$-providing technologies T. All flexibility options are included for downward flexibility $\Delta P_{xx'}^{\mathrm{down}}$.

Technology T for $\Delta P_{xx',T}^{\mathrm{up}}$	S^E	S^t
Curtailed wind-power	0.05	0.16
PV batteries	0.28	0.25
Power-to-heat	0.49	0.36
Wind-power and P2H	0.50	0.40
All technologies	0.64	0.58

available as curtailed generation or used by other similar flexible assets.

If such assets are connected in similar voltage levels as the existing or future P2H assets, similar values as listed in Table 5.3 can be expected. However, if flexibility is provided from lower voltage levels, curative transmission operation would require new communication techniques and a regulatory framework giving the DSOs the permission to access it quickly enough. To show the influence of voltage level allocation for P2H and wind-power, Figure 5.7 depicts a sensitivity analysis.

This sensitivity analysis shows that wind-power shares have significantly smaller impact than P2H shares. For large P2H shares, V_T of wind-power has little effect, while for the inverse relation the opposite is true. If only a small part of P2H assets are available for curative operation, having access to all curtailed wind farms does not hold great flexibility potential. The reason behind this phenomenon is also visible in Figure 5.1 in the previous section on page 97: A stressed grid coincides with large renewable power injections from wind-power and usage of all flexible loads, as for example power-to-heat.

In Table 5.3, for all technologies T the value for S^E is greater than the one for S^t, except for wind-power. This means that for all other options for ΔP^{up}, often a part of the dropped power $P_{xx'}^{\mathrm{drop}}$ can be compensated, but rarely all of it. Figure 5.4 already shows this result: Especially on the HVDC corridors, the distributed flexibility is not enough to completely compensate the dropped power. However, as shown in the next Figure 5.5, on these very transmission lines the averaged possibly compensated power is over one gigawatt. Wind-power is mainly installed in the north, and curtailment of it also happens mainly in the north. Here, it can more often compensate the total $P_{xx'}^{\mathrm{drop}}$, but with much lower total power.
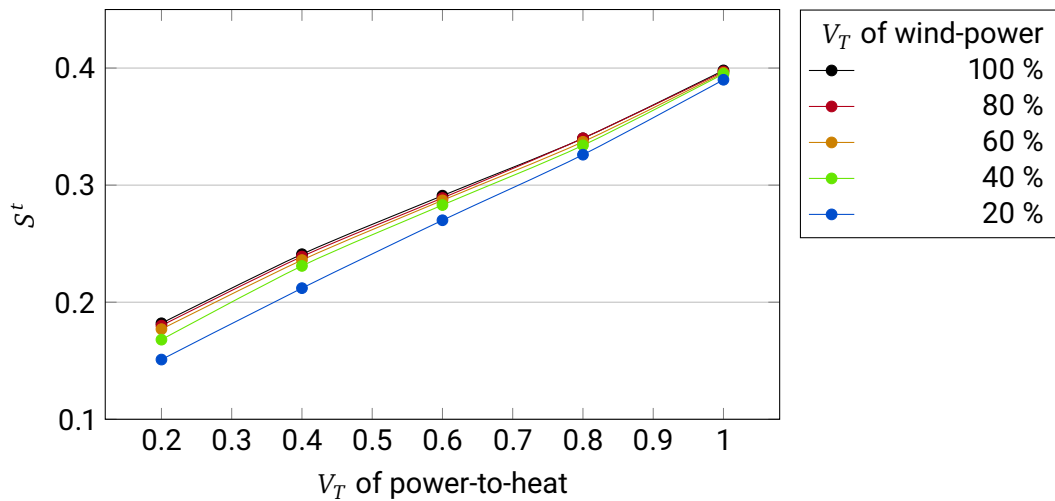
Figure 5.7.: Influence of the voltage share V_T of wind-power onto the flexibility potential as a function of the voltage share V_T of P2H.

5.3. Discussion

Results of the flexibility potential calculation using the simulated redispatch method show that flexibility from decentral batteries, wind-power, and P2H amounts to values of several gigawatt. These potentials are robust against changes in the merit order, in contrast to those from PV. However, no information about the usefulness of these flexibilities can be obtained with this method.

The calculation of corridor-resolved flexibility shows contrasting results: Only at very few corridors, the distributed flexibility sources show enough potential to completely compensate simulated transmission losses. Especially on the North-South oriented HVDC-systems, $S^t_{xx'}$ exhibits values smaller than 10%. These results seem to contradict those from the simulated redispatch method.

However, looking at average compensated power per corridor $\langle P^{\text{comp}}_{xx'} \rangle$, the conclusion changes, as distributed flexibilities from only wind-power and P2H alone already offer average values of over 500 MW for the HVDC-systems. This shows, that flexibility from distribution systems might not be the sole solution or source of operational degrees of freedom for curative operation, but an integral part. Especially P2H can take a central role, as it offers valuable upward flexibility in most cases the grid can become critical. If P2H will not be build in such large quantities as it is modeled here, other flexible assets can take its role if these

alternative assets are also controllable by DSOs.

The modeling of the transmission grid in this thesis is not as accurate as modeling individual power-lines. As a consequence, the sensitivity of setpoint changes onto the power-line-loadings cannot be accurately determined. The exact efficacy of distribution system flexibility for curative grid operation is therefore hard to analyze. In the InnoSys consortium, the power transfer distribution factor (PTDF) of power injections by possible grid-boosters were calculated. These factors drop to values below 10 % for power-lines that are not directly connected to the grid-booster. Distributed flexibilities probably have even less direct effect onto the critical branch as they are not concentrated at one node. This has two consequences:

1. more flexible power is needed in comparison with grid boosters to achieve the same results, and

2. flexibility from distribution grids is not only usable for single power-lines in the system, but for several.

As more and more RES are integrated into the energy system, it becomes a priority to include the new assets into the processes of providing flexibility. The more assets are connected, the more controllable and flexible the whole power system becomes, enabling a higher utilization of the transmission grid.

In those cases, when distributed flexibility is not sufficient to completely compensate losses of transmission capacity, it can serve as collateral for other measures or as one component in a bundle of measures, which together are able to compensate the loss in transmission capacity. In future and more advanced grid operation processes, distributed flexibilities can also serve as a curative backup to a curative measure by increasing the TATL, so that other, slower measures can be integrated into the curative grid operation.

Even if flexibility from distribution grids is not used in the curative measures, it can serve as a restoring remedial action by helping to return to a new n-1-safe state after a loss in transmission capacity has been compensated.

One of the main advantages of flexibility from distribution grids is, that the available capacity rises automatically with the need. More installed RES will result in higher transmission need and also in a larger number of controllable, flexible assets on the generation side as well as the demand side. This is in contrast to specialized assets like grid-boosters, that only serve a limited purpose and must be built additionally to the occurring increase in installed RES.

Summary

In this chapter, the results for the calculation of flexibility potentials from distribution systems for curative transmission system operation are shown. The analysis provides a series of insights:

- Time-steps in which the grid is at its capacity limit are characterized by large power injections from RES and large consumption of flexible loads, as for example P2H.

- While the amount of curtailed wind-power might be large and robust against changes in merit order, it does not contribute a lot to the useful flexibility due to its location in the grid. However, if flexible assets were not running, curtailed wind-power might become more relevant in providing flexibility.

- An aggregate measure of flexibility potential typically overestimates the flexibility that is helpful in compensating losses of transmission capacity, but establishes an order-of-magnitude understanding of the relevant phenomena.

- Even in situations when the flexibility from distribution grids is not sufficient to completely compensate losses of transmission capacity, it can take part in curative operation by providing a part of the needed flexibility or serving as a collateral for other curative measures.

Part II.

Robust Provisioning of Distribution System Flexibility

The modeling framework, method, and results in this part of the thesis closely resemble the paper [191].

6. Modeling for Safe Flexibility Calculation and Aggregation

In this chapter, the modeling for the task of providing flexibility from distribution grids is introduced. The methods and approaches developed here are only used for provisioning of flexibility from distribution to transmission grids. However, the same methods can be used to provide flexibility from any distribution grid to a connected grid of a higher voltage level.

While in the first part of this thesis the potential of distributed flexibility sources for curative transmission grid operation is evaluated, this second part deals with the details of the provisioning process itself. As the objective is a different one, the modeling, method, and results are therefore not comparable and introduced separately. In this chapter, the general theory behind modeling of power-flows and distribution system flexibility are outlined, before dealing with the constraints to guarantee a safe operation.

6.1. Modeling Distribution System Flexibility

In this section, the basics behind distribution system flexibility modeling are outlined, including a transmission line model, power-flow calculation, and initial and safe flexibility sets. In general, this thesis follows the notation introduced in [192] and [193].

Looking at a distribution grid or a model thereof, two categories of operating equipment are immediately distinguishable: power lines, branches, or edges and buses or nodes. These names can be used interchangeably, where the first ones stem from the engineering side, while the second set of terms, branches or edges and nodes, stem from graph theory, a field going back to Leonhard Euler and his problem to cross all seven bridges of Königsberg only once while still reaching all three parts of the town[194]. While the original bridges of Königsberg problem is proven to be unsolvable, power-flow calculation is a solved problem being performed many hundreds of times each day by the grid operators all around the world. The following notation is used:

- The number of power lines or branches l is denoted by n_l.

- The number of nodes or buses b is denoted n_{b}.

For both of these categories, further subcategories exists, for which subscripts are added to always keep a clear notation.

6.2. Types of Buses in Electrical Power Grids

The first subcategory that is introduced here, are the different types of buses b. Depending on the information known about a bus b, different names are given:

- For *PQ*-buses, both the active and reactive power p_b and q_b are known, while there is no information about voltages v_b with real and imaginary components of the rectangular form of the complex voltage phasors $v_{b,\mathrm{r}}$ and $v_{b,\mathrm{j}}$, or v_b and ϑ_b in polar coordinates. In a classical power system, those are the buses without generation capacity to control the voltage.

- A *PV*-bus has known active power injections p_b and voltage $v_{b,\mathrm{r}}$, or, in case of polar coordinates, voltage magnitude v_b, while reactive power q_b and $v_{b,\mathrm{j}}$ are variable. Classically, these are buses where synchronous generators are connected, that feed in variable reactive power to keep the voltage at a set point.

- In a power system model, at least one bus has to be a slack-bus or $V\vartheta$-bus, that is setting the reference voltage angle or $v_{b,\mathrm{j}}$ and makes up the losses occurring in the system. It is thereby balancing the whole power grid.

The first two types of buses are subsumed into another category and are denoted non-slack-buses b_{ns}. There are n_{bns} non-slack-buses in the grid and n_{bs} slack-buses.

6.3. Basic Power Flow Calculation

In this section, the basics of power-flow calculation are introduced to establish both the notation and the basics on which the following linearization is built. The notation mainly follows [193] and [168], while basics of power-flow calculation can be found in many publications, for example [165], [168], [193], [195]–[198].[1]

For each bus in the power system the sum of all complex powers s is always zero:

$$s_{\mathrm{in}} + s_{\mathrm{out}} + s_{\mathrm{loads}} \overset{!}{=} 0 \tag{6.1}$$

[1]All following equations in this section until Equation 6.32 are describing these foundations upon which the optimization method is based and are therefore not the author's original work.

Flows between different buses are driven by the difference in potential between them. In this case, the potential is the voltage. The transmitted power on the line from a bus f ("from") to a neighboring one t ("to") is a function of said voltage difference. In the case of direct current or DC, this relation is formulated the following way:

$$s_{ft} \sim v_f - v_t \tag{6.2}$$

As complex power does not occur in case of DC-systems, active power p_{ft} can be used here instead of s_{ft}. In case of alternating current or AC, the voltage is, besides its amplitude, described by the phase denoted by the angle ϑ. In a simplified version of the power-flow, neglecting reactive power and losses, assuming a flat voltage profile, the flows are proportional to the difference in voltage angle between two nodes. This is referred to as DC-power-flow [193]:

$$s_{ft} \sim \vartheta_f - \vartheta_t \tag{6.3}$$

For a more realistic model of a power-flow, these simplifications are dropped, and admittances introduced to adjust for losses and the correct distribution of flows. Losses in an AC-system are not only functions of the resistance r producing ohmic losses, caused by the scattering of charge carriers inside the conductor, but also of the reactance x, which describes losses due to the recurring build of the magnetic field surrounding the conductor:

$$z = r + j \cdot x \qquad\qquad y = \frac{1}{z} \tag{6.4}$$

The inverse of the sum of both parts is defining the functional dependence of current and voltage and is called admittance y. When dealing with more than one power line, the complex admittance matrix Y is needed:

$$Y = G + j \cdot B \tag{6.5}$$

The conductance G is the real and the susceptance B the imaginary part of the complex nodal admittance matrix Y. The entry Y_{ft} in row f and column t of this admittance matrix is used to specify Equation 6.3 for an AC-system:

$$s_{ft} = v_f i_{ft}^* \tag{6.6}$$
$$= v_f (v_f - v_t)^* Y_{ft}^* \tag{6.7}$$
$$= |v_f|^2 Y_{ft}^* - |v_f||v_t| Y_{ft}^* e^{j\vartheta_{ft}} \tag{6.8}$$

Here, $\vartheta_{\mathrm{ft}} = \vartheta_{\mathrm{f}} - \vartheta_{\mathrm{t}}$ is the difference in voltage phase between buses f and t and the star denotes a complex conjugation. Splitting the complex power s into real and imaginary parts, expressions for active power p and reactive power q are obtained:

$$\mathrm{Re}(s_{\mathrm{ft}}) = p_{\mathrm{ft}} = |v_{\mathrm{f}}|^2 G_{\mathrm{ft}} - |v_{\mathrm{f}}||v_{\mathrm{t}}|(G_{\mathrm{ft}} \cdot \cos\vartheta_{\mathrm{ft}} + B_{\mathrm{ft}} \sin\vartheta_{\mathrm{ft}}) \qquad (6.9)$$

$$\mathrm{Im}(s_{\mathrm{ft}}) = q_{\mathrm{ft}} = -|v_{\mathrm{f}}|^2 B_{\mathrm{ft}} - |v_{\mathrm{f}}||v_{\mathrm{t}}|(G_{\mathrm{ft}} \cdot \sin\vartheta_{\mathrm{ft}} - B_{\mathrm{ft}} \cos\vartheta_{\mathrm{ft}}) \qquad (6.10)$$

When not only considering one branch, but all n_{lb} branches l connected to a bus b, and taking into account the power or load injections $s_b = p_b + \mathrm{j} \cdot q_b$ at this node, the following equations can be formulated:

$$\sum_{k=1}^{n_{\mathrm{lb}}} [|v_k||v_b|(G_{bk} \cdot \cos\vartheta_{bk} + B_{bk} \sin\vartheta_{bk})] + p_b = 0$$

$$\sum_{k=1}^{n_{\mathrm{lb}}} [|v_k||v_b|(G_{bk} \cdot \sin\vartheta_{bk} - B_{bk} \cos\vartheta_{bk})] + q_b = 0$$

The polar coordinates can be rewritten into Cartesian coordinates, so that information about voltage angles and magnitude are included in the real and imaginary parts of the complex voltages:

$$0 = \sum_{k=1}^{n_{\mathrm{lb}}} \big[v_{b,\mathrm{r}} \cdot G_{bk} \cdot v_{k,\mathrm{r}} - v_{b,\mathrm{r}} \cdot B_{bk} \cdot v_{k,\mathrm{j}} \qquad (6.11)$$
$$+ v_{b,\mathrm{j}} \cdot G_{bk} \cdot v_{k,\mathrm{j}} + v_{b,\mathrm{j}} \cdot B_{bk} \cdot v_{k,\mathrm{r}} \big] + p_b$$

$$0 = \sum_{k=1}^{n_{\mathrm{lb}}} \big[-v_{b,\mathrm{r}} \cdot G_{bk} \cdot v_{k,\mathrm{j}} - v_{b,\mathrm{r}} \cdot B_{bk} \cdot v_{k,\mathrm{r}} \qquad (6.12)$$
$$+ v_{b,\mathrm{j}} \cdot G_{bk} \cdot v_{k,\mathrm{r}} - v_{b,\mathrm{j}} \cdot B_{bk} \cdot v_{k,\mathrm{j}} \big] + q_b$$

Since these equations are valid for all nodes, they can be reformulated into an equation for all buses using vectors $\vec{v}$ for voltages and matrices Y for admittances:

$$\vec{s} = \mathrm{diag}(\vec{v})Y^*\vec{v}^* \qquad (6.13)$$
$$= \mathrm{diag}(\vec{v}_{\mathrm{r}} + \mathrm{j} \cdot \vec{v}_{\mathrm{j}})(G - \mathrm{j} \cdot B)(\vec{v}_{\mathrm{r}} - \mathrm{j} \cdot \vec{v}_{\mathrm{j}}) \qquad (6.14)$$
$$\mathrm{Re}(\vec{s}) = \vec{p} = \mathrm{diag}(\vec{v}_{\mathrm{r}})G\vec{v}_{\mathrm{r}} - \mathrm{diag}(\vec{v}_{\mathrm{r}})B\vec{v}_{\mathrm{j}} + \mathrm{diag}(\vec{v}_{\mathrm{j}})G\vec{v}_{\mathrm{j}} + \mathrm{diag}(\vec{v}_{\mathrm{j}})B\vec{v}_{\mathrm{r}} \qquad (6.15)$$
$$\mathrm{Im}(\vec{s}) = \vec{q} = -\mathrm{diag}(\vec{v}_{\mathrm{r}})G\vec{v}_{\mathrm{j}} - \mathrm{diag}(\vec{v}_{\mathrm{r}})B\vec{v}_{\mathrm{r}} + \mathrm{diag}(\vec{v}_{\mathrm{j}})G\vec{v}_{\mathrm{r}} - \mathrm{diag}(\vec{v}_{\mathrm{j}})B\vec{v}_{\mathrm{j}} \qquad (6.16)$$

Here, $\text{diag}(\vec{x})$ means diagonal matrix of vector $\vec{x}$, or $\text{diag}(\vec{x}) = \vec{x}\mathbb{1}$. In the following, all voltage vectors $\vec{v}$ and power vectors $\vec{s}$, $\vec{p}$ and $\vec{q}$ will be denoted with capital letters V, S, P, Q. The following notation is used to describe the power injections into all nodes:

$$S = \text{diag}(V)Y^*V^* \tag{6.17}$$

$$P = \text{diag}(V_\text{r})GV_\text{r} - \text{diag}(V_\text{r})BV_\text{j} + \text{diag}(V_\text{j})GV_\text{j} + \text{diag}(V_\text{j})BV_\text{r} \tag{6.18}$$

$$Q = -\text{diag}(V_\text{r})GV_\text{j} - \text{diag}(V_\text{r})BV_\text{r} + \text{diag}(V_\text{j})GV_\text{r} - \text{diag}(V_\text{j})BV_\text{j} \tag{6.19}$$

To see if this set of equations solves uniquely, so that all voltages and power injections or loads are known, the problem needs to be properly determined. Taking the set of equations where active and reactive components are already separated, it becomes visible, that there are $2 \cdot n_\text{b}$ equations, two for each bus. With given admittances, this system of equations holds $4 \cdot n_\text{b}$ variables: active and reactive power injections P_b, Q_b and real and imaginary voltages $V_{b,\text{r}}$, $V_{b,\text{j}}$ for each bus b. To solve for all variables, $2 \cdot n_\text{b}$ of them need to be known, so that the number of unknown variables equals the number of equations.

Fortunately, in Subsection 6.2, the different types of buses are defined, which are used to encode this information. In ordinary distribution grids, the large part of buses are PQ-buses, while, depending on the voltage level, there is no, or are only very few PV-buses. In LV-grids, normally there are only PQ-buses, and one $V\vartheta$-bus, the local distribution substation. In HV distribution grids however, there are often several slack-buses, to enhance reliability by redundancy. Most substations are connected via two separate power lines, so that one of them may fail without disconnecting the substation. The number of PV-buses is heavily dependent on the individual grid, while some rural grids might have several ones, for example from larger biomass or hydro power plants, urban ones might have none.

In the case of aggregating flexibility while guaranteeing a safe state in the providing grid, all non-slack-buses with flexible energy resources can be treated as PQ-buses, since the amount of active and reactive power they inject into or draw from the grid is known. The slack-buses are the buses balancing the provided flexibility, which is exactly what is wanted, as this means the operator at those buses can use the aggregated power or load to his benefit.

Now, knowing the power injections, the voltages can be calculated. However, if the power flows between all buses are also needed, a second step in the calculation has to be added. Before trying to calculate the power-flows, it is necessary to know which branch is connected to which nodes. This information can be encoded in so called incidence matrices C_f and C_t for the "from"- and "to"-ends of the branches. Since an incidence matrix denotes which bus is connected to which branch, its dimensions are $n_\text{l} \times n_\text{b}$. These matrices can be calculated in

the following way:

$$C_{f,b,l} = \begin{cases} 1 & \text{if bus } b \text{ at "from"} - \text{end of branch } l \\ 0 & \text{else} \end{cases} \tag{6.20}$$

$$C_{t,b,l} = \begin{cases} 1 & \text{if bus } b \text{ at "to"} - \text{end of branch } l \\ 0 & \text{else} \end{cases} \tag{6.21}$$

The power-flow in a grid does change as a function of the power injections at the buses, therefore it is not guaranteed that the "from"-end is always the one injecting power and the "to"-end the one withdrawing it.
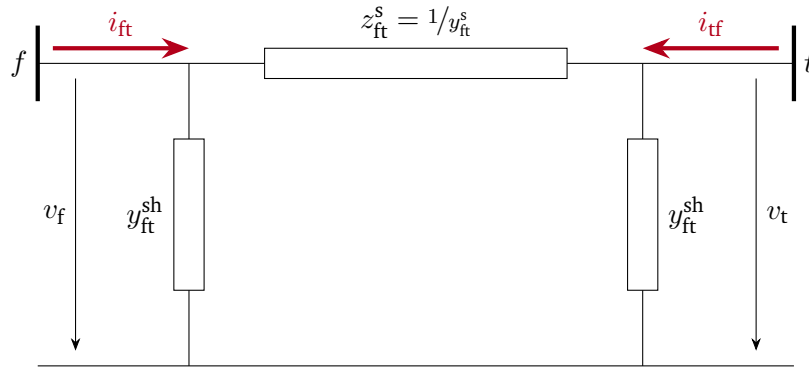
Figure 6.1.: π-model of transmission lines from bus f to bus t with shunt admittances y_{ft}^{sh} and series admittance y_{ft}^{s}. Graphic after [193].

Figure 6.1 shows a simple model of a transmission line, where the current i_{ft} is injected at bus f with voltage v_f and i_{tf} at bus t with voltage v_t. The series impedance z_{ft}^{s} poses as the impedance of the power line in the sense of an electrical equivalent circuit diagram. The variable y_{ft}^{sh} represents the shunt admittances caused by the non-infinite resistors to hold the power-lines and other shunts to ground.

With the help of these three parts, the shunt admittance y_{ft}^{sh}, the series admittance y_{ft}^{s}, and the voltages v_f and v_t at both ends, the currents i_{ft} and i_{tf} can be calculated:

$$\begin{pmatrix} i_{ft} \\ i_{tf} \end{pmatrix} = \underbrace{\begin{pmatrix} y_{ft}^{s} + y_{ft}^{sh} & -y_{ft}^{s} \\ -y_{tf}^{s} & y_{ft}^{s} + y_{ft}^{sh} \end{pmatrix}}_{Y_{br}} \begin{pmatrix} v_f \\ v_t \end{pmatrix} \tag{6.22}$$

The branch admittance matrix Y_{br} can be simplified by summing up and relabeling the entries:

$$Y_{\mathrm{br}} = \begin{pmatrix} y_{\mathrm{ff}} & y_{\mathrm{ft}} \\ y_{\mathrm{tf}} & y_{\mathrm{tt}} \end{pmatrix} \tag{6.23}$$

In a more general model including transformers, with $\tau = n_{\mathrm{primary}}/n_{\mathrm{secondary}}$ the ratio of primary to secondary windings at bus f, a phase shift Θ is introduced. In this case, the matrix entries are:

$$y_{\mathrm{ff}} = \frac{1}{\tau^2}(y_{\mathrm{ft}}^{\mathrm{s}} + y_{\mathrm{ft}}^{\mathrm{sh}}) \qquad\qquad y_{\mathrm{ft}}^{\mathrm{s}} = -\frac{1}{\tau e^{j\Theta}} y_{\mathrm{ft}}^{\mathrm{s}}$$

$$y_{\mathrm{tf}} = -\frac{1}{\tau e^{-j\Theta}} y_{\mathrm{ft}}^{\mathrm{s}} \qquad\qquad y_{\mathrm{tt}} = y_{\mathrm{ft}}^{\mathrm{s}} + y_{\mathrm{ft}}^{\mathrm{sh}}$$

The derivation of these entries is omitted here, but can be looked up in [193] or similar literature.

To generalize these equations so that all currents can be calculated in matrix form, another matrix Y_{f} is needed. It describes the currents into all branch at buses f and is constructed by using the incidence matrices and the entries of the branch admittance matrix:

$$Y_{\mathrm{f}} = Y_{\mathrm{ff}} C_{\mathrm{f}} + Y_{\mathrm{ft}} C_{\mathrm{t}} \tag{6.24}$$

Here, Y_{ff} and Y_{ft} are diagonal matrices of the vectors that describe the branches shunt- and series-admittances Y_{ff} and Y_{ft} respectively:

$$Y_{\mathrm{ff}} = \begin{pmatrix} y_{\mathrm{ff},1} & & \\ & \ddots & \\ & & y_{\mathrm{ff},n_1} \end{pmatrix} \qquad\qquad Y_{\mathrm{ft}} = \begin{pmatrix} y_{\mathrm{ft},1} & & \\ & \ddots & \\ & & y_{\mathrm{ft},n_1} \end{pmatrix} \tag{6.25}$$

Using these variables, the currents into all branches can be written down:

$$I_{\mathrm{f}} = Y_{\mathrm{f}} V \tag{6.26}$$

To obtain power-flows, complex conjugation and multiplication by voltages is performed:

$$S_{\mathrm{f}} = C_{\mathrm{f}} V I_{\mathrm{f}}^* \tag{6.27}$$

$$S_{\mathrm{f}} = \mathrm{diag}(V_{\mathrm{f}}) Y_{\mathrm{f}}^* V^* \tag{6.28}$$

$$= \mathrm{diag}(V_{\mathrm{f}}) Y_{\mathrm{ff}}^* V_{\mathrm{f}}^* + \mathrm{diag}(V_{\mathrm{f}}) Y_{\mathrm{ft}}^* V_{\mathrm{t}}^* \tag{6.29}$$

$$= \mathrm{diag}(C_{\mathrm{f}} V)(Y_{\mathrm{ff}} C_{\mathrm{f}} + Y_{\mathrm{ft}} C_{\mathrm{t}})^* V^* \tag{6.30}$$

V_f and V_t are voltages at the "from" and "to"-end of the branches. Again, the power can be split in active and reactive part by separating real and imaginary parts:

$$P_f = \text{Re}(S_f) = \text{diag}(V_{f,r})Y_{ff,r}V_{f,r} - \text{diag}(V_{f,r})Y_{ff,j}V_{f,j} \tag{6.31}$$
$$+ \text{diag}(V_{f,j})Y_{ff,j}V_{f,r} + \text{diag}(V_{f,j})Y_{ff,r}V_{f,j}$$
$$+ \text{diag}(V_{f,r})Y_{ft,r}V_{t,r} - \text{diag}(V_{f,r})Y_{ft,j}V_{t,j}$$
$$+ \text{diag}(V_{f,j})Y_{ft,j}V_{t,r} + \text{diag}(V_{f,j})Y_{ft,r}V_{t,j}$$
$$Q_f = \text{Im}(S_f) = -\text{diag}(V_{f,j})Y_{ff,j}V_{f,j} + \text{diag}(V_{f,j})Y_{ff,r}V_{f,r} \tag{6.32}$$
$$- \text{diag}(V_{f,r})Y_{ff,r}V_{f,j} - \text{diag}(V_{f,r})Y_{ff,j}V_{f,r}$$
$$- \text{diag}(V_{f,j})Y_{ft,j}V_{t,j} + \text{diag}(V_{f,j})Y_{ft,r}V_{t,r}$$
$$- \text{diag}(V_{f,r})Y_{ft,r}V_{t,j} - \text{diag}(V_{f,r})Y_{ft,j}V_{t,r}$$

6.4. Boundary Conditions to Guarantee a Safe Operation

In Section 2.2, the safe operating state is defined on page 59: Two different categories of operating equipment, buses and lines, lead to two categories of operational limits, buses have voltage limits and lines have power or current limits. Due to the grid model used in this thesis, power limits are used, but the same procedure is also possible for current limits.

Now, using the notation introduced above, this definition can be put into formulas: A safe operating state is defined by three boundary conditions, that can be set in vector-form as follows:

$$V_{\min} \leq V(t) \tag{6.33}$$
$$V_{\max} \geq V(t) \tag{6.34}$$
$$S_{f,\max} \geq S_f(t) \tag{6.35}$$

If a description is wanted in a non-vector form, the following can be used:

$$v_{b,\min} \leq v_b \leq v_{b,\max} \qquad \forall \text{ buses } b \tag{6.36}$$
$$s_l \leq s_{l,\max} \qquad \forall \text{ lines } l \tag{6.37}$$

6.5. Initial and Safe Flexibility Sets

The goal of this chapter is to calculate how much flexibility each flexible energy resource can provide without the grid leaving its safe operating space. There are n_{FA} flexible assets with the following properties:

- A setpoint for active and reactive power for each flexible asset $n = 1, \ldots, n_{\text{FA}}$: $p_{\text{FA},n}^{(0)}$ and $q_{\text{FA},n}^{(0)}$. These individual setpoints can be put into vectors $P_{\text{FA}}^{(0)} \in \mathbb{R}^{n_{\text{FA}}}$ and $Q_{\text{FA}}^{(0)} \in \mathbb{R}^{n_{\text{FA}}}$ or be combined to include both reactive and active power $S_{\text{FA}}^{(0)} \in \mathbb{C}^{n_{\text{FA}}}$.

- These assets were not flexible, if they could not change their power injections or withdrawals from the grid. This change is denoted by the variables $\delta p_{\text{FA},n}$ and $\delta q_{\text{FA},n}$. They denote absolute changes.

- Since the flexibility is not infinite, limits for active $\delta p_{\text{FA,max},n}$, $\delta p_{\text{FA,min},n}$ and reactive power changes $\delta q_{\text{FA,max},n}$, $\delta p_{\text{FA,min},n}$ are needed. As these are absolute changes, all for all four variables are positive: $\delta p_{\text{FA,max},n} \geq 0$, $\delta p_{\text{FA,min},n} \geq 0$, $\delta q_{\text{FA,max},n} \geq 0$, $\delta q_{\text{FA,min},n} \geq 0$.

Knowing all these flexibilities and their limits, these values can be aggregated and the initial flexibility set $F^{(0)}$ containing the reference powers $S_{\text{FA}}^{(0)} \in \mathbb{C}^{n_{\text{FA}}}$ and initial flexibility limits $\delta p_{\text{FA,max},n}^{(0)}$, $\delta p_{\text{FA,min},n}^{(0)}$, $\delta q_{\text{FA,max},n}^{(0)}$, $\delta q_{\text{FA,min},n}^{(0)}$ can be obtained. In a perfect power grid that is built without monetary boundaries, allowing all connected energy resources to inject or withdraw any power they want, this set is equal to the safe flexibility set F, allowing all flexibilities to be used to the TSO's taste. However, this would be very uneconomical, since most of all possible combinations of setpoints do not occur in real life. Therefore, grids are built to allow most combinations of setpoints, but operators have the power to limit the power injections of all energy resources if necessary to remain in a safe operating state.

The more RES are installed, the less are their marginal gains in benefit for the energy system: As a consequence, it is more economical to not build the grid for the situation when all RES inject their installed power, but only for some share of it. The share is usually defined by the regulator. For example, in Germany, DSOs can curtail 3 % of the output energy of all PV installations without financial compensation. This usually corresponds to a curtailment of 70 % of the installed capacity [36]. With rising numbers of RES it is therefore increasingly probable that the initial flexibility set $F^{(0)}$ needs to be reduced in some manner to achieve a safe flexibility set F.

This safe flexibility set F is defined by new, more conservative limits for all n_{FA} flexible energy resources:

$$-\delta p_{\text{FA,min},n}^{(0)} \leq -\delta p_{\text{FA,min},n} \leq \delta p_{\text{FA},n} \leq \delta p_{\text{FA,max},n} \leq \delta p_{\text{FA,max},n}^{(0)} \qquad n = 1, \ldots, n_{\text{FA}} \qquad (6.38)$$

$$-\delta q_{\text{FA,min},n}^{(0)} \leq -\delta q_{\text{FA,min},n} \leq \delta q_{\text{FA},n} \leq \delta q_{\text{FA,max},n} \leq \delta q_{\text{FA,max},n}^{(0)} \qquad n = 1, \ldots, n_{\text{FA}}, \qquad (6.39)$$

with the premise, that all flexibility activation or combinations of such lead to a safe operating state. The task the algorithm has to perform is to reduce the initial individual
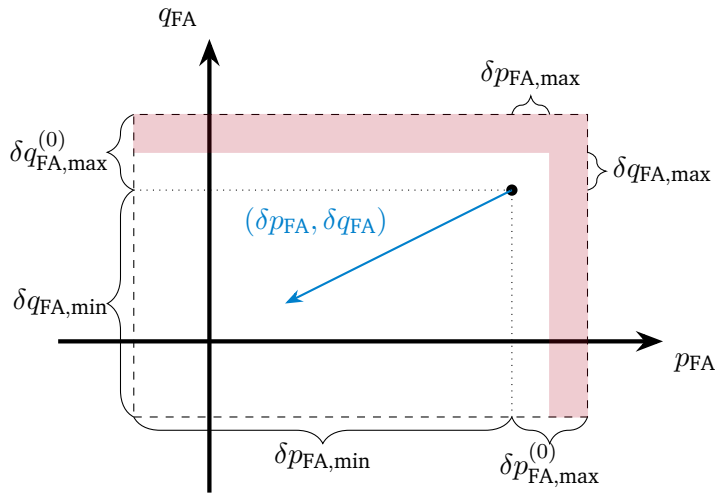
Figure 6.2.: Initial flexibility area of a flexible energy resource and its limitations to achieve a safe operating state. The shaded area in red is set to reduce the flexible energy resource's initial upper flexibility limits $\delta q_{\mathrm{FA,max}}^{(0)}$ and $\delta q_{\mathrm{FA,max}}^{(0)}$ to safe values $\delta q_{\mathrm{FA,max}}$ and $\delta q_{\mathrm{FA,max}}$. An admissible change in the setpoint is shown as a blue arrow.

flexibilities to safe flexibilities and achieve a safe flexibility set. In case that the initial flexibility set is already safe, the algorithm should not enforce more conservative limits.

Figure 6.2 shows this reduction in a general example: The boundary of the initial area, defined by the setpoint and the flexible energy resource's active and reactive power flexibilities, is depicted as a dashed line. The algorithm calculates if all setpoints in this area are leading to a safe operating state, which is not the case. However, limitations of the initial flexibilities are only necessary at the upper boundaries, $\delta p_{\mathrm{FA,max}}^{(0)}$ and $\delta q_{\mathrm{FA,max}}^{(0)}$, which are reduced to the new limits $\delta p_{\mathrm{FA,max}}$ and $\delta q_{\mathrm{FA,max}}$. For the lower limits, $\delta p_{\mathrm{FA,min}}^{(0)} = \delta p_{\mathrm{FA,min}}$ and $\delta q_{\mathrm{FA,min}}^{(0)} = \delta q_{\mathrm{FA,min}}$ are kept. A request for flexibility, resulting in a setpoint shift, as displayed as a blue arrow, is possible, since it does not end in or traverse a red area.

In general, the flexibility area is not rectangular. In Figure 6.3, a triangular area is shown as an example. The shape of the area depends on the generation technology and the reactive power limits may change as a function of active power injection. Some more examples are shown in [135]. The inclusion of such areas requires a more general solution than the one developed here, as here the non-rectangular areas are simplified by inscribing rectangles. As the need for flexibility stems from curative transmission grid operation, active power is more important than reactive power to immediately help relieve active power congestion. Therefore, such inscribed rectangles would be chosen with a focus on active power flexibility, as the blueish area in Figure 6.3.
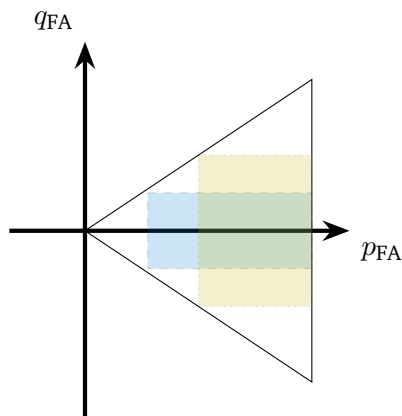
Figure 6.3.: For flexibility areas that are not rectangular, rectangles can be inscribed in with different objectives: maximize the area (yellow), or get more active power flexibility (blue).

6.6. Data Preparation and Needs

Every model needs data to work. In this case, however, the data needs are very manageable:

- A grid model: Here, a bus-branch model is used to calculate power-flows. A different type of grid model, for example a node-breaker, could also be used or transformed into a bus-branch model. Test grids are available from many different sources. For example, built-in models from Matpower [168] or IEEE test grids can be used. In this thesis, a small generic test grid created for the InnoSys consortium [52] and a real distribution grid provided in the same consortium are used.

- Time-series: For different assets connected to the grid model, time-series are needed. In theory, randomly generated values for power injections or loads can be used, but phenomena become more tangible with real or realistic time-series. Here, real data from the InnoSys partners is used.

- Installed generation and load capacities: This data is a part of the grid model. If not present, values for installed loads and generators can be artificially generated. For the conceptual test grid, the capacities are added by hand to the grid model, while for the real grid, the data is included in the original grid model.

- Flexibility factors: Upper and lower bounds for active and reactive power injection or withdrawal are needed to parameterize the installed energy resources. If these values are not available, they can be artificially generated, as done in this thesis.

Summary

In this chapter, the necessary modeling to calculate a safe flexibility set F from an initial flexibility set $F^{(0)}$ is introduced:

- Power-flow calculation is used to determine voltages at all buses in the power grid and the resulting flows over all power lines.

- To solve the calculation of power-flows that comprises a set of equations, slack- or reference-buses are needed, which absorb surplus power or inject missing power and set a reference angle to reduce the number of variables in the set of equations.

- A safe operating state is characterized by the non-violation of voltage and power-flow bounds that stem from physical boundaries to ensure the safety not only for the grid operator, but also the environment around the operating equipment and for the operating equipment itself.

- Initial flexibility sets might need restrictions to guarantee that all setpoints within the set result in a safe operating state. To comply with this restriction, an algorithm is developed in the following chapters of this thesis. The resulting safe flexibility set F guarantees that all setpoints and all combinations of setpoints of all n_{FA} flexible energy resources result in a safe operating state.

- Rectangular flexibility areas are introduced as a simplification in this thesis. For non-rectangular flexibility areas, rectangles can be inscribed.

- Data requirements to perform the modeling for the calculation of safe flexibility sets can be reduced to publicly available test grids, while all other data can be generated artificially.

7. Calculation of Safe and Reliable Flexibility

This chapter introduces a novel method to reliably calculate safe flexibility sets from an initial flexibility set. Not only the optimization itself is described, but also the method by which the individual flexibilities are aggregated onto the grid interconnection points to the TSO. The method of this aggregation is not the authors original work, but was conceptualized in non-public work by several DSOs. However, it has never been formulated or published so far and, to the author's knowledge, has not been tested or used in any application. In the project "connect +" by German grid operators [199], the concept seems to be used, but no detailed information is found with regard to this aspect.

The chapter is structured as follows: at first, the method for aggregation of individual flexibilities is introduced before the optimization problem to limit initial individual flexibilities to safe flexibilities is described.

7.1. Flexibility Cluster

In a distribution grid with more than one grid interconnection point (GICP), the power of the connected assets distributes among the GICPs according to the impedance of each asset with each GICP. The closer a flexible energy resource is located electrically to a GICP, the more of its flexibility will be available at this GICP.

The TSO receiving or requesting this flexibility needs to know how much will be delivered at which bus in his grid. In addition, the TSO is not allowed to request setpoint changes of flexible energy resources not connected in his responsibility area, as this might cause a transition into unsafe operating states. Therefore, a method must be found to both aggregate the individual flexibilities and calculate the sensitivity onto the GICPs.

The method introduced here is called "Wirksamkeitscluster" or flexibility cluster. The idea behind it is to calculate the efficacy of each setpoint change onto each GICP and create clusters incorporating these efficacies or sensitivities. In addition, the method incorporates how a request for flexibility is split between all flexible energy resources.
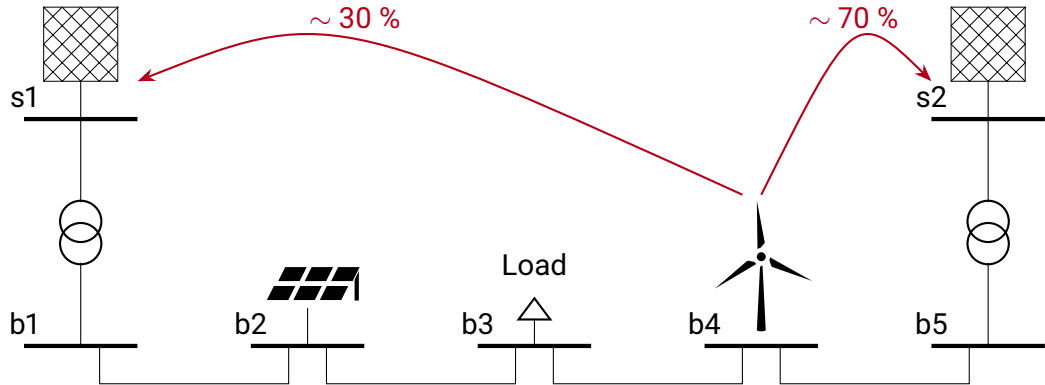
Figure 7.1.: Distribution of flexibility onto grid interconnection points: the power and therefore the flexibility of a flexible energy resource is distributed between the grid interconnection points of the distribution grid in which it is connected. This distribution factor is inversely proportional to the impedance of the connection between the bus and the GICPs.

7.1.1. Aggregation of Individual Assets onto Grid Interconnection Points

The first task to be fulfilled by the flexibility cluster is to aggregate individual flexible energy resources and their flexibility onto the GICPs. For each flexible energy resource, the partial derivative or sensitivity can be computed with which it acts onto a GICP:

$$\delta P_{GICP,t} = \frac{\partial P_{GICP}}{\partial \delta p_{\text{FA}}} \delta p_{\text{FA},t} \tag{7.1}$$

As the sensitivities of interest here are time independent, the index t will be dropped. For several flexible energy resources, the sensitivity becomes a vector, which becomes a matrix if several GICPs are to be observed at once:

$$\begin{pmatrix} \delta P_{GICP,1} \\ \vdots \\ \delta P_{GICP,n_{\text{bs}}} \end{pmatrix} = \underbrace{\begin{pmatrix} \frac{\partial P_{GICP,1}}{\partial \delta p_{\text{FA},1}} & \cdots & \frac{\partial P_{GICP,1}}{\partial \delta p_{\text{FA},n_{\text{FA}}}} \\ \vdots & \ddots & \vdots \\ \frac{\partial P_{GICP,n_{\text{bs}}}}{\partial \delta p_{\text{FA},1}} & \cdots & \frac{\partial P_{GICP,n_{\text{bs}}}}{\partial \delta p_{\text{FA},n_{\text{FA}}}} \end{pmatrix}}_{D} \begin{pmatrix} \delta p_{\text{FA},1} \\ \vdots \\ \delta p_{\text{FA},n_{\text{FA}}} \end{pmatrix} \tag{7.2}$$

This matrix can be called the sensitivity matrix D as it calculates all the sensitivities for all GICPs and flexible energy resources. The sensitivities are in linear order, since only the first

order derivatives are calculated. The validity of this approximation is analyzed in the results on page 158.

The sensitivity matrix does not have to be calculated for all flexible energy resources at once, but a selection of only some of them can be performed and several clusters be created for the different assets. For example, all wind-power is grouped into one cluster, or all assets that have specific reaction times. Due to the linearity of the problem, clusters can be added and the same results be obtained:

$$
\begin{pmatrix} \delta P_{GICP,1} \\ \vdots \\ \delta P_{GICP,n_{\text{bs}}} \end{pmatrix} = D_1 \begin{pmatrix} \delta p_{\text{FA},1} \\ \vdots \\ \delta p_{\text{FA},n_x} \end{pmatrix} + D_2 \begin{pmatrix} \delta p_{\text{FA},n_{x+1}} \\ \vdots \\ \delta p_{\text{FA},n_{\text{FA}}} \end{pmatrix}, \tag{7.3}
$$

where n_x denotes some arbitrary number of assets which is chosen to be included in the first cluster. Such clusters can also be optimized with respect to sensitivities, so that some cluster affects mainly one GICP and another cluster affects mainly another GICP.

For the TSO, a sensitivity vector $\vec{d}$ is calculated for each cluster, containing the sensitivities of the total upward ΔP^{up} and downward ΔP^{down} flexibility onto the GICPs. This way, the TSO can easily see how much total flexibility is available and how it translates onto the GICPs. The total upward and downward flexibilities are obtained by addition of all individual upward and downward flexibilities. The vector $\vec{d}$ is calculated in the following way:

$$
\vec{d} = D \begin{pmatrix} \delta p_{\text{FA},1} \\ \vdots \\ \delta p_{\text{FA},n_{\text{FA}}} \end{pmatrix} \cdot \frac{1}{\Delta P^{\text{up}}} \qquad\qquad \Delta P^{\text{up}} = \sum_{i=1}^{n_{\text{FA}}} \delta p_{\text{FA},i}^{\text{up}} \tag{7.4}
$$

Here, the example is for upward flexibility. However, the same is valid for downward flexibility. If only some assets are to be included, the summation to obtain ΔP^{up} is only performed over these assets. The sum over the components of $\vec{d}$ does not need to be equal to one, as losses can occur or be avoided, depending on the power-flow before and after the request for flexibility. If the providing grid is in a state where it is injecting power into the transmission grid, and upward flexibility is needed, the losses will rise and for example only 90 % of the total flexibility will be available at the GICPs. However, if in the same situation downward flexibility is needed, losses will be reduced, and the aggregated amount is greater than the sum of the individual amounts.

7.1.2. Disaggregation of Requests onto Individual Assets

The moment a TSO needs to activate the flexibility that was aggregated before, the call must be disaggregated onto the individual assets. There are several ways, how such a disaggregation

can be performed: proportional to the offered flexibility, proportional to the rated power of the asset, governed by a minimization of losses, or by another metric. As a distribution proportional to the offered flexibility is free of discrimination and might be favored by future regulation, in this thesis, the disaggregation is performed proportional to the offered flexibility of each flexible energy resource:

$$\begin{pmatrix} \delta P_{GICP,1} \\ \vdots \\ \delta P_{GICP,n_{bs}} \end{pmatrix} = \frac{\delta P}{\Delta P^{\mathrm{up}}} \begin{pmatrix} \delta p_{\mathrm{FA},1} \\ \vdots \\ \delta p_{\mathrm{FA},n_{\mathrm{FA}}} \end{pmatrix} \qquad \delta P \in [0, \Delta P^{\mathrm{up}}] \qquad (7.5)$$

$$\begin{pmatrix} \delta P_{GICP,1} \\ \vdots \\ \delta P_{GICP,n_{bs}} \end{pmatrix} = \frac{\delta P}{\Delta P^{\mathrm{down}}} \begin{pmatrix} \delta p_{\mathrm{FA},1} \\ \vdots \\ \delta p_{\mathrm{FA},n_{\mathrm{FA}}} \end{pmatrix} \qquad \delta P \in [\Delta P^{\mathrm{down}}, 0] \qquad (7.6)$$

This proportionality together with the linearization allowing the summation of clusters leads to a very simple interface: the TSO only needs to specify the cluster and the amount of power desired.
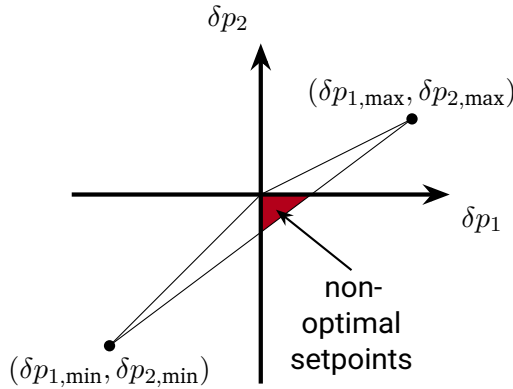
Figure 7.2.: Non-optimal setpoints due to different gradients in upward and downward flexibility provision in a case of two flexible energy resources and active power flexibility. In the red area, the first asset shifts its power injection upwards, while the second one shifts downwards.

As one can see in equations 7.5 and 7.6, the clusters for upward and downward flexibility are called upon separately. This is done to avoid non-optimal setpoint combinations, where in case of a request for flexibility, some flexible energy resources shift their setpoints toward more power injection, while others do the opposite. Figure 7.2 depicts such a case for two flexible energy resources and their active power flexibility limits. In a case with more assets, the problem remains the same, but becomes more-dimensional, turning the red triangle into a pyramid for three assets or a 5-cell for four. Only if gradients for both upward and downward flexibility are the same, such behavior is avoided.

7.2. Robust Optimization

In this section, the optimization model to reduce the initial flexibility sets $F^{(0)}$ to safe sets F is developed. At first, the problem is described and a linearization of power-flow is introduced before the actual robust optimization model is developed.

7.2.1. Optimization to Calculate Power Flows

One first thought about optimization to solve power flow problems is, why it is possible to use optimization to solve the problem of power-flow calculation. The easiest and most apparent method to calculate all power-flows between all buses is using a standard method for a system of non-linear equations, as the Newton-Raphson method. This iterative approach uses partial differentiation to find the roots of the system. However, the physical properties of electromagnetism can also be used, in this case the fact, that the current in a system will always take the route of least resistance. This means, that power-flows in the system will always flow such that the losses are minimal.

Rephrasing the problem as an optimization, the objective is simple: minimize all losses while adhering to certain boundary conditions, which are the power balance equations, based on the physical conversation laws. A nice side-benefit to using optimization is the possibility to include additional boundary conditions and costs, for example operating limits of assets in the grid, or in case of an optimal power-flow, generation costs for electrical power.

7.2.2. Problem Description

The flexibility provisioning problem has two main objectives:

1. Reduce individual initial flexibility limitations $\delta p_{\mathrm{FA,max}}^{(0)}$, $\delta p_{\mathrm{FA,min}}^{(0)}$, $\delta q_{\mathrm{FA,max}}^{(0)}$, $\delta q_{\mathrm{FA,min}}^{(0)}$ to such values $\delta p_{\mathrm{FA,max}}$, $\delta p_{\mathrm{FA,min}}$, $\delta q_{\mathrm{FA,max}}$, $\delta q_{\mathrm{FA,min}}$, that a safe operation is guaranteed for all setpoint combinations inside those boundaries.

2. Keep as much of the initial flexibility as possible to provide a maximum of aggregated flexibility.

In an optimization problem, the first objective is formulated as boundary conditions while the second point is the objective function:

$$f_{\mathrm{obj}} = \sum_{n}^{n_{\mathrm{FA}}} \Big[c_p(\delta p_{n,\mathrm{max}}^{(0)} - \delta p_{n,\mathrm{max}}) + c_p(\delta p_{n,\mathrm{min}}^{(0)} - \delta p_{n,\mathrm{min}}) \tag{7.7}$$
$$+ c_q(\delta q_{n,\mathrm{max}}^{(0)} - \delta q_{n,\mathrm{max}}) + c_q(\delta q_{n,\mathrm{min}}^{(0)} - \delta q_{n,\mathrm{min}}) \Big],$$

where c_p and c_q are cost factors for active and reactive flexibility reductions. These cost factors reflect the marginal economic value of flexibility. To address the first point, boundary conditions are added:

$$\min f_{\text{obj}} \text{ so that } \begin{array}{ll} V_{\min} & \leq V \\ V_{\max} & \geq V \\ S_{\text{f,max}} & \geq S_{\text{f}} \end{array} \quad \forall \delta p \in [\delta p_{\min}, \delta p_{\max}], \ \forall \delta q \in [\delta q_{\min}, \delta q_{\max}] \qquad (7.8)$$

To be able to fulfill both points, it is necessary to asses the effect of a change in power or load injection of each asset onto the power grid. For all non-slack-buses, the voltage $V_{\text{ns}} = V_{\text{ns}}^{(0)} + \delta V_{\text{ns}}$ changes from its initial, unperturbed values $V_{\text{ns}}^{(0)}$ to a new value V_{ns} due to changes in the power injection at the non-slack-buses $S_{\text{ns}} = S_{\text{ns}}^{(0)} + \delta S_{\text{ns}}$. Here, δS_{ns} are changes in power injections as caused by a request for flexibility and $S_{\text{ns}}^{(0)}$ the initial injections. $S_{\text{ns}}^{(0)}$ is also called the reference point or linearization point, as the linearization of power-flows is performed at this point.

7.2.3. Linearization of the Power Flow

Linearization is used to be able to simplify the problem and later transform it into a robust optimization problem. Therefore, higher orders of derivatives are dropped. Taking the power balance equation 6.13, the functional dependence with respect to voltage changes δV can be obtained. This can be done by using partial derivatives $\frac{\partial}{\partial \delta V}$, which is the same as $\frac{\partial}{\partial V}\delta V$ or by using perturbations δV. In general, when writing δX, this is a linear approximation and the same as $\frac{\partial X}{\partial Y}\delta Y$, where $Y = V$ if not specified otherwise. To show that both the derivations, via perturbation theory and via partial derivatives, are the same and can be used interchangeably, they are shortly demonstrated, and only the second will be used in the following. At first the introduction of a perturbation δV:

$$S = \text{diag}(V)Y^* \cdot V^* \qquad (7.9)$$

$$S + \delta S = \text{diag}(V + \delta V)Y^* \cdot (V + \delta V)^* \qquad (7.10)$$

$$\delta S = \text{diag}(\delta V)Y^*V^* + \text{diag}(V)Y^*\delta V^* + \underline{\text{diag}(\delta V)Y^*\delta V^*} \qquad (7.11)$$

Now, the same as a product of partial derivation:

$$S = \text{diag}(V)Y^* \cdot V^* \qquad (7.12)$$

$$\frac{\partial S}{\partial \delta V} = \text{diag}(\frac{\partial V}{\partial \delta V})Y^*V^* + \text{diag}(V)Y^*\frac{\partial V^*}{\partial \delta V} \qquad (7.13)$$

$$\delta S = \text{diag}(\delta V)Y^*V^* + \text{diag}(V)Y^*\delta V^* \qquad (7.14)$$

The third term in Equation 7.11 is dropped, because it contains perturbations of second order. Analogously, derivatives of higher order are excluded, to simplify the problem to a desired level. Here, the goal is a linear problem, so that robust optimization can be used and the speed with which the problem can be solved increases.

In the above equations, S and δS are node-injections. However, in the problem of distributed flexibilities, a number of flexible assets that are connected to these nodes are put into the problem. To calculate bus injections from the available asset injections, an asset allocation matrix A_{FA} is introduced for all n_{FA} flexible assets, describing the relation which asset is connected to which bus. Node-injections S can be calculated by multiplying the injections S_{FA} of all assets by the allocation matrix A_{FA}:

$$S = A_{\mathrm{FA}} S_{\mathrm{FA}} \tag{7.15}$$

The dimensions of this matrix A_{FA} are $\mathbb{N}^{n_{\mathrm{b}} \times n_{\mathrm{FA}}}$. An example: Assume a grid with three buses and five assets, of which three are connected to the second node. The allocation matrix then looks like this:

$$A_{\mathrm{FA}} = \begin{pmatrix} 1 & 0 & 0 & 0 & 0 \\ 0 & 1 & 1 & 1 & 0 \\ 0 & 0 & 0 & 0 & 1 \end{pmatrix} \tag{7.16}$$

As the voltage at the slack-buses b_{s} are kept constant and do not change due to changes in power injections at non-slack-buses, the problem's dimension can be reduced. This can be done by multiplying the vectors or matrices by another allocation matrix $A_{\mathrm{ns}} \in \mathbb{N}^{n_{\mathrm{bns}} \times n_{\mathrm{b}}}$. It is defined by the following relation:

$$V_{\mathrm{ns}} = A_{\mathrm{ns}} V \tag{7.17}$$

Here, V_{ns} is the voltage-vector of non-slack-nodes and V the vector containing all voltages. An example for a four-bus system is:

$$A_{\mathrm{ns}} = \begin{pmatrix} 0 & 1 & & \\ & & 1 & \\ & & & 1 \end{pmatrix} \qquad V_{\mathrm{ns}} = \begin{pmatrix} v_{2,\mathrm{ns}} \\ v_{3,\mathrm{ns}} \\ v_{4,\mathrm{ns}} \end{pmatrix} \qquad V = \begin{pmatrix} v_{1,s} \\ v_{2,\mathrm{ns}} \\ v_{3,\mathrm{ns}} \\ v_{4,\mathrm{ns}} \end{pmatrix} \tag{7.18}$$

Of course, a similar relation for the admittance matrix is needed which is $Y_{\mathrm{ns}} = A_{\mathrm{ns}} Y A_{\mathrm{ns}}^{T}$, with A_{ns}^{T} the transpose of A_{ns}. To construct A_{ns}, an identity matrix $\mathbb{1}$ is taken and the rows at the indices of the slack-nodes are deleted. To perform a reverse operation, that is the addition of slack-buses into a vector of size n_{bns}, the transposed allocation matrix A_{ns}^{T} is multiplied

by the non-slack voltage vector V_{ns}. The result is a vector of original dimension n_{b}, but the entries for slack-buses are replaced by zeros. Using this allocation matrix from Equation 7.17, Equation 7.14 is rewritten:

$$\delta S_{\mathrm{ns}} = \mathrm{diag}(\delta V_{\mathrm{ns}})Y_{\mathrm{ns}}^* V_{\mathrm{ns}}^* + \mathrm{diag}(V_{\mathrm{ns}})Y_{\mathrm{ns}}^* \delta V_{\mathrm{ns}}^* \tag{7.19}$$

Using linear algebra, this equation can be reformulated so that all voltage deviations δV are at one side:

$$\delta S_{\mathrm{ns}} = \mathrm{diag}(V_{\mathrm{ns}})Y_{\mathrm{ns}}^* \delta V_{\mathrm{ns}}^* + \mathrm{diag}(Y_{\mathrm{ns}}^* V_{\mathrm{ns}}^*)\delta V_{\mathrm{ns}} \tag{7.20}$$

Also, real and imaginary parts can be separated to get the equations for active and reactive power:

$$\delta S_{\mathrm{ns}} = \delta P_{\mathrm{ns}} + \mathrm{j} \cdot \delta Q_{\mathrm{ns}} \tag{7.21}$$

Writing the separated components in a matrix-equation, the following simplification is possible:

$$\begin{pmatrix} \delta P_{\mathrm{ns}} \\ \delta Q_{\mathrm{ns}} \end{pmatrix} = \begin{pmatrix} A & B \\ C & D \end{pmatrix} \begin{pmatrix} \delta V_{\mathrm{r,ns}} \\ \delta V_{\mathrm{j,ns}} \end{pmatrix}, \tag{7.22}$$

where the entries A, B, C and D are partial derivatives:

$$A = \frac{\partial P_{\mathrm{ns}}}{\partial V_{\mathrm{r}}} = \mathrm{diag}(V_{r,\mathrm{ns}})Y_{r,\mathrm{ns}} + \mathrm{diag}(V_{\mathrm{j,ns}})Y_{j,\mathrm{ns}} \tag{7.23}$$

$$+ \mathrm{diag}(Y_{r,\mathrm{ns}}V_{r,\mathrm{ns}}) - \mathrm{diag}(Y_{j,\mathrm{ns}}V_{\mathrm{j,ns}})$$

$$B = \frac{\partial P_{\mathrm{ns}}}{\partial V_{\mathrm{j}}} = \mathrm{diag}(V_{\mathrm{j,ns}})Y_{r,\mathrm{ns}} - \mathrm{diag}(V_{r,\mathrm{ns}})Y_{j,\mathrm{ns}} \tag{7.24}$$

$$+ \mathrm{diag}(Y_{r,\mathrm{ns}}V_{\mathrm{j,ns}}) + \mathrm{diag}(Y_{j,\mathrm{ns}}V_{r,\mathrm{ns}})$$

$$C = \frac{\partial Q_{\mathrm{ns}}}{\partial V_{\mathrm{r}}} = \mathrm{diag}(V_{\mathrm{j,ns}})Y_{r,\mathrm{ns}} - \mathrm{diag}(V_{r,\mathrm{ns}})Y_{j,\mathrm{ns}} \tag{7.25}$$

$$- \mathrm{diag}(Y_{j,\mathrm{ns}}V_{r,\mathrm{ns}}) - \mathrm{diag}(Y_{r,\mathrm{ns}}V_{\mathrm{j,ns}})$$

$$D = \frac{\partial Q_{\mathrm{ns}}}{\partial V_{\mathrm{j}}} = -\mathrm{diag}(V_{r,\mathrm{ns}})Y_{r,\mathrm{ns}} - \mathrm{diag}(V_{\mathrm{j,ns}})Y_{j,\mathrm{ns}} \tag{7.26}$$

$$+ \mathrm{diag}(Y_{r,\mathrm{ns}}V_{r,\mathrm{ns}}) - \mathrm{diag}(Y_{j,\mathrm{ns}}V_{\mathrm{j,ns}})$$

This equation now shows the change of power or load injection as a function of voltage changes. The Matrix is also commonly referred to as Jacobi-matrix or *Jacobian*. However, the

inverse relation of voltage changes due to variations in active and reactive power is needed, which can be achieved by inverting the matrix:

$$\begin{pmatrix} \delta V_{\text{r,ns}} \\ \delta V_{\text{j,ns}} \end{pmatrix} = \begin{pmatrix} A & B \\ C & D \end{pmatrix}^{-1} \begin{pmatrix} \delta P_{\text{ns}} \\ \delta Q_{\text{ns}} \end{pmatrix} \tag{7.27}$$

To simplify notation, this inverted matrix is denoted by $\frac{\partial V_{\text{ns}}}{\partial S}$, Equation 7.27 then simplifies to:

$$\delta V_{\text{ns}} = \frac{\partial V_{\text{ns}}}{\partial S} \delta S_{\text{ns}} \tag{7.28}$$

Note, that this inversion is only possible since the slack-nodes are removed. To calculate power-flow deviations in addition to voltage deviation, Equation 6.28, that describes how to calculate power-flows into one end of a power line, is used:

$$S_{\text{f}} = \text{diag}(V_{\text{f}})Y_{\text{f}}^{*}V^{*} \tag{7.29}$$

Now, the same approach used to calculate voltage deviations as a function of power injection changes is used for all branches l to calculate changes in power-flows as a function of voltage changes:

$$\delta S_{\text{f}} = \frac{\partial S_{\text{f}}}{\partial V} \delta V \tag{7.30}$$

$$\frac{\partial S_{\text{f}}}{\partial V} = \frac{\partial \text{diag}(V_{\text{f}})}{\partial V} Y^{*}V^{*} + \text{diag}(V_{\text{f}})Y^{*}\frac{\partial V^{*}}{\partial V} \tag{7.31}$$

Here, δV is a vector of dimension n_{b}. Fortunately, the voltage deviation $\delta V = 0$ for slack-nodes, and the δV_{ns}-vectors from Equation 7.28 can be filled with zeros for the slack-buses with the help of the transposed allocation matrix A_{ns}^{T} from Equation 7.18:

$$\delta V_{\text{r}} = A_{\text{ns}}^{T} \delta V_{\text{r,ns}} \qquad\qquad \delta V_{\text{j}} = A_{\text{ns}}^{T} \delta V_{\text{j,ns}} \tag{7.32}$$

To obtain the correct allocation-matrix for δV, the Kronecker-product which is denoted by the $\otimes$ symbol is used:

$$\delta V = \begin{pmatrix} 1 & 0 \\ 0 & 1 \end{pmatrix} \otimes A_{\text{ns}}^{T} \delta V_{\text{ns}} = \begin{pmatrix} A_{\text{ns}}^{T} & 0 \\ 0 & A_{\text{ns}}^{T} \end{pmatrix} \delta V_{\text{ns}} \tag{7.33}$$

As for the voltages, active and reactive components are separated to establish equations for active power injections $\delta P_{\text{f}} = \text{Re}(\delta S_{\text{f}})$ and reactive power injections $\delta Q_{\text{f}} = \text{Im}(\delta S_{\text{f}})$ into

each line:

$$\delta P_f = \frac{\partial P_f}{\partial V} \delta V \tag{7.34}$$

$$\delta Q_f = \frac{\partial Q_f}{\partial V} \delta V \tag{7.35}$$

As for the voltages in equations 7.23 to 7.26, this can be expressed in terms of partial derivatives:

$$\begin{pmatrix} \delta P_f \\ \delta Q_f \end{pmatrix} = \underbrace{\begin{pmatrix} A & B \\ C & D \end{pmatrix}}_{\frac{\partial S_f}{\partial V}} \begin{pmatrix} \delta V_r \\ \delta V_j \end{pmatrix} \tag{7.36}$$

The block-components of the $\frac{\partial S_f}{\partial V}$ matrix can be written down as partial derivatives:

$$A = \frac{\partial P_f}{\partial V_r} = \mathrm{diag}(Y_{f,r} V_r) C_f - \mathrm{diag}(Y_{f,j} V_j) C_f \tag{7.37}$$
$$+ \mathrm{diag}(C_f V_r) Y_{f,r} + \mathrm{diag}(C_f V_j) Y_{f,j}$$

$$B = \frac{\partial P_f}{\partial V_j} = \mathrm{diag}(Y_{f,r} V_j) C_f + \mathrm{diag}(Y_{f,j} V_r) C_f \tag{7.38}$$
$$- \mathrm{diag}(C_f V_r) Y_{f,j} + \mathrm{diag}(C_f V_j) Y_{f,r}$$

$$C = \frac{\partial Q_f}{\partial V_r} = -\mathrm{diag}(Y_{f,j} V_r) C_f - \mathrm{diag}(Y_{f,r} V_j) C_f \tag{7.39}$$
$$+ \mathrm{diag}(C_f V_j) Y_{f,r} - \mathrm{diag}(C_f V_r) Y_{f,j}$$

$$D = \frac{\partial Q_f}{\partial V_j} = -\mathrm{diag}(Y_{f,j} V_j) C_f + \mathrm{diag}(Y_{f,r} V_r) C_f \tag{7.40}$$
$$- \mathrm{diag}(C_f V_j) Y_{f,j} - \mathrm{diag}(C_f V_r) Y_{f,r}$$

The matrix formula can also be written as a product of partial derivatives:

$$\delta S_f = \frac{\partial S_f}{\partial V} \frac{\partial V}{\partial S} \delta S_{ns} \tag{7.41}$$

Using the Kronecker-product, the power-flow into a branch is formulated as a functional dependence of power injection changes analogously to the voltages:

$$\delta S_f = \frac{\partial S_f}{\partial V} \mathbb{1}_{2\times2} \otimes A_{ns}^T \frac{\partial V_{ns}}{\partial S} \delta S_{ns} \tag{7.42}$$

7.2.4. Linearization of Voltage Limits

Now, knowing the change in complex voltages as a function of a variation in power injections, the boundary conditions for voltages can be formulated to adhere operational limits. These voltage limits are functions of magnitudes or absolute values. If $|V|$ is set as the vector of absolute values of the entries of the V vector, the conditions can be formulated:

$$|V_{\text{max}}| \geq \left|V^{(0)} + \delta V\right| \qquad\qquad \forall\ \delta S_{\text{ns}} \qquad\qquad (7.43)$$

$$|V_{\text{min}}| \leq \left|V^{(0)} + \delta V\right| \qquad\qquad \forall\ \delta S_{\text{ns}} \qquad\qquad (7.44)$$

These equations are valid for all nodes, including the slack-nodes, but no deviations $\delta V = 0$ are assumed for all slack-buses. These inequalities must hold for all injection-change vectors δS_{ns}. The purpose of the optimization problem is to limit the injection changes to only those δS_{ns}, for which boundary conditions are not violated. However, the power injections, that can lead to critical voltage changes δV_{ns} at non-slack buses, are different for Equation 7.43 and for Equation 7.44. In Equation 7.43, the δS_{ns} causing the biggest change of voltage in positive direction is searched for, while in Equation 7.44, the δS_{ns} causing the biggest change in negative direction is of interest. It is therefore important, to optimize in the correct direction of voltage changes and not just to maximize δV_{ns}. A formulation of the above formulas, that makes this more obvious is as follows:

$$|V_{\text{max}}| \geq \max_{\delta S_{\text{ns}}} \left|V_{\text{ns}}^{(0)} + \delta V_{\text{ns}}\right| \qquad\qquad (7.45)$$

$$|V_{\text{min}}| \leq \min_{\delta S_{\text{ns}}} \left|V_{\text{ns}}^{(0)} + \delta V_{\text{ns}}\right| \qquad\qquad (7.46)$$

This way, the equations not only provide better understanding, but also the problem is transformed from a "for-all"-type problem into a problem of finding an extreme.

These equations are solved to get a term describing the dependence of the voltage magnitudes from the changes in power injections. The dependency $\delta V_{\text{ns}} = \frac{\partial V_{\text{ns}}}{\partial S} \delta S_{\text{ns}}$ is already known. Now, the absolute value function has to be linearized, to obtain a linear problem in the end. The linearization is set to be:

$$\left|V_{\text{ns}}^{(0)} + \delta V_{\text{ns}}\right| \approx \left|V_{\text{ns}}^{(0)}\right| + \delta|V_{\text{ns}}| \qquad\qquad (7.47)$$

$$\delta|V_{\text{ns}}| = \frac{\partial\, \delta\left|V_{\text{ns}}^{(0)}\right|}{\partial S} \delta S_{\text{ns}} \qquad\qquad (7.48)$$

These last equations are also valid if squared absolute values are used, which helps when differentiating the absolute value function as a differentiable function of real- and imaginary

part, which can be rewritten as $|z|^2 = z \cdot z^*$:

$$\delta |V_{\mathrm{ns}}|^2 = \frac{\partial \left|V_{\mathrm{ns}}^{(0)}\right|^2}{\partial S} \delta S_{\mathrm{ns}} \tag{7.49}$$

$$\frac{\partial \left|V_{\mathrm{ns}}^{(0)}\right|^2}{\partial S} = \frac{\partial \operatorname{diag}(V_{\mathrm{ns}}^{(0)}) \cdot V_{\mathrm{ns}}^{(0)*}}{\partial S} \tag{7.50}$$

$$= \frac{\partial \operatorname{diag}(V_{\mathrm{ns}}^{(0)})}{\partial S} V_{\mathrm{ns}}^{(0)*} + \operatorname{diag}(V_{\mathrm{ns}}^{(0)}) \frac{\partial V_{\mathrm{ns}}^{(0)*}}{\partial S} \tag{7.51}$$

$$= 2 \left(\frac{\partial \operatorname{diag}(V_{\mathrm{r,ns}}^{(0)})}{\partial S} V_{\mathrm{r}} + \frac{\partial \operatorname{diag}(V_{\mathrm{j,ns}}^{(0)})}{\partial S} V_{\mathrm{j}} \right) \tag{7.52}$$

For the absolute value of $V_{\mathrm{ns}}^{(0)}$, it can analogously be written as:

$$\operatorname{diag}(V_{\mathrm{r,ns}}^{(0)}) V_{\mathrm{r,ns}}^{(0)} + \operatorname{diag}(V_{\mathrm{j,ns}}^{(0)}) V_{\mathrm{j,ns}}^{(0)} = \left|V_{\mathrm{ns}}^{(0)}\right|^2 \tag{7.53}$$

Using this linearization, boundary conditions for voltages from Equation 7.45 and Equation 7.46 are reformulated:

$$\left|V_{\mathrm{max,ns}}\right|^2 \geq \max_{\delta S_{\mathrm{ns}}} \left(\left|V_{\mathrm{ns}}^{(0)}\right|^2 + \delta |V_{\mathrm{ns}}|^2 \right) \tag{7.54}$$

$$\left|V_{\mathrm{min,ns}}\right|^2 \leq \min_{\delta S_{\mathrm{ns}}} \left(\left|V_{\mathrm{ns}}^{(0)}\right|^2 + \delta |V_{\mathrm{ns}}|^2 \right) \tag{7.55}$$

With Equation 7.28, voltage boundaries are formulated as a function of changes in power injection:

$$\delta |V_{\mathrm{ns}}|^2 = \frac{\partial |V_{\mathrm{ns}}|^2}{\partial V} \frac{\partial V_{\mathrm{ns}}}{\partial S} \delta S_{\mathrm{ns}} \tag{7.56}$$

$$= \frac{\partial |V_{\mathrm{ns}}|^2}{\partial S} \delta S_{\mathrm{ns}} \tag{7.57}$$

Now, the boundary conditions from equations 7.54 and 7.54 are reformulated with the help of the new matrix $\frac{\partial |V_{\mathrm{ns}}|^2}{\partial V}$:

$$\left|V_{\mathrm{max,ns}}\right|^2 \geq \max_{\delta S_{\mathrm{ns}}} \left(\left|V_{\mathrm{ns}}^{(0)}\right|^2 + \frac{\partial |V_{\mathrm{ns}}|^2}{\partial V} \frac{\partial V_{\mathrm{ns}}}{\partial S} \delta S_{\mathrm{ns}} \right) \tag{7.58}$$

$$\left|V_{\mathrm{min,ns}}\right|^2 \leq \min_{\delta S_{\mathrm{ns}}} \left(\left|V_{\mathrm{ns}}^{(0)}\right|^2 + \frac{\partial |V_{\mathrm{ns}}|^2}{\partial V} \frac{\partial V_{\mathrm{ns}}}{\partial S} \delta S_{\mathrm{ns}} \right) \tag{7.59}$$

These equations must hold for all vectors δS. Indeed, the goal is to limit the extremes of the flexibilities $\delta p_{\text{max},k}$, $\delta p_{\text{min},k} \in \delta P$ and $\delta q_{\text{max},k}$, $\delta q_{\text{min},k} \in \delta Q$ to be provided at each non-slack-node b_{ns} to such values, that this is just the case. In addition, the $V_{\text{ns}}^{(0)}$ vectors can be taken out of the min and max functions, since $V_{\text{ns}}^{(0)}$ is independent of changes in power injections:

$$\left|V_{\text{max,ns}}\right|^2 \geq \left|V_{\text{ns}}^{(0)}\right|^2 + \max_{\delta S_{\text{ns}}} \left(\frac{\partial |V_{\text{ns}}|^2}{\partial V} \frac{\partial V_{\text{ns}}}{\partial S} \delta S_{\text{ns}} \right) \tag{7.60}$$

$$\left|V_{\text{min,ns}}\right|^2 \leq \left|V_{\text{ns}}^{(0)}\right|^2 + \min_{\delta S_{\text{ns}}} \left(\frac{\partial |V_{\text{ns}}|^2}{\partial V} \frac{\partial V_{\text{ns}}}{\partial S} \delta S_{\text{ns}} \right) \tag{7.61}$$

$$\leq \left|V_{\text{ns}}^{(0)}\right|^2 - \max_{\delta S_{\text{ns}}} \left(-\frac{\partial |V_{\text{ns}}|^2}{\partial V} \frac{\partial V_{\text{ns}}}{\partial S} \delta S_{\text{ns}} \right) \tag{7.62}$$

This can be rewritten, to explicitly show the inequality in known parts on the left and unknown parts on the right:

$$\left|V_{\text{max,ns}}\right|^2 - \left|V_{\text{ns}}^{(0)}\right|^2 \geq \max_{\delta S_{\text{ns}}} \left(\frac{\partial |V_{\text{ns}}|^2}{\partial V} \frac{\partial V_{\text{ns}}}{\partial S} \delta S_{\text{ns}} \right) \tag{7.63}$$

$$\left|V_{\text{ns}}^{(0)}\right|^2 - \left|V_{\text{min,ns}}\right|^2 \geq \max_{\delta S_{\text{ns}}} \left(-\frac{\partial |V_{\text{ns}}|^2}{\partial V} \frac{\partial V_{\text{ns}}}{\partial S} \cdot \delta S_{\text{ns}} \right) \tag{7.64}$$

Following [143, p. 288], this maximum condition can be rewritten into a norm of our choosing to find an analytical solution of the inner optimization problem.

$$\max_{\|z\|_r \leq 1} w^T z = \|w\|_{r'} \qquad \frac{1}{r} + \frac{1}{r'} = 1, \tag{7.65}$$

where $w, z \in \mathbb{R}^n$, $r, r' \in \mathbb{Z}$, and $\| \ \|_{r'}$ is the dual norm of $\| \ \|_r$. However, to be able to perform this step, it is necessary to transform the boundary conditions to achieve a normed and symmetric z. First, the symmetrization transformation T_1 is performed by shifting the reference point into the middle of the flexibility range:

$$\max_{\substack{\delta S_{\text{min,ns}} \leq \delta S_{\text{ns}} \\ \delta S_{\text{ns}} \leq \delta S_{\text{max,ns}}}} \frac{\partial |V_{\text{ns}}|^2}{\partial S} \delta S_{\text{ns}} \stackrel{T_1}{=} \max_{\|\delta \tilde{S}_{\text{ns}}\| \leq \delta \tilde{S}_{lim,\text{ns}}} \frac{\partial |V_{\text{ns}}|^2}{\partial S} (\delta \tilde{S}_{\text{ns}} + S_{\text{shift,ns}}) \tag{7.66}$$

As before, $\delta S_{ns} = \begin{pmatrix} \delta P_{ns} \\ \delta Q_{ns} \end{pmatrix}$. For $\delta \tilde{S}_{ns}$ and $S_{shift,ns}$, the following holds:

$$\delta P_{ns} = \delta \tilde{P}_{ns} + P_{shift,ns} \qquad\qquad \delta Q_{ns} = \delta \tilde{Q}_{ns} + Q_{shift,ns} \qquad (7.67)$$

$$P_{shift,ns} = \frac{\delta P_{max,ns} - \delta P_{min,ns}}{2} \qquad\qquad Q_{shift,ns} = \frac{\delta Q_{max,ns} - \delta Q_{min,ns}}{2} \qquad (7.68)$$

$$\delta \tilde{S}_{ns} = \begin{pmatrix} \delta \tilde{P}_{ns} \\ \delta \tilde{Q}_{ns} \end{pmatrix} \qquad\qquad S_{shift,ns} = \begin{pmatrix} P_{shift,ns} \\ Q_{shift,ns} \end{pmatrix}$$

The symmetric limit $\delta \tilde{P}_{lim,ns}$ instead of the unsymmetrical $\delta P_{max,ns}$ and $\delta P_{min,ns}$ can be formulated:

$$\delta \tilde{P}_{lim,ns} = \delta P_{max,ns} - P_{shift,ns} = P_{shift,ns} + \delta P_{min,ns} \qquad (7.69)$$

$$= \frac{\delta P_{max,ns} + \delta P_{min,ns}}{2} \qquad (7.70)$$

Now, parts of the boundary conditions from Equation 7.66 are reformulated using this transformation:

$$\max_{\substack{\delta S_{min,ns} \leq \delta S_{ns} \\ \delta S_{ns} \leq \delta S_{max,ns}}} \frac{\partial |V_{ns}|^2}{\partial S} \delta S_{ns} \stackrel{T_1}{=} \max_{\|\delta \tilde{S}_{ns}\| \leq \delta \tilde{S}_{lim,ns}} \frac{\partial |V_{ns}|^2}{\partial S} (\delta \tilde{S}_{ns} + S_{shift,ns}) \qquad (7.71)$$

$$= \max_{\|\delta \tilde{S}_{ns}\| \leq \delta \tilde{S}_{lim,ns}} \frac{\partial |V_{ns}|^2}{\partial S} \delta \tilde{S}_{ns} \qquad (7.72)$$

$$+ \frac{\partial |V_{ns}|^2}{\partial S} S_{shift,ns}$$

However, to apply Equation 7.65 the vector $\delta \tilde{S}_{ns}$ must be normalized, so that $\left\| \delta \tilde{S}_{ns} \right\| \leq 1$. To achieve this, another transformation T_2 is performed as in the following example:

$$\max_{\|z\| \leq a} (w^T z) = \max_{\left\| \frac{z}{a} \right\| \leq 1} (w^T z) \qquad (7.73)$$

$$= \max_{\|\tilde{z}\| \leq 1} (w^T \tilde{z} \cdot a) \qquad\qquad z = \tilde{z} \cdot a \qquad (7.74)$$

When using the $\| \ \|_\infty$ as r-norm, only the largest component of z is needed and all components of the vector need to be divided by it. However, it is unknown which component is the largest. Therefore a component-wise division by their maxima which are to be found

by the optimization is performed:

$$\max_{\substack{\|z_1\|\le a_1 \\ \vdots \\ \|z_{2n_{\mathrm{bns}}}\|\le a_{2n_{\mathrm{bns}}}}} (w^T z) = \max_{\|\tilde{z}\|\le 1}(w^T \operatorname{diag}(A)\tilde{z}) \qquad A = \begin{pmatrix} a_1 \\ \vdots \\ a_{2n_{\mathrm{bns}}} \end{pmatrix} \tag{7.75}$$

$$z = \operatorname{diag}(A)\cdot\tilde{z} \qquad \tilde{z} = \begin{pmatrix} \frac{1}{a_1} & 0 & 0 \\ 0 & \ddots & 0 \\ 0 & 0 & \frac{1}{a_{2n_{\mathrm{bns}}}} \end{pmatrix}\cdot z \tag{7.76}$$

Here, these factors $a_1,\dots,a_{2n_{\mathrm{bns}}}$ are the maxima for active $\delta\tilde{p}_{1,\mathrm{lim}},\dots,\delta\tilde{p}_{n_{\mathrm{bns}},\mathrm{lim}}$ and reactive power flexibility $\delta\tilde{q}_{1,\mathrm{lim}},\dots,\delta\tilde{q}_{n_{\mathrm{bns}},\mathrm{lim}}$. Using this transformation, Equation 7.72 is rewritten:

$$\max_{\|\delta\tilde{S}_{\mathrm{ns}}\|\le\delta\tilde{S}_{\mathrm{lim,ns}}} \frac{\partial|V_{\mathrm{ns}}|^2}{\partial S}\delta\tilde{S}_{\mathrm{ns}} \overset{T_2}{=} \max_{\|\tilde{z}\|_\infty\le 1} \frac{\partial|V_{\mathrm{ns}}|^2}{\partial S}\tilde{z} \tag{7.77}$$

$$= \left\|\frac{\partial|V_{\mathrm{ns}}|^2}{\partial S}\delta\tilde{S}_{\mathrm{lim,ns}}\right\|_1 \tag{7.78}$$

The complete term including the shift from equation 7.72 then reads:

$$\max_{\substack{\delta S_{\mathrm{min,ns}}\le\delta S_{\mathrm{ns}} \\ \delta S_{\mathrm{ns}}\le\delta S_{\mathrm{max,ns}}}} \frac{\partial|V_{\mathrm{ns}}|^2}{\partial S}\delta S_{\mathrm{ns}} = \left\|\frac{\partial|V_{\mathrm{ns}}|^2}{\partial S}\delta\tilde{S}_{\mathrm{lim,ns}}\right\|_1 + \frac{\partial|V_{\mathrm{ns}}|^2}{\partial S}S_{\mathrm{shift,ns}} \tag{7.79}$$

Since $S_{\mathrm{shift,ns}}$ and $\delta\tilde{S}_{\mathrm{lim,ns}}$ can be calculated trivially, Equation 7.78 can be formulated for each bus b_{ns}. For better readability $\frac{\partial|V_{\mathrm{ns}}|^2}{\partial V}\frac{\partial V_{\mathrm{ns}}}{\partial S} = \frac{\partial|V_{\mathrm{ns}}|^2}{\partial S} = M$ is set, with $M_{b,k}$ the (b,k) component of that matrix (row b, column k):

$$M_b(S_{\mathrm{shift,ns}}) = M_b\left(\begin{pmatrix} 0.5\cdot\delta P_{\mathrm{max,ns}} - 0.5\cdot\delta P_{\mathrm{min,ns}} \\ 0.5\cdot\delta Q_{\mathrm{max,ns}} - 0.5\cdot\delta Q_{\mathrm{min,ns}} \end{pmatrix}\right) \tag{7.80}$$

$$= M_{b,1}(\frac{\delta p_{1,max} - \delta p_{1,\mathrm{min}}}{2}) + \cdots \tag{7.81}$$

$$+ M_{b,2n_{\mathrm{bns}}}(\frac{\delta q_{n_{\mathrm{bns}},max} - \delta q_{n_{\mathrm{bns}},\mathrm{min}}}{2})$$

$$\left\|M_b(\operatorname{diag}(\delta\tilde{S}_{\mathrm{lim,ns}}))\right\|_1 = \left|M_{b,1}\left(\frac{\delta p_{1,\mathrm{max}}}{2} + \frac{\delta p_{1,\mathrm{min}}}{2}\right)\right| + \cdots \tag{7.82}$$

$$+ \left|M_{b,2n_{\mathrm{bns}}}\left(\frac{\delta q_{n_{\mathrm{bns}},\mathrm{max}}}{2} + \frac{\delta q_{n_{\mathrm{bns}},\mathrm{min}}}{2}\right)\right|$$

Using these formulations, the voltage bounds can be written for each bus individually:

$$V_{b,\max}^2 - |V_b|^2 \geq \sum_{n=1}^{n_{\mathrm{bns}}} \frac{(|M_{b,n}| + M_{b,n}) \cdot \delta p_{n,\max}}{2} + \frac{(|M_{b,n}| - M_{b,n}) \cdot \delta p_{n,\min}}{2} \tag{7.83}$$

$$+ \frac{(|M_{b,n+n_{\mathrm{bns}}}| + M_{b,n+n_{\mathrm{bns}}}) \cdot \delta q_{n,\max}}{2} + \frac{(|M_{b,n+n_{\mathrm{bns}}}| - M_{b,n+n_{\mathrm{bns}}}) \cdot \delta q_{n,\min}}{2}$$

$$|V_b|^2 - V_{b,\min}^2 \geq \sum_{n=1}^{n_{\mathrm{bns}}} \frac{(|M_{b,n}| - M_{b,n}) \cdot \delta p_{n,\max}}{2} + \frac{(|M_{b,n}| + M_{b,n}) \cdot \delta p_{n,\min}}{2} \tag{7.84}$$

$$+ \frac{(|M_{b,n+n_{\mathrm{bns}}}| - M_{b,n+n_{\mathrm{bns}}}) \cdot \delta q_{n,\max}}{2} + \frac{(|M_{b,n+n_{\mathrm{bns}}}| + M_{b,n+n_{\mathrm{bns}}}) \cdot \delta q_{n,\min}}{2}$$

By introducing a function $f(x) = \frac{|x| + x}{2}$, the notation significantly simplifies:

$$V_{b,\max}^2 - |V_b|^2 \geq \sum_{n=1}^{n_{\mathrm{bns}}} f(M_{b,n}) \cdot \delta p_{n,\max} + f(-M_{b,n}) \cdot \delta p_{n,\min} \tag{7.85}$$

$$+ f(M_{b,n+n_{\mathrm{bns}}}) \cdot \delta q_{n,\max} + f(-M_{b,n+n_{\mathrm{bns}}}) \cdot \delta q_{n,\min}$$

$$|V_b|^2 - V_{b,\min}^2 \geq \sum_{n=1}^{n_{\mathrm{bns}}} f(-M_{b,n}) \cdot \delta p_{n,\max} + f(M_{b,n}) \cdot \delta p_{n,\min} \tag{7.86}$$

$$+ f(-M_{b,n+n_{\mathrm{bns}}}) \cdot \delta q_{n,\max} + f(M_{b,n+n_{\mathrm{bns}}}) \cdot \delta q_{n,\min}$$

The indices (b,n) and $(b,n+n_{\mathrm{bns}})$ can also be interpreted as parts of the partial derivatives in the Matrix M:

$$V_{b,\max}^2 - |V_b|^2 \geq \sum_{n=1}^{n_{\mathrm{bns}}} f\left(\left(\frac{\partial |V_{\mathrm{ns}}|^2}{\partial P}\right)_{b,n}\right) \cdot \delta p_{n,\max} + f\left(-\left(\frac{\partial |V_{\mathrm{ns}}|^2}{\partial P}\right)_{b,n}\right) \cdot \delta p_{n,\min} \tag{7.87}$$

$$+ f\left(\left(\frac{\partial |V_{\mathrm{ns}}|^2}{\partial Q}\right)_{b,n}\right) \cdot \delta q_{n,\max} + f\left(-\left(\frac{\partial |V_{\mathrm{ns}}|^2}{\partial Q}\right)_{b,n}\right) \cdot \delta q_{n,\min}$$

$$|V_b|^2 - V_{b,\min}^2 \geq \sum_{n=1}^{n_{\mathrm{bns}}} f\left(-\left(\frac{\partial |V_{\mathrm{ns}}|^2}{\partial P}\right)_{b,n}\right) \cdot \delta p_{n,\max} + f\left(\left(\frac{\partial |V_{\mathrm{ns}}|^2}{\partial P}\right)_{b,n}\right) \cdot \delta p_{n,\min} \tag{7.88}$$

$$+ f\left(-\left(\frac{\partial |V_{\mathrm{ns}}|^2}{\partial Q}\right)_{b,n}\right) \cdot \delta q_{n,\max} + f\left(\left(\frac{\partial |V_{\mathrm{ns}}|^2}{\partial Q}\right)_{b,n}\right) \cdot \delta q_{n,\min}$$

As can be seen, clear and robust conditions are obtained for the optimization problem. The matrix M can be calculated before the optimization is performed, essentially externalizing the problem of a power-flow. It can also be seen, what robustness means: If the matrix entry

$M_{b,n}$ is positive, the linear response of the voltage magnitude to a change in power injection δp_n at bus n is positive. As a consequence, this boundary becomes active for $\delta p_{n,\max}$. The same is valid for $\delta q_{n,\max}$ and the corresponding entry $M_{b,n+N}$ or, on the other side of the flexibility plane, for $\delta p_{n,\min}$ and $\delta q_{n,\min}$. This means, that the solution chooses the maximally possible change in voltage as a function of power injection changes. On the other hand, if a term is negative, it vanishes. This way, for each bus, two of the four terms are equal to zero, one of the first pair and one of the second pair.

7.2.5. Linearization of Power Flow Limits

As introduced in the modeling subsection in the previous chapter on page 116, not only voltages have boundary conditions, but also power-flows. In this subsection, the linearization of power-flow limits is developed analogously to the development for the voltage limits above. Since the development is different in some details, the boundary conditions are covered once again, this time for the n_l branches l. As for the voltages, the linearized power-flow boundary can be set in absolute values:

$$\left|S_{f,\max}\right|^2 \geq \left|S_f^{(0)} + \delta S_l\right|^2 \approx \left|S_f^{(0)}\right|^2 + \delta|S_f|^2 \tag{7.89}$$

$$\delta|S_f|^2 = 2 \cdot (\mathrm{diag}(P_f^{(0)})\delta P_f + \mathrm{diag}(Q_f^{(0)})\delta Q_f) \tag{7.90}$$

However, in contrast to the voltages, the absolute value is of no great help here. To understand why, a look at the per-unit system has to be taken. Optimization methods and power-flow algorithms work best if all values are in a similar order of magnitude. In the per-unit system, voltages take values around one, independent of their voltage level, as the respective voltage level is encoded in a base-value. A linearization of voltages therefore takes place at values of about one. The voltage boundaries are symmetric around this linearization point. For power-flows, the linearization might take place at flows of $p_f = 0$ for many branches. Here, the absolute value function is not well approximated by a linearization. This approximation is additionally weakened by the fact that the linearization of power-flows is flawed at this point due to the underestimation of transmission losses. This problem can only in part be compensated by a clever choice of the linearization point. Therefore, another approach has to be taken.

To achieve results that are better in guaranteeing the adherence of all boundary conditions, another set of limits is added, in which linearization is only performed once, in contrast to the voltages as done above. The idea behind the alternative boundary conditions is simple: The sum of the power-flow into a branch $S_{f,l}^{(0)}$ and its linearized change $\delta S_{f,l}$ as a function of the power injection changes S_{ns} is set to be less than the allowed power-flow $S_{f,\max}$. However,
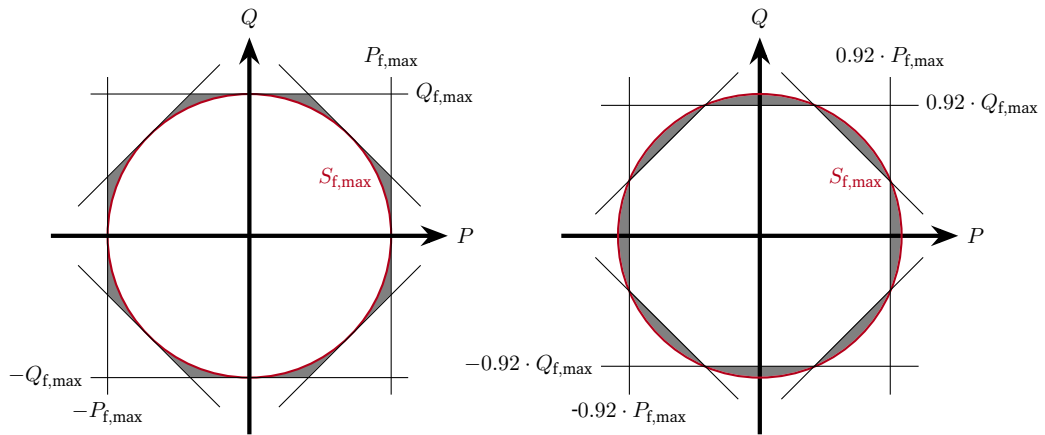
Figure 7.3.: Alternative boundaries for power-flows: On the left, non-conservative boundaries are added which do not cut away feasible solutions, but allow boundary violations (gray areas). On the right, boundaries are set conservatively, guaranteeing no power-flow limit violations, but viable solutions are lost (gray). To reduce the areas, in addition to the boundaries in P and Q, conditions are introduced at angles of 45°. The factor of 0.92 on the right is rounded from $\cos(22.5°)$, the maximal distance from the octagons edge to its circumcircle.

since $S_{f,l}^{(0)}$ can take any orientation in the PQ-plane, and it is not desired to leave the linear problem optimization class by introducing a circular boundary, this circular boundary is approximated by an inscribed polygon. Figure 7.3 depicts the concept behind the idea. The boundary is always circular as it is is defined by the power-rating of the power-line. This rating is given in apparent power, creating a circle in the PQ-plane.

These new conditions can be added in arbitrary ratios of P_f and Q_f in the PQ-plane and can be either conservative, cutting away feasible solution space, but guarantee compliance with boundary conditions, or non-conservative, not cutting away feasible solutions, but allowing violations of power-flow limits. Figure 7.3 shows the difference of these two options for boundaries solely in P and Q-direction and also in a mixed direction of 45°. These eight additional boundary conditions essentially form an octagon in the solution space.

Figure 7.4 shows the solution space that is lost when using conservative limitations depending on the number of additional boundary conditions. Of course, the more limitations are introduced, the better they approximate the physical conditions, but also the slower the algorithm will be. The same is valid for non-conservative limitations, in which case the mean
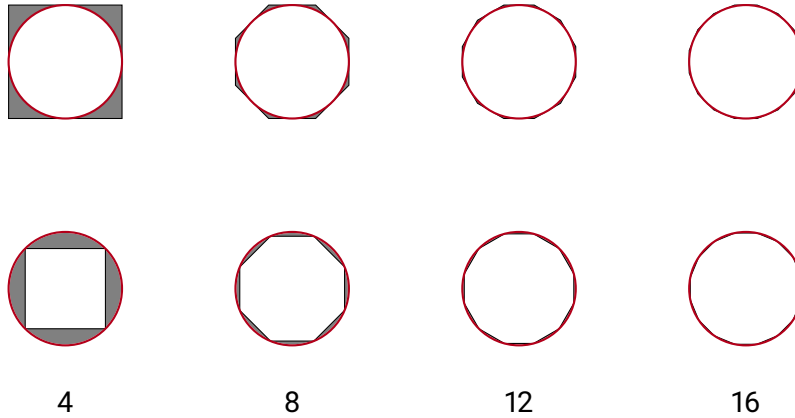
Figure 7.4.: Overestimation and underestimation of the solution space limited by polygonal boundary conditions as a function of the order of the polygon in the non-conservative (top) and conservative case (bottom).

Table 7.1.: Ratio of conservative and non-conservative polygonal limitations to the real solution given by the power-flow limit $S_{\text{f,max}}$.

Corners of polygon	4	8	12	16
Non-conservative	1.41	1.08	1.04	1.02
Conservative	0.71	0.92	0.97	0.98

overestimation will decrease with rising number of limits.

In Table 7.1, the maximum distance between the circumference of polygons with circumradius/conservative and inner radius/non-conservative with respect to the circle that is defined by the thermal limits $S_{\text{f,max}}$ are listed. Only polygons that are of an order of multiples of four are shown, since only those can be used to add the "easy" conditions in directions of P and Q, which are computationally half as expensive to instantiate as the other ones. As one can see, the jump in accuracy from four corners to eight increases the accuracy by over 20 %, while adding more corners has smaller marginal returns. The factor of $\cos(22.5°) \approx 0.92$ is the difference of the height of a triangle of $45°$[1] to the circumradius.

---

[1]The angle of the inner corner of each of the eight triangles inside an octagon, as $360/8 = 45$

In this thesis, to achieve a short runtime and sufficient accuracy, a conservative octagonal limit is chosen. Following Equation 7.91, these eight additional limits can be formulated by using a normal vector pointing in the respective directions. For each $\hat{n}_\alpha$ in $\alpha = 45° \cdot \{0, \ldots, 7\}$ the limit can be written as:

$$\hat{n}_\alpha \delta S_{\mathrm{f}} \leq \cos(22.5°) S_{\mathrm{f,max}} - \hat{n}_\alpha S_{\mathrm{f}}^{(0)} \tag{7.91}$$

With the help of the new unit vector $\hat{n}_\alpha$, the new inequalities are set that must hold true for all maximal δS_{ns}:

$$\max_{\delta S_{\mathrm{ns}}} \hat{n}_\alpha \delta S_{\mathrm{f}} \leq \cos(22.5°) S_{\mathrm{f,max}} - \hat{n}_\alpha S_{\mathrm{f}}^{(0)} \tag{7.92}$$

Here, as in Equation 7.42, $\delta S_{\mathrm{f}} = \frac{\partial S_{\mathrm{f}}}{\partial V} \mathbb{1}_{2\times2} \otimes A_{\mathrm{ns}}^T \frac{\partial V_{\mathrm{ns}}}{\partial S} \delta S_{\mathrm{ns}}$. For reasons of brevity, we set:

$$W = \frac{\partial S_{\mathrm{f}}}{\partial S} = \frac{\partial S_{\mathrm{f}}}{\partial V} \mathbb{1}_{2\times2} \otimes A_{\mathrm{ns}}^T \frac{\partial V_{\mathrm{ns}}}{\partial S} \tag{7.93}$$

Following reformulation is done:

$$\max_{\delta S_{\mathrm{ns}}} \hat{n}_\alpha \delta S_{\mathrm{f}} = \max_{\delta S_{\mathrm{ns}}} \hat{n}_\alpha W \delta S_{\mathrm{ns}} \tag{7.94}$$

Using the transformation T_1 already introduced for voltages in Equation 7.66 is used to make the problem symmetric:

$$\max_{\substack{\delta S_{\mathrm{min,ns}} \leq \delta S_{\mathrm{ns}} \\ \delta S_{\mathrm{ns}} \leq \delta S_{\mathrm{max,ns}}}} \hat{n}_\alpha W \delta S_{\mathrm{ns}} \overset{T_1}{=} \max_{\left\| \delta \tilde{S}_{\mathrm{ns}} \right\| \leq \delta \tilde{S}_{\mathrm{lim,ns}}} \hat{n}_\alpha W (\delta \tilde{S}_{\mathrm{ns}} + S_{\mathrm{shift,ns}}) \tag{7.95}$$

Now, applying the second transformation T_2 as in Equation 7.78 to normalize the vectors, the desired simplification is obtained:

$$\max_{\left\| \delta \tilde{S}_{\mathrm{ns}} \right\| \leq \delta \tilde{S}_{\mathrm{lim,ns}}} \hat{n}_\alpha W \delta \tilde{S}_{\mathrm{ns}} \overset{T_2}{=} \left\| \hat{n}_\alpha W \delta \tilde{S}_{\mathrm{lim,ns}} \right\|_1 \tag{7.96}$$

As for the voltages, these two transformations result in:

$$\max_{\delta S_{\mathrm{ns}}} \hat{n}_\alpha \delta S_{\mathrm{f}} = \left\| \hat{n}_\alpha W \delta \tilde{S}_{\mathrm{lim,ns}} \right\|_1 + \hat{n}_\alpha W S_{\mathrm{shift,ns}} \tag{7.97}$$

Inserting $S_{\mathrm{shift,ns}} = \frac{1}{2} \begin{pmatrix} \delta P_{\mathrm{max,ns}} - \delta P_{\mathrm{min,ns}} \\ \delta Q_{\mathrm{max,ns}} - \delta Q_{\mathrm{min,ns}} \end{pmatrix}$ and $\tilde{S}_{\mathrm{lim,ns}} = \frac{1}{2} \begin{pmatrix} \delta P_{\mathrm{max,ns}} + \delta P_{\mathrm{min,ns}} \\ \delta Q_{\mathrm{max,ns}} + \delta Q_{\mathrm{min,ns}} \end{pmatrix}$ and writing Equation 7.92 component wise and using $f(x) = \frac{|x|+x}{2}$, the following is obtained for

all lines l:

$$\cos(22.5°)S_{\mathrm{f},l,\max} - \hat{n}_\alpha S_{\mathrm{f},l}^{(0)} \geq \sum_{n=1}^{n_{\mathrm{bns}}} f(\hat{n}_{\alpha,1}W_{l,n} + \hat{n}_{\alpha,2}W_{l+n_1,n})\delta p_{n,\max} \tag{7.98}$$
$$+ f(-\hat{n}_{\alpha,1}W_{l,n} - \hat{n}_{\alpha,2}W_{l+n_1,n})\delta p_{n,\min}$$
$$+ f(\hat{n}_{\alpha,1}W_{l,n+n_{\mathrm{bns}}} + \hat{n}_{\alpha,2}W_{l+n_1,n+n_{\mathrm{bns}}})\delta q_{n,\max}$$
$$+ f(-\hat{n}_{\alpha,1}W_{l,n+n_{\mathrm{bns}}} - \hat{n}_{\alpha,2}W_{l+n_1,n+n_{\mathrm{bns}}})\delta q_{n,\min}$$

For a better intuition, the equation can be rewritten in terms of partial derivatives:

$$\cos(22.5°)S_{\mathrm{f},l,\max} - \hat{n}_\alpha S_{\mathrm{f},l}^{(0)} \geq \sum_{n=1}^{n_{\mathrm{bns}}} f\left(\hat{n}_{\alpha,1}\left(\frac{\partial P_{\mathrm{f}}}{\partial P}\right)_{l,n} + \hat{n}_{\alpha,2}\left(\frac{\partial Q_{\mathrm{f}}}{\partial P}\right)_{l,n}\right)\delta p_{n,\max} \tag{7.99}$$
$$+ f\left(-\hat{n}_{\alpha,1}\left(\frac{\partial P_{\mathrm{f}}}{\partial P}\right)_{l,n} - \hat{n}_{\alpha,2}\left(\frac{\partial Q_{\mathrm{f}}}{\partial P}\right)_{l,n}\right)\delta p_{n,\min}$$
$$+ f\left(\hat{n}_{\alpha,1}\left(\frac{\partial P_{\mathrm{f}}}{\partial Q}\right)_{l,n} + \hat{n}_{\alpha,2}\left(\frac{\partial Q_{\mathrm{f}}}{\partial Q}\right)_{l,n}\right)\delta q_{n,\max}$$
$$+ f\left(-\hat{n}_{\alpha,1}\left(\frac{\partial P_{\mathrm{f}}}{\partial Q}\right)_{l,n} - \hat{n}_{\alpha,2}\left(\frac{\partial Q_{\mathrm{f}}}{\partial Q}\right)_{l,n}\right)\delta q_{n,\min},$$

where the indices $(\cdots)_{l,n}$ stand for the (l,n) entries in the matrices. As for the voltages, this result captivates the eye by its simplicity: All power-flow boundary conditions are provided in a pre-computed matrix and the secondary problem of keeping power-flows inside boundaries is put into one formula. The optimization problem becomes a simple minimization of flexibility limitations with two boundary equations for voltages and eight for power-flows.

If different boundary conditions instead of octagonal ones are chosen, it is necessary to use the correct $\hat{n}_{\alpha,x}$ and adapt the factor of $\cos(22.5°)$. The argument $\sphericalangle$ of the cosine function is easily determined by corners of the polygon:

$$\sphericalangle = {360°}/{2 \cdot n_{\mathrm{corners}}} \tag{7.100}$$

However, a compromise has to be found between speed, which favors lower order polygons, and accuracy, which favors higher orders. In this work, octagonal boundaries were chosen as they offer arguably the best compromise.

7.3. Implementation

The algorithm itself consists of the optimization model, which itself consists of the objective function and the boundary conditions, and the corresponding functions to prepare and

transform the input data, namely the linearization functions. This results in a very simple optimization model, as the more complex calculations are externalized.

7.3.1. Optimization Model

In the optimization model, at first the cost function as defined in Equation 7.7 is used to set the goal of the optimization. The objective is to minimize the cost function in order to achieve an optimal result. Here, the optimum is that initial flexibilities are not limited, such that the safe flexibilities are equal to the initial flexibilities. To lessen the computation time, this upper limit in optimality can be given explicitly to the numerical solver.

The boundary conditions for voltages from Equation 7.87 and for power-flows from Equation 7.99 are added to restrict the possible solutions to those that guarantee a safe operating state.

The algebraic modeling language AMPL [200] is used to formulate this problem, including additional formulas to aggregate power injections by flexible assets onto nodes. To solve the formulated optimization problem, a numerical solver is needed. In this thesis, the open-source SCIP solver [201] is used, which uses an evolved Simplex algorithm [202].

The simplex algorithm follows a simple approach: the objective is expected to be extreme if a bound is active, which can mathematically be shown to be true. This way, the algorithm "only" needs to walk the borders of the multi-dimensional solution space that is set by the boundary conditions. Somewhere along this walk it has to find the extreme value of the cost function if the problem is properly defined. If the problem is not properly defined, such that is is unbound in some direction in this multi-dimensional space, it becomes infeasible. As the theory behind this algorithm already in its base form is very complex, no further elaboration on this topic follows.

7.3.2. Conceptual Description of the Algorithm

The optimization model itself is only a part of the algorithm to calculate safe flexibilities. One part that is externalized from the optimization itself is the linearization of the power-flow and the calculation of the linear factors being used in the boundary conditions in Equations 7.87 and 7.99. To better understand how these parts interact, the algorithm is described as an instruction in the following:

1. Using a grid model and a set of flexible and inflexible loads that are connected in this grid, the power-flow at the reference point is calculated. If the initial power-flow calculations at the reference point fail, it is not possible to calculate safe flexibility ranges, as the rest of the algorithm is based on the result of said power-flow. In this case, the algorithm is stopped.

2. Using the allocation matrix A_{FA}, which maps flexible assets onto grid nodes, and the allocation matrix A_{ns}, as defined in Equation 7.17, which reduces the grid dimension to only non-slack buses, voltage vectors and the Jacobi-matrix $\frac{\partial S}{\partial V_{\mathrm{ns}}}$ is calculated.

3. An inversion of the Jacobi-matrix returns the sensitivity matrix $\frac{\partial V_{\mathrm{ns}}}{\partial S}$ as defined in Equation 7.27. Following Equation 7.56, the sensitivity of voltage amplitudes as a function of power-injection changes $\frac{\partial |V_{\mathrm{ns}}|^2}{\partial S}$ is calculated.

4. The inverted matrix from equation 7.27 is used to calculate the sensitivity matrix for power-flows $\frac{\partial S_{\mathrm{f}}}{\partial V}$ as defined in 7.41. At this point, all pre-optimization steps have been performed.

5. To instantiate the optimization problem, the parameters in the boundary conditions are filled with the pre-calculated sensitivity values. Now, the safe flexibility ranges of the flexible assets are the only variables in the linear program. The algebraic formulation is converted into a formulation readable by the solver.

6. The minimization of the cost function defines, that the difference between initial flexibility ranges and safe flexibility ranges is to be minimized while the boundary conditions restrict the solution space, if any become active. The solver, here SCIP 7, chooses a starting point and walks along the edges of the polyhedron defined by the boundary conditions until the minimum value for the cost function is found.

7. After minimal limitations to the initial flexibilities have been calculated, these values are communicated back to the user who can check the result by running power-flows in the extreme corners given by the safe flexibilities.

7.3.3. Integration and Tool-Chain

To implement the algorithm, a pre-existing tool-chain from a previous project [89] was taken and adapted to the needs of the algorithm. It uses Matlab as the interface to the user to enable fast scripting and development. To perform power-flow calculations and manage grid models, Matpower [168], an open source library for solving power flow problems, is used.
  To integrate the chosen solver, SCIP 7 [201], a series of interfaces is needed:

- At first, the user provides matlab with the data needed to run a power-flow calculation: a grid model, loads and generators, and time-series or set-points for the loads and generators. Additionally, flexibility factors are used to create flexible loads if they are not already parameterized.

- A web-service is hosted locally to wrap the C++ code that includes the optimizer. After creating the necessary objects, the functions in Matlab send them to the web-service.

- The web-service receives the objects and converts them to fill the C++ classes with the corresponding data. The linearization functions and matrix algebra is performed by using the matrix algebra library Eigen [203]. Afterwards, the optimization problem is instantiated and SCIP is called as the solver.

- As the optimization problem itself is written in AMPL [200], it is converted to C++ to be readable by the chosen solver. This has to be done every time a change is performed to the optimization code itself.

- The solver returns the solved problem. The solution includes the last objective value and the optimized flexibilities.

- This solution is sent to the Matlab client via the web-service.

This whole tool-chain is depicted in Figure 7.5. So far, no optimization to parallelize the program has been done, which results in the fact that the whole algorithm only runs on a single core of the computer.
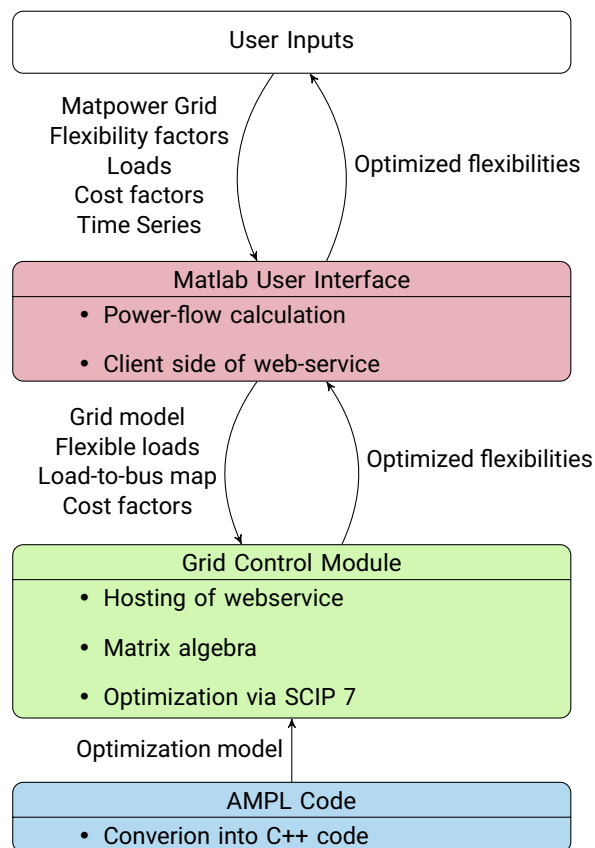
Figure 7.5.: Tool-chain and integration of the optimization model to perform calculations of safe flexibility sets.

Summary

In this chapter, two main topics are outlined: flexibility clusters to aggregate individual flexibilities and disaggregate requests back onto individual flexible energy resources, and robust optimization with linearized power-flow calculation to minimize individual flexibility reductions while guaranteeing a safe operating state. To achieve both points the following aspects are covered:

- Individual power injections distribute their power onto grid interconnection points according to the impedance of the respective connection. In a sensitivity matrix D, all these distribution factors can be collected in a linearized manner by calculating derivatives.

- Disaggregation of requests for flexibility is done proportional to the offered amount.

- Flexibility clusters can easily be split and added if needed due to their linear nature.

- To avoid non-optimal setpoints, upward and downward flexibility are provisioned separately.

- An objective function is formulated to minimize reductions in initial individual flexibilities, while boundary conditions are needed to guarantee a safe operation for all setpoint combinations.

- Power-flow calculation can be linearized and both voltages and power-flows into lines can be calculated as functions of power injection changes at non-slack-buses.

- Voltage limits can be linearized in their absolute values, allowing the transformation of the optimization problem into a master problem, minimizing flexibility limitations, and an analytical formulation of boundary conditions for voltages.

- A similar approach is chosen for power-flows, but linearization of the absolute value function does not work as well as it does for voltages. A set of new conservative boundary conditions can be introduced to approximate power-flow bounds.

- For both voltage and power-flow bounds, the boundary conditions can be solved analytically as functions of the flexibility limits. This creates an optimization problem with a very simple and enlightening formulation, which gives insights why the optimization is robust: Sensitivities determine if a boundary condition becomes active for the flexibilities that are maximized by the objective function.

- Implementation of the algorithm was done in a pre-existing tool-chain that was adapted to enable matrix calculations and the handling of large grids.

8. Results

In this chapter, the results of the application of the algorithm to calculate optimized safe flexibility ranges are listed and discussed. At first, conceptual results are discussed to explain how the algorithm performs, followed by the evaluation of the validity of linearization, both in the case of the flexibility cluster and the linearization for power-flow calculation. On a conceptual test grid, optimality and adherence to boundary conditions are tested, before superimposed power-flows are added to evaluate their influence. At last, the algorithm is tested on a real distribution grid and compared with a nonlinear approach.

8.1. Conceptual Results

To get an idea how the optimization works and what the results are, a suitable state in the grid is needed. This state ideally includes large amounts of flexibility, that, if no limitation is performed, lead to violations of boundary conditions. Also, it is important, that the reference values for all assets do not lead to such violations, as the optimization becomes infeasible. To show exemplary results, a period with high availability of RES is chosen, in this case, an evening in June. Additionally, the flexibility is scaled up, to achieve violations of boundary conditions for extreme setpoint changes in the initial flexibility set $F^{(0)}$, so that a reduction of initial individual flexibilities becomes necessary.

Figure 8.1 shows the results of the flexibility optimization. The initial flexibility is plotted as dotted area in Figure 8.1a. There are combinations of individual setpoint activations, that can lead to currents on the power line with index 40 that exceed the branch limits, as depicted in Figure 8.1b. Here, the horizontal dashed line in orange shows the current limit. If the initial flexibility set was not limited, a request for this flexibility could lead to currents that exceed this current limit, as plotted with the dashed black line. The optimization process limits the initial flexibility set $F^{(0)}$ to a safe set F, which is shaded in blue. In case of a request for flexibility provision, all possible setpoints inside this safe area lead to currents that are less than the rated current on branch 40[1].

---

[1]The difference between rated current and maximum allowed by the optimizer is due to conservative boundary conditions, which cut away feasible solution space. Quantification follows in Section 8.3.
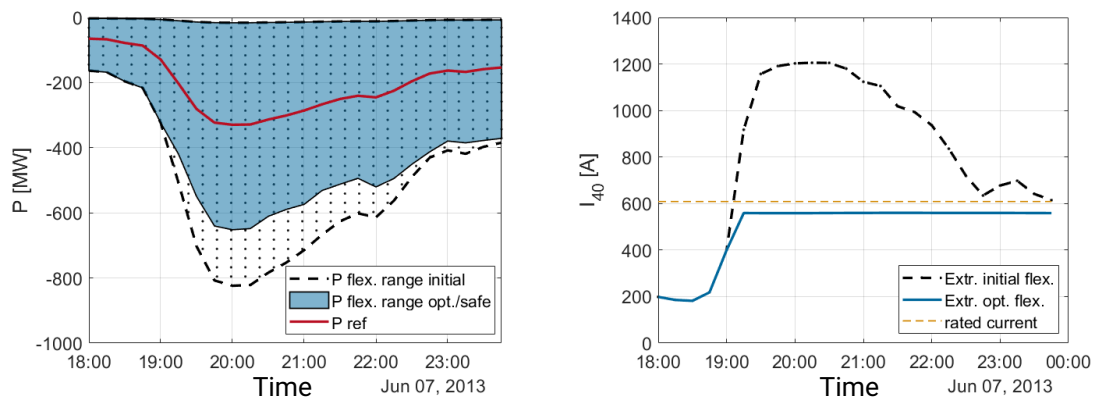
(a) Aggregated flexibility from wind-power in a test grid. Initial flexibility (dotted area, dashed boundary) is reduced to a safe flexibility set (colored area) around the reference injection (red).

(b) Initial current over a power line in the test grid (dashed line) and current reduced by the optimizer (blue line). The orange dahshed line denotes the rated current below which the current must be reduced.

Figure 8.1.: Reduction of flexibility from wind-power to meet operational boundary conditions.

The choice of conservative boundary conditions reduces the solution space and in turn produces less-than-optimal results. Less-than-optimal here means, that flexibility is reduced in excess of the necessary reduction. However, conservative boundaries also guarantee a safe operating state, which is very important for grid operation. To illustrate the importance of this guarantee of safe flexibility, consider the following scenario of using the initial, unsafe flexibility set: A DSO aggregates the individual flexibilities of the flexible energy resource connected to his grid and communicates the aggregated amount. The TSO includes this aggregated value into his calculations and, after the occurrence of a critical outage, requests the aggregated flexibility. After the provision of this flexibility and the activation of all individual setpoint changes, the providing distribution grid exceeds some operation limits. Now, the DSO needs to adapt the power injections and load flows and, as a consequence, the setpoints at the GICPs change a second time. This makes the control problem uncertain from the TSO's perspective and leads to new problems in the transmission level. However, if the provided flexibility is slightly less than what could have been provided given optimality, the TSO will plan with this smaller amount of flexibility and can adapt his preventive redispatch process to reduce transmission line loadings. The possible costs of slightly increased redispatch measures are much lower than those of a cascading outage due to unavailable flexibility in a

n-1 situation.

As a side-note: As the flexibility areas are aggregated for TSOs, upward flexibility ΔP^{up} is plotted at negative ordinates, while downward flexibility ΔP^{down} is plotted at positive ordinates. This is due to the fact, that the TSO sees loads as positive values in his control center, while generation is seen as negative load. In the following graphics, the same convention, called passive sign convention, is used.

8.2. General Applicability of Linearization

To assess the general applicability of linearization, a small test grid is created which can be seen in Figure 8.2. The flexible load's injection is varied between -1300 and 1300 MW at a constant -100 Mvar of reactive power injection. To get smooth gradients, the number of steps is chosen to be 200. As a result, the increment from one simulated state to the next is 13 MW in power injection. Voltage at bus 2 as well as power-flow into the connecting branch are calculated and plotted. To analyze the influence of the linearization point, three points are investigated: at 0 MW, +500 MW, and -500 MW injection of the flexible load.

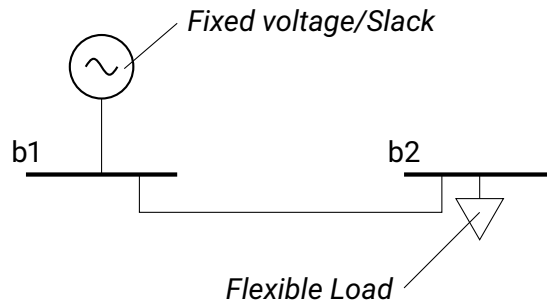

Figure 8.2.: Two bus test grid for analyzing the scope of the linearization and get an estimation of the resulting errors. The line rating is $S_{\text{f,max}} = 259$ MVA.

At first, linear and analytical solutions for voltage magnitudes at bus 2 are compared and plotted in Figure 8.3. The analytical solution is calculated using equation 6.28:

$$s_{\text{f}} = v_1 (y_{1,2}^{\text{s}} + y_{1,2}^{\text{sh}})^* v_1^* + v_1 (-y_{1,2}^{\text{s}})^* v_2^* \tag{8.1}$$

This equation can be solved for the complex voltage at bus 2:

$$v_2 = \left(\frac{v_1 (y_{1,2}^{\text{s}} + y_{1,2}^{\text{sh}})^* v_1^* - s_{\text{f}}}{(-y_{1,2}^{\text{s}})^* v_2^*} \right)^* \tag{8.2}$$

For the linearized voltages, formulas introduce in Equation 7.28 are used:

$$|v|^2 = V_r^2 + V_j^2 + 2 \cdot (V_r \delta V_r + V_j \delta V_j) \tag{8.3}$$

$$\delta V_r = \frac{\partial V_r}{\partial p} \delta p + \frac{\partial V_r}{\partial q} \delta q \tag{8.4}$$

$$\delta V_j = \frac{\partial V_r}{\partial p} \delta p + \frac{\partial V_r}{\partial q} \delta q \tag{8.5}$$

As displayed in Figure 8.3, the analytical solution is a curve with a larger negative slope for the positive power injections than for the negative ones. This part of the curve is sometimes called "Nasenkurve" in German, which translates to "nose-curve" and it describes the nose-shaped voltage drop for high loads.

The three linearization points and the tangents describing the linearization itself, are plotted in yellow, red, and blue. Of course, the further the linearization point is located from the evaluation, the higher the errors become with respect to the exact solution. However, the power-flow limits here are already passed at ±250 MW power injections. Therefore, the difference between the linearization at point 0 MW and the black analytical solution do not differ much in states that occur in operation. In fact, at $p_2 = -254$ MW, the difference is less than 0.15 % or 0.015 kV. At $p_2 = 255$ MW, the difference is less than 0.34 % or 0.38 kV. An error of 1 % is reached at $p_2 = -460$ and $p_2 = 435$ respectively.

For the power-flows, the same procedure is performed and can be seen in Figure 8.4. Here, the linearized power-flow is calculated with the formula from Equation 7.42:

$$|s_f|^2 = p_f^2 + q_f^2 + 2 \cdot (p_f \delta p_f + q_f \delta q_f) \tag{8.6}$$

$$\delta p_f = \frac{\partial p_f}{\partial V} \frac{\partial V}{\partial S} \delta s \tag{8.7}$$

Only positive values are plotted, as negative values do not make sense here. As the linearization at the point $p_{in} = 0$ would be a horizontal line, the linearization point is set at $\Delta P_{in} = -6.2$ MW to the left of the zero point. To get a true value for comparison, the Newton-Raphson power-flow calculated value is also plotted in Figure 8.4.

As is depicted, the absolute value of the power-flow is not linearized very well, which is the reason why the algorithm does not use it. Especially, if linearization is done close to $P_{in} = 0$, the linearization produces results that are far off. For example, at $p_{in} = -125$ MW, the linearization performed at $\Delta P_{in} = -6.2$ MW is already 50 % below the true value and does not reach the power-flow boundary in the evaluated interval[2]. The contrast to the linearization of the voltage is evident at first glance. However, if the linearization point is

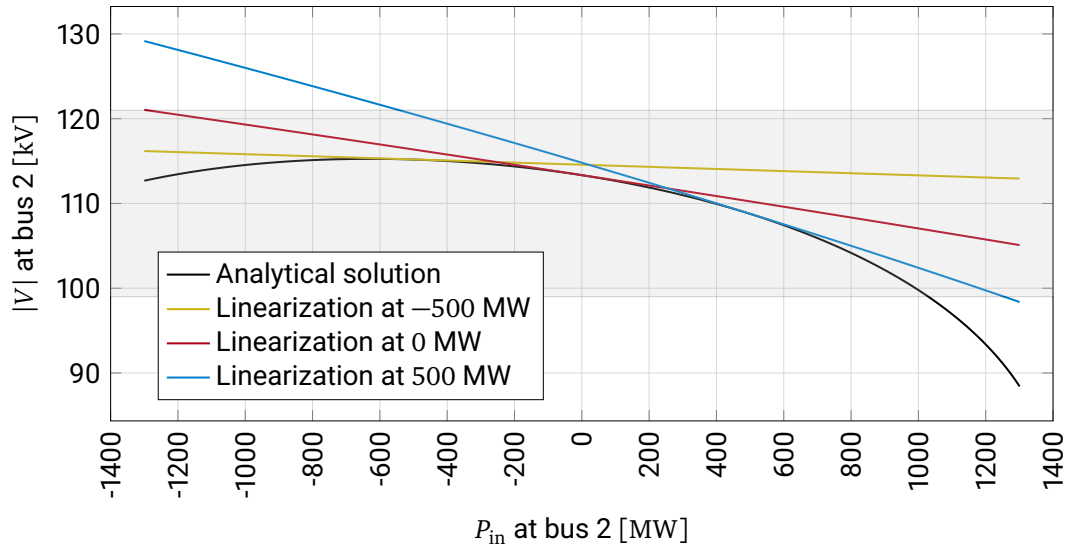[2]Values given here are square-roots of the values plotted.

Figure 8.3.: Comparison between the analytical and linearized solution of the voltage magnitude calculation at bus 2 in the grid shown in Figure 8.2. The gray area depicts the voltage boundaries, which are at $\pm 10\,\%$ of the nominal value.

close to the evaluation point, the approximation performs better. For example at -607 MW, the inaccuracy of the linearization performed at -500 MW is less than 1.5 %.

From the analysis, it is concluded that a linearization of power-flows at reference points closer to zero than the evaluation point will lead to an underestimation of losses. This is due to the fact that the linearization extrapolates the losses at the linearization point, which are lower than the ones closer to the power ratings or current boundaries. A linearization outside the boundaries is possible in theory, but the robust optimization model does not converge for such reference points, excluding this option from practical use. It is possible to calculate the linear sensitivities at points outside the boundaries, but provide the optimizer with reference power injections for states inside the limits, which in turn mimics the robust approach chosen here by a much more complex process. In this thesis, instead of shifting linearization points to get better estimates, octagonal power flow boundaries are used, as shown in Figure 7.4 in the previous chapter.
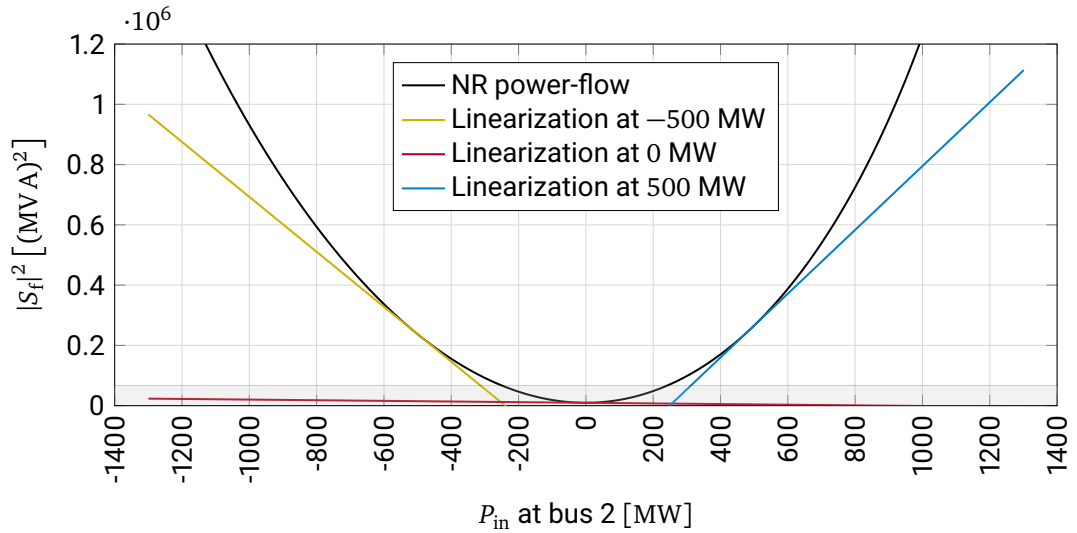
Figure 8.4.: Analytical and linearized solution of the power-flow calculation over the branch connecting bus 1 and bus 2 in the grid shown in Figure 8.2. The gray area depicts the power-flow boundaries, which are at $\pm259\,\mathrm{MV\,A}$.

8.3. Tests on a Conceptual Test Grid

Figure 8.5 shows a conceptual test grid, following the test grid that was created for the demonstrator used in the InnoSys project [52]. It consists of five buses in the distribution grid, here 110 kV, and two slack-buses in the transmission grid, here 380 kV. The power ratings are 260 MVA for power lines and 400 MVA for the transformers. Resistances, reactances, and line charging susceptances are taken from real power grids.

At each of the buses b2, b3, and b4, loads, PV plants, and wind farms are connected, with different flexibility factors. Both the installed capacity as well as the flexibility factors can be scaled. This scaling is performed to get non-critical reference cases and initial flexibility sets in which the most critical activations violate the operational boundaries.

On this test grid, a few tests can be performed concerning the two main aspects of quality for the developed algorithm:

1. Adherence to boundaries: It is important, that the operational boundaries are not transgressed.

2. Optimality: Only necessary limitations of initial individual flexibilities should be performed by the algorithm.
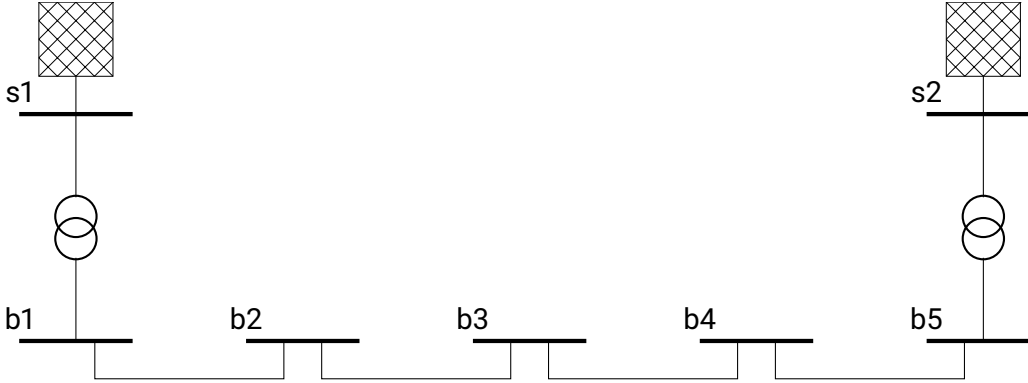
Figure 8.5.: The conceptual test grid with five HV buses and two UHV slack-buses. Transformers have a power rating of 400 MVA each, while power lines are rated at 260 MVA.

To analyze how the developed linear optimization algorithm performs with respect to these two aspects, the first week of each of the twelve months of the year are simulated in 15-minute resolution. To determine the adherence of boundary conditions, the maximum utilization of all assets at each time-steps is determined. A value higher than 100 % would indicate over-utilization. The maximum utilization is defined as:

$$\mu_t = \max_C \frac{\max_{\delta p, \delta q} u_{C,t}}{u_{C,\text{lim}}} \qquad \forall \; C \in \{\text{lines l, buses b}\}, \qquad (8.8)$$

where $u_{C,t}$ is the usage of asset C at time t and $u_{C,\text{lim}}$ its operational boundary.

In Figure 8.6, the maximum utilization μ_t is plotted over time in 15-minute resolution. As the figure shows, at no time the maximum utilization exceeds 100 %, which means that no boundary conditions were violated.

To test the efficiency of the approach or determine how close the maximum utilization μ_t is getting to 100 %, it is necessary to know when a reduction of the initial flexibilities is performed and evaluate the average maximum utilization $\langle \mu_t \rangle$ for these time-steps.

Figure 8.7 depicts the monthly means over $\langle \mu_t \rangle$ with error bars representing the standard deviations of the average values. As becomes visible, the mean values are, including errors, between 98 % and 99 %. This means that the power lines and buses that are closest to their operating boundaries and therefore become the active boundary are only between one and two percent away from a full utilization. The active boundary is the boundary condition in the optimization problem which is the limit that enforces a reduction in the objective function.
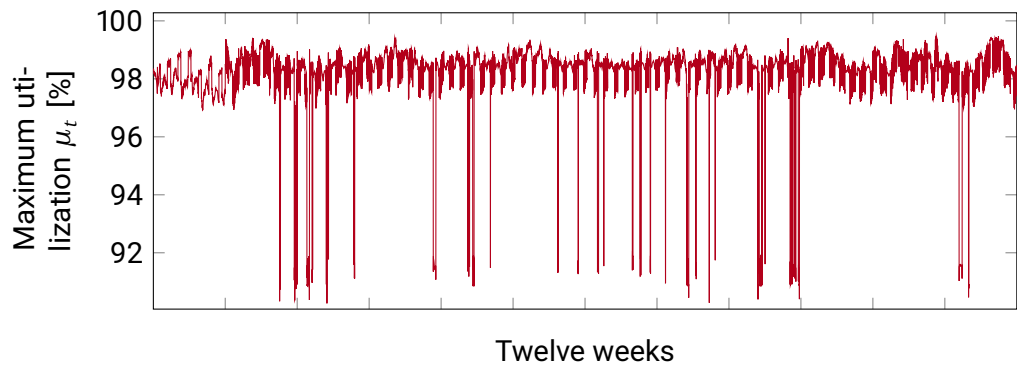
Figure 8.6.: Maximum utilization μ_t for all assets in the test grid over 12 first weeks in 15 minute resolution.

If the boundary becomes active at 100 % utilization, the objective function is at its theoretical maximum. However, as conservative boundary conditions are used, this theoretical maximum cannot be reached. Depending on the orientation of the s_{f}-vector in the complex pq-plane for each power line, in the worst case reductions can reach 8 %, as is displayed in Figure 7.3. However, in the application to the conceptual grid, it turns out that reductions seldomly reach 3 %, as is shown in Figure 8.7.

The objective function from Equation 7.7 also evaluates to lower values due to the conservative boundaries. In Section 8.6, the magnitude of this reduction is evaluated.
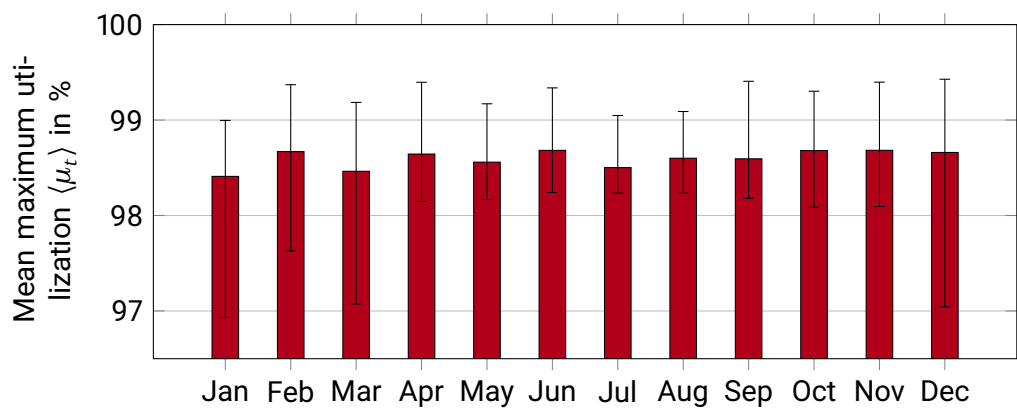

Figure 8.7.: Mean utilization μ_t for all assets in the test grid over each months first weeks in 15 minute resolution. Error bars indicate extreme values

8.4. Superimposed Power-Flows and their Effect on Flexibility Provision

Figure 2.3 shows the effects of slack angle differences $\delta\vartheta$. Slack angle differences cause power-flows on the power lines in the connected transmission grid. Proportional to the impedance of the two paths the power-flow can take, either via the transmission or distribution grid, a part of the power-flow is shifted into the distribution grid. This effect is analyzed by taking the conceptual grid shown in Figure 8.5 and setting a new slack angle at bus s2. The angle ϑ is incremented in steps of 1°, from -7°to 7°, resulting in 15 samples.

(a) Sensitivity for ΔP^{up} and ΔP^{down} at bus s1

(b) Aggregated ΔP^{up} and ΔP^{down} in the grid

(c) Sensitivity for ΔP^{up} and ΔP^{down} at bus s2

(d) Initial and safe flexibility of a flexible energy resource at b3

(e) Initial and safe flexibility of a flexible energy resource at b4

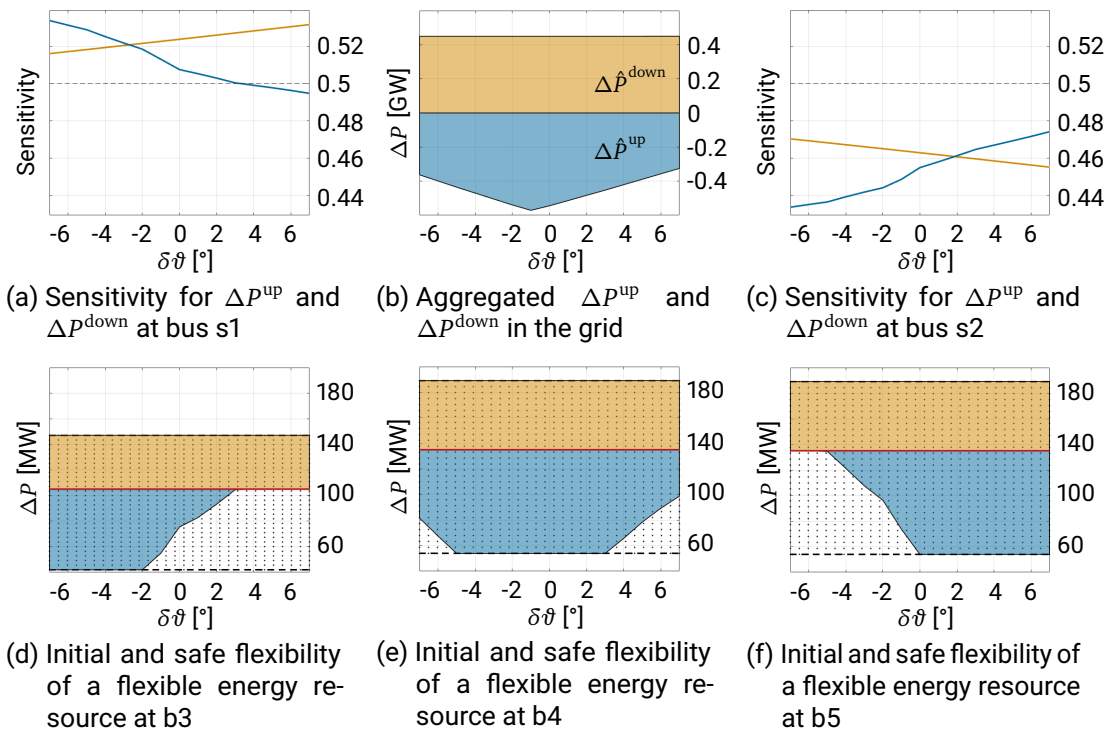(f) Initial and safe flexibility of a flexible energy resource at b5

Figure 8.8.: Influence of the slack angle difference $\delta\vartheta$ onto aggregated flexibilities and sensitivities onto the grid interconnection point (GICP). Yellow areas are downward and blue areas upward flexibilities.

Figure 8.8 shows the results of this analysis. Negative slack angle differences $\delta\vartheta < 0$ mean, that the power-flow in the transmission grid points from the right slack-bus s2 to the left slack-bus s1: At a slack angle difference of $\delta\vartheta = -1°$, the superimposed power-flow cancels

the power-flow caused by the energy resources connected in the distribution grid itself. This power-flow from the lower bus numbers to the higher ones is caused by a non-symmetrical load distribution, with a load of 105 MW being connected at b2, while at buses b3 and b4, 135 MW are installed. The generation capacities and power injections are distributed equally, with power injections from PV of -45 MW and -210 MW from wind-power at each bus. As a consequence, the total flexibility shown in Figure 8.8b shows the largest amounts at an angle of $\delta\vartheta = -1°$.

As the slack angle difference is further reduced, in the area of $\delta\vartheta = [-1°,\ldots,-7°]$, the superimposed power-flow puts a preloading on all power lines, reducing the amount of flexibility that can be provided by the flexible energy resources. Only the flexible energy resources that are connected at the left buses with lower indices can continue to provide flexibility. In the lower three figures 8.8d, 8.8e, and 8.8f, the upward and downward flexibility that can be provided by the loads at each bus are displayed. Indeed. the upward flexibility (blue) is decreased at first for bus b5 and for higher $\delta\vartheta$ also for bus b4. As a consequence of the reduction in flexibility for buses b4 and b5, the sensitivity with respect to the total flexibility at bus s1 rises for smaller $\delta\vartheta$ in Figure 8.8a, while it is reduced for bus s2 in Figure 8.8c.

For slack angles differences $\delta\vartheta = [0°,\ldots,7°]$, the same phenomenon can be observed, just in the opposite direction: Now, flexibility from bus b3 is limited first, while b5 can provide its initial, unlimited flexibility. The downward flexibility depicted in yellow is not reduced in any case, as the distribution grid itself is injecting power into the transmission grid. If its loads were withdrawing more power than the generation provides, the yellow areas would be reduced. The sensitivity for downward flexibility also shifts as a function of $\delta\vartheta$. This shift is also due to the changes in power-flow into the distribution grid in dependence of $\delta\vartheta$ while providing downward flexibility: Power flows are proportional to $\delta\vartheta$ and therefore the sensitivity at one GICP rises with the difference in ϑ relative to the other GICP.

These results show, that considering superimposed power-flows is of importance when providing flexibility due to the additional limitations these superimposed power-flows can cause. This is in contrast to distribution grids in a star-topology, with only one GICP, where these superimposed power-flows do not exist and therefore this phenomenon does not need to be taken into account.

8.5. Validity Considerations of Flexibility Clusters

The flexibility clusters introduced in Section 7.1 are a simplification: Sensitivities are only calculated in linear order, which lead to possible errors in flexibility provisioning. The same conceptual test grid is used to determine if the errors caused by this simplification are

significant.

In this test grid, three flexible energy resources are modeled at buses b3, b4, and b5, with 100 MW (b3) and 280 MW (each b4 and b5) installed generation capacity. Now, the power injections are reduced in 30 steps and a power-flow is calculated for each step. As a result of the power-flow calculation, the power flowing over the GICPs between s1 and b1 is known, as well as the one between s2 and b5. These values are taken as true values and are plotted in the upper part of Figure 8.9 in black dashed lines.
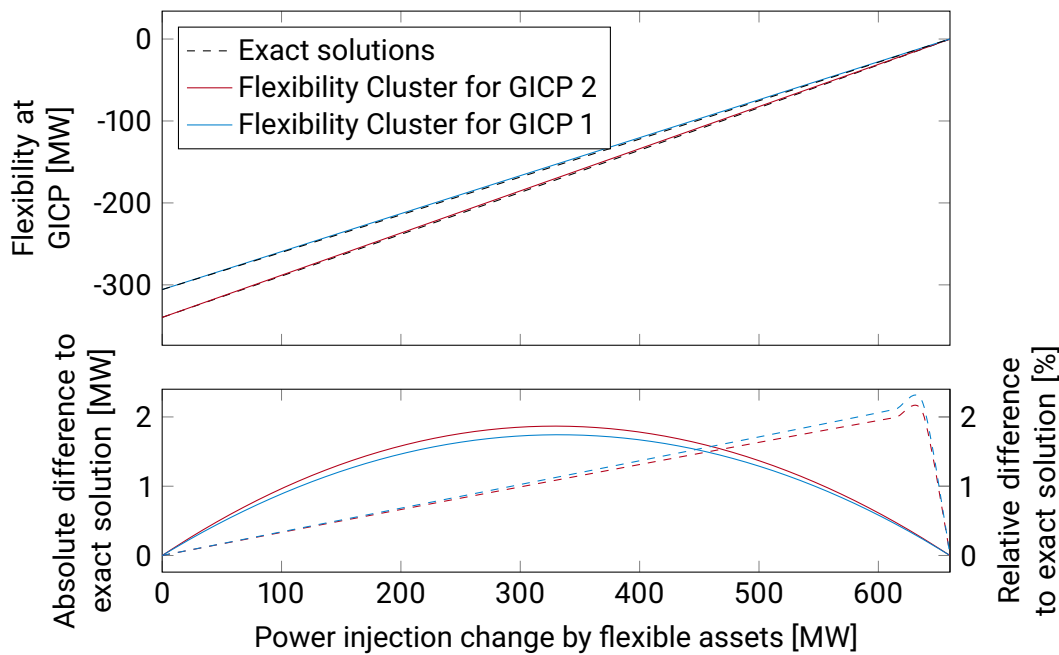
Figure 8.9.: Comparison of flexibility provision by flexibility cluster and exact calculations. Absolute values are shown in the upper half, while differences between exact calculations and the flexibility cluster are plotted in the lower half. Dashed values in the lower plot correspond to right axis and depict relative differences.

For the flexibility cluster, values for sensitivities are calculated once and evaluated for the same power injections as the true values. The results of this evaluation are compared to one another in the upper half of Figure 8.9, with the red line displaying values for the GICP at $s2$, and the blue line for bus $s1$.

In the lower part of Figure 8.9, the relative difference between solutions are plotted as dashed lines, while absolute differences are plotted as solid lines. The absolute difference is highest for values around 325 MW, while the relative difference is highest for values of 640 MW. This is due to the small base values, resulting in large relative errors. The worst error in absolute numbers is less than 2 MW, which corresponds to a relative error of less than 1 %. This does not pose a problem, as the optimization process produces conservative boundaries, which counter an overestimation of flexibility. In addition, the flexibility cluster does underestimate the available flexibility, which means that the TSO does not receive values for possible setpoints that cannot be reached.

8.6. Application to a German 110 kV Distribution Grid

Of course, the algorithm is not developed to optimize flexibilities on grids with seven buses. An application to a real distribution grid is needed to determine its performance in a realistic setting. Real-life distribution grids can span several hundreds of kilometers with several hundreds of nodes. However, since controlling such large grids is much harder than it is to control parts of these grids, some operators split their grids into groups, that are not directly and horizontally connected in the HV level. Splitting grids at suitable buses also leads to less superimposed power-flows and can simplify the communication with lower voltage grids operated by different DSOs due to the lower number of communication partners.

In the scope of this thesis, a real grid model in Baden-Württemberg was provided by Netze BW. The regional extent of this grid is shown in Figure 8.10. Netze BW is the only HV grid operator in Baden Württemberg and operates a 110 kV grid with a combine length of over 7500 km of power lines and 280 substations [204]. The HV grid is split into several groups that are denoted with colors. The group that is used here is the "red" group in the north-east of the state.

This part of the grid exhibits high numbers of renewable installations in the HV level in comparison with other parts in Baden-Württemberg and injects up to 500 MW back into the transmission grid given the right circumstances. Table 8.1 shows the key parameters of this grid used in the simulation.

As the power-flow calculation on parts of the grid model did not converge in Matpower, six buses with water power plants in the south of the model are removed. This removal does not change the outcome of flexibility calculations, as these run-of-river power plants are not modeled to provide flexibility. The remaining branch-bus model features 94 buses and 114 branches. In addition to the flexible energy resources that are already installed today, planned wind-power and PV farms are added and the grid model is selectively reinforced to be able to handle the additional power injections. With these additional flexible energy resources, 21
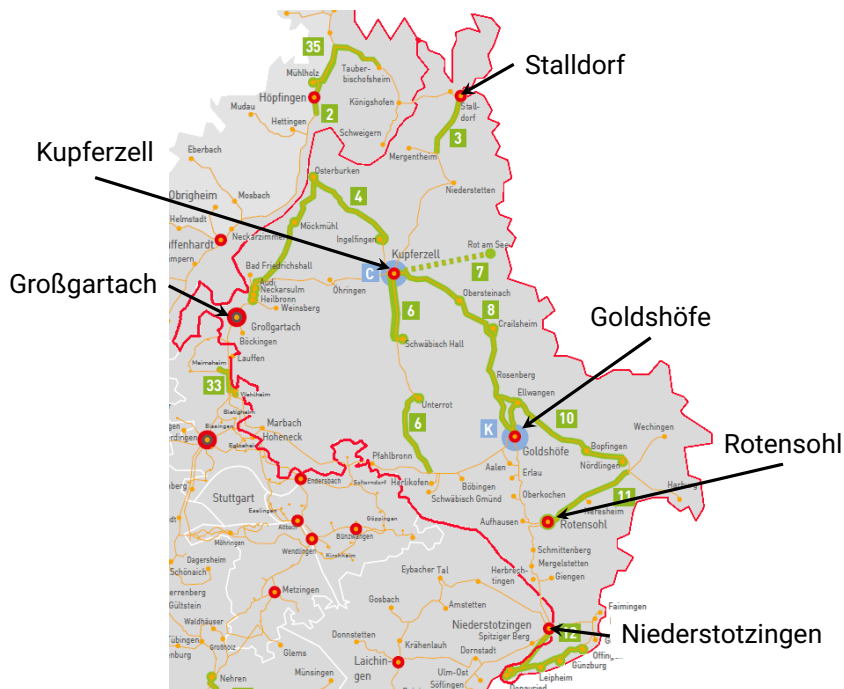
Figure 8.10.: A representation of the real power grid "Netzgruppe Rot" on which the algorithm is tested. The group that is modeled here is marked with a red border. The original graphic is from Netze BW [205]. Thick green lines display grid expansions. Red circles show the GICPs to the transmission grid.

wind farms and 9 large scale PV farms are installed, while there are 50 connected loads. In order to test the algorithm, is is necessary to observe situations, during which activations of the initially provided flexibility lead to violations of boundary conditions. These situations do not necessarily need to be real, but a diverse sample is needed to test the algorithm in different settings. As the grid is very well developed, flexibilities from wind-power are scaled by 150 % to create artificial reductions of possible flexibility provisioning.

8.6.1. Total Aggregated Flexibilities

One key parameter for the analysis of the algorithm on a real grid is the aggregated flexibility while guaranteeing a safe operation. To define which amount of flexibility is indeed optimal, another algorithm is used which was developed in the REGEES project [89]. This alternative

Table 8.1.: Key information about the real grid used to evaluate the algorithms.

Substations to UHV	6
Substations to MV	73
Combine line length	1200 km
Installed RES	1800 MW
Peak load	1130 MW
Peak power injection	500 MW
Branch bus model	
Number of buses	94
Number of branches	114

algorithm uses an intelligent sampling approach without any linearization. This intelligent sampling is done by simultaneously shifting individual power injections into the corners of the flexibility area. If the calculation of power-flows in these points are invalid, in the next iteration the point is shifted a little bit more to the center of the initial flexibility area. This approach circumvents a lot of the scaling problems for large numbers of flexible energy resources as discussed in the literature review in Section 1.3.2 and analysis in Section 2.2, by not sampling all combinations of setpoints. However, as the convergence behavior is not very robust and strongly dependent on the starting-point, its application in curative operation is not possible.

To generate the data that is needed to compare both approaches, the first week of each month is simulated in hourly resolution[3]. Of these, one case already violated operational constraints in the base-case and had to be excluded. In 300 remaining cases, the initial flexibility of at least one flexible energy resource had to be limited, making them the a subject of this analysis. Another 14 cases had to be excluded, since the alternative approach did not converge, proving some benefit of robust optimization, as the linear algorithm did always produce results. In summary, the final set of time-steps that is taken for comparison consists of 286 different cases.

In Table 8.2, the result of this comparison can be seen. The average downward flexibility ΔP^{down} is the same in both approaches, as most of the flexibility stems from wind-power. Exemplary, this result can also be seen in Figure 8.1, where only upward flexibility is limited. For the upward flexibility ΔP^{up}, the robust algorithm calculates slightly smaller values, which

---

[3]As the first value is missing from the time-series, this results in 1739 different grid-use-cases.

Table 8.2.: Evaluation of the performance of the linear algorithm on the real grid in comparison with the REGEES algorithm.

	Robust linear algorithm	Alternative algorithm from [89]
Average ΔP^{down} [MW]	241.0 ± 46.6	241.0 ± 46.6
Average ΔP^{up} [MW]	294.3 ± 39.6	307.4 ± 40.2
Average Objective function [a.u.]	1.711 ± 0.425	1.582 ± 0.515

are about 4 % less in average. This is to be expected, as this approach uses conservative boundaries that cut away feasible solution space. These 4 % are a price that is worth paying to obtain an approach that does not have to deal with convergence problems the non-linear method exhibits. Of course, starting points for the non-linear approach can be repeatedly changed in order to find a spot in which the optimization does converge, but as this way does not guarantee convergence times, it is not a feasible approach for curative grid operation.

If uncertainties of power injections from RES are included, it is likely that the difference in flexibility provision from both approaches vanishes. If uncertainties of about 10 % are assumed, their effect is already over twice as big as the difference in aggregated flexibility from the nonlinear and linear approach.

8.6.2. Influence of Slack-Angle Differences

To evaluate the influence of slack angles in the real grid, the same day as in Figure 8.1 is taken at 8 o'clock in the evening, and slack angle differences are imposed onto the six UHV buses in the grid: Stalldorf in the north of the grid is set to $\delta\vartheta = 0°$, with an increasing difference in slack angle, the further south the other buses are located.

In Table 8.3, the parameters for the slack angle adaptions are shown. As for the conceptual grid, these angles are set and the resulting flexibility and its sensitivity plotted in Figure 8.11.

As the power-flow did not converge for angles $\delta\vartheta > 3°$, only results between $-7° \leq \delta\vartheta \leq 3°$ are shown. Also, as Niederstotzingen is only connected to the rest of the grid via Rotensohl and no flexible assets are installed in this area of the grid, sensitivities are zero. Therefore, sensitivities for Niederstotzingen are trivial and not shown here.

A large part of the flexibility is located in the north, as at Kupferzell over one third of the downward flexibility is available. This means, that for each Megawatt of activated flexibility, about one third flows over the GICP at Kupferzell. For the upward flexibility, the sensitivities

Table 8.3.: Parameters to introduce slack angle differences in the real grid.

Grid node	slack-angle parameter
Stalldorf	$0 \cdot \delta\vartheta$
Kupferzell	$0.3 \cdot \delta\vartheta$
Großgartach	$0.5 \cdot \delta\vartheta$
Goldshöfe	$0.7 \cdot \delta\vartheta$
Rotensohl	$0.8 \cdot \delta\vartheta$
Niederstotzingen	$1 \cdot \delta\vartheta$

change with rising $\delta\vartheta$. However, as the grid topology is much more complex than the one of the conceptual test grid, relations are not linear and not strictly in the North-South direction. For example Großgartach, which is located in the middle in north-south direction in a mesh between Kupferzell and Goldshöfe, sensitivities rise for rising $\delta\vartheta$. For Goldshöfe and Kupferzell, sensitivities decrease with rising $\delta\vartheta$. The central north-south connections between Kupferzell and Goldshöfe, where a lot of the wind-power is connected, is getting congested by the superimposed power-flow, reducing the amount of flexibility that is available. This can also be seen in the aggregated flexibility in Figure 8.8a. The other sensitivities rise, as the aggregated flexibility decreases and the respective shares of the aggregate that is available at these other buses (Stalldorf, Großgartach, and Rotensohl) stays constant.

The slack-angle differences assumed in this scenario are not necessarily realistic. However, the importance of the fact that they can be taken into account is shown, as the total upward flexibility is reduced by about 100 MW. A more thorough analysis of the influence of slack-angle differences requires a combined and detailed modeling of transmission and distribution grid. Also, such an analysis would greatly profit from an integrated market and grid model, for example by using the results from the first part of this thesis as input for a grid analysis.

8.7. Runtime and Scaling Behavior

To determine how fast the algorithm converges on a solution, the runtime was determined for different grid sizes. Seven test grids from the grid-library included in Matpower were chosen with different numbers of buses $n_b = \{30, 57, 85, 118, 141, 300, 1345\}$. At each node, a flexible load was connected, so that $n_b = n_{FA}$. As parameterizing these loads is not trivial, for some of the test-grids the power-flow does not converge. However, non-convergence does
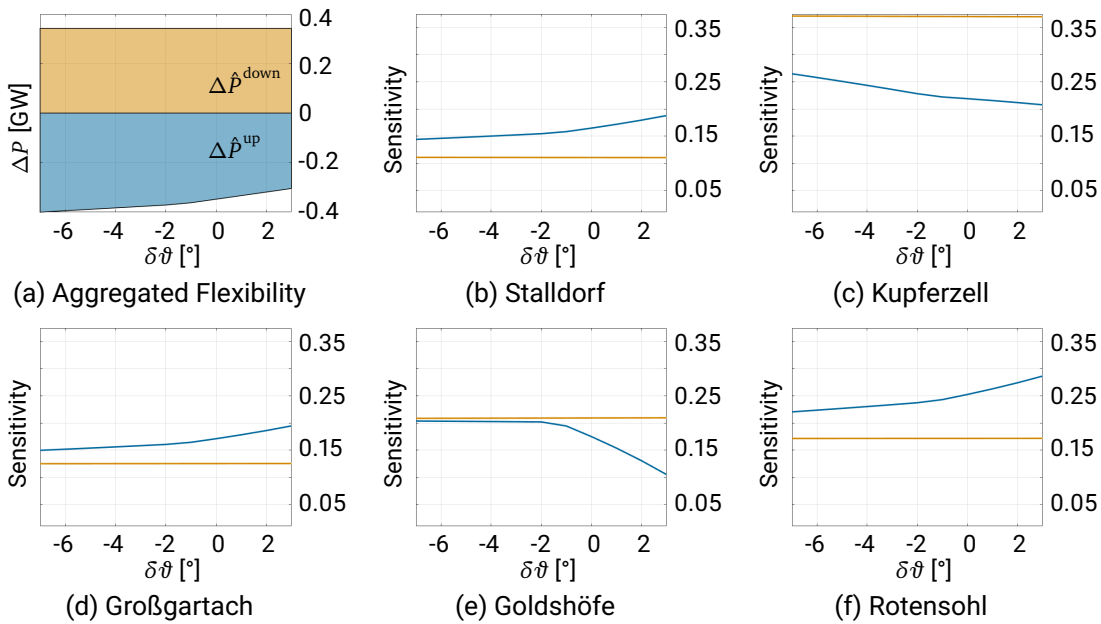
Figure 8.11.: Influence of the slack angle difference $\delta\vartheta$ onto aggregated flexibilities and sensitivities in the real grid. Niederstotzingen is not shown, as the sensitivity is close to zero at all angles.

not have an influence on all parts of the components that define the runtime. For example matrix inversion is independent of convergence behavior. However, the solver itself takes more time, if the problem is infeasible.

All calculations are performed on the same machine, a laptop equipped with Windows 10, an Intel i7-7820HQ CPU at 2.9 GHz, and 32 GB of RAM. The code is not optimized to be run in parallel, using only one of the CPU's cores. Determination of the runtime of different components of the code was performed using Visual Studio's performance analysis tools, which return millisecond values for CPU-times at lines of code.

Figure 8.12 depicts the two components of the runtime that are of the most interest: matrix inversion to calculate the functional dependence of voltage deviations from power injection changes as depicted in Equation 7.28, and the time the solver needs for the solution of the problem. The solver used here is SCIP 7 [201], a non-commercial solver developed by the Zuse Institut Berlin. For both processes, a fit has been added in red to show the cubic scaling behavior of matrix inversion and the quadratic scaling for the solution process. The scaling behavior for matrix inversion is expected, as the classical Gaussian-Jordan algorithm scales
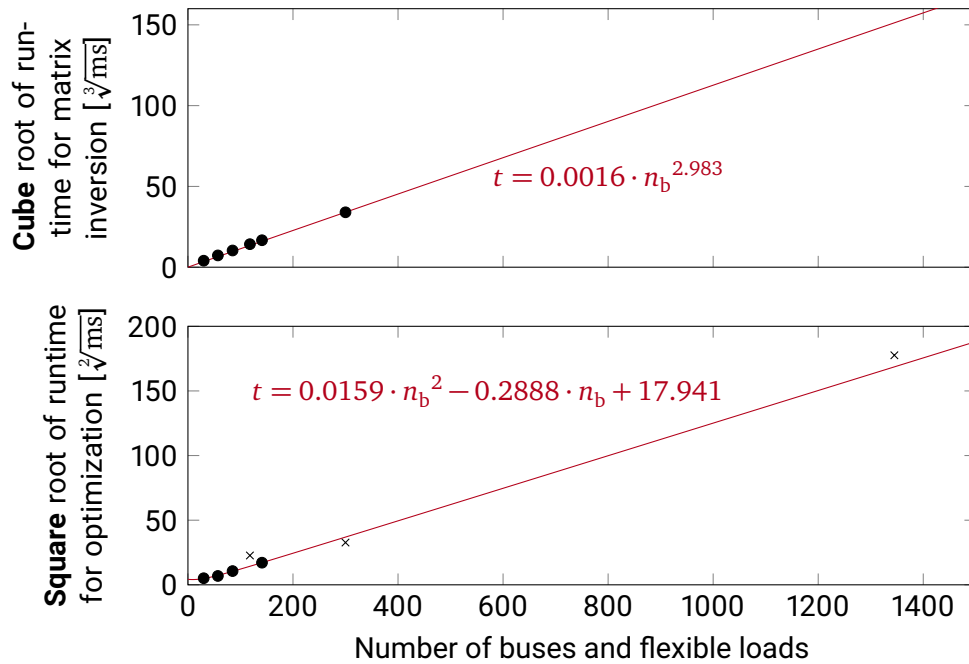
Figure 8.12.: Runtimes of different processes in the robust algorithm: Matrix inversion scales in cubic manner, while the optimization itself scales quadratically as a function of n_b. Marks that are depicted as crosses indicate that the optimization was not possible due to non-converging power-flows.

with n^3, while newer algorithms achieve lower exponents, for example $n^{2.376}$ in [206]. In actual numbers, the comparison of inversion and optimization becomes more tangible: While the matrix inversion for 1300 buses takes about 4000 seconds, the solver only takes 30 seconds. For grids with $n_b \leq 300$, the solver takes less than one second, while inversion times cross the one second mark at about $n_b = 80$.

For small grids with $n_b \leq 50$, the solution of the problem is obtained in a matter of seconds. For grids that are of the size of real-world distribution or sub-transmission grids, e.g. $50 \leq n_b \leq 300$, inversion and optimization is done in less than a minute on the laptop used for this analysis. However, for large grids, solution times are dominated by matrix inversion. While better algorithms can reduce this behavior to lower exponents [206], they still scale worse than quadratically. Further speed improvements can be achieved by using sparse matrices and solvers for systems of linear equations, but this path was not pursued in

this thesis.

Comparison with other approaches is difficult, as most publications do not state the explicit runtime or are not directly comparable. However, in [142], a runtime of 500 seconds was achieved on a 33-bus grid on a server, using GUROBI [207] as solver for a comparable solution using scenario sampling and optimal power flow (OPF). The algorithm developed here is over two orders of magnitude faster taking 1.6 seconds for the whole process for a similar grid. The approach in [142] also takes into account uncertainty from different sources and is developed for planning purposes, therefore the comparison is not very fair. However, it is done without including effects caused by computation hardware, commercial vs. academic solvers, or optimization of code.

It must be noted, that the code used for this thesis was not optimized for performance by any expert, but only small steps to increase performance were performed, as for example buffering of the number of entries in a vector instead of calculating it at each call. For matrix operations, the C++ library Eigen [203] was used, without any changes to the choices of algorithms being used. However, even at this state, the algorithm developed here is sufficiently fast for curative grid operation purposes on reals grids and can be run in short cycles in the DSOs control center. For grids larger than a few hundreds of nodes, further optimization is necessary, especially in the choice of algorithms to perform the matrix inversion.

8.8. Discussion

As the results show, linearization of power flows can be used to achieve a robust optimization problem. While linearization of voltage magnitudes does not pose a problem, it is inaccurate for power-flow magnitudes and quickly leads to large errors. Therefore, instead of linearization of power-flow magnitudes, octagonal boundaries in the complex P_f-Q_f-plane are introduced to guarantee a safe state in the flexibility providing grid.

As a consequence of the choice of conservative conditions, which cut away feasible solution space, the corresponding results amount to less than the theoretical optimum. The results show, that indeed the boundary conditions are always adhered, while the efficiency on a conceptual grid is between 97-99 % of the theoretically achievable values. In the application on real grids, an inclusion of uncertainties probably introduces a greater reduction in aggregated flexibilities than the different approaches to calculate safe flexibility sets. The difference observed here amounts to less than 4.5 %. Such uncertainty is not yet included in the method, a master thesis dealing with this topic is currently underway.

On the real test grid, the robust approach also shows values less effective than a sampling approach while converging at all simulated time-steps, a quality that is important for curative operation. In time-sensitive operation, algorithms cannot just be re-run with different starting

values until they converge, as the results might be obtained too late for the application. In such a case, it is imperative that explicit results are achieved in foreseeable time, a quality which is provided by the robust approach developed here.

On both the real and the conceptual grid, slack angles and the corresponding power-flows, that are imposed onto the distribution grid, are of great importance: Not only the total aggregated flexibility reduces its values down to about 50 % of the the values without the introduction of slack-angles, but also the sensitivity where the flexibility is present changes significantly. For curative operation it is very important, that the communicated flexibility is indeed provided in the communicated way, as missing flexibility might lead to cascading outages in the transmission system. Therefore it is of importance to take the effects of slack-angle differences into account when calculating and aggregating safe flexibility sets.

To further analyze the influence of transmission system power-flows, it is possible to couple the results of the first part of the thesis with the second part, to create scenarios that can then be tested in detail on the real distribution grid model. Of course, the installed capacities of flexible assets in both parts of this coupling must be aligned to enable transferring schedules for all assets from the energy system model to the distribution system simulation. This would be an interesting subject for further research.

The communication of flexibility from one grid operator to another is performed via flexibility clusters in this thesis. These clusters and the underlying linearization of sensitivities are sufficiently accurate to be used in the application chosen here. However, it is important to split upward and downward flexibility clusters, as sensitivities in a combined approach lead to non-optimal setpoint shifts that in turn lead to higher losses and costs.

The runtime achieved with the robust optimization approach is dominated by matrix inversion, which scales cubically. Usage of sparse matrix algebra with corresponding solvers can help to reduce the runtime without changes to the core algorithm. In addition, competing sampling algorithms scale exponentially and OPF-based approaches also use matrix inversion to calculate power-flows, leading to similar runtime scaling while lacking robustness.

Summary

In this chapter, the algorithm developed in the course of this thesis is applied to two test grids: a conceptual, seven-bus grid, and a real grid with about 100 buses. The following results were determined and discussed:

- Exemplary time-steps show reductions in initial flexibility to reduce power-flows below the operational limits.

- Conservative boundary conditions lead to a non-optimality or over-reduction of power-flows.

- The robust linear approach is indeed robust. Convergence was always achieved if it was possible. In contrast, a non-linear approach failed to converge in about 5 % of the simulated cases.

- Linearization of voltages has proven to be an approximation with acceptable accuracy. For power-flow magnitudes deviations from true values are larger. Therefore, boundary conditions in the algorithm are reformulated to not use the absolute value function for power-flows in order to bypass this issue.

- On the conceptual test grid, the algorithm did always adhere to the boundary conditions. Conservative boundary conditions lead to reduction in efficiency between 1 % and 3 %.

- Superimposed power-flows can reduce or increase the flexibility that can safely be provided to the TSO. In grids with more than one grid interconnection point (GICP), it is imperative to consider these superimposed power-flows.

- Flexibility clusters as a method to aggregate the safe individual flexibilities are a valid choice, as deviations caused by linearization are not large and do not lead to an overestimation of aggregated flexibility.

- The developed algorithm reliably converges on real grid data, producing results that are at about 96 % of the theoretical maximum. While it is less optimal than the non-linear approach, its stable convergence guarantees that a safe set of flexibilities is always found.

- The runtime achievable with the approach chosen here is significantly faster than previous approaches. The scaling behavior is dominated by matrix inversion, which scales cubically with the number of buses. However, different approaches are conceivable to counter this behavior and speed up the total process.

- The differences in aggregated flexibility from the nonlinear and the linear approach are likely to be negligible compared to uncertainties from forecasts of injections of RES. However, this is a topic for further research.

9. Conclusion and Outlook

This chapter provides a summary of the thesis. Also, a brief overview of some aspects that are under-explored so far or could not further be delineated in this thesis is given.

The goal of this thesis is to evaluate if distributed flexible energy resources can help transmission system operators to operate grids curatively instead of preventively n-1 safe. Two research questions are posed to analyze the feasibility of this concept:

1. Are flexible assets in distribution grids a viable source of flexibility for curative transmission system operation?

2. How can flexibility from underlying grids be safely and quickly aggregated and offered for curative use?

These two questions are answered in two methodologically independent parts of this thesis. The first part uses an energy system model to simulate a German energy system in the year 2030, while the second develops and tests a grid control algorithm.

To answer the first question, two methods are developed and analyzed. Both determine time-steps during which the grid could slip into a critical state before calculating the available flexibility at this time. The simulated redispatch model performs determination of critical times globally, by approximating redispatch amounts, while the simulation of transmission capacity losses performs its analysis locally. After knowing which time-steps are of interest, the amount of available flexibility can be calculated as a function of the technologies that are available.

While the global analysis by simulated redispatch shows amounts in the magnitude of several gigawatts of curtailed wind-power being available, the simulation of transmission capacity losses demonstrates, that a large part of usable flexibility actually stems from flexible loads, as for example power to heat (P2H). These flexible loads are taking advantage of low electricity prices when many renewable energy sources (RES) are generating electricity. These time-steps coincide with large transmission loadings in the grid when a loss of 2 GW transmission capacity could lead to a critical outage.

The presented analysis of the potential of distributed flexible energy resources also shows, that flexibility from distribution grids can indeed contribute to a higher transmission grid

utilization. In addition, if it is not actively used for such an increase in utilization, it can be used as collateral for other measures used for curative operation, indirectly contributing to the higher utilization.

The simulated loss of transmission capacity can also be used to determine suitable locations for grid-boosters: In each region, a grid booster can be simulated with a desired power and its value can be determined by the number of situations where it can compensate transmission capacity losses or by the amount of energy loss that is avoided. Such an analysis was performed during the course of the thesis but is left out as it does not thematically fit here.

The second research question is addressed in the latter part of this thesis with the development of a linearized robust optimization approach to limit individual flexibility boundaries such that only safe combinations of setpoints within these boundaries are possible. The aggregation of these individual flexibilities is done with a concept called "Wirksamkeitscluster" or flexibility cluster, which is introduced and evaluated.

While the linearization and the conservative boundary conditions chosen for power-flows lead to results that are about one to five percent less effective than what is theoretically possible, the approach converges reliably. A sampling approach to benchmark the newly developed algorithm does not converge reliably, which is not acceptable for curative or real-time usage.

Uncertainty of power injections is not analyzed yet. A possible extension of the robust optimization to include uncertainties can be performed by transforming flexible loads into flexible loads with uncertainty. For example, the present formulation of the optimization problem can be altered to include flexible loads whose flexibility may not be limited to represent the uncertain part of the power injection. Such an approach is set to be pursued in a following master thesis.

The algorithm developed here is not only usable for operation, but can also be applied for planning processes: If a new energy resource is to be installed in the grid, the optimally installed power can be determined for which only a preset amount or share of energy is set to be curtailed. This can be done by placing virtual assets in the grid at several buses and equip these assets with large flexibilities. After simulating a set of time-steps, average curtailments and power injections can be calculated, helping in the decision which power is to be installed.

Another benefit of distributed flexibility and of curatively usable concepts in general is, that even without operating the grid curatively, a reliability-gain in operation can be obtained, as these measures, once developed and deployed, can also be used as remedial actions after a critical outage. Even if the algorithm developed in this thesis is not used for curative grid operation, it can still help relieve congestion after losses of transmission capacity and increase the reliability of preventively operated grids.

In this thesis, it is shown that flexibility from distribution grids is not only present when and where it is needed in magnitudes usable for curative grid operation, but also that provisioning

of such distributed flexibility to transmission system operators can be performed quickly and reliably.

Acknowledgments

and Katharina, Olof, Lena, and Eva not only for proofreading, but also general help and support and help in the completion of this thesis. Especially I thank Meike for staying up late in the final months and enduring the nerd-talk about the future of our energy system and the necessary steps to achieve a more sustainable society.

Bibliography

[1] P. Shukla, J. Skea, E. Calvo Buendia, V. Masson-Delmotte, H.-O. Pörtner, D. C. Roberts, P. Zhai, R. Slade, S. Connors, R. van Diemen, M. Ferrat, E. Haughey, S. Luz, S. Neogi, M. Pathak, J. Petzold, J. Portugal Pereira, P. Vyas, E. Huntley, K. Kissick, M. Belkacemi, and J. Malley, "Climate Change and Land: An IPCC special report on climate change, desertification, land degradation, sustainable land management, food security, and greenhouse gas fluxes in terrestrial ecosystems", IPCC, 2019.

[2] T. M. Lenton, J. Rockström, O. Gaffney, S. Rahmstorf, K. Richardson, W. Steffen, and H. J. Schellnhuber, "Climate tipping points too risky to bet against", *Nature*, vol. 575, no. 7784, pp. 592–595, Nov. 28, 2019, ISSN: 0028-0836, 1476-4687. DOI: `10/ggdmkg`. [Online]. Available: `http://www.nature.com/articles/d41586-019-03595-0` (visited on 09/08/2021).

[3] J. Rockström, W. Steffen, K. Noone, Å. Persson, F. S. Chapin, E. F. Lambin, T. M. Lenton, M. Scheffer, C. Folke, H. J. Schellnhuber, B. Nykvist, C. A. de Wit, T. Hughes, S. van der Leeuw, H. Rodhe, S. Sörlin, P. K. Snyder, R. Costanza, U. Svedin, M. Falkenmark, L. Karlberg, R. W. Corell, V. J. Fabry, J. Hansen, B. Walker, D. Liverman, K. Richardson, P. Crutzen, and J. A. Foley, "A safe operating space for humanity", *Nature*, vol. 461, no. 7263, pp. 472–475, Sep. 2009, ISSN: 0028-0836, 1476-4687. DOI: `10/bjgw48`. [Online]. Available: `http://www.nature.com/articles/461472a` (visited on 09/08/2021).

[4] M. Madrigal and S. Stoft, *Transmission Expansion for Renewable Energy Scale-Up: Emerging Lessons and Recommendations*. The World Bank, Jun. 14, 2012, ISBN: 978-0-8213-9598-1. DOI: `10.1596/978-0-8213-9598-1`. [Online]. Available: `http://elibrary.worldbank.org/doi/book/10.1596/978-0-8213-9598-1` (visited on 11/18/2021).

[5] ENTSO-E, "Continental Europe Operation Handbook P3", ENTSO-E, p. 21.

[6] E. Foote, *Circumstances Affecting the Heat of the Sun's Rays* (American Journal of Science and Arts), Second Series, B. Silliman, B. J. Silliman, J. D. Dan, A. Gray, L. Agassiz, and W. Gibbs, Eds. 1856. [Online]. Available: `https://archive.org/stream/mobot31753002152491/mobot31753002152491_djvu.txt`.

[7] M. Hulme, "On the origin of the greenhouse effect': John Tyndall's 1859 interrogation of nature", *Royal Meteorological Society*, pp. 121–123, 2005.

[8] C. MacFarling Meure, D. Etheridge, C. Trudinger, P. Steele, R. Langenfelds, T. van Ommen, A. Smith, and J. Elkins, "Law Dome CO2 , CH4 and N2O ice core records extended to 2000 years BP", *Geophysical Research Letters*, vol. 33, no. 14, p. L14810, 2006, ISSN: 0094-8276. DOI: `10/cdqx54`. [Online]. Available: `http://doi.wiley.com/10.1029/2006GL026152` (visited on 09/08/2021).

[9] M. E. Mann, R. S. Bradley, and M. K. Hughes, "Northern hemisphere temperatures during the past millennium: Inferences, uncertainties, and limitations", *Geophysical Research Letters*, vol. 26, no. 6, pp. 759–762, Mar. 15, 1999, ISSN: 00948276. DOI: `10/fk95w9`. [Online]. Available: `http://doi.wiley.com/10.1029/1999GL900070` (visited on 09/08/2021).

[10] S. Arrhenius, "On the Influence of Carbonic Acid in the Air upon the Temperature of the Earth", *Publications of the Astronomical Society of the Pacific*, vol. 9, no. 54, p. 14, 1897. DOI: `10/cvz3qd`.

[11] P. Friedlingstein, M. O'Sullivan, M. W. Jones, *et al.*, "Global Carbon Budget 2020", *Earth System Science Data*, vol. 12, no. 4, pp. 3269–3340, Dec. 11, 2020, ISSN: 1866-3516. DOI: `10/ghn75s`. [Online]. Available: `https://essd.copernicus.org/articles/12/3269/2020/` (visited on 09/08/2021).

[12] Bundesministerium für Umwelt, Naturschutz und nukleare Sicherheit. "Treibhausgasemissionen sinken 2020 um 8,7 Prozent", Bundesministerium für Umwelt, Naturschutz und nukleare Sicherheit. (Mar. 16, 2021), [Online]. Available: `https://www.bmu.de/pressemitteilung/treibhausgasemissionen-sinken-2020-um-87-prozent/`.

[13] Alexandre Edmond Becquerel, "Recherche sur les effets de la radiation chimique de la lumière solaire, au moyen des courants électriques", *Comptes rendus hebdomadaires des séances de l'Académie des sciences*, vol. 9, pp. 145–149, 1839. [Online]. Available: `https://archive.org/details/comptes-rendus-hebdomadaires-des-seances-...-academie-des-bpt-6k-2968p`.

[14] D. M. Chapin, C. S. Fuller, and G. L. Pearson, "A New Silicon pn Junction Photocell for Converting Solar Radiation into Electrical Power", *Journal of Applied Physics*, vol. 25, no. 5, pp. 676–677, May 1954, ISSN: 0021-8979, 1089-7550. DOI: `10/cn6qct`. [Online]. Available: `http://aip.scitation.org/doi/10.1063/1.1721711` (visited on 09/01/2021).

[15] A. P. Cracknell and C. A. Varotsos, "Editorial and cover: Fifty years after the first artificial satellite: From Sputnik 1 to ENVISAT", *International Journal of Remote Sensing*, vol. 28, no. 10, pp. 2071–2072, May 2007, ISSN: 0143-1161, 1366-5901. DOI: `10/cwb7q7`. [Online]. Available: `https://www.tandfonline.com/doi/full/10.1080/01431160701347147` (visited on 09/01/2021).

[16] C. Leepa and M. Unfried, "Effects of a cut-off in feed-in tariffs on photovoltaic capacity: Evidence fromGermany", *Energy Policy*, vol. 56, pp. 536–542, May 2013, ISSN: 03014215. DOI: `10/f4wbxf`. [Online]. Available: `https://linkinghub.elsevier.com/retrieve/pii/S0301421513000256` (visited on 09/01/2021).

[17] Harold Anuta, Pablo Ralon, Michael Taylor, Dolf Gielen, Rafael De Sa Ferreira, Paul Komor, Adrian Whiteman, and Jon Gorvett, *Renewable Power Generation Costs in 2018*. Abu Dhabi: International Renewable Energy Agency, 2019, ISBN: 978-92-9260-126-3. [Online]. Available: `www.irena.org/publications`.

[18] Michael Taylor, Pablo Ralon, Harold Anuta, and Sonia Al-Zoghoul, *Renewable Power Generation Costs in 2019*. Abu Dhabi: International Renewable Energy Agency, 2020, ISBN: 978-92-9260-244-4. [Online]. Available: `www.irena.org/publications`.

[19] D. C. Kost, D. T. Schlegl, Shammugan, Shevenes, Jülich, Verena, and Nguyen, Huyen-Tran, "Stromgestehungskosten erneuerbare Energien", Frauenhofer-Institut für Solare Energiesysteme, Mar. 2018, p. 44.

[20] S. Mathew, *Wind Energy: Fundamentals, Resource Analysis, and Economics*. Berlin ; New York: Springer, 2006, 246 pp., ISBN: 978-3-540-30905-5.

[21] T. J. Price, "James Blyth Britain's First Modern Wind Power Pioneer", *Wind Engineering*, vol. 29, no. 3, pp. 191–200, May 2005, ISSN: 0309-524X, 2048-402X. DOI: `10/fs82fw`. [Online]. Available: `http://journals.sagepub.com/doi/10.1260/030952405774354921` (visited on 09/01/2021).

[22] P. Maegaard, Ed., *Wind Power for the World. 1* (Pan Stanford Series on Renewable Energy Vol. 2). Signapore: Pan Stanford Publ, 2013, 642 pp., ISBN: 978-981-4364-93-5.

[23] E. F. Moran, M. C. Lopez, N. Moore, N. Müller, and D. W. Hyndman, "Sustainable hydropower in the 21st century", *Proceedings of the National Academy of Sciences*, vol. 115, no. 47, pp. 11 891–11 898, Nov. 20, 2018, ISSN: 0027-8424, 1091-6490. DOI: `10/gfhknq`. [Online]. Available: `http://www.pnas.org/lookup/doi/10.1073/pnas.1809426115` (visited on 09/01/2021).

[24] Bundesnetzagentur, *EEG in Zahlen 2018*. [Online]. Available: `https : / / www . bundesnetzagentur . de / DE / Sachgebiete / ElektrizitaetundGas / Unternehmen _ Institutionen / ErneuerbareEnergien / ZahlenDatenInformationen / zahlenunddaten - node . html` (visited on 02/19/2020).

[25] T. Ackermann, G. Andersson, and L. Söder, "Distributed generation: A definition", *Electric Power Systems Research*, vol. 57, no. 3, pp. 195–204, Apr. 2001, ISSN: 03787796. DOI: `10 / cvs5kv`. [Online]. Available: `https : / / linkinghub . elsevier . com/retrieve/pii/S0378779601001018` (visited on 06/10/2021).

[26] International Energy Agency, *World Energy Outlook 2020* (World Energy Outlook). OECD, Oct. 13, 2020, ISBN: 978-92-64-62199-2. DOI: `10.1787/557a761b-en`. [Online]. Available: `https://www.oecd-ilibrary.org/energy/world-energy-outlook-2020_557a761b-en` (visited on 09/08/2021).

[27] 50Hertz Transmission GmbH, "50Hertz Energiewende Outlook 2035", Berlin, Abschlussbericht, Jun. 2016, p. 72. [Online]. Available: `https : / / www . 50hertz . com / de / Netz / Netzentwicklung / WofuerNetzausbau / 50HertzEnergiewendeOutlook2035` (visited on 05/10/2021).

[28] IEA, "Installed power generation capacity by source in the Stated Policies Scenario, 2000-2040", Paris, 2020. [Online]. Available: `https://www.iea.org/data-and-statistics/charts/installed-power-generation-capacity-by-source-in-the-stated-policies-scenario-2000-2040`.

[29] Lazard, "Lazards Levelized Cost of Energy Analysis Version 13.0", Lazard, 13.0, 2019. [Online]. Available: `https://www.lazard.com/media/451086/lazards-levelized-cost-of-energy-version-130-vf.pdf`.

[30] "Why did renewables become so cheap so fast?", Our World in Data. (Dec. 1, 2020), [Online]. Available: `https://ourworldindata.org/cheap-renewables-growth` (visited on 09/08/2021).

[31] *Directive (EU) 2018/844 of the European Parliament and of the Council of 30 May 2018 amending Directive 2010/31/EU on the energy performance of buildings and Directive 2012/27/EU on energy efficiency*. [Online]. Available: `https : / / eur-lex . europa . eu / legal - content / EN / TXT / ?uri=uriserv%3AOJ.L_ .2018.156.01.0075.01.ENG`.

[32] *Directive (EU) 2018/2002 of the European Parliament and of the Council of 11 December 2018 amending Directive 2012/27/EU on energy efficiency*. [Online]. Available: `https://eur-lex.europa.eu/legal-content/EN/TXT/?uri=uriserv%3AOJ.L_.2018.328.01.0210.01.ENG`.

[33] *Directive (EU) 2018/2001 of the European Parliament and of the Council of 11 December 2018 on the promotion of the use of energy from renewable sources*. [Online]. Available: `https://eur-lex.europa.eu/legal-content/EN/TXT/?uri=uriserv:OJ.L_.2018.328.01.0082.01.ENG&toc=OJ:L:2018:328:TOC`.

[34] *Regulation (EU) 2019/942 of the European Parliament and of the Council of 5 June 2019 establishing a European Union Agency for the Cooperation of Energy Regulators*. [Online]. Available: `https://eur-lex.europa.eu/legal-content/EN/TXT/?uri=uriserv:OJ.L_.2019.158.01.0022.01.ENG&toc=OJ:L:2019:158:TOC`.

[35] Bundesministerium der Justiz und Verbraucherschutz, *Netzausbaubeschleunigungsgesetz Übertragungsnetz,* Aug. 5, 2011. [Online]. Available: `https://www.gesetze-im-internet.de/nabeg/BJNR169010011.html` (visited on 05/13/2019).

[36] Bundesministerium der Justiz und Verbraucherschutz, *Gesetz für den Ausbau erneuerbarer Energien (Erneuerbare-Energien-Gesetz - EEG 2017)*, 2017. [Online]. Available: `http://www.gesetze-im-internet.de/eeg_2014/__14.html` (visited on 04/01/2020).

[37] Bundesministerium der Justiz und Verbraucherschutz, *Gesetz für die Erhaltung, die Modernisierung und den Ausbau der Kraft-Wärme-Kopplung*. [Online]. Available: `https://www.gesetze-im-internet.de/kwkg_2016/`.

[38] Bundesministerium der Justiz und Verbraucherschutz, *Gesetz über die Elektrizitäts- und Gasversorgung*, May 18, 2021. [Online]. Available: `https://www.gesetze-im-internet.de/enwg_2005/__13.html` (visited on 05/28/2021).

[39] Dr. Sandu-Daniel Kopp, "Redispatch 2.0", BDEW. [Online]. Available: `https://www.bdew.de/energie/redispatch-20/`.

[40] Mitnetz Strom, e.dis, WEMAG Netz GmbH, BWE WindEnergie, BASF, energiequelle, Entelios, Nodes, and E.-B. C. GmbH, *Masterplan Flexibilität in Brandenburgs Verteilnetzen*, Mar. 24, 2021. [Online]. Available: `https://www.e-bridge.de/2021/06/konsortium-um-e-bridge-veroeffentlicht-den-masterplan-flexibilitaet-in-brandenburgs-verteilnetzen/`.

[41] B. WindEnergie. "Zahlen und Fakten: Statistische Kennziffern zur Erfolgsgeschichte Windenergie", Bundesverband WindEnergie. (Feb. 2021), [Online]. Available: `https://www.wind-energie.de/themen/zahlen-und-fakten/` (visited on 09/15/2021).

[42] Strom-Report. "Photovoltaik in Deutschland", Strom-Report: Zahlen. Daten. Fakten. (Oct. 1, 2021), [Online]. Available: `https://strom-report.de/photovoltaik` (visited on 10/01/2021).

[43] Patrick Fekete, *Redispatch in Deutschland*, Nov. 10, 2020. [Online]. Available: `https://www.bdew.de/service/anwendungshilfen/redispatch-deutschland/`.

[44] "TYNDP 2018 Executive Summary: Connecting Europe: Electricity, 2025 - 2030 - 2040 Final version after consultation and ACER opinion", Avenue de Cortenbergh 100, 1000 Brussels, Belgium, Oct. 2019. [Online]. Available: `https://tyndp.entsoe.eu/Documents/TYNDP%20documents/TYNDP2018/consultation/Main%20Report/TYNDP2018_Executive%20Report.pdf`.

[45] Bundesnetzagentur für Elektrizität, Gas, Telekommunikation, Post und Eisenbahnen, *Quartalsbericht zu Netz- und SystemsicherheitsmaSSnahmen Gesamtjahr und Viertes Quartal 2017*. [Online]. Available: `https://www.bundesnetzagentur.de/DE/Sachgebiete/ElektrizitaetundGas/Unternehmen_Institutionen/Versorgungssicherheit/Netz_Systemsicherheit/Netz_Systemsicherheit.html` (visited on 03/20/2019).

[46] "PJM", PJM Interconnection. (), [Online]. Available: `https://www.pjm.com/`.

[47] "Midcontinent Independent System Operator", misoenergy. (), [Online]. Available: `https://www.misoenergy.org/`.

[48] T. Alvey, D. Goodwin, Xingwang Ma, D. Streiffert, and D. Sun, "A security-constrained bid-clearing system for the New Zealand wholesale electricity market", *IEEE Transactions on Power Systems*, vol. 13, no. 2, pp. 340–346, May 1998, ISSN: 08858950. DOI: `10/b6rqck`. [Online]. Available: `http://ieeexplore.ieee.org/document/667349/` (visited on 11/18/2021).

[49] M. Ambrosius, V. Grimm, T. Kleinert, F. Liers, M. Schmidt, and G. Zöttl, "Endogenous Price Zones and Investment Incentives in Electricity Markets: An Application of Multilevel Optimization With Graph Partitioning", *SSRN Electronic Journal*, 2018, ISSN: 1556-5068. DOI: `10/gm4gn9`. [Online]. Available: `https://www.ssrn.com/abstract=3271827` (visited on 09/09/2021).

[50] Bundesministerium der Justiz und Verbraucherschutz, *Verordnung über den Zugang zu Elektrizitätsversorgungsnetzen*. [Online]. Available: `https://www.gesetze-im-internet.de/stromnzv/BJNR224300005.html`.

[51] Markus Kahles, "Überprüfung der einheitlichen deutschen Stromgebotszone nach der Elektrizitätsbinnenmarkt-Verordnung", Stiftung Umweltenergierecht, Würzburg, 44, Jul. 17, 2019. [Online]. Available: `https://stiftung-umweltenergierecht.de/wp-content/uploads/2019/07/Stiftung_Umweltenergierecht_WueBerichte_44_Gebotszonenkonfiguration.pdf`.

[52] TenneT TSO GmbH. "InnoSys2030", Innovationen in der Systemführung bis 2030. (Oct. 1, 2021), [Online]. Available: `www.innosys2030.de` (visited on 10/01/2021).

[53] T. van Leeuwen, A.-K. Meinerzhagen, A. Roehder, and S. Raths, "Integration kurativer MaSSnahmen in das Engpassmanagement im deutschen Übertragungsnetz", in *16. Symposium Energieinnovation*, Graz, 2020.

[54] "Stresstest für die Netzausbauplanung, Studie im Auftrag der TenneT TSO GmbH", Consentec GmbH, Nov. 25, 2016. [Online]. Available: `https://www.tennet.eu/de/unser-netz/rund-um-den-netzausbau/netzstresstest/` (visited on 09/07/2021).

[55] K. Kollenda, A. Hoffrichter, Maximilian Schneider, Alexander Schrief, and Albert Moser, "Planungsorientierte Simulation kurativer MaSSnahmen im Deutschen Übertragungsnetz", in *16. Symposium Energieinnovation*, Graz, 2020.

[56] Dimitri Pescia, *Flexibility in thermal power plants With a focus on existing coal-fired power plants*, 2017. [Online]. Available: `www.agora-energiewende.de`.

[57] *Directive (EU) 2009/72/EC of the European Parliament and of the Council of 13 July 2009 concerning common rules for the internal market in electricity and repealing Directive 2003/54/EC*. [Online]. Available: `https://eur-lex.europa.eu/legal-content/EN/ALL/?uri=celex%3A32009L0072`.

[58] *Directive (EU) 2019/944 of the European Parliament and of the Council of 5 June 2019 on common rules for the internal market for electricity and amending Directive 2012/27/EU*. [Online]. Available: `https://eur-lex.europa.eu/legal-content/EN/TXT/?uri=CELEX%3A32019L0944`.

[59] ENTSO-E, CEDEC, GEODE, Eurelectric, and E.DSO, "Data Management Report", Jun. 10, 2018, p. 72. [Online]. Available: `https://docs.entsoe.eu/dataset/tso-dso-data-management-report` (visited on 06/09/2021).

[60] ENTSO-E, E.DSO, CEDEC, Eurelectric, and GEODE, "An Integrated Approach to Active System Management", TSO-DSO Report, Apr. 2019, p. 48. [Online]. Available: `https://www.edsoforsmartgrids.eu/a-toolbox-for-tsos-and-dsos-to-make-use-of-new-system-and-grid-services-2/`.

[61] F. Bouffard and M. Ortega-Vazquez, "The value of operational flexibility in power systems with significant wind power generation", in *2011 IEEE Power and Energy Society General Meeting*, San Diego, CA: IEEE, Jul. 2011, pp. 1–5, ISBN: 978-1-4577-1000-1. DOI: `10/bdt42v`. [Online]. Available: `https://ieeexplore.ieee.org/document/6039031/` (visited on 06/08/2021).

[62] E. Lannoye, D. Flynn, and M. O'Malley, "Evaluation of Power System Flexibility", *IEEE Transactions on Power Systems*, vol. 27, no. 2, pp. 922–931, May 2012, ISSN: 0885-8950, 1558-0679. DOI: `10/fzcjvk`. [Online]. Available: `http://ieeexplore.ieee.org/document/6125228/` (visited on 06/08/2021).

[63] J. Ma, V. Silva, R. Belhomme, D. S. Kirschen, and L. F. Ochoa, "Evaluating and Planning Flexibility in Sustainable Power Systems", *IEEE Transactions on Sustainable Energy*, vol. 4, no. 1, pp. 200–209, Jan. 2013, ISSN: 1949-3029, 1949-3037. DOI: `10/gkzmmw`. [Online]. Available: `http://ieeexplore.ieee.org/document/6313967/` (visited on 06/08/2021).

[64] T. Kolster, R. Krebs, S. Niessen, and M. Duckheim, "The contribution of distributed flexibility potentials to corrective transmission system operation for strongly renewable energy systems", *Applied Energy*, vol. 279, p. 115 870, Dec. 2020, ISSN: 03062619. DOI: `10/ghk65g`. [Online]. Available: `https://linkinghub.elsevier.com/retrieve/pii/S0306261920313428` (visited on 10/23/2020).

[65] *Technical Connection Rules for High-Voltage (VDE-AR-N 4120)*, Oct. 19, 2018. [Online]. Available: `https://www.vde.com/en/fnn/topics/technical-connection-rules/tar-for-high-voltage`.

[66] *Cascading of measures for the system security of electrical energy supply networks (VDE-AR-N 4140)*, Feb. 1, 2017. [Online]. Available: `https://www.vde-verlag.de/standards/0100363/vde-ar-n-4140-anwendungsregel-2017-02.html`.

[67] Bundesministerium der Justiz und Verbraucherschutz, *Gesetz zum Schutz vor schädlichen Umwelteinwirkungen durch Luftverunreinigungen, Geräusche, Erschütterungen und ähnliche Vorgänge*, Aug. 31, 2021. [Online]. Available: `https://www.gesetze-im-internet.de/bimschg/`.

[68] Dan van Holst Pellekaan. "South Australia helps keep the lights on in Queensland". (Nov. 15, 2019), [Online]. Available: `https://web.archive.org/web/20191214223336/https://premier.sa.gov.au/news/south-australia-helps-keep-the-lights-on-in-queensland`.

[69] Government of South Australia. "South Australia's Virtual Power Plant: VIRTUAL POWER PLANT REACHES 1,100 HOMES". (), [Online]. Available: `https://virtualpowerplant.sa.gov.au/`.

[70] Lichtblick. "Lichtblick Schwarmenergie", Bringt euch ins Schwärmen: die Schwarm-Batterie. (Oct. 1, 2021), [Online]. Available: `https://www.lichtblick.de/schwarmenergie/schwarmbatterie/`.

[71] Christoph Kost, Shivenes Shammugam, Verena Jülch, Huyen-Tran Nguyen, and Thomas Schlegl, *Stromgestehungskosten erneuerbare Energien März 2018*, Mar. 2018.

[72] "Dena Netzstudie II: Integration of Renewable Energy Sources in the German Power Supply System from 2015 2020 with an Outlook to 2025", Deutsche Energie-Agentur GmbH (dena), 2012. [Online]. Available: `https://www.dena.de/themen-projekte/projekte/energiesysteme/netzstudie-i-und-ii/`.

[73] N. Hartmann, J. Thomsen, and N. Wanapinit, "Using demand side management and CHP in renewable dominated decentral energy systems: A case study", *Computer Science - Research and Development*, vol. 33, no. 1-2, pp. 193–198, Feb. 2018, ISSN: 1865-2034, 1865-2042. DOI: `10.1007/s00450-017-0358-3`. [Online]. Available: `http://link.springer.com/10.1007/s00450-017-0358-3` (visited on 05/06/2021).

[74] T. Müller and D. Möst, "Demand Response Potential: Available when Needed?", *Energy Policy*, vol. 115, pp. 181–198, Apr. 2018, ISSN: 03014215. DOI: `10/gdb39d`. [Online]. Available: `https://linkinghub.elsevier.com/retrieve/pii/S0301421517308509` (visited on 05/06/2021).

[75] C. Zöphel, S. Schreiber, T. Müller, and D. Möst, "Which Flexibility Options Facilitate the Integration of Intermittent Renewable Energy Sources in Electricity Systems?", *Current Sustainable/Renewable Energy Reports*, vol. 5, no. 1, pp. 37–44, Mar. 2018, ISSN: 2196-3010. DOI: `10/gj8ktq`. [Online]. Available: `http://link.springer.com/10.1007/s40518-018-0092-x` (visited on 05/06/2021).

[76] D. Koraki and K. Strunz, "Wind and Solar Power Integration in Electricity Markets and Distribution Networks Through Service-Centric Virtual Power Plants", *IEEE Transactions on Power Systems*, vol. 33, no. 1, pp. 473–485, Jan. 2018, ISSN: 0885-8950,

1558-0679. DOI: `10/gctgz6`. [Online]. Available: `http://ieeexplore.ieee.org/document/7937825/` (visited on 05/06/2021).

[77]   M. Alizadeh, M. Parsa Moghaddam, N. Amjady, P. Siano, and M. Sheikh-El-Eslami, "Flexibility in future power systems with high renewable penetration: A review", *Renewable and Sustainable Energy Reviews*, vol. 57, pp. 1186–1193, May 2016, ISSN: 13640321. DOI: `10.1016/j.rser.2015.12.200`. [Online]. Available: `https://linkinghub.elsevier.com/retrieve/pii/S136403211501583X` (visited on 02/19/2020).

[78]   A. Jakhar, "A comprehensive review of power system flexibility", in *2017 IEEE International Conference on Power, Control, Signals and Instrumentation Engineering (ICPCSI)*, Chennai: IEEE, Sep. 2017, pp. 1747–1752, ISBN: 978-1-5386-0814-2. DOI: `10.1109/ICPCSI.2017.8392013`. [Online]. Available: `https://ieeexplore.ieee.org/document/8392013/` (visited on 02/19/2020).

[79]   Joachim Gruber, Richard Tretter, and Matthias Wesseis, "Anreizmechanismen für die Bereitstellung von Flexibilität", *ew-magazin*, Jul. 31, 2018. [Online]. Available: `https://www.ew-magazin.de/anreizmechanismen-fuer-bereitstellung-von-flexibilitaet/`.

[80]   Julia Radecke, Joseph Hefele, and Lion Hirth, "Markets for Local Flexibility in Distribution Networks", *Preprint,* [Online]. Available: `https://www.econstor.eu/handle/10419/204559` (visited on 02/19/2020).

[81]   M. Vogel and D. Bauknecht, "Flexibilität für das Netz", 2020. [Online]. Available: `https://www.oeko.de/fileadmin/oekodoc/Flexibilitaet-fuer-das-Netz.pdf`.

[82]   M. Zipf and D. Most, "Cooperation of TSO and DSO to provide ancillary services", in *2016 13th International Conference on the European Energy Market (EEM)*, Porto, Portugal: IEEE, Jun. 2016, pp. 1–6, ISBN: 978-1-5090-1298-5. DOI: `10.1109/EEM.2016.7521273`. [Online]. Available: `http://ieeexplore.ieee.org/document/7521273/` (visited on 02/19/2020).

[83]   EU-SySFlex. "EU-SySFlex", Demonstrating innovative approaches to coordinate flexibilities. (Oct. 1, 2021), [Online]. Available: `https://eu-sysflex.com/`.

[84]   Jonas Buhr, Holger Hänchen, Anne-Katrin Marten, Jens Schwedler, Markus Kreutziger, Constantin Dierstein, Sebastian Wende v. Berg, Nils Bornhorst, Thomas Wagner, Uwe Schmidt, Jürgen Götz, and Andrei Szabo, "Projektabschlussbericht - Bundesforschungsprojekt SysDL 2.0", Nov. 9, 2018. [Online]. Available: `https://`

`www.sysdl20.de/ergebnisse/abschlu%C3%9Fbericht/` (visited on 04/27/2020).

[85] Imowen. "IMOWEN", IMOWEN. (Apr. 9, 2020), [Online]. Available: `http://forschung-stromnetze.info/projekte/windpark-cluster-sicher-ins-netz-integrieren/`.

[86] Interplan. "Interplan", Interplan. (Apr. 9, 2020), [Online]. Available: `https://interplan-project.eu/`.

[87] Netze BW and TransnetBW GmbH. "DA/RE". (Apr. 9, 2020), [Online]. Available: `https://www.dare-plattform.de/`.

[88] enera. "Enera", enera. (Apr. 9, 2020), [Online]. Available: `https://projekt-enera.de/`.

[89] S. Klaiber, S. Naumann, P. Bretschneider, B. Arendarski, P. Kormarnicki, A. Richter, M. Wolter, S. Schlegel, D. Westermann, M. Duckheim, and T. Donlagic, "Verbundprojekt "REGEES": Optimale Betriebs- und Regelungsstrategien für das zuverlässige elektrische Energieversorgungssystem Deutschlands bei vollständiger Integration der Einspeisung aus erneuerbaren Energien im Zeithorizont 2030 : Schlussbericht REGEES", Fraunhofer IOSB-AST, version 1.0, 2018, 1 Online–Ressource (159 Seiten, 10, 26 MB). DOI: `10.2314/KXP:1665338806`. [Online]. Available: `https://www.tib.eu/suchen/id/TIBKAT:1665338806/` (visited on 09/05/2021).

[90] R. Schwerdfeger, D. Westermann Univ.-Prof. Dr.-Ing., and F. Berger Univ.-Prof. Dr.-Ing., "Vertikaler Netzbetrieb: ein Ansatz zur Koordination von Netzbetriebsinstanzen verschiedener Netzebenen", Ph.D. dissertation, Universitätsverlag Ilmenau, Ilmenau, Dec. 2016. [Online]. Available: `http://uri.gbv.de/document/gvk:ppn:720080177`.

[91] M. Klobasa, G. Angerer, A. Lüllmann, J. Schleich, T. Buber, A. Gruber, M. Hünecke, and S. von Roon, "Lastmanagement als Beitrag zur Deckung des Spitzenlastbedarfs in Süddeutschland", *Endbericht einer Studie von Fraunhofer ISI und der Forschungsgesellschaft für Energiewirtschaft, erstellt im Auftrag von Agora Energiewende*, 2013.

[92] S. von Roon and T. Gobmaier, "Demand response in der industrie: Status und potenziale in deutschland", *München: Forschungsstelle für Energiewirtschaft eV (FfE)*, 2010.

[93] P. Elsner, B. Erlach, M. Fischedick, B. Lunz, and D. U. Sauer, *Flexibilitätskonzepte Für Die Stromversorgung 2050: Technologien-Szenarien-Systemzusammenhänge* (Energiesysteme Der Zukunft). acatech, 2015.

[94] F. Adamek, T. Aundrup, W. Glaunsinger, M. Kleimaier, H. Landinger, M. Leuthold, B. Lunz, A. Moser, C. Pape, H. Pluntke, *et al.*, "Energiespeicher für die Energiewende: Speicherungsbedarf und Auswirkungen auf das Übertragungsnetz für Szenarien bis 2050", *VDE Verband der Elektrotechnik Elektronik Informationstechnik eV, Frankfurt am Main*, 2012.

[95] S. Auer, F. Steinke, W. Chunsen, A. Szabo, and R. Sollacher, "Can distribution grids significantly contribute to transmission grids' voltage management?", in *2016 IEEE PES Innovative Smart Grid Technologies Conference Europe (ISGT-Europe)*, Ljubljana, Slovenia: IEEE, Oct. 2016, pp. 1–6, ISBN: 978-1-5090-3358-4. DOI: `10/gj8ktp`. [Online]. Available: `http://ieeexplore.ieee.org/document/7856194/` (visited on 05/06/2021).

[96] Kaspar Knorr, Britta Zimmermann, Dirk Kirchner, Markus Speckmann, Spiecker-mann, Raphael, Martin Widdel, Manuela Wunderlich, Reinhard Mackensen, Kurt Rohrig, Florian Steinke, Philipp Wolfrum, Thomas Leveringhaus, Thomas Lager, Lutz Hofmann, Dirk Filzek, Tina Göbel, Bettina Kusserow, Lars Nicklaus, and Peter Ritter, "Abschlussbericht des Forschungsprojektes Kombikraftwerk 2", Abschlussbericht, 2014. [Online]. Available: `http://www.kombikraftwerk.de/mediathek/abschlussbericht.html`.

[97] Bundesnetzagentur für Elektrizität, Gas, Telekommunikation, Post und Eisenbahnen. "Marktstammdatenregister", Marktstammdatenregister. (Apr. 22, 2020), [Online]. Available: `https://www.marktstammdatenregister.de/MaStR/` (visited on 04/22/2020).

[98] 50Hertz Transmission GmbH, Amprion GmbH, TenneT TSO GmbH, and TransnetBW GmbH, *Szenariorahmen für die Netzentwicklungspläne Strom 2030 - Entwurf der Über-tragungsnetzbetreiber*, 2019. [Online]. Available: `www.netzentwicklungsplan.de`.

[99] A. Silva, J. Sumaili, J. Silva, L. Carvalho, L. Seca, M. Matos, R. Bessa, G. Schaarschmidt, and R. Hermes, "Assessing Der Flexibility In A German Distribution Network For Different Scenarios And Degrees Of Controllability", Jun. 14, 2016. DOI: `10/gkzmmv`. [Online]. Available: `https://zenodo.org/record/57663` (visited on 06/07/2021).

[100] V. d. E. E. Informationstechnik eV, *Demand Side Integration-Lastverschiebungspotenziale in Deutschland*. VDE, Frankfurt am Main, Germany, 2012.

[101] N. Krzikalla, S. Achner, and S. Brühl, *Möglichkeiten Zum Ausgleich Fluktuierender Einspeisungen Aus Erneuerbaren Energien: Studie Im Auftrag Des Bundesverbandes Erneuerbare Energie*. Ponte Press, 2013. [Online]. Available: `https://www.bee-ev.de/fileadmin/Publikationen/Studien/Plattform/BEE-Plattform-Systemtransformation_Ausgleichsmoeglichkeiten.pdf`.

[102] Gasunie Deutschland and TenneT TSO GmbH, *Phase 2 - Pathways to 2050*. [Online]. Available: `https://www.tennet.eu/de/news/news/gasunie-und-tennet-klimapolitische-ziele-lassen-sich-nur-mit-einem-integrierten-europaeischen-energi/` (visited on 02/19/2020).

[103] S. Raths, S. Koopmann, C. Mueller, A. Meinerzhagen, T. Falke, M. Cramer, T. Kulms, D. Beulertz, H. Barrios, A. Schnettler, M. Tackenberg, F. Steinke, P. Wolfrum, M. Metzger, B. Schlageter, W. Kusian, and A. Schmidt, "The Energy System Development Plan (ESDP)", in *Die Energiewende - Blueprints for the New Energy Age*, 2015, ISBN: 978-3-8007-4121-2.

[104] P. Gerbert, P. Herhold, J. Burchardt, S. Schönberger, F. Rechenmacher, A. Kirchner, A. Kemmler, and M. Wünsch, *Klimapfade Für Deutschland*. BCG, The Boston Consulting Group, 2018.

[105] Philip Sterchele, Julian Brandes, Judith Heilig, Daniel Wrede, Christoph Kost, Thomas Schlegl, Andreas Bett, and Hans-Martin Henning, "Wege zu einem klimaneutralen Energiesystem: Die deutsche Energiewende im Kontext gesellschaftlicher Verhaltensweisen", Fraunhofer-Institut für Solare Energiesysteme ISE, Freiburg, Feb. 2020. [Online]. Available: `https://www.ise.fraunhofer.de/de/veroeffentlichungen/studien/wege-zu-einem-klimaneutralen-energiesystem.html` (visited on 02/27/2020).

[106] Martin Robinius, Peter Markewitz, Peter Lopion, Felix Kullmann, Philipp-Matthias Heuser, Konstantinos Syranidis, Simonas Cerniauskas, Markus Reuss, Severin Ryberg, Leander Kotzur, Dilara Caglayan, Lara Welder, Jochen Linssen, Thomas Grube, Heidi Heinrichs, Peter Stenzel, and Detlef Stolten, "Kosteneffiziente und klimagerechte Transformationsstrategien für das deutsche Energiesystem bis zum Jahr 2050. (Kurzfassung)", Institut für Techno-Ökonomische Systemanalyse (IEK3), Forschungszentrum Jülich.

[107] C. Müller, A. Hoffrichter, L. Wyrwoll, C. Schmitt, M. Trageser, T. Kulms, D. Beulertz, M. Metzger, M. Duckheim, M. Huber, M. Küppers, D. Most, S. Paulus, H. Heger, and A. Schnettler, "Modeling framework for planning and operation of multi-modal energy systems in the case of Germany", *Applied Energy*, vol. 250, pp. 1132–1146, Sep. 2019, ISSN: 03062619. DOI: `10/gf5p76`. [Online]. Available: `https://`

linkinghub.elsevier.com/retrieve/pii/S0306261919309559 (visited on 04/17/2020).

[108] V. Krishnan, J. Ho, B. F. Hobbs, A. L. Liu, J. D. McCalley, M. Shahidehpour, and Q. P. Zheng, "Co-optimization of electricity transmission and generation resources for planning and policy analysis: Review of concepts and modeling approaches", *Energy Systems*, vol. 7, no. 2, pp. 297–332, May 2016, ISSN: 1868-3967, 1868-3975. DOI: 10.1007/s12667-015-0158-4. [Online]. Available: http://link.springer.com/10.1007/s12667-015-0158-4 (visited on 01/29/2020).

[109] B. Müller, F. Gardumi, and L. Hülk, "Comprehensive representation of models for energy system analyses: Insights from the Energy Modelling Platform for Europe (EMP-E) 2017", *Energy Strategy Reviews*, vol. 21, pp. 82–87, Aug. 2018, ISSN: 2211467X. DOI: 10/gd8vdf. [Online]. Available: https://linkinghub.elsevier.com/retrieve/pii/S2211467X18300154 (visited on 05/14/2021).

[110] Sebastian Miehling, Benedikt Schweiger, Wolf Wedel, Andreas Hanel, Jakob Schweiger, René Schwermer, Maximilian Blume, and Hartmut Spliethoff, "100 % erneuerbare Energien für Bayern. Potenziale und Strukturen einer Vollversorgung in den Sektoren Strom, Wärme und Mobilität", Lehrstuhl für Energiesysteme der Technischen Universität München, Bayerische Zentrum für Angewandte Energieforschung, May 11, 2021. [Online]. Available: https://www.mw.tum.de/es/publikationen/bayernstudie/.

[111] H. Lund and B. Mathiesen, "Energy system analysis of 100% renewable energy systemsThe case of Denmark in years 2030 and 2050", *Energy*, vol. 34, no. 5, pp. 524–531, May 2009, ISSN: 03605442. DOI: 10/cf6qxs. [Online]. Available: https://linkinghub.elsevier.com/retrieve/pii/S0360544208000959 (visited on 05/17/2021).

[112] W. Zappa, M. Junginger, and M. van den Broek, "Is a 100% renewable European power system feasible by 2050?", *Applied Energy*, vol. 233–234, pp. 1027–1050, Jan. 2019, ISSN: 03062619. DOI: 10/gf8fz5. [Online]. Available: https://linkinghub.elsevier.com/retrieve/pii/S0306261918312790 (visited on 04/17/2020).

[113] M. Child, C. Kemfert, D. Bogdanov, and C. Breyer, "Flexible electricity generation, grid exchange and storage for the transition to a 100% renewable energy system in Europe", *Renewable Energy*, vol. 139, pp. 80–101, Aug. 2019, ISSN: 09601481. DOI: 10/gf8fz3. [Online]. Available: https://linkinghub.elsevier.com/retrieve/pii/S0960148119302319 (visited on 05/17/2021).

[114] C. Ripp and F. Steinke. "Modeling Time-dependent CO2 Intensities in Multi-modal Energy Systems with Storage". arXiv: `1806.04003 [eess]`. (Feb. 19, 2019), [Online]. Available: `http://arxiv.org/abs/1806.04003` (visited on 03/31/2021).

[115] C. Ripp and F. Steinke, "A First Shot at Time-Dependent CO2 Intensities in Multi-Modal Energy Systems", in *2018 15th International Conference on the European Energy Market (EEM)*, Lodz: IEEE, Jun. 2018, pp. 1–5, ISBN: 978-1-5386-1488-4. DOI: `10/gj8ktm`. [Online]. Available: `https://ieeexplore.ieee.org/document/8469841/` (visited on 09/09/2021).

[116] A. García-Olivares, J. Solé, and O. Osychenko, "Transportation in a 100% renewable energy system", *Energy Conversion and Management*, vol. 158, pp. 266–285, Feb. 2018, ISSN: 01968904. DOI: `10/gf3js3`. [Online]. Available: `https://linkinghub.elsevier.com/retrieve/pii/S0196890417312050` (visited on 05/17/2021).

[117] D. G. Caglayan, N. Weber, H. U. Heinrichs, J. LinSSen, M. Robinius, P. A. Kukla, and D. Stolten, "Technical potential of salt caverns for hydrogen storage in Europe", *International Journal of Hydrogen Energy*, vol. 45, no. 11, pp. 6793–6805, Feb. 2020, ISSN: 03603199. DOI: `10/gh6j9c`. [Online]. Available: `https://linkinghub.elsevier.com/retrieve/pii/S0360319919347299` (visited on 05/17/2021).

[118] R. Ortiz-Imedio, D. G. Caglayan, A. Ortiz, H. Heinrichs, M. Robinius, D. Stolten, and I. Ortiz, "Power-to-Ships: Future electricity and hydrogen demands for shipping on the Atlantic coast of Europe in 2050", *Energy*, vol. 228, p. 120 660, Aug. 2021, ISSN: 03605442. DOI: `10/gj8ktg`. [Online]. Available: `https://linkinghub.elsevier.com/retrieve/pii/S0360544221009099` (visited on 05/17/2021).

[119] C. Syranidou, J. Linssen, D. Stolten, and M. Robinius, "On the Curtailments of Variable Renewable Energy Sources in Europe and the Role of Load Shifting", in *2020 55th International Universities Power Engineering Conference (UPEC)*, Torino, Italy: IEEE, Sep. 2020, pp. 1–6, ISBN: 978-1-72811-078-3. DOI: `10/ghdwjr`. [Online]. Available: `https://ieeexplore.ieee.org/document/9209846/` (visited on 05/17/2021).

[120] J. Horsch and T. Brown, "The role of spatial scale in joint optimisations of generation and transmission for European highly renewable scenarios", in *2017 14th International Conference on the European Energy Market (EEM)*, Dresden, Germany: IEEE, Jun. 2017, pp. 1–7, ISBN: 978-1-5090-5499-2. DOI: `10.1109/EEM.2017.7982024`.

[Online]. Available: http://ieeexplore.ieee.org/document/7982024/ (visited on 01/29/2020).

[121] F. Steinke, P. Wolfrum, and C. Hoffmann, "Grid vs. storage in a 100% renewable Europe", *Renewable Energy*, vol. 50, pp. 826–832, Feb. 2013, ISSN: 09601481. DOI: 10/f4jmr5. [Online]. Available: https://linkinghub.elsevier.com/retrieve/pii/S0960148112004818 (visited on 05/14/2021).

[122] L. Kotzur, P. Markewitz, M. Robinius, and D. Stolten, "Time series aggregation for energy system design: Modeling seasonal storage", *Applied Energy*, vol. 213, pp. 123–135, Mar. 2018, ISSN: 03062619. DOI: 10.1016/j.apenergy.2018.01.023. [Online]. Available: https://linkinghub.elsevier.com/retrieve/pii/S0306261918300242 (visited on 01/29/2020).

[123] B. Bahl, A. Kümpel, H. Seele, M. Lampe, and A. Bardow, "Time-series aggregation for synthesis problems by bounding error in the objective function", *Energy*, vol. 135, pp. 900–912, Sep. 2017, ISSN: 03605442. DOI: 10.1016/j.energy.2017.06.082. [Online]. Available: https://linkinghub.elsevier.com/retrieve/pii/S0360544217310769 (visited on 01/29/2020).

[124] H.-K. Ringkjøb, P. M. Haugan, and I. M. Solbrekke, "A review of modelling tools for energy and electricity systems with large shares of variable renewables", *Renewable and Sustainable Energy Reviews*, vol. 96, pp. 440–459, Nov. 2018, ISSN: 13640321. DOI: 10.1016/j.rser.2018.08.002. [Online]. Available: https://linkinghub.elsevier.com/retrieve/pii/S1364032118305690 (visited on 05/14/2021).

[125] A. Fattahi, J. Sijm, and A. Faaij, "A systemic approach to analyze integrated energy system modeling tools: A review of national models", *Renewable and Sustainable Energy Reviews*, vol. 133, p. 110 195, Nov. 2020, ISSN: 13640321. DOI: 10/gj8ktn. [Online]. Available: https://linkinghub.elsevier.com/retrieve/pii/S1364032120304858 (visited on 05/14/2021).

[126] S. Dierkes, Laura Emmermacher, Andreas Ernst, Kevin Goldermann, J. Gruber, Sandra Maeding, Marcus Merkel, Stefan Nykamp, Nikolaus Pleister, Henning Schuster, Richard Tretter, and Matthias Wessels, "Flex-Router-Konzept", Diskussionspapier, p. 7. [Online]. Available: https://www.bdew.de/service/stellungnahmen/diskussionspapier-flex-router-konzept/.

[127] Stephan Börries, Andre Herrmann, Ralf Ott, Benjamin Petters, and Jonas Höckner, "Netzbetreiberkoordination im Kontext eines Flexibilitätsmarkts und der "gelben Ampelphase"", *e|m|w*, Energie. Markt. Wettbewerb, vol. Special Smart Grids, no. 6.2018, Jun. 2018. [Online]. Available: https://www.emw-online.com/

artikel/187968/netzbetreiberkoordination-im-kontext-eines-flexibilit-tsmarkts-und-der-gelben-ampelphase`.

[128] Martin Braun, Lutz Hofmann, Axel Braun, Jan Dobschinski, Rafael Fritz, Reinhard Mackensen, Christoph Scholz, Sebastian Wende - von Berg, André Baier, Holger Becker, Juliane Liebelt, Denis Mende, and David Sebastian Stock, "Generation and Laod Data Provision Methodology (GLDPM)", Fraunhofer IEE, Kassel, Whitepaper, 2018. [Online]. Available: `https : / / www . iee . fraunhofer . de / de / geschaeftsbereiche / energiewirtschaft / energiemeteorologische - informationssysteme / white - paper - gldpm.html`.

[129] D. Stock, F. Sala, A. Berizzi, and L. Hofmann, "Optimal Control of Wind Farms for Coordinated TSO-DSO Reactive Power Management", *Energies*, vol. 11, no. 1, p. 173, Jan. 11, 2018, ISSN: 1996-1073. DOI: `10 / gc6pgz`. [Online]. Available: `http://www.mdpi.com/1996-1073/11/1/173` (visited on 04/21/2020).

[130] Philipp Goergens, Fabian Potratz, Markus Gödde, and Armin Schnettler, "Determination of the potential to provide reactive power from distribution grids to the transmission grid using optimal power flow", in *Proceedings of the 2015 50th International Universities Power Engineering Conference (UPEC)*, Piscataway, NJ: IEEE, 2015, p. 6, ISBN: 978-1-4673-9682-0.

[131] P. Aristidou, G. Valverde, and T. Van Cutsem, "Contribution of Distribution Network Control to Voltage Stability: A Case Study", *IEEE Transactions on Smart Grid*, vol. 8, no. 1, pp. 106–116, Jan. 2017, ISSN: 1949-3053, 1949-3061. DOI: `10 / f9mfzp`. [Online]. Available: `http://ieeexplore.ieee.org/document/7271075/` (visited on 06/10/2021).

[132] P. Cuffe and A. Keane, "Voltage Responsive Distribution Networks: Comparing Autonomous and Centralized Solutions", *IEEE Transactions on Power Systems*, vol. 30, no. 5, pp. 2234–2242, Sep. 2015, ISSN: 0885-8950, 1558-0679. DOI: `10 / gkzmmt`. [Online]. Available: `http://ieeexplore.ieee.org/document/6926878/` (visited on 06/10/2021).

[133] G. Valverde and T. Van Cutsem, "Model Predictive Control of Voltages in Active Distribution Networks", *IEEE Transactions on Smart Grid*, vol. 4, no. 4, pp. 2152–2161, Dec. 2013, ISSN: 1949-3053, 1949-3061. DOI: `10/gkzmms`. [Online]. Available: `http://ieeexplore.ieee.org/document/6464620/` (visited on 06/10/2021).

[134]   J. Silva, J. Sumaili, R. J. Bessa, L. Seca, M. A. Matos, V. Miranda, M. Caujolle, B. Goncer, and M. Sebastian-Viana, "Estimating the Active and Reactive Power Flexibility Area at the TSO-DSO Interface", *IEEE Transactions on Power Systems*, vol. 33, no. 5, pp. 4741–4750, Sep. 2018, ISSN: 0885-8950, 1558-0679. DOI: `10.1109/TPWRS.2018.2805765`. [Online]. Available: `https://ieeexplore.ieee.org/document/8291006/` (visited on 05/06/2021).

[135]   D. A. Contreras and K. Rudion, "Improved Assessment of the Flexibility Range of Distribution Grids Using Linear Optimization", in *2018 Power Systems Computation Conference (PSCC)*, Dublin, Ireland: IEEE, Jun. 2018, pp. 1–7, ISBN: 978-1-910963-10-4. DOI: `10/gftskc`. [Online]. Available: `https://ieeexplore.ieee.org/document/8442858/` (visited on 04/14/2020).

[136]   F. Capitanescu, "TSODSO interaction: Active distribution network power chart for TSO ancillary services provision", *Electric Power Systems Research*, vol. 163, pp. 226–230, Oct. 2018, ISSN: 03787796. DOI: `10/ggsr5p`. [Online]. Available: `https://linkinghub.elsevier.com/retrieve/pii/S0378779618301822` (visited on 04/21/2020).

[137]   D. A. Contreras and K. Rudion, "Computing the feasible operating region of active distribution networks: Comparison and validation of random sampling and optimal power flow based methods", *IET Generation, Transmission & Distribution*, vol. 15, no. 10, pp. 1600–1612, May 2021, ISSN: 1751-8687, 1751-8695. DOI: `10/gkzmm3`. [Online]. Available: `https://onlinelibrary.wiley.com/doi/10.1049/gtd2.12120` (visited on 06/07/2021).

[138]   M. Heleno, R. Soares, J. Sumaili, R. Bessa, L. Seca, and M. A. Matos, "Estimation of the flexibility range in the transmission-distribution boundary", in *2015 IEEE Eindhoven PowerTech*, Eindhoven, Netherlands: IEEE, Jun. 2015, pp. 1–6, ISBN: 978-1-4799-7693-5. DOI: `10.1109/PTC.2015.7232524`. [Online]. Available: `http://ieeexplore.ieee.org/document/7232524/` (visited on 06/07/2021).

[139]   D. Mayorga Gonzalez, J. Hachenberger, J. Hinker, F. Rewald, U. Hager, C. Rehtanz, and J. Myrzik, "Determination of the Time-Dependent Flexibility of Active Distribution Networks to Control Their TSO-DSO Interconnection Power Flow", in *2018 Power Systems Computation Conference (PSCC)*, Dublin, Ireland: IEEE, Jun. 2018, pp. 1–8, ISBN: 978-1-910963-10-4. DOI: `10.23919/PSCC.2018.8442865`. [Online]. Available: `https://ieeexplore.ieee.org/document/8442865/` (visited on 02/19/2020).

[140] N. Savvopoulos and N. Hatziargyriou, "Estimating Operational Flexibility from Active Distribution Grids", in *2020 17th International Conference on the European Energy Market (EEM)*, Stockholm, Sweden: IEEE, Sep. 2020, pp. 1–6, ISBN: 978-1-72816-919-4. DOI: 10/gkzmmx. [Online]. Available: `https://ieeexplore.ieee.org/document/9221991/` (visited on 06/07/2021).

[141] Y. Song, M. Wang, and M. Wang, "Aggregated Power Flexibility of Active Distribution Network Considering Reliability and Uncertainty", in *2020 IEEE/IAS Industrial and Commercial Power System Asia (I&CPS Asia)*, Weihai, China: IEEE, Jul. 2020, pp. 701–707, ISBN: 978-1-72814-303-3. DOI: 10/gkzmmz. [Online]. Available: `https://ieeexplore.ieee.org/document/9208425/` (visited on 06/07/2021).

[142] M. Kalantar-Neyestanaki, F. Sossan, M. Bozorg, and R. Cherkaoui, "Characterizing the Reserve Provision Capability Area of Active Distribution Networks: A Linear Robust Optimization Method", *IEEE Transactions on Smart Grid*, vol. 11, no. 3, pp. 2464–2475, May 2020, ISSN: 1949-3053, 1949-3061. DOI: 10/gkzmm2. [Online]. Available: `https://ieeexplore.ieee.org/document/8917723/` (visited on 06/07/2021).

[143] A. Ben-Tal, L. El Ghaoui, and A. S. Nemirovski, *Robust Optimization* (Princeton Series in Applied Mathematics). Princeton: Princeton University Press, 2009, 542 pp., ISBN: 978-0-691-14368-2.

[144] U. Munz, A. Mesanovic, M. Metzger, and P. Wolfrum, "Robust Optimal Dispatch, Secondary, and Primary Reserve Allocation for Power Systems With Uncertain Load and Generation", *IEEE Transactions on Control Systems Technology*, vol. 26, no. 2, pp. 475–485, Mar. 2018, ISSN: 1063-6536, 1558-0865. DOI: 10.1109/TCST.2017.2670535. [Online]. Available: `http://ieeexplore.ieee.org/document/7866878/` (visited on 05/06/2021).

[145] A. Mesanovic, U. Munz, and C. Ebenbauer, "Robust Optimal Power Flow for Mixed AC/DC Transmission Systems With Volatile Renewables", *IEEE Transactions on Power Systems*, vol. 33, no. 5, pp. 5171–5182, Sep. 2018, ISSN: 0885-8950, 1558-0679. DOI: 10.1109/TPWRS.2018.2804358. [Online]. Available: `https://ieeexplore.ieee.org/document/8288668/` (visited on 05/06/2021).

[146] Thomas Estermann, Simon Pichlmaier, Andrej Guminski, and Christoph Pellinger, *Kurzstudie Power-to-X Ermittlung des Potenzials von PtX-Anwendungen für die Netzplanung der deutschen ÜNB*, Nov. 2017. [Online]. Available: `www.ffe.de`.

[147] *Power-to-Heat zur Integration von ansonsten abgeregeltem Strom aus Erneuerbaren Energien - Handlungsvorschläge basierend auf einer Analyse von Potenzialen und energiewirtschaftlichen Effekten*, Jun. 2014. [Online]. Available: `www.agora-energiewende.de`.

[148] *Glood: Power to Heat Überschussstrom sinnvoll speichern*. [Online]. Available: `https://glood.de/wp-content/uploads/2017/05/Produkte.pdf`.

[149] 50hertz. "'Exploiting instead of curtailing': First power-to-heat units now operational in northern Germany", www.50hertz.com. (Nov. 29, 2021), [Online]. Available: `https://www.50hertz.com/en/News/Details/11600/exploiting-instead-of-curtailing-first-power-to-heat-units-now-operational-in-northern-germany` (visited on 12/21/2021).

[150] sonnengroup. "sonnenCommunity". (Feb. 20, 2020), [Online]. Available: `https://sonnengroup.com/sonnencommunity/` (visited on 02/20/2020).

[151] "SA batteries paid to charge as solar sends electricity prices negative", pv magazine. (Dec. 6, 2021), [Online]. Available: `https://www.pv-magazine-australia.com/2021/12/06/sa-batteries-paid-to-charge-as-solar-sends-electricity-prices-negative/`.

[152] L. Day and I. McNeil, Eds., *Biographical Dictionary of the History of Technology* (Routledge Reference), 1. publ. in paperback. London: Routledge, 1998, 844 pp., ISBN: 978-0-415-19399-3.

[153] D. Bäzold, C. Tietze, and B. Rampp, *Elektrische Lokomotiven deutscher Eisenbahnen* (Eisenbahn-Fahrzeug-Archiv 4), 2., überarb. Aufl. Düsseldorf: Alba, 1993, 471 pp., ISBN: 978-3-87094-143-7.

[154] W. Fischer, Ed., *Die Geschichte Der Stromversorgung*, 1. Aufl. Frankfurt am Main: Verlags- und Wirtschaftsgesellschaft der Elektrizitätswerke, 1992, 267 pp., ISBN: 978-3-8022-0298-8.

[155] A. Hauer, Tosato, Giancarlo, and Gielen, Dolf, "Thermal Energy Storage", Energy Technology System Analysis Programme and International Renewable Energy Agency, Technology-Policy Brief E17 - January 2013, Jan. 2017. [Online]. Available: `https://iea-etsap.org/E-TechDS/PDF/E17IR%20ThEnergy%20Stor_AH_Jan2013_final_GSOK.pdf`.

[156] J. H. Merrick, "On representation of temporal variability in electricity capacity planning models", *Energy Economics*, vol. 59, pp. 261–274, Sep. 2016, ISSN: 01409883. DOI: `10.1016/j.eneco.2016.08.001`. [Online]. Available: `https://linkinghub.elsevier.com/retrieve/pii/S0140988316302018` (visited on 01/29/2020).

[157] J. N. Schupbach and J. Sprenger, "The Logic of Explanatory Power", *Philosophy of Science*, vol. 78, no. 1, pp. 105–127, Jan. 2011, ISSN: 0031-8248, 1539-767X. DOI: `10/b2b3zh`. [Online]. Available: `https://www.journals.uchicago.edu/doi/10.1086/658111` (visited on 11/22/2021).

[158] M. Metzger, M. Duckheim, M. Franken, H. J. Heger, M. Huber, M. Knittel, T. Kolster, M. Kueppers, C. Meier, D. Most, S. Paulus, L. Wyrwoll, A. Moser, and S. Niessen, "Pathways toward a decarbonized future - impact on security of supply and system stability in a sustainable german energy system", *Energies*, vol. 14, no. 3, p. 560, Jan. 22, 2021, ISSN: 1996-1073. DOI: `10.3390/en14030560`. [Online]. Available: `https://www.mdpi.com/1996-1073/14/3/560` (visited on 05/12/2021).

[159] ENTSO-E, "Ten Year Network Development Plan", 2018.

[160] ENTSO-E, "Midterm Adequacy Forecast", ENTSO-E, 2018. [Online]. Available: `https://www.entsoe.eu/Documents/SDC%20documents/MAF/MAF_2018_Executive_Report.pdf`.

[161] L. V. Kantorovich, "Mathematical methods of organizing and planning production", *Management science*, vol. 6, no. 4, pp. 366–422, 1960. DOI: `10/ff82t5`.

[162] T. Yang, X. Yi, J. Wu, Y. Yuan, D. Wu, Z. Meng, Y. Hong, H. Wang, Z. Lin, and K. H. Johansson, "A survey of distributed optimization", *Annual Reviews in Control*, vol. 47, pp. 278–305, 2019, ISSN: 13675788. DOI: `10/gg5vdj`. [Online]. Available: `https://linkinghub.elsevier.com/retrieve/pii/S1367578819300082` (visited on 09/11/2021).

[163] P. Olivella-Rosell, F. Rullan, P. Lloret-Gallego, E. Prieto-Araujo, R. Ferrer-San-Jose, S. Barja-Martinez, S. Bjarghov, V. Lakshmanan, A. Hentunen, J. Forsstrom, S. O. Ottesen, R. Villafafila-Robles, and A. Sumper, "Centralised and Distributed Optimization for Aggregated Flexibility Services Provision", *IEEE Transactions on Smart Grid*, vol. 11, no. 4, pp. 3257–3269, Jul. 2020, ISSN: 1949-3053, 1949-3061. DOI: `10/gm4gn8`. [Online]. Available: `https://ieeexplore.ieee.org/document/8978550/` (visited on 09/11/2021).

[164] *Planungsgrundsätze für 110-kV-Netze (VDE-AR-N 4121)*, Apr. 1, 2018. [Online]. Available: `https://www.vde.com/de/fnn/arbeitsgebiete/netzbetrieb-sicherheit/netzplanung/planungsgrundsaetze-hochspannung-vde-ar-n-4121`.

[165] D. Oeding and B. R. Oswald, *Elektrische Kraftwerke und Netze*. Berlin, Heidelberg: Springer Berlin Heidelberg, 2011, ISBN: 978-3-642-19245-6. DOI: `10.1007/978-3-642-19246-3`. [Online]. Available: `http://link.springer.com/10.1007/978-3-642-19246-3` (visited on 09/30/2021).

[166] T. Rogalla. "Vattenfall stellt Kraftwerk Klingenberg von Braunkohle auf Erdgas um", Berliner Zeitung. (May 24, 2017), [Online]. Available: `https://www.berliner-zeitung.de/mensch-metropole/vattenfall-stellt-kraftwerk-klingenberg-von-braunkohle-auf-erdgas-um-li.10519?pid=true` (visited on 09/17/2021).

[167] ENTSO-E. "Common Information Model", entso-e Common Information Model. (Sep. 21, 2021), [Online]. Available: `https://www.entsoe.eu/digital/common-information-model/` (visited on 09/21/2021).

[168] R. D. Zimmerman and C. E. Murillo-Sánchez, *MATPOWER*, version 7.0, Zenodo, Jun. 20, 2019. DOI: `10.5281/ZENODO.3251119`. [Online]. Available: `https://zenodo.org/record/3251119` (visited on 06/18/2021).

[169] GAMS. "GAMS", General Algebraic Modeling System. (Sep. 21, 2021), [Online]. Available: `https://www.gams.com/` (visited on 09/21/2021).

[170] I. I. Cplex, "V12. 1: Users manual for CPLEX", *International Business Machines Corporation*, vol. 46, no. 53, p. 157, 2009.

[171] Simone Besgen, "Ergebnisse messtechnischer Untersuchungen an landwirtschaftlichen Biogasanlagen im Rheinland", Rheinischen Friedrich-Wilhelm-Universität zu Bonn, 174 pp. [Online]. Available: `http://hss.ulb.uni-bonn.de/2006/0720/0720.pdf`.

[172] Manuela Bücken, Herbert Freischlad, Jochen Kalunka, Armin Kraft, Mario Leisten, Sabine Milatz, Oliver Weltz, Thomas Wolter, Tibor Güntzel, Jens Hache, and Ronald Halbauer, *Potenziale der Sektorkupplung und Nutzung von Strom aus Erneuerbaren Energien im Wärmebereich in Sachsen-Anhalt*, Nov. 2, 2017.

[173] Danish Energy Agency and Energinet, *Technology Data - Energy Plants for Electricity and District heating generation*, Aug. 2016. [Online]. Available: `http://www.ens.dk/teknologikatalog`.

[174] eia - U.S. Energy Inforamtion Administration, *Capital Cost Estimates for Utility Scale Electricity Generating Plants*, Nov. 2016. [Online]. Available: `www.eia.gov`.

[175] Mario Bachhiesl, Oliver Then, Sven Göhring, Thomas Linnemann, Ludger Mohrbach, Stefan Prost, and Christopher WeSSelmann, *Stromerzeugung 2018|2019 - Zahlen und Fakten*, Aug. 2018. [Online]. Available: `www.vgb.org`.

[176] V. PowerTech, *Levelised Cost of Electricity LCOE 2015*. VGB PowerTech Service GmbH Verlag technisch-wissenschaftlicher Schriften, ISBN: 978-3-86875-876-4.

[177] E. Vartiainen, G. Masson, C. Breyer, D. Moser, and E. Román Medina, "Impact of weighted average cost of capital, capital expenditure, and other parameters on future utilityscale PV levelised cost of electricity", *Progress in Photovoltaics: Research and Applications*, pip.3189, Aug. 29, 2019, ISSN: 1062-7995, 1099-159X. DOI: `10.1002/pip.3189`. [Online]. Available: `https://onlinelibrary.wiley.com/doi/abs/10.1002/pip.3189` (visited on 02/19/2020).

[178] Johannes Weniger, Selina Maier, Lena Kranz, Nico Orth, Nico Böhme, and Volker Quaschning, *Stromspeicher - Inspektion 2018*, Nov. 2018. [Online]. Available: `www.stromspeicher-inspektion.de`.

[179] Thomas Geissmann, "Computation of the Levelized Cost of Electricity under Uncertainty and Endogeneities in Inputs", *IAEE Energy Forum*, IAEE Energy Forum, no. 1/2017, pp. 15–18, 2017.

[180] Sabine Flamme, Jörg Hanewinkel, Peter Quicker, and Kathrin Weber, *Energieerzeugung aus Abfällen: Stand und Potenziale in Deutschland bis 2030*. [Online]. Available: `http://www.umweltbundesamt.de/publikationen`.

[181] RWE Power AG, *RWE Power die ganze Kraft Kraftwerk Huckingen*. [Online]. Available: `www.rwe.com`.

[182] H. R. Europe. "Profiles and Baselines for heating and cooling energy demands in 2015 for EU28 countries", Heat Roadmap Europe. (Sep. 21, 2021), [Online]. Available: `https://heatroadmap.eu/heating-and-cooling-energy-demand-profiles/`.

[183] M. Küppers, "Data-Driven Modeling of Decarbonization Pathways for Worldwide Energy Systems Based on Archetypes and Spatial Clustering Methods", Technische Universität Darmstadt, Darmstadt, 2021. [Online]. Available: `https://doi.org/10.26083/tuprints-00019824`.

[184] Eurostat. "European Statistical Recovery Dashboard", eurostat: Your key to European statistics. (Sep. 21, 2021), [Online]. Available: `https://ec.europa.eu/eurostat/web/main/data/database`.

[185] E. C. J. R. Centre., *EMHIRES Dataset.Part II, Solar Power Generation* . LU: Publications Office, 2017. [Online]. Available: `https://data.europa.eu/doi/10.2760/044693` (visited on 09/21/2021).

[186] E. C. J. R. Centre., *EMHIRES Dataset. Part I, Wind Power Generation.* LU: Publications Office, 2016. [Online]. Available: `https://data.europa.eu/doi/10.2790/831549` (visited on 09/21/2021).

[187] W. Biener and K. R. Garcia Rosas, "Grid reduction for energy system analysis", *Electric Power Systems Research*, vol. 185, p. 106 349, Aug. 2020, ISSN: 03787796. DOI: `10.1016/j.epsr.2020.106349`. [Online]. Available: `https://linkinghub.elsevier.com/retrieve/pii/S0378779620301553` (visited on 05/19/2020).

[188] 50hertz and PSE, *Meilenstein zur besseren Lastflusssteuerung zwischen deutschem und polnischem Strom-übertragungsnetz*, Apr. 13, 2016. [Online]. Available: `https://www.50hertz.com/Portals/1/Dokumente/Markt/Internationale%20Leitungen/20160413_Pressemitteilung_PSE_50Hertz.pdf?ver=2016-04-13-131031-033`.

[189] "ARGE FNB OST", ARGE FNB OST. (Sep. 23, 2021), [Online]. Available: `https://www.arge-fnb-ost.de/`.

[190] e.dis, Thüringer Energienetze, avacon, enso Netz, Mitnetz Strom, and WEMAG Netz GmbH, *Gemeinsamer Netzausbauplan der Arbeitsgemeinschaft der ostdeutschen 110-kV-Flächennetzbetreiber 2017*. [Online]. Available: `https://www.arge-fnb-ost.de/arbeitsfelder/netzausbauplan`.

[191] T. Kolster, S. Niessen, and M. Duckheim, "Providing Distributed Flexibility for Curative Transmission System Operation Using a Scalable Robust Optimization Approach", *Electric Power Systems Research*, vol. 211, Jul. 2022. DOI: `https://doi.org/10.1016/j.epsr.2022.108431`. [Online]. Available: `https://www.sciencedirect.com/science/article/abs/pii/S0378779622005764?via%3Dihub` (visited on 07/13/2022).

[192] R. D. Zimmerman, C. E. Murillo-Sanchez, and R. J. Thomas, "MATPOWER: Steady-State Operations, Planning, and Analysis Tools for Power Systems Research and Education", *IEEE Transactions on Power Systems*, vol. 26, no. 1, pp. 12–19, Feb. 2011, ISSN: 0885-8950, 1558-0679. DOI: `10/b94mfs`. [Online]. Available: `http://ieeexplore.ieee.org/document/5491276/` (visited on 06/18/2021).

[193]   G. Anderson, *Power System Analysis* (Lecture 227-0526-00, ITET ETH Zĺurich). Zürich: ETH Zürich, Sep. 2012, 185 pp. [Online]. Available: `https://web.archive.org/web/20170215042633/http://www.eeh.ee.ethz.ch/uploads/tx_ethstudies/modelling_hs08_script_02.pdf`.

[194]   L. Euler, "Solutio problematis ad geometriam situs pertinentis", *Commentarii academiae scientiarum Petropolitanae*, pp. 128–140, 1741.

[195]   M. Albadi, "Power Flow Analysis", in *Computational Models in Engineering*, K. Volkov, Ed., IntechOpen, Mar. 11, 2020, ISBN: 978-1-78923-869-3. DOI: `10.5772/intechopen.83374`. [Online]. Available: `https://www.intechopen.com/books/computational-models-in-engineering/power-flow-analysis` (visited on 01/07/2022).

[196]   H. Seifi and M. S. Sepasian, *Electric Power System Planning* (Power Systems). Berlin, Heidelberg: Springer Berlin Heidelberg, 2011, ISBN: 978-3-642-17988-4. DOI: `10.1007/978-3-642-17989-1`. [Online]. Available: `http://link.springer.com/10.1007/978-3-642-17989-1` (visited on 01/07/2022).

[197]   S. W. Blume, *Electric Power System Basics: For the Nonelectrical Professional*. 2017, ISBN: 978-1-119-18020-3. [Online]. Available: `http://site.ebrary.com/id/11300193` (visited on 11/22/2021).

[198]   K. Heuck, K.-D. Dettmann, and D. Schulz, *Elektrische Energieversorgung*. Wiesbaden: Springer Fachmedien Wiesbaden, 2013, ISBN: 978-3-8348-1699-3. DOI: `10.1007/978-3-8348-2174-4`. [Online]. Available: `http://link.springer.com/10.1007/978-3-8348-2174-4` (visited on 01/07/2022).

[199]   connect+. "Connect +Netzbetreiberkooperation", connect +Netzbetreiberkooperation. (Sep. 29, 2021), [Online]. Available: `https://netz-connectplus.de/` (visited on 09/29/2021).

[200]   R. Fourer, D. M. Gay, and B. W. Kernighan, *AMPL: A Modeling Language for Mathematical Programming*, 2nd ed. Pacific Grove, CA: Thomson/Brooks/Cole, 2003, 517 pp., ISBN: 978-0-534-38809-6.

[201]   G. Gamrath, D. Anderson, K. Bestuzheva, W.-K. Chen, L. Eifler, M. Gasse, P. Gemander, A. Gleixner, L. Gottwald, K. Halbig, G. Hendel, C. Hojny, T. Koch, P. Le Bodic, S. J. Maher, F. Matter, M. Miltenberger, E. Mühmer, B. Müller, M. E. Pfetsch, F. Schlösser, F. Serrano, Y. Shinano, C. Tawfik, S. Vigerske, F. Wegscheider, D. Weninger, and J. Witzig, "The SCIP optimization suite 7.0", Zuse Institute Berlin, ZIB-Report 20-10, Mar. 2020. [Online]. Available: `http://nbn-resolving.de/urn:nbn:de:0297-zib-78023`.

[202] G. B. Dantzig, "Origins of the simplex method", in *A History of Scientific Computing*, S. G. Nash, Ed., New York, NY, USA: ACM, Jun. 1990, pp. 141–151, ISBN: 978-0-201-50814-7. DOI: `10.1145/87252.88081`. [Online]. Available: `http://dl.acm.org/doi/10.1145/87252.88081` (visited on 01/18/2022).

[203] G. Guennebaud, B. Jacob, *et al.*, *Eigen v3*, 2010. [Online]. Available: `http://eigen.tuxfamily.org`.

[204] "Unser Stromnetz", Netze BW. (Oct. 1, 2021), [Online]. Available: `https://www.netze-bw.de/unser-netz` (visited on 10/01/2021).

[205] "Netzausbauplan Grafik 2021", Netze BW. (2021), [Online]. Available: `https://assets.ctfassets.net/xytfb1vrn7of/4ZJ0qWIGus8EsoSa6ykccy/a703dccc3c99732a5531a9ac0ad6a536/Netzausbauplan_Grafik_2021.pdf` (visited on 10/01/2021).

[206] D. Coppersmith and S. Winograd, "Matrix multiplication via arithmetic progressions", *Journal of Symbolic Computation*, vol. 9, no. 3, pp. 251–280, Mar. 1990, ISSN: 07477171. DOI: `10/ct7x67`. [Online]. Available: `https://linkinghub.elsevier.com/retrieve/pii/S0747717108800132` (visited on 10/08/2021).

[207] Gurobi Optimization, LLC, *Gurobi optimizer reference manual*, 2021. [Online]. Available: `https://www.gurobi.com`.